JPRS L/8237

23 January 1979

[redacted]

USSR

[redacted]

[redacted]

EXPERIMENTAL SEISMIC STUDIES OF THE EARTH'S INTERIOR

U. S. JOINT PUBLICATIONS RESEARCH SERVICE

[redacted]

NOTE

JPRS publications contain information primarily from foreign newspapers, periodicals and books, but also from news agency transmissions and broadcasts. Materials from foreign-language sources are translated; those from English-language sources are transcribed or reprinted, with the original phrasing and other characteristics retained.

Headlines, editorial reports, and material enclosed in brackets [] are supplied by JPRS. Processing indicators such as [Text] or [Excerpt] in the first line of each item, or following the last line of a brief, indicate how the original information was processed. Where no processing indicator is given, the information was summarized or extracted.

Unfamiliar names rendered phonetically or transliterated are enclosed in parentheses. Words or names preceded by a question mark and enclosed in parentheses were not clear in the original but have been supplied as appropriate in context. Other unattributed parenthetical notes within the body of an item originate with the source. Times within items are as given by source.

The contents of this publication in no way represent the policies, views or attitudes of the U.S. Government.

PROCUREMENT OF PUBLICATIONS

JPRS publications may be ordered from the National Technical Information Service, Springfield, Virginia 22151. In ordering, it is recommended that the JPRS number, title, date and author, if applicable, of publication be cited.

Current JPRS publications are announced in Government Reports Announcements issued semi-monthly by the National Technical Information Service, and are listed in the Monthly Catalog of U.S. Government Publications issued by the Superintendent of Documents, U.S. Government Printing Office, Washington, D.C. 20402.

Indexes to this report (by keyword, author, personal names, title and series) are available through Bell & Howell, Old Mansfield Road, Wooster, Ohio, 44691.

Correspondence pertaining to matters other than procurement may be addressed to Joint Publications Research Service, 1000 North Glebe Road, Arlington, Virginia 22201.

50272-101

REPORT DOCUMENTATION PAGE	1. REPORT NO. JPRS L/8237	2.	3. Recipient's Accession No.
4. Title and Subtitle: EXPERIMENTAL SEISMIC STUDIES OF THE EARTH'S INTERIOR			5. Report Date: 23 January 1979
			6.
7. Author(s): L. V. Antonova, F. F. Antikayev, et al.			8. Performing Organization Rept. No.
9. Performing Organization Name and Address: Joint Publications Research Service, 1000 N. Glebe Rd., Arlington, Va. 22201			10. Project/Task/Work Unit No.
			11. Contract(C) or Grant(G) No. (C) (G)
12. Sponsoring Organization Name and Address: As above			13. Type of Report & Period Covered
			14.

15. Supplementary Notes: EKSPERIMENTAL'NYYE SEYSMICHESKIYE ISSLEDOVANIYA NEDR ZEMLI, Moscow, 1978

16. Abstract (Limit: 200 words)

This report contains an examination of the procedures and results of an experimental study of patterns of seismic wave propagation in the inhomogeneous earth. Principles are worked out for resolving the observed wave field into a regular (background) component and fluctuations. New morphological wave field characteristics are introduced as well as methods of quantitative evaluations of these characteristics.

17. Document Analysis a. Descriptors

USSR
Geophysics
Seismic waves
Upper mantle
Fluctuations
Travel times
Gravitational anomalies

b. Identifiers/Open-Ended Terms

c. COSATI Field/Group 8K, 17J

18. Availability Statement	19. Security Class (This Report)	21. No. of Pages
FOR OFFICIAL USE ONLY. Limited Number of Copies Available From JPRS.	20. Security Class (This Page)	174
		22. Price

(See ANSI-Z39.18) See Instructions on Reverse OPTIONAL FORM 272 (4-77) (Formerly NTIS-35) Department of Commerce

JPRS L/8237

23 January 1979

EXPERIMENTAL SEISMIC STUDIES OF THE EARTH'S INTERIOR

Moscow EKSPERIMENTAL'NYYE SEYSMICHESKIYE ISSLEDOVANIYA NEDR ZEMLI in Russian 1978 signed to press 23 Dec 77, pp 1-159

[Book by L.V. Antonova, F.F. Antikayev, et al., Nauka, 1,350 copies]

CONTENTS

CONTENTS (Continued)

CONTENTS (Continued)

PUBLICATION DATA

English title	: EXPERIMENTAL SEISMIC STUDIES OF THE EARTH'S INTERIOR
Russian title	: EKSPERIMENTAL'NYYE SEYSMICHESKIYE ISSLEDOVANIYA NEDR ZEMLI
Author (s)	: L. V. Antonova, F. F. Antikayev, et al.
Editor (s)	: A. M. Epinat'eva
Publishing House	: Nauka
Place of Publication	: Moscow
Date of Publication	: 1978
Signed to press	: 23 Dec 77
Copies	: 1,350
COPYRIGHT	: Izdatel'stvo "Nauka", 1978

[Annotation]

[Text] The book examines the procedure and results of an experimental study of patterns of seismic wave propagation in the inhomogeneous earth. Principles are worked out for resolving the observed wave field into a regular (background) component and fluctuations (deviations from the background); new morphological wave field characteristics are introduced as well as methods of quantitative evaluation of these characteristics. In a number of regions of the Soviet Union and throughout the earth with appreciably different geological structure, a study is done on the mutual relation between fluctuations of the characteristics of longitudinal waves and the inhomogeneity of the earth's mantle. A detailed analysis is given of the particulars of propagation of Pn, Pg, P, Sn, S, Lg and Rg waves over an extensive territory of Central Asia. The interior structure of the crust and upper mantle of Pamir-Baykal are studied in detail in accordance with data on the seismologic profile of this region. Crust-mantle blocks with different velocity characteristics are distinguished, a quality cross section is obtained for the medium down to the mantle-core boundary, and regional calibration curves are plotted for an extensive class of waves. New experimental data are given on the mutual relation between the amplitude characteristics of seismic waves and

gravitational and magnetic anomalies observed within the territorial limits of the USSR, as well as the position of seismic stations relative to tectonic structures. Recommendations are made on choosing points for setting up high-sensitivity seismic stations.

Introduction

The present concept of the internal structure of the earth is based on fundamental results provided by experimental seismology. In the last decade experimental seismology has made appreciable progress in studying the interior of the earth. At the present time there are several thousand seismic stations and several dozen grouping stations in operation throughout the earth. Hundreds of thousands of earthquakes are recorded every year. However, despite the enormous volume of material accumulated, the structure of individual regions of the earth is known only roughly. Remaining unknown until recently have been what would seem to be primary facts about the structure of the earth such as the range of natural regional and local variations in seismic wave velocities and depths of interfaces and the nature of these variations for the principal shells of the earth and geological structures. This book is devoted to a study of these questions.

Formulation of the problem of study requires solution of two major problems: selection of a model of the medium whose parameters are to be determined, and selection of the informative characteristics of the wave field. These problems are closely interrelated and ways to solve them are informal; they depend on many additional circumstances: the available preliminary information on the object of study, quality and quantity of experimental data, the possibility of processing them, and finally, the specific problem of study.

Model of the Medium. As the volume of experimental data increases and methods of processing them improve, the ideas about the earth change and the models of its structure become more complicated.

The development of ideas about the structure of the earth progresses from a uniform spherically symmetric model to a complex three-dimensional model that contains horizontal inhomogeneities of different sizes.

The development of recording technology and the creation of dense networks of seismic stations have improved precision in determining the coordinates of a focus and the magnitude [of a disturbance], and have enabled establishment of the considerable influence of horizontal inhomogeneities of different scales (from thousands of kilometres to tens of metres) on the formation of a wave pattern. This in turn has raised the problem of studying inhomogeneities.

At the present time, intense development is taking place in methods of studying the horizontally inhomogeneous earth, and even though they are in the developmental stage and still have not been formulated as a definite system, they can be classified and described to put a model of the medium together.

1°. *Homogeneous spherically symmetric model of the earth.* For many decades this was the only model. During its formulation it was established that the earth is layered in shells, and the main characteristics of the layers were found: velocities of longitudinal and transverse waves, mechanical quality of the medium. These results were based on enormous experimental material of quality sufficient to show the deviations of the model from spherical symmetry. However, the efforts of researchers were concentrated on perfecting this "ideal" model, on finding unified global patterns. In recent years, the concept of a horizontally homogeneous mantle was formulated with a comparatively homogeneous crust of variable thickness. Such a model justified extensive use of surface waves in research, the interpretation being done on the assumption of spherical symmetry or horizontal stratification of the medium. The success of experimental and theoretical research associated with this model, support on the part of other geophysical methods, and the authority of leading scientists have dictated a certain conformity in ideas about the structure of the earth and unmerited vitality of the spherically symmetric model right up to the last decade.

2°. *Locally homogeneous model.* According to this model, individual large structures -- continents, oceans, mountain chains, platforms -- are horizontally homogeneous regions distinguished by the nature of change in seismic parameters with depth. Developed methods can be applied to investigation of such regions; however, the preparation of experimental material requires a certain sampling of data.

In the course of detailed studies carried out in regional seismological observations and depth probes of the earth a pronounced horizontal mosaic structure has been detected in the crust and upper mantle. This has led to the development of a laminar-block model in which the medium is divided into comparatively small horizontally layered blocks. At present this model is widely used in seismology and in deep seismic sounding.

3°. *Spherically symmetric model containing large horizontal inhomogeneities.* It is assumed that the velocity contrast of these inhomogeneities is low, and therefore seismic rays lie in the vertical plane.

Profile observations yield data that enable redefinition of the coordinates and depths of earthquake foci and parameters relative to the profile. This method was developed at the computing center of the Siberian Department of the Soviet Academy of Sciences (Alekseyev et al., 1969).

4°. *Inhomogeneous block model.* This is a three-dimensional model made up of several layers broken up into comparatively small blocks. To solve the inverse kinematic problem with respect to travel times of the P-wave, it is assumed that the anomalies of velocities of seismic waves in the blocks are small, and therefore rays travel through the medium without refraction. The initial information is provided by data on the travel times of waves from remote sources lying in different azimuths to stations of an area group.

Solution of the problem reduces to finding anomalies of velocity in the individual blocks that best correspond to the observed anomalies in travel time. To determine the velocity in some volume of the medium beneath a group of stations the seismic rays must penetrate elementary volumes repeatedly and in different directions. Such an approach to solution of the problem was proposed independently by A. S. Alekseyev and K. Aki (Alekseyev et al., 1971; Aki, 1973).

This method has been used in practice for determining the velocity profile of the earth's crust and the upper mantle in a number of territories -- Kamchatka, California and elsewhere -- and has given rather good results.

The comparatively thin network of stations and the incomplete range of azimuths of arrival of seismic waves limit the possibilities of determining the structure of the medium beneath the stations. This requires a qualitatively different statistical approach to investigation of the medium.

5°. *Random inhomogeneities, seismically hazy media.* This is a complicated model comprised of a deterministic background constructed according to one of the schemes 1°-4° given above, and a random field of fluctuations in velocities and absorbing properties that approximates the difference of the actual medium from the deterministic model. Usually it is assumed that this field is locally homogeneous, isotropic, smooth and low in contrast. As a result of interpretation such characteristics of the medium are determined as the predominant size of inhomogeneities, their contrast and the coefficient of turbidity (Nikolayev, 1973).

Initial Stage of Investigation of the Three-Dimensional Model of the Earth. Statistical models take on especially important significance on the initial stage of investigation of the horizontally inhomogeneous earth. This is due to a lack of data that might be used to construct a deterministic model. At the same time, even a comparatively incomplete system of data (thin network of stations, small number of earthquakes) is sufficient to establish some general characteristics of inhomogeneities. These characteristics are of independent geological interest, and can be used besides in planning future studies.

Basic Problems. Our study deals with three problems: 1°. To establish the natural range of variations in velocities of propagation of seismic waves and absorbing properties, their characteristic scale and coarse stratification. 2°. To determine the main characteristic features of the wave field associated with horizontal inhomogeneities, to evaluate local and regional variability of characteristics of body and surface waves. 3°. To work out the elements of a simple and constructive research technique that corresponds to conditions 1° and 2°; this requires first of all the introduction of new morphological characteristics of the wave field that are based on statistical estimates.

Research Technique. The study is based on resolving the observed seismic fields into two main components: the background and the deviation from the

background -- fluctuations. Depending on scale, the background component characterizes the average value over a larger or smaller territory.

Such an approach requires introducing a certain hierarchy of scales. We have introduced five scales: global, continental, regional, local and detailed. Corresponding to the global scale are patterns found by averaging data over the entire earth, to the continental scale -- over parts of the earth of the continent-ocean type, to the regional scale -- over areas with a transverse size from 3000 to 6000 km, to the local scale -- from 200 to 2000 km, and to the detailed scale -- less than 200 km.

The spherically symmetric model of the earth corresponds to the global scale. The general patterns of change in the characteristics of the major types of waves have been well studied, and therefore existing data (hodographs, calibration and amplitude curves) are taken as the background characteristics.

The level of detail of the research depends on the detail of the system of observations. Low detail, scant experimental material enable investigation of only deviations from the global background, including the influence of regional, local and district conditions; the most detailed studies that use data of observations of dense networks of seismic stations enable investigation of the fine spatial structure of fluctuations distinguished relative to the local background.

Initial Experimental Data. This work is based on experimental material obtained by the Comprehensive Seismological Expedition of the Institute of Physics of the Earth in various years in the course of carrying out a variety of seismological research aimed chiefly at solving problems of seismic zoning, earthquake prediction and investigation of the degree of seismic danger of hydroelectric plants being planned and under construction in the Northern Tyan'-Shan', in Kirgizia, in the Naryn River basin, in Garmskiy Rayon of the Tadzhik SSR, in the Central Sayan Mountains and in the territory of the Zeya River. The system of observations in each region was a network of stations usually numbering up to 10-12 separated by distances of from tens to hundreds of kilometres.

For the purpose of getting more general material on the nature of regional inhomogeneities of the earth, short-term observations were organized by groups of stations in regions with low earthquake danger: the Ukraine, North Kazakhstan. To supplement the detailed systems of observations described above and the system of observations in the European part of the USSR and the central territories of the nation, in many instances data were included from the Unified Network of Seismic Observations [YeSSN service]. Seismographic material used in the work is provided by observational data from more than 100 stations.

The observations were made with standard seismic channels SK, SKM-3M, SM-2 and ChISS (Zapol'skiy, 1971) with photographic or visual registration. A description of the corresponding equipment can be found in the book "Apparatura i metodika seysmometricheskikh nablyudeniy v SSSR" [Equipment and Methods of Seismometric Observations in the USSR] (1974).

More than 6000 seismograms of earthquakes covering the entire range of epicentral distances and located at the most diverse azimuths relative to the recording stations were used to different extents -- from isolated measurements of the amplitude and time of arrival of a P-wave to spectral analysis. More detailed information on initial data is contained in the corresponding sections of the book. Measurements of the dynamic characteristics of waves -- amplitudes, periods -- were done in strict conformity with the scheme described in the book (Antonova et al., 1968).

A. P. Andreychenko, L. M. Vlasova, P. S. Glazkov, A. M. Sokolova and S. G. Starchenko took part in the production of this monograph.

The book uses seismographic material obtained by the Comprehensive Seismological Expedition of the Institute of Physics of the Earth in different territories of the USSR. The considerable work of the members of the expedition is incorporated in the organization and successful completion of field observations and also in the processing of experimental materials. The authors express their gratitude to all of them, and especially to detachment leaders G. I. Aksenovich, Yu. P. Kolobashkin, V. N. Krivosheyev, K. K. Kuznetsov, V. D. Pavlov, G. G. Starchenko, G. G. Tarasov and V. I. Sheloputov.

I. EXPERIMENTAL STUDY OF PATTERNS OF PROPAGATION OF SEISMIC WAVES IN THE INHOMOGENEOUS EARTH

Chapter 1. Seismic Waves in the Inhomogeneous Earth

The first experimental evidence of stratification in the deep interior of the earth according to seismological data was found in the early twentieth century. Hodographs of fundamental modes of elastic oscillations -- longitudinal and transverse -- were the foundation on which a model of a radially inhomogeneous and spherically symmetric earth was constructed over the next 25-30 years.

The development of radial inhomogeneity on a planetary scale was shown by such typical features of hodographs as splitting of refracted and reflected waves into branches, sharp bends and breaks. The most pronounced of these features were confined to the interfaces of shells of the earth: crust and mantle, mantle and core.

As a result of careful analysis of the hodographs of fundamental waves, other divisions were distinguished in the earth's cross section, and numerous averaged models of its structure were found. Typically, all these models were in "good" agreement with the data of observations. In the final analysis this caused uncertainty in choosing a suitable standard cross section of the earth.

This ambiguity was the impetus for numerous refinements in the model of the earth. This process led to the conclusion that the structure of the shells

deviates on various scales from spherical symmetry, and to the necessity of expanding the class of models of the earth that account for radial and horizontal inhomogeneity of the structure of its shells. The problem of standardization assumed the aspect of refinement of general patterns in the structure of the shells based on specific stipulation of deviations from spherical symmetry in different regions.

The leading area of experimental seismology is becoming the study of comparatively fine details of the structure of the earth's interior, especially those parts characterized by different types of geological-tectonic evolution.

Obviously the selection and refinement of a model of the earth under specific conditions should be oriented toward some characteristic scale of inhomogeneity of structure matched to the detail of studies and the accuracy of data. In this connection it is of considerable interest to establish the co-dependence of scales of inhomogeneities of the structure of the earth's interior and their manifestation in the seismic characteristics of the medium, as well as the correlation of scales of seismic inhomogeneities and the characteristic elements of schemes of geological-tectonic zoning.

In particular, according to materials of geological-tectonic zoning of the folded complexes of Central Asia it has been established that the most frequently encountered structures are elongated with predominant longitudinal dimensions of about 500-600 km, and transverse dimensions of about 100-150 km (Belyayevskiy, 1974).

According to materials of deep seismic sounding in various regions of Siberia, typical values of the horizontal extent of surfaces of the crystalline basement and the Mohorovičič discontinuity are 100-200 km, predominant dimensions of undulation of the Mohorovičič discontinuity are 5-8 km, and for the crystalline basement -- 3-5 km. Variations of the boundary velocity on the surface of the basement may reach values of 1.0-1.2 km/s (with a predominant value of about 0.3 km/s), and the horizontal extent of such anomalies is up to 40 km (Puzyrev et al., 1975).

Available experimental data on travel times and amplitudes of body waves and on the phase velocities of surface waves enable us to differentiate the inhomogeneities of the internal structure of the earth in the first approximation into five characteristic scales: global, continental, regional, local and detailed, which were discussed above.

Radial spherically symmetric inhomogeneity corresponds to the global scale.

This model satisfactorily explains the major experimental patterns observed over the entire earth.

1. Relation between radial inhomogeneity of the earth and travel times and amplitudes of seismic waves

In a homogeneous and infinite elastic medium a wave field has comparatively simple properties. Seismic recordings in this case would be represented by

just two waves: longitudinal P and transverse S. In particular, for a homogeneous sphere we can construct hodographs of P and S waves, but they will differ appreciably from the hodographs observed in the actual earth.

The main difference is that the travel times of P and S waves increase with epicentral distance much faster in a homogeneous sphere than in the actual earth. This implies in particular that in the real earth velocity in general increases with depth.

It is also known that on the whole the hodographs of P and S waves are rather well approximated by smooth functions such as a parabola (Hales et al., 1968). The greatest deviations from smooth functions are observed at epicentral distances below 30°, and from 105 to 142°. In general, as data are analyzed more intently and in greater detail, more justifications show up for differentiating them into separate parts.

Analysis of the derivative of a hodograph $dt/d\Delta$ of a longitudinal wave with respect to data of direct measurements on groups of seismic stations for the distance range of 30-100° shows that characteristic dips can be observed in the behavior of this function most frequently close to distances that are equal to approximately 35-36, 48-49, 60, 68-70 84-85 and 95° (Corbishley, 1970). This is an indication of a possible anomalous change in the velocity gradient close to depths equal to approximately 850-900, 1200, 1550, 1800-1900, 2500 and 2800 km. Analysis of data on $d^2t/d\Delta^2$ also indicates the presence of singularities within the limits of the mentioned depths. Fig. 1 summarizes

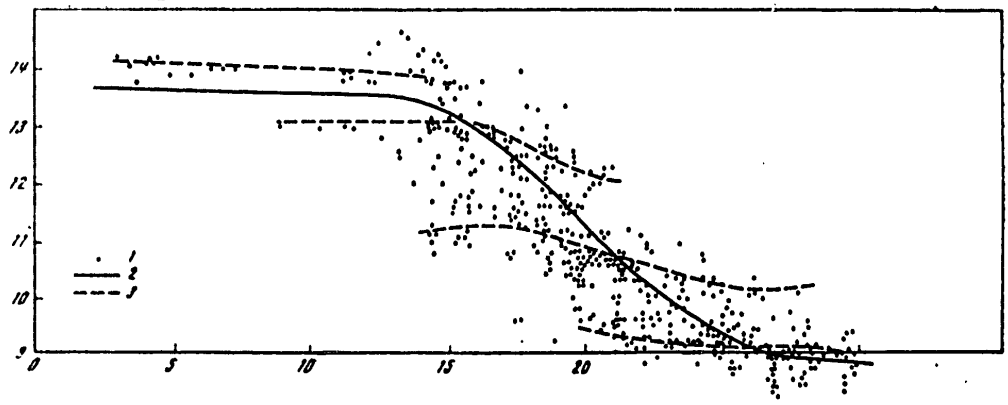

Fig. 1. Direct measurements of hodograph derivative $dt/d\Delta$ from non-Soviet data (the epicentral distance Δ is plotted in degrees along the axis of abscissas)

1--Isolated measurements
2--E. Herrin's standard curve (1968)
3--Data of K. Kaila and D. Sarkar (1975)

data from direct measurements of the derivative dt/dΔ on a number of groups of seismic stations (Chinnery, 1969; Chinnery, Toksöz, 1967; Corbishley, 1970; Johnson, 1967, 1969; Kanamory, 1972b; Niazi, Anderson, 1965; Simpson et al., 1974). Shown here for comparison is E. Herrin's standard dt/dΔ profile (Herrin, 1968) and an approximation of L. Johnson's data (1967) made by K. Kaila and D. Sarkar (1975).

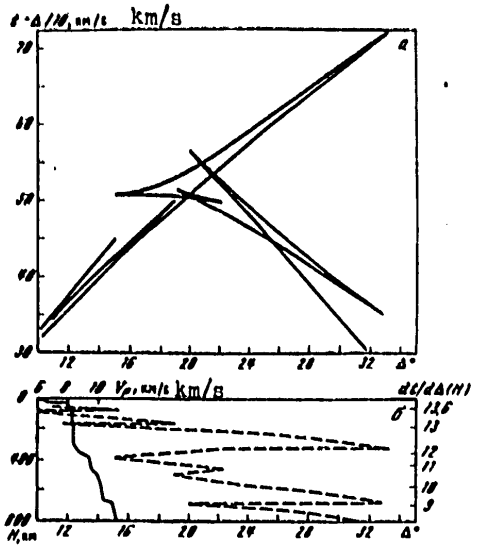

Fig. 2. Model of the structure of the crust and upper mantle according to P waves in the territory of the Warramunga group in Australia from research data of D. Simpson et al. (1974). a--reduced hodograph: b--velocity profile (solid line) and projection of the derivative of the hodograph dt/dΔ (H) (dotted line)

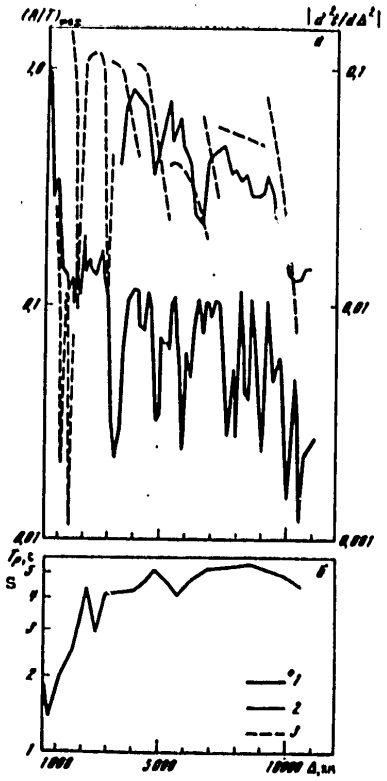

Fig. 3. Distance dependences of the ratio $(A/T)_{max}$ (a) and the period of recording of the wave (b): 1--curves from stations of the Northern Tyan'-Shan' (Antonova et al., 1968); 2--azimuthal curve for roughly confocal earthquakes according to data of M. Sengupta and B. Julian (1976); 3--theoretical curves of $|d^2t/d\Delta^2|$ from the work of K. Kaila and D. Sarkar (1975)

However, the most pronounced changes in travel time are observed at distances of less than 30°. For instance let us consider the data of the Warramunga group in Australia (Simpson et al., 1974) shown in Fig. 2. The SMAKI model includes a crust 35 km thick with a jump in velocity of longitudinal waves on the Mohorovičić discontinuity from 6.5 to 8 km/s. At depths of from 150 to 300 km a low velocity gradient zone is observed with change from 8.3 to 8.5 km/s.

Such a fine differentiation of the upper mantle is reflected in the structure of the hodograph and the derivative $dt/d\Delta$.

The radial inhomogeneity of the earth shows up in other parameters of seismic waves as well. A previous monograph (Antonova et al., 1968) gives extensive composite data on variation in the way that the predominant period of the recordings of longitudinal and transverse waves depends on the epicentral distance, and also on the same dependence for the maximum A/T ratio of these waves.

Fig. 3 shows distance dependences of the ratio $(A/T)_{max}$ and apparent period for P waves as found from data of SK channel registration on a group of stations in Northern Tyan'-Shan' and on the Talgar station respectively.

Let us examine these data in more detail. The behavior of the apparent period of a P wave with distance is determined by the characteristic stepped form of the curve. The lower level of the step is observed at a distance of from 200 to 700 km and is equal to approximately 1.5 s, while the upper level, equal to approximately 4-4.5 s, stretches from about 2,000 to 10,000 km, a relatively smooth transition being noted between these levels.

Particular attention should be given to the presence of relative maxima on the curve, that are confined to distances of approximately 2,500, 6,000 and beyond 10,000 km.

The curves for the ratio $(A/T)_{max}$ as a function of distance that are shown in Fig. 3a have rather interesting properties. If we compare the intervals of distances where characteristic jumps in the function $dt/d\Delta$ are observed (see Fig. 1) with the position of the sharp minima on the graph of $(A/T)_{max}$ for a longitudinal wave, we can see that they coincide. We can convince ourselves that this agreement is not accidental by comparing our data with those found by M. Sengupta and B. Julian (1976) for roughly confocal earthquakes (see Fig. 3a).

Besides, the relation between amplitude and profile parameters can be analyzed if we consider the following expression (Volkov and Yanovskaya, 1974):

$$A(\omega, \Delta) = A_0 Q(p) \exp(-\omega l_0(p)), \qquad (*)$$

where A_0 is a constant that determines the intensity of the P wave in the vicinity of the source,

$$G(p) = R^{-1}\left[p\,(p_0^2 - p_m^2)^{-1}\left(\sin\Delta p_m \frac{dp}{d\Delta}\right)^{-1}\right]^{1/2},$$

$$I_0(p) = \int_{r_m}^{R} rQ^{-1}V^{-1}\left|(r/V)^2 - p_m^2\right|^{-1/2} dr,$$

$$\Delta p_m = 2p_m \int_{r_m}^{R} r^{-1}\left|(r/V)^2 - p_m^2\right|^{-1/2} dr,$$

$$p_0 = R/V(R), \quad p_m = r_m/V(r_m).$$

Here r_m is the radius of penetration of a seismic ray; p_m is the parameter of this ray; Δp_m is the epicentral distance at which this ray penetrates to r_m; $V(r_m)$ is the velocity corresponding to the radius r_m; R is the radius of the earth; Q is mechanical quality.

The expression (*) describes the behavior of the amplitude curve $A(\omega,\Delta)$ as a function of the geometric divergence of the wave front G(p) that in turn is determined by the velocity profile V(r) and also as a function of the parameters of the inelastic profile Q(r).

If for the time being we disregard the influence of the profile Q(r) and the loss of wave energy at interfaces, the main contribution to the behavior of the amplitude curve $A(\omega,\Delta)$ comes from the term G(p). In this case expression (*) can be conveniently represented as

$$A(\Delta) \sim K\left[(\sin\Delta)^{-1}\,(dt/d\Delta)\,(d^2t/d\Delta^2)\right]^{1/2},$$

hence it is apparent that the behavior of the amplitude curve is determined by the second derivative of the hodograph $d^2t/d\Delta^2$, and consequently the curve should be more sensitive to peculiarities of the velocity profile.

At the same time, there are grounds for assuming that the change in the quality factor with depth may also have a considerable effect on the amplitude curve.

To illustrate this assumption let us use the calculations of K. Kaila and D. Sarkar (1975). In their work, the authors used data of L. Johnson (1967, 1969) on $dt/d\Delta$ and calculated the second derivative $d^2t/d\Delta^2$ for comparison with the known amplitude curves of B. Gutenberg and C. Richter (1956) and O. Nuttli (1972).

These data are reproduced in Fig. 3a together with the amplitude curve of a P wave found on a group of stations of Northern Tyan'-Shan', and the amplitude curve of M. Sengupta and B. Julian (1976) for stations in the United States. A comparison of the results convinces us that the behavior of the amplitude curves can be attributed only in part to the influence of the function $d^2t/d\Delta^2$.

Noteworthy in this connection is the work of K. Veith and G. Clawson (1972) in which the authors used data of numerous amplitude measurements to study the influence of the inelastic profile Q(r). They calculated and eliminated from the observed data the effect of geometric divergence G(p). As a result it is shown that the inelastic profile does indeed have an appreciable

influence of the behavior of the amplitude curve, the greatest effect of Q(r) being observed at epicentral distances of less than 30°.

In general outline, the radial inhomogeneity of the earth has now been rather well studied. The physicochemical evolution of the earth has led to the formation of shells with appreciably different properties. The most pronounced changes in the seismic properties of the medium are confined to depths of 10-70, 150-270, 350-450 and 620-870 km (Press, 1975), 2885-2889 and 5141-5156 km (Adams, Engdahl, 1974; Dziewonski, Haddon, 1974).

The depths of 10-70 km are associated with the earth's crust, which is thinnest under the oceans.The interval of depths of 150-270 km is generally associated with the asthenospheric zone, whose distinguishing features are low values of the velocity of transverse waves and mechanical quality. The depths from 350 to 870 km are associated with a transition zone in which a relatively high increase in velocity and quality is observed. The region from 870 to 2885 km belongs to the lower mantle for which lower gradients of velocity, density and quality factor are characteristic on the average. The depth range of 2885-2889 km is associated with the boundary passing between the lower mantle and the outer core. The boundary between the outer and inner core is situated at depths from 5141 to 5156 km.

At the present time the internal shells of the earth have been comparatively little investigated. Therefore it is of considerable interest to study the travel times and amplitudes of waves that have traversed the outer and inner cores, particularly waves of the PKP type. In this section an examination is made of the travel times of PKP waves; the amplitudes of these waves are considered in the next section.

The investigation of the characteristics of PKP waves is of fundamental importance for studying the structure of the earth. From these waves we can also determine the characteristics of foci, which usually are determined from P waves (moment of onset, coordinates, depth, magnitude, parameters of the mechanism). At the same time, an improvement in the effectiveness of using PKP waves requires accounting for the peculiarities of their spatial structure, which show up primarily in characteristic distortions of amplitudes and travel times that are inherent in individual seismic stations and epicentral regions.

On the territory of the USSR PKP waves are recorded from earthquakes in South America, the region of underwater mountain chains to the south of Africa and in the southern part of the Pacific Ocean. In the investigation of kinematic characteristics, about 700 recordings were used. To get more reliable data, only the strong earthquakes in South America were selected. All recording stations are equipped with short-period instruments with standard frequency responses and magnification from 40,000 to 250,000. Earthquake information -- time of onset, focus depth, coordinates and magnitude -- was taken from seismological bulletins of the United States, the USSR, and the International Seismological Center.

In plotting the hodographs of first arrivals and maximum phases of PKP waves no assumptions were made about the form of the hodograph itself. As a result it was possible to trace some clear branches that do not always coincide with the well-known hodograph of B. Bolt (1968).

In the range of epicentral distances from 12,000 to 18,000 km the most stable phase of the PKP wave corresponds to the DF branch of the hodograph (Fig. 4). At distances $\Delta = 15,300$-$15,900$ km it copies the B. Bolt hodograph with a lead of 3 s, with a delay of up to 1 s at $\Delta = 16,600$-$16,700$ km, and with a delay of 2 s at $\Delta = 17,400$-$17,600$ km. The observed leads and lags do not exceed the standard deviations calculated for the corresponding distances.

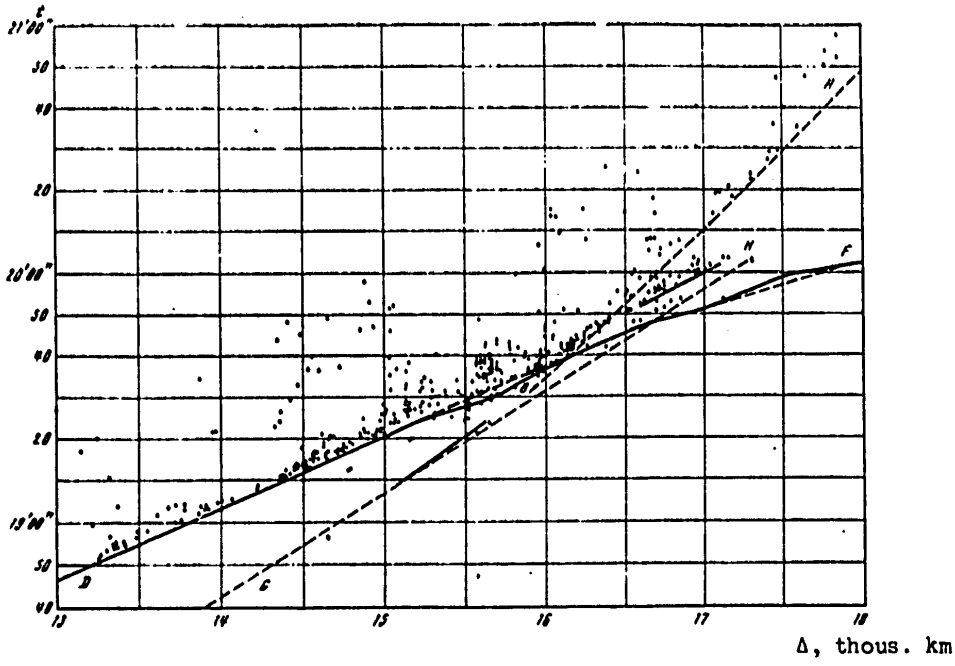

Fig. 4. Hodograph of first arrivals (solid line) and times of maximum phases (points) of PKP waves. B. Bolt's hodograph (1968) is shown by the broken curves.

Arrivals of the PKP phase that are identified as the GH branch (see Fig. 4) are distinguished only in fairly strong ($m_{PV}^{SKM} > 0.6$) earthquakes at epicentral distances $\Delta = 15,100$-$15,700$ km and $\Delta = 16,700$-$17,100$ km. Let us note that at a distance equal to 15,100 km the travel time of this phase according to our estimates corresponds to B. Bolt's hodograph. At the same time the derivative for the hodograph here reaches values of p = 3 s/deg, i. e. somewhat greater than for B. Bolt's case. The second section of the GH branch deviates from Bolt's hodograph by about 4 s, and at $\Delta = 17,000$ km has a parameter p = 2.15 s/deg.

One might think that with such values of the parameter p the observed sections of the GH branch could scarcely belong to a single straight line as suggested by B. Bolt, and possibly are independent branches. Besides, the observed values of the parameter p eliminate the possibility of intersection of the GH and DF branches.

Let us note that the parameters obtained relative to the GH branch are quite close to T. B. Yanovskaya's results (1971).

The standard deviation of the experimental data does not remain constant with a change in epicentral distance, responding sensitively to inhomogeneities in the structure of the medium. In the distance range of 12,100-15,100 km the DF branch is characterized by a standard deviation of $\sigma = \pm 1.5$ s. On the 15,100-15,600 km segment the standard deviation for this branch increases to $\sigma = \pm 2.1$ s. The increase in variance may possibly be due to the fact that on this section one sees waves of the GH branch in the first arrivals, while waves of the DF branch are in evidence in the second arrivals. The standard deviation is $\sigma = \pm 1.8$ s for the GH branch on this section.

on the 15,600-16,000 km section one cannot see the first entries of the GH branch, and at later times, interference of several wave groups is observed, the most stable among them being the group corresponding to the DF branch. The standard deviation on this section is $\sigma = \pm 3.1$ s. Beyond 16,000 km the waves of the DF branch again go out to the first entries, and the standard deviation once more falls to $\sigma = \pm 1.9$ s on the 16,000-16,500 km section. With a further increase in distance, the GH and DF branches diverge still more, and the standard deviation decreases: to $\sigma = \pm 1.4$ s for the DF branch, and to $\sigma = \pm 1.2$ s for the GH branch.

Thus it turns out that the wave pattern in the given range of distances is very complicated and the differentiation of different branches will inevitably be accompanied by errors, particularly in the case of slight earthquakes.

Analysis of the hodographs of maximum PKP phases shows that the maximum amplitudes may also correspond to different branches. It is clear from Fig. 4 that at distances up to 16,000 km the maximum amplitudes as a rule correspond to the DF branch. They are observed on the average 4 s after the first entry of waves of the given branch; the variance in time of arrival of the maxima is not much greater than for the first entries. In the interval of epicentral distances between 15,000 and 16,000 km the first entries of the GH branch are poorly distinguishable, although the maximum amplitudes in approximately 15% of the cases correspond to just this branch.

In the 16,000-16,200 km interval the DF and GH branches are indistinguishable, and in the 16,200-16,400 interval the maximum amplitudes fall to the GH branch in the overwhelming majority of cases. In the 16,400-17,200 km interval the maximum amplitudes are associated with the DF branch in only 10% of the cases, and fall to the GH and AB branches each in about 40% of the cases. The AB branch predominates after 17,000 km.

2. Correlation between scales of fluctuations in seismic wave parameters and horizontal inhomogeneities of the earth

The horizontal inhomogeneity of the earth has been little investigated even though it has a very strong influence on kinematic and dynamic wave characteristics. The effect of inhomogeneity on level, shape and phase difference (travel time anomalies) depends on the size of the inhomogeneity, "intensity," and the relative placement of the source and the observation point. With respect to "intensity," i. e. the deviation of velocity (quality factor) from the average, it is known that in most instances the magnitudes of anomalies do not exceed a few percent. This circumstance considerably simplifies the calculations of wave fields, since the effect of the action of the inhomogeneity is linearly dependent on its "intensity."

A great deal of theoretical and experimental research has been devoted to the propagation of seismic waves in plane-laminar and spherically symmetric media. Although the effect of horizontal inhomogeneity of the medium shows up rather clearly in isolated instances, it has been very little investigated. Therefore, we have examined chiefly the problems of wave propagation in weakly inhomogeneous media where slight (horizontal or three-dimensional) inhomogeneity is superimposed on one-dimensional, plane-laminar or spherically symmetric inhomogeneity. Corresponding to such differentiation of the medium is an analogous differentiation of the field.

Influence that Inhomogeneity of the Medium has on the Level and Phase of a Seismic Wave. Terminology. The natural logarithm of amplitude of an oscillatory process is called the level ($\ln A$), and the product of travel time of the wave by angular frequency is called the phase. In the following discussion we will be concerned only with deviations of travel time or phases from the average. We will call these characteristics simply the time deviation δt or the phase deviation $\delta\psi = (2\pi f)\delta t$. Without going in detail into the theory of wave propagation in inhomogemeous media that has been worked out in acoustics, optics and radio physics, we will take up only the main results. To do this, we introduce concepts that are not used in the seismics of horizontally layered and spherically symmetric media.

Random inhomogeneity of a medium is small-scale inhomogeneity that is approximated by a three-dimensional random field. We will assume that the actual field of the inhomogeneity is one sample of a general set that contains all possible specimens of the random field. The simplest and physically most applicable model of a random field is a smooth, homogeneous and isotropic field. Smoothness means continuity in variation of the field and its derivative; homogeneity means steadiness in space, sameness of the statistical characteristics of the field throughout the entire region of the medium under consideration; isotropy means equivalence of all directions, i. e. the absence of directions in which the statistical characteristics of the medium will differ from the average characteristics taken in other directions.

The term "size of inhomogeneity" can have two meanings. In the case of a local isolated inhomogeneity it means the average size of its thickness.

In the description of a field with homogeneities of different sizes, the maximum size is usually considered, which is identified with the interval of spatial correlation a of fluctuations in seismic wave parameters. This interval -- the distance between two points where the correlation coefficient reaches some threshold such as 0.2 -- may serve as an estimate of the average sizes of inhomogeneities. It is necessary to distinguish longitudinal and transverse correlation intervals: longitudinal meaning correlation along rays, and transverse -- along wavefronts.

The geometric region is the part of the medium filled with the "shadow" cast by the inhomogeneity. The boundary of this region extends to a distance of about $\sqrt{\lambda a}$ from the inhomogeneity; λ is the predominant wavelength.

The diffraction region lies beyond the geometric region at distances greater than $\sqrt{\lambda a}$ from the inhomogeneity.

The point of observation for nearby inhomogeneities lies in the geometric region, and for remote inhomogeneities -- in the diffraction region. As a consequence of the principle of reversibility it turns out that if the receiver is in the geometric region relative to some inhomogeneity and seismic source, then when the source and receiver change places the latter will also be in the geometric region. Thus, inhomogeneities located close to the receiver cast a shadow over the entire length of the seismic ray.

In media with large inhomogeneities wave propagation takes place in accordance with the laws of geometric seismics. We will call such media inhomogeneous. In media with small inhomogeneities wave propagation takes place in accordance with the laws of nongeometric diffraction seismics. We will call such media turbid (Nikolayev, 1972). Actual media contain inhomogeneities of different sizes and are simultaneously inhomogeneous and turbid.

The main peculiarities of the wave field in an inhjomgeneous medium (we mean here a large three-dimensional inhomogeneity rather than a change in velocity in one direction): a) good correlation is observed between fluctuations of amplitudes and phases; b) the anomalies of wave field characteristics on the plane of observations coincide with the region into which the seismic rays project the inhomogeneity; c) seismic oscillations are subject to a change of amplitude and phase, but their shape is preserved, i. e. the amplitude fluctuations of individual phases of an oscillation are strongly correlated.

The main peculiarities of the wave field in a turbid medium:

a) fluctuations of amplitudes and phases are uncorrelated;

b) longitudinal correlation of fluctuations extends to the same distances as the region of geometric shadow. The transverse correlation of fluctuations for plane waves is the same as the correlation of the inhomogeneities themselves, and the correlation interval is equal to a. When waves with complex

wavefront surfaces pass through the medium the correlation interval is al_2/l_1, where l_1 is the geometric divergence of the wavefront close to the inhomogeneity, and l_2 is the geometric divergence close to the surface of observation. The quantity l_2 is nearly always greater than l_1, which means that the interval of transverse correlation increases as the inhomogeneity approaches the source and gets further away from the plane of observation. The quantities l_1 and l_2 are directly proportional to the cross sections of tubes of rays;

c) in a medium with large inhomogeneities ($a \gg \lambda$) scattering is directed forward and is concentrated in a cone with small vertex angle. In a medium with small inhomogeneities ($a \ll \lambda$) scattering is isotropic, and therefore a comparatively small fraction of the energy of the scattered field follows in the direction of propagation of the transmitted wave. Fluctuations in the times of first entries occur chiefly under the effect of a large inhomogeneity. Scattering by small inhomogeneities is accompanied by a substantial exchange of the P→S type. The scattered waves arrive at the point of observation with large delays from different directions, and therefore the intensity of fluctuations increases with depth of the seismogram;

d) fluctuations of amplitudes and times are related by the following expression:

$$D\delta \ln A = 4\pi^2 f^2 D\delta t = D\delta\Phi.$$

Here A is amplitude, t is time, D is the symbol for the mean square or variance, δ is the symbol for fluctuation, Φ is phase. This relation means that the variance of fluctuations in the natural logarithm of the amplitude is equal to the variance of fluctuations in phase. Let us note that

$$\delta \ln A \approx \delta A/\bar{A}, \text{ if } \delta A \ll \bar{A},$$

where δA is the fluctuation of amplitude, and $\bar{A}$ is the average amplitude.

In a turbid medium, the fluctuations of amplitudes and times increase as the wave propagates. The quantities $D\delta \ln A$ and $D\delta t$ in a homogeneous turbid medium are proportional to the path L traveled by the ray:

$$D\delta \ln A = 4\pi^2 f^2 D\delta t = gL,$$

where g is a proportionality factor called the coefficient of turbidity. It has the dimensions of $[\text{length}]^{-1}$ and characterizes the scattering action of the medium. In the case of large inhomogeneities, g coincides with the coefficient of scattering.

Method of Studying the Spatial Structure of the Field of Amplitudes and Hodographs. Investigation of the spatial structure of amplitudes and travel times requires first of all the differentiation of the observed fields into components that correspond to change in velocity with depth, large horizontal inhomogneity, small inhomogeneity -- turbidity, inhomogeneity close to the source and receiver. This resolution is carried out by spatial averaging of the characteristics of the field, and therefore is based on combined

processing of data of a large number of seismic stations and sources. Depending on requirements for detail, the seismic stations must be situated more or less closely together.

The investigation of the influence that a change in velocity of seismic waves with depth has on the amplitudes and times does not require a dense network of stations, and has been well studied both for the earth as a whole and for its individual regions. The results of these studies are hodographs of waves and calibration curves of A and A/T.

Investigation of the influence of regional inhomogeneity associated with large velocity anomalies and anomalies of the absorbing properties in the crust and upper mantle requires a well developed regional network of seismic stations. The procedure for distinguishing anomalies consists in averaging of data over areas, and calculating the corresponding background values and deviations from the background. These deviations in turn are averaged over smaller sections (local sections), which enables determination of the local background of the anomaly and deviations even from this background that are associated with still smaller inhomogeneities. The systematic deviations for each station depend on seismogeological peculiarities, i. e. inhomogeneity of the upper part of the profile close to the stations. The remaining fluctuations are caused by the minor inhomogeneity of the earth on the trajectories of rays from the sources to the seismic stations; they cannot be localized, and are described in statistical terms: the mean square of the fluctuations is determined, their law of distribution is studied and so on.

Possibilities of Using the Kinematic and Dynamic Characteristics of Waves for Studying the Structure of the Earth. The amplitudes and travel times are unequally sensitive to inhomogeneities of the earth. The travel time is a stable parameter that depends primarily on change in velocity with depth and the large-scale inhomogeneity of the medium. Minor inhomogeneities of the medium cause very small fluctuations in the travel times with little distortion of its characteristic features associated with the most appreciable elements of the structure of the earth. Therefore the kinematic characteristics of waves play a major role in the study of the principal large-scale features of the earth's structure.

The amplitudes of oscillations are a less stable characteristic that reacts sensitively to both large and comparatively small inhomogeneities. Therefore the amplitudes of oscillations are used as an auxiliary parameter in plotting velocity profiles. However, small inhomogeneity, turbidity, is revealed better by amplitudes than by the travel times of waves.

A detailed study of the space and time structure of the P-wave became possible comparatively recently: simultaneously with the deployment of dense networks of recording stations and seismic groups. At present we have only preliminary results on space and time organization of the longitudinal wave (Aki et al., 1976; Sedova, 1974).

In the general case the space-time structure of a P wave can be represented as follows:

$$P(S, t) = A(S)\,\varphi(S, t + \delta t),$$

where A(S) is the amplitude of the signal recorded on area S(X,Y); δ(S,t) is the pulse shape of the longitudinal wave normalized with respect to amplitude and registered at the instant corresponding to the hodograph t(S) and the travel time anomaly δt. Thus the variations of space-time organization of the P wave are associated with fluctuations of amplitude δA, travel time δt and pulse shape $\delta\phi$.

The spatial variability of shape ϕ is associated with distortion of the signal spectrum that can be expressed in terms of the spatial fluctuations of the spectral components of the signal. The spatial variation of the spectral components of the pulse of the P wave can be evaluated by using the coherence function. For instance if on some area S(X,Y) the waveshape ϕ(S,t) can be described by the spectral function Φ(S,ω), then the spatial coherence is determined by the expression

$$G(S_j, S_k, \omega) = k \bmod\left(\int_S \Phi(S, \omega)\, e^{i\omega(S_j - S_k)}\, dS\right),$$

where Φ(S,ω) is the spectral function of the P wave; k is a constant; S_j and S_k are the points of observation on the area S for which $\Phi(s,\omega) \neq 0$. By studying the spatial variability of coherence G we can get an idea of the nature of distribution of wave numbers in the investigated medium.

In practice it is more usual to estimate the coherence function of time realization of a process taken as a steady-state ergodic random process. If at points S_j and S_k we get realizations $f_j(t)$ and $f_k(t)$, then the estimate of their coherence function takes the form

$$G_{jk}^2(\omega) = |F_{jk}(\omega)^2|\,|F_j(\omega)\, F_k(\omega)|^{-1}, \qquad (*)$$

where $F_{jk}(\omega)$ is the mutual spectral density of realizations $f_j(t)$ and $f_k(t)$: $F_j(\omega)$ and $F_k(\omega)$ are the spectral densities of individual realizations.

Analysis of the known results of evaluation of the coherence of the P wave on groups and systems of stations (Capon et al., 1968; Hasegawa, 1970; Jansson, Husebye, 1968) shows that the coherence of the P wave on the average attenuates with an increase in the relative distance between points of registration. Simultaneously with this the coherence function undergoes appreciable spatial variations, probably associated with spatial inhomogeneities in the earth's interior.

There is a direct analogy between the estimate $G_{jk}(\omega)$ that is equal to the square root of the expression (*) and the estimate of the correlation ratio

$$K_{ij} = |\sigma_{ij}^2\,(\sigma_i^2\sigma_j^2)^{-1}|^{1/2},$$

where $\sigma_{i,j}^2$ is the mutual variance of the signals $f_i(t)$ and $f_j(t)$; σ_i^2 and σ_j^2 are the variances of the individual signals. Therefore in studying the spatial variability of the shape of the P wave, an estimate of the correlation ratio is frequently used.

Fisher's z-test is ordinarily used to check the accuracy of the correlation

$$Z = \frac{1}{2}\ln\left(\frac{1+K_{xy}}{1-K_{xy}}\right) = \operatorname{arcth} K_{xy}.$$

For $n > 20$, Z conforms approximately to normal distribution with average

$$m_z = \frac{1}{2}\ln\left(\frac{1+\kappa}{1-\kappa}\right)$$

and variance

$$\sigma_z^2 = 1/(n-3),$$

where κ is the correlation ratio, n is the sample space.

The confidence limits for κ are determined from the relation

$$-\lambda_\alpha < \sqrt{n-3}\,(Z - m_z) < \lambda_\alpha,$$

where λ_α is the quantile of normal distribution for confidence level α.

Thus the true correlation ratio with probability α will be in the interval

$$\kappa_1 < \kappa < \kappa_2,$$

where

$$\kappa_1 = \operatorname{th} Z - l;\ \kappa_2 = \operatorname{th} Z + l;\ l = \lambda_\alpha/\sqrt{n-3}.$$

In many instances simpler methods are used to estimate the reliability of the correlation ratio. In particular, it is convenient to use the estimate of the mean square error of the correlation ratio

$$\sigma_K = (1 - K^2)/\sqrt{n}.$$

In this case it can be approximately assumed that with probability 0.95 the random error will not exceed $2\sigma_K$, i. e.

$$\kappa = K \pm 2\sigma_K.$$

Besides, if the ratio $(K/\sigma_K) > 3$ when $n \geq 50$, it can be assumed that the sample correlation ratio is reliable and reflects the sought relation.

In our studies, wherever necessary, the reliability of the correlation ratio was evaluated in accordance with the rules we have described above. Shown in

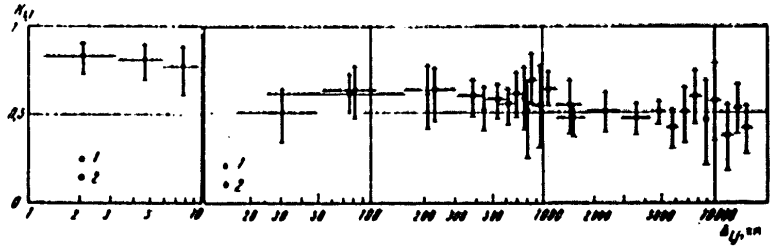

Fig. 5. Dependence of the correlation ratio of the shape of a P wave on distance between stations and epicenters of earthquakes for different regions of the world. 1--V. Din's data (1968); 2--data of B. Jansson and E. Husebye (1968); the horizontal lines represent averaging intervals: the vertical lines show the 70% confidence interval of the average values.

Fig. 5 are average estimates of the correlation ratio of the shape of the P wave as a function of the relative distance between recording stations found by V. Din (1965) on the Tonto-Forest group, and by B. Jansson and E. Husebye (1968) on stations of Fennoscandia and the WWSSN world-wide network.

Analysis of these data shows that a characteristic feature of the spatial correlation of the shape of the P wave is a tendency toward systematic attenuation with an increase in the relative distance between recording stations, and also the presence of comparatively sharp spikes and extinctions superimposed on the general pattern of the curve. The trend component of the function $K_{ij}(\Delta)$ asymptotically approaches the 0.5 level. The most clearly pronounced spikes and dips in the function $K_{ij}(\Delta)$ are confined to distance intervals of 40, 120, 1500, 2500, 5000, 8000 and 11,000 km.

To study the spatial structure of fluctuations of the parameters $\delta \lg A$, δt and $\delta\phi$ of the P wave, the structure function introduced by A. I. Kolmogorov (1941) is of great interest. Sometimes this is called an autostructure function. The structure function is understood as the mean square of the difference in values of the function x(r) separated by interval τ:

$$C(\tau) = \langle |X(r) - X(r+\tau)|^2 \rangle = (N-\tau)^{-1} \sum_{i=1}^{N-\tau} |X_i(r) - X_i(r+\tau)|^2.$$

If we take the deviation of the X(r) from the average rather than their actual values, then

$$C(\tau) = \langle |X'(r) - X'(r+\tau)|^2 \rangle,$$
$$X'(r) = X(r) - \langle X(r) \rangle, \; X'(r+\tau) = X(r+\tau) - \langle X(r) \rangle.$$

There is a definite relation between the structure function and the correlation ratio. As a matter of fact, from the preceding expression we get

$$C(\tau) = \langle |X'(r)|^2 \rangle - 2\langle X'(r) X'(r+\tau) \rangle + \langle |x'(r+\tau)|^2 \rangle.$$

Since $\langle |X'(r)|^2 \rangle = \langle |X'(r+\tau)|^2 \rangle = \sigma^2$, where σ^2 is the standard deviation, we have

$$C(\tau) = 2|\sigma^2 - K(\tau)|.$$

As $t \to \infty$, $K(\tau) \to 0$, whence $C(\infty) = 2\sigma^2$, and the normalized correlation ratio is

$$K'(\tau) = K(\tau)/\sigma^2 = 1 - C(\tau)/2\sigma^2. \qquad (**)$$

Formula (**) establishes a simple relation between the structure function and the correlation function: when $\tau = 0$, $C(\tau) = 0$, and $K'(\tau) = 1$; when $\tau \to \infty$, $C(\tau) = 2\sigma^2$ and $K'(\tau) \to 0$.

For the sake of convenience we arbitrarily denote the structure function of fluctuations $\delta \lg A$, δt, $\delta\phi$ by $\langle \delta\delta A^2 \rangle$, $\langle \delta\delta t^2 \rangle$, $\langle \delta\delta\phi^2 \rangle$. Fig. 6 shows the structure functions $\langle \delta\delta t^2 \rangle$ for fluctuations of travel time of the P wave, and

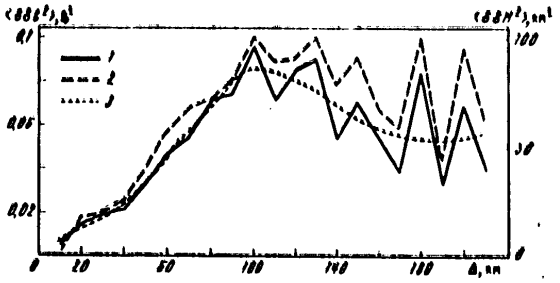

Fig. 6. Structure function of fluctuations in travel time and variations in thickness of the earth's crust for the territory of the LASA group in accordance with data of H. Iyer and J. Healy (1972). 1--variations in thickness of the earth's crust; 2--fluctuations of travel time; 3--smoothed structure function of variations in crust thickness

also the structure function $\langle \delta\delta H^2 \rangle$ for variations in thickness of the earth's crust δH according to data of the LASA group and 20 portable USGS stations (Iyer, Healy, 1972).

As can be seen, the structure function has an absolute maximum at a distance of 100 km and a series of relatively low extrema. If we consider the smoothed function $\langle \delta\delta H^2 \rangle$ we can see that the first maximum comes at a distance equal to 100 km, and the first minimum is close to 180-190 km. This indicates that in the change of crustal thickness in the territory of the LASA group a characteristic rhythm can be observed that has a period of the order of 180 km and accordingly a half-period of the order of 90 km. In addition, other characteristic rhythms are observed as well, but less pronounced, e. g. of the order of 35, 110 km, etc.

If we look at the structure function of fluctuations of travel time of the P wave, we can see that it is practically identical in shape to the function $\langle \delta\delta H^2 \rangle$. This indicates a direct genetic relation between fluctuations of travel time of the P wave and variations in the thickness of the earth's crust, and apparently the upper mantle.

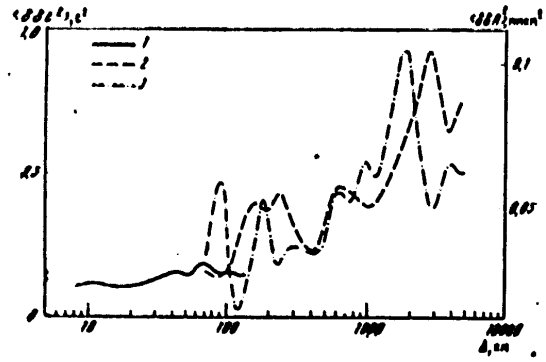

Fig. 7. Structure functions of fluctuations in travel time and logarithms of amplitudes of P waves for stations of the United States and Canada: 1--travel times from California stations (Robinson, Iyer, 1976); 2--travel times for U. S. and Canadian stations (Carder et al., 1966): 3--amplitudes from data of U. S. stations (Cleary, 1967)

Fig. 7 shows structure functions $\langle\delta\delta t^2\rangle$ and $\langle\delta\delta A^2\rangle$ according to the data of a system of seismic stations in the United States and Canada. The structure function $\langle\delta\delta t^2\rangle$ for relative distances of up to 150 km was obtained from data of a system of stations in California (Robinson, Iyer, 1976). Analysis of this structure function shows its considerable similarity to the structure function of the LASA group. At the same time some differences are observed; for instance the absolute maximum here comes at a distance equal to 70 km. In addition, relative maxima are observed here at distances of about 10 and 45 km, and relative minima -- close to 20 and 55 km. These facts show the appreciable difference of the structure of the core and mantle within the limits of the central and extreme western part of the United States.

The structure functions $\langle\delta\delta t^2\rangle$ and $\langle\delta\delta A^2\rangle$ within the limits of distances from 70 to 4500 km (see Fig. 7) are plotted from the data of a system of seismic stations in the United States and Canada (Carder et al., 1966; Cleary, 1967). Analysis of the structure function of fluctuations in the travel time of the P wave shows that the mean square of the second differences $\langle\delta\delta t^2\rangle$ systematically increases with an increase in the relative distances between seismic stations. In fact, for distances between recording points of less than 100 km the mean square $\langle\delta\delta t^2\rangle$ does not exceed 0.2 of a log unit, while for $\Delta = 4{,}000$-$4{,}500$ km the mean square is equal to aproximately 0.7-0.8 log unit. The behavior of the structure function $\langle\delta\delta t^2\rangle$ shows relative minima and maxima that show the presence of characteristic scales of fluctuations in the travel time of the P wave. The presence of maxima and minima of the mean square of fluctuations in the time of arrival of the P wave, just as in the case of the LASA group, show the probable presence of characteristic scales of inhomogeneities in the structure of the earth's crust and mantle. Minima in the structure function are observed at distances of the order of 80-90, 200, 400, 1000 and 4000 km.

An examination of the structure function of fluctuations in the logarithm of amplitude $\langle\delta\delta A^2\rangle$ shows its considerable similarity to the structure function of fluctuations in the time of arrival of the P wave. It is worth noting that fluctuations of the parameters $\delta \lg A$ and δt were obtained on the same system of recording stations. At the same time, the systems of seismic sources were different: the deviations of $\delta \lg A$ were found from earthquakes, while the deviations of δt were found from underground nuclear explosions. In contrast to $\langle\delta\delta t^2\rangle$ the structure function $\langle\delta\delta A^2\rangle$ has an inherent somewhat greater expressiveness of shape. Besides, it is evident that the structure function of fluctuations in amplitude contains "phase-wise" the structure function of fluctuations in time of arrival of the P wave so that the maxima of the mean square of the fluctuations in the logarithm of the amplitude as a rule have corresponding minima of the mean square of the time fluctuations.

The reason for the observed peculiarities of structure functions of fluctuations in travel time and logarithm of the amplitude of the P wave can be seen if we compare the velocity profiles of the crust and upper mantle for the territory of the United States and Canada. Shown on Fig. 8 are the

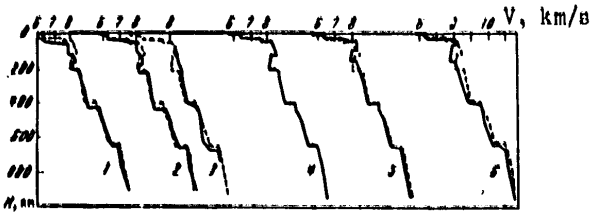

Fig. 8. Velocity profiles of longitudinal waves for a number of territories of North America. The WCB profile (broken line) is taken as the reference: 1--HWA profile for southwest territories of the United States; 2--HWB profile for northwest territories of the United States; 3---VIC-3 profile for southeast territories of Canada; 5--WCA profile for coastal territories of western Canada; 6--WCC profile for northwest territories of Canada

velocity profiles of longitudinal waves found by R. Wiggins and D. Helmberger (1973), by G. McMechan (1975) and also by S. Dey-Sarkar and R. Wiggins (1976).

An examination of relative differences in the velocity profiles of the crust and mantle of different territories of North America convinces us that the observed fluctuations in travel time and amplitudes of the longitudinal wave are engendered by horizontal inhomogeneities that contrast most highly near the principal divisions in the crust and upper mantle.

Horizontal inhomogeneity is apparently inherent in the deeper interior of the earth as well. Shown on Fig. 9 is the structure function of fluctuations $\langle \delta\delta t^2 \rangle$, s^2

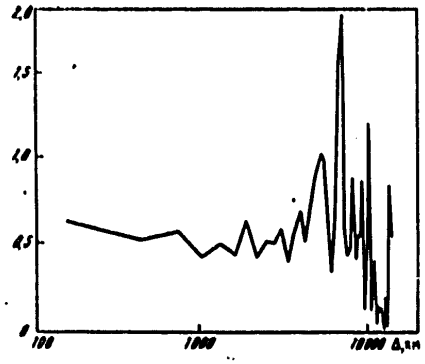

Fig. 9. Structure function of fluctuations in travel time of a PcP wave calculated from data of the LONG-SHOT underground nuclear explosion (Herrin, 1968)

in travel time of a PcP wave plotted from data of registration of the LONG-SHOT underground nuclear explosion reduced to the well known summary of E. Herrin et al. (1968).

The mean square of fluctuations in travel time for a PcP wave depends quite uniquely on distances between seismic stations. For a relative distance equal to approximately 100-200 km the mean square of time fluctuations

reaches 0.6 s^2 on the average. With an increase in distance to 3000-3500 km, the mean square of the fluctuations decreases to 0.45-0.5 s^2. With a further increase in relative distance, $\langle \delta\delta t^2 \rangle$ increases rapidly, and at a distance equal to approximately 7000 km it reaches a value of 1.85-1.9 s^2. With an increase in distance to 8000-9000 km, the mean square decreases to 0.5-0.55 s^2, and further, by 12,000-13,000 km it becomes equal to 0.05-0.1, i. e. it falls almost to zero.

The uniqueness of the structure function of fluctuations in travel time of the PcP wave consists in the nature of its oscillations. Actually, the most pronounced spikes in the mean square of fluctuations are confined to distances that are multiples of the radius of the outer core ($R_1 = 3486 \pm 3$ km); an absolute maximum is observed at a distance equal to $2R_1$; the second and third maxima with respect to magnitude are observed at distances of $3R_1$ and $4R_1$ respectively. In addition, the observed minimum in the mean square of the fluctuations is confined to a distance equal to half the length of the circumference of the outer core.

A comparison of structure functions $\langle \delta\delta t^2 \rangle$ for P and PcP waves convinces us that they reflect essentially different elements in the inhomogeneous structure of the earth. A confirmation of this conclusion can be found if we examine materials on the amplitudes of P and PKP waves of 11 stations of the Comprehensive Seismological Expedition that were used to plot calibration curves to be discussed in the next chapter, and also the azimuthal amplitude curves of the P wave plotted from data of the SK channel of a group of stations situated in the Northern Tyan'-Shan'.

From data of measurements of more than 50,000 recordings of P and PKP waves by short-period channels, individual stationary calibration curves and a summary calibration curve were plotted. Graphs were plotted for each station for the way that the absolute value of the deviation $\delta \lg A$ depends on epicentral distance, which were then averaged (Fig. 10). Thus, corresponding to

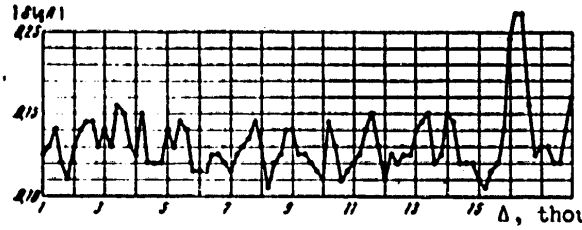

Fig. 10. Absolute value of deviation of the logarithm of amplitude of P and PKP waves as a function of epicentral distance from data of 11 stations of the Comprehensive Seismological Expedition

each value of Δ on the main graph is a broad set of stations and epicentral regions. Therefore the fluctuations in the graph of $\delta \lg A$ characterize the inhomogeneity of the earth's structure on the average, irrespective of any specific region.

We can see from Fig. 10 that at epicentral distances of 1,000-15,800 km the average deviation of amplitude at an arbitrary station for arbitrary earth tremors is equal to about 0.13 log unit. The greatest differences between individual calibration functions are observed at epicentral distances of 3400-3600, 4200, 11,600, 13,400, 14,000, 15,900 and 16,600 km. Minimum differences are confined to distances of 1800, 8200, 10,000, 10,600, 12,000, and 15,000-15,300 km.

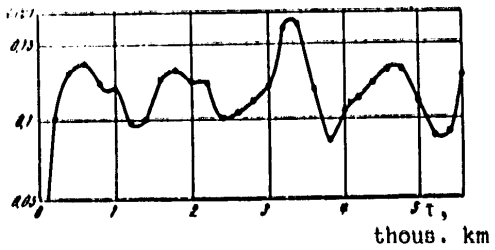

Fig. 11. Structure function of fluctuations in the logarithm of the amplitude of P and PKP waves from data of 11 stations of the Comprehensive Seismological Expedition

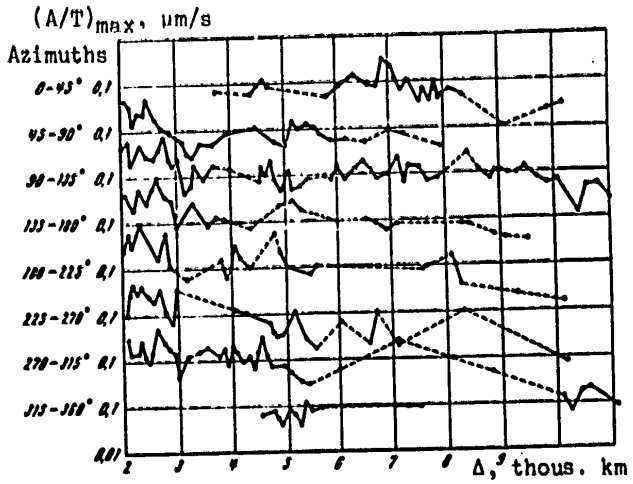

Fig. 12. $(A/T)_{max}$ as a function of distance for longitudinal waves with respect to different azimuths. Data obtained from the network of stations of Northern Tyan'-Shan' by SK equipment.

Shown on Fig. 11 is the structure function found from data on $|\delta \lg A|$ (see Fig. 10). One can see that the mean square of the fluctuations of the logarithm of the amplitude has minimum values with displacement in the epicentral distance equal to 1300, 2400, 3800 and 5300 km, and vice versa, the maximum values are observed at displacements of 600, 1800, 3300 and 4700 km.

Fig. 12 shows the azimuthal amplitude curves of $(A/T)_{max}$ obtained from data of the SK channel of the group of stations in the Northern Tyan'-Shan'. Analysis of these data shows that the individual amplitude curves have considerable deviations from the average trend. A number of peculiarities

indicate that in the area of location of the stations the isotach surfaces of divisions in the crust and upper mantle experience a considerable slope in the direction with azimuth of 180-225°. This question is examined in more detail in the third part of the monograph with interpretation of materials obtained on the Pamir-Baykal seismic profile.

Chapter 2. Using Regional Calibration Curves to Improve Magnitude Determinations

1. Regional calibration curves of waves propagating in the crust and mantle of the earth

Estimation of the magnitude of earthquakes is subject to rather wide variance as a consequence of the effect of factors of the focus, path of propagation and the relative location of the station and the source, as well as deviation of the characteristics of the reception equipment from standard. Numerous studies have been aimed at finding methods to compensate for the action of specific mechanisms of fluctuations in magnitude.

In the first approximation, formation of the wave process can be described by the following linear system:

$$A(\omega) = A_0(\omega, \theta, \Phi)\, A_1(\omega, \Delta) A_2(\omega), \qquad (*)$$

where $A(\omega)$ is the spectral amplitude of the wave recording, A_0 is the spectral function of the source, A_1 is the transfer function of the medium in the vicinity of the source, the receiver, and on the path of wave propagation; A_2 is the transfer function of the receiver.

In practice, seismic services estimate magnitude according to the following scheme:

$$M = \lg(A/T) + Q_M(\Delta).$$

Here $Q_M(\Delta)$ is an empirical function of damping. In accordance with (*)

$$\lg A(\omega) = \lg A_0 + (\lg A_1 + \lg A_2). \qquad (**)$$

where $\lg A_0$ in principle corresponds to the estimated value of M, so that the function $Q_M(\Delta)$ is determined by the sum of the factors in parentheses in expression (**) and has the purpose of compensating for their action. The function $Q_M(\Delta)$ has come to be called the calibration function.

There are two methods of plotting calibration curves: the first is to plot individual calibration curves for each separate wave, and the second is to plot a unified calibration curve for the maximum value of A/T regardless of which group of waves of the given type this maximum belongs to. The first method requires identification of individual phases since each wave uses its own calibration curve. Incorrect identification of waves is an additional source of errors.

Erroneous identification of waves is associated not only with insufficient skill of the analyst, but also with such objective factors as fluctuations

in travel times, losses of first entries in the case of weak signals, a large number of waves with close travel times including some waves that are unstable in space that have a nature about which we are still uncertain. The use of a system of calibration curves with respect to each type of waves, e. g. with respect to many Pn phases can ensure higher accuracy only under condition that the system of magnitude corrections is known with respect to each group of waves for each station relative to each epicentral region. In the final analysis, such a system of calibration functions will be extremely sensitive and unstable. The integrated amplitude curve $(A/T)_{max}$ is more stable, particularly in regions of wave change, where a complicated interference pattern is observed. Therefore calibration curves plotted by the second method, despite a number of simplifications, frequently ensure higher accuracy. At the same time, the reliability of calibration can be improved by using integrated calibration curves of other types of waves such as Pg, Lg, Sn, etc.

The most extensively used have been magnitude scales plotted for surface and longitudinal waves. Scales in which surface waves are used will be designated by the symbol M in the following presentation, while those in which body waves are used will be denoted by the symbol m. For longitudinal waves, scales have been developed with the use of both a vertical component (we will denote the vertical component by the subscript V) and a horizontal (H) component. Determination of magnitude from surface waves is based on the total horizontal displacement vector. Calibration of earthquakes with respect to other types of waves has not been extensively practiced. Magnitude scales of both types have numerous modifications, depending on the equipment used and the measurement technique.

Analysis of station discrepancies in evaluation of magnitudes has shown that sometimes even the very determination of magnitude leaves room for subjective evaluation of experimental material. For instance in determining the maximum values of A/T on two horizontal components, synchronism is violated (Aranovich et al., 1966).

Our studies have shown that using only a single component does not reduce the convergence of magnitude estimates, and at the same time simplifies the measurement procedure, considerably weakening the role of the subjective factor. In this connection, when plotting calibration functions for longitudinal waves and Rayleigh waves we used the vertical component, and for transverse waves -- the component on which the value of A/T is maximum. This is usually one of the horizontal components.

The convergence of magnitude estimates with respect to body waves depends to a large extent on the method of measurement, and first of all on the choice of the time interval used for the magnitude estimates. A careful analysis of this assumption was made with respect to earthquake recordings on seismic stations of Talgar, Frunze and elsewhere on standard SK, SKD-0 and SKM-3M equipment. It was established that more than 95% of earthquakes with magnitude M exceeding 7.5 have maximum values of the ratio A/T in the longitudinal wave within the first 20 s of the recording, and in only 55% is the maximum A/T recorded in the first 5 s.

Apparently one of the principal reasons that the NOS service of the United States consistently understates estimates of earthquake magnitudes from PV wave data as compared with the YeSSN service of the USSR is that a short interval of measurements is used for the maximum value of the A/T ratio.

Besides, it should be borne in mind that for strong earthquakes with magnitude $M \geq 7.5$ the maximum value of A/T in a PV wave may be delayed relative to the first entry by 60 s or more. Let us note that analogous results were found by K. K. Zapol'skiy (Zapol'skiy, 1971; Zapol'skiy et al., 1974) with respect to data of analysis of frequency-time fields.

In plotting calibration curves from longitudinal waves which are shown below, the maximum value of A/T was sought and measured in a 20-second interval for earthquakes with $M < 7.5$, and in an interval with duration of 60 s for earthquakes with $M \geq 7.5$.

Quite appreciable blunders leading to systematic errors of the order of 0.1-0.15 unit of magnitude can arise as a consequence of imperfect methods of finding and measuring the actual maximum ratio A/T. For instance in a number of cases the quantity A_{max}/T is used instead of $(A/T)_{max}$. It is appropriate to mention here that B. Gutenberg's magnitude classification (1963) was based on the maximum ratio $(A/T)_{max}$.

Experience has shown that the best estimate of $(A/T)_{max}$ is given by the amplitude A measured from the zero line of the recording, and the corresponding half-period T/2.

In plotting the calibration curves we used recordings of seismic stations at Alma-Ata, Shchel'-Dal'nyaya, Talgar, Rybach'ye, Kadzhi-Say, Przheval'sk and Frunze for earthquakes with normal depth of focus. These stations are equipped with sets of standard equipment SK (SKD-0) and SKM-3M that have fairly similar amplitude-frequency responses. Constant magnification is observed in the range of periods from 0.3 to 10 (15) s for the SK (SKD-0) channels, and from 0.1-1.2 s for the SKM-3M channels. With increasing periods the amplitude-frequency responses fall off as the third power.

To improve the convergence of the calibration curves during plotting, the well known method of B. Gutenberg was used that consists in tying the calibration curve of a body wave in with data of the calibration curve of surface waves. In doing this it is important that the step of the new scale be constant, and that the curves be parallel in different ranges of magnitudes of the reference scale with respect to surface waves.

This coordination of calibration curves was done for all the wave types indicated above. To do this, individual $(A/T)_{max}$ curves were plotted as a function of the epicentral distance for six levels of the scale of magnitudes M_{LH} of the YeSSN service: 3, 4, 5, 6, 7 and 8. For each wave type, about 1500 earthquake recordings were used in the distance range from 200 to 11,000 km, and a range of magnitudes M_{LH} from 3 to 8. The data on the M_{LH} were

taken from the bulletin of the YeSSN service and spot checked with respect to recordings of the stations at Frunze, Alma-Ata and Przheval'sk.

It was found that earthquakes with $M_{LH} = 3$ are representative for distances up to 400 km, with $M_{LH} = 4$ up to 1800 km, with $M_{LH} = 5$ up to 6000 km, earthquakes with $M_{LH} = 6$ are representative for the entire distance range, with $M_{LH} = 7$ from 1500 to 11,000 km and with $M_{LH} = 8$ for distances greater than 5000 km.

In averaging experimental data of $\lg(A/T)_{LH}$ the step with respect to distance was usually equal to 200 km. The averaging curves were plotted within confidence intervals estimated from the formula

$$q_i = \sigma_i t_{(p,k)} / \sqrt{n_i - 1},$$

where the q_i are confidence limits for the true value of Q_M in the i-th epicentral distance interval; the σ_i is the corresponding value of the mean square deviation; n_i is the number of data of $\lg(A/T)_{max}$; $t_{(p,k)}$ is the Student test for a confidence coefficient of $p = 0.68$ and number of degrees of freedom $k = n_i - 1$.

The mean square deviation σ_i was estimated by a simplified method. Since the distribution law for the quantity $\lg(A/T)_{max}$ is close to normal, the mean square value in the i-th distance interval was estimated on the graph from the width of the 68% interval of values of $\lg(A/T)_{max}$. A check of estimates of σ_i by the formula

$$\sigma_i = \sqrt{\sum_{i=1} [(A/T)_{ii} - (\overline{A/T})_k]^2 / (n_i - 1)}$$

showed that when $n \geq 10$ the discrepancy in the estimates does not exceed 10-15%. The calibration curves found in this way are shown on Fig. 13.

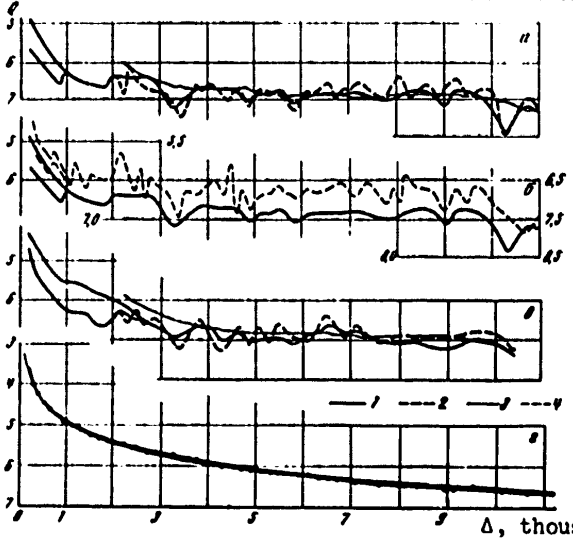

Fig. 13. Calibration curves for longitudinal (*а*, *б*), transverse (*в*) and surface (*г*) waves: 1--from data of Northern Tyan'-Shan' stations, SK equipment; 2--from data of the Talgar station, SK equipment; 3--YeSSN summary curves; 4--from data of Northern Tyan'-Shan' stations, SKM-3 equipment; axis of ordinates marked off to the right (*б*).

Analysis of the results shows that curves for $\lg(A/T)_{max}$ as a function of epicentral distance for a Rayleigh wave are parallel to each other practically throughout the range of epicentral distances. The step between curves is constant, does not depend on the range of magnitudes of the reference scale of M_{LH}, and practically coincides with the step of the M_{LH} scale. The relative level of the calibration curve of the R wave is such that on the average it satisfies the relation

$$\lg (A/T)_{LH}' - \lg (A/T)_R = 0{,}1.$$

Thus we can take as fully justified the calibration of earthquakes with respect to a Rayleigh wave with the use of the known calibration curve for M_{LH} for medium-period SK (SKD-0) equipment.

The calibration curve for a Rayleigh wave found over the network of Northern Tyan'-Shan' stations is shown in Fig. 13*a*. Also shown here for comparison is the M_{LH} calibration curve of the YeSSN service.

An examination of the calibration curve shows that in the distance interval of 200-2000 km its level falls off on the average as $\Delta^{-1/6}$. In this connection the exponent may vary from -1.52 to -1.66. At greater distances, the curve falls in accordance with a law of $\Delta^{-1.66}$. In the case of a spherically symmetric model of the earth and isotropic radiation of the seismic source, the amplitude of the Airy phase of the surface wave can be described by the expression

$$A = k\Delta^{-1/2} (\sin \Delta)^{-1/2} \exp (-\gamma\Delta), \qquad (***)$$

where k is a constant, $\gamma = \pi(VTQ)^{-1}$ is the attenuation factor, V is group velocity, T is the period and Q is the quality factor of the medium.

In matching the theoretical amplitude curve according to (***), the best agreement with experimental data is obtained when $\gamma = 0.025$ (deg)$^{-1}$. At a group velocity V = 3 km/s and period T = 9-16 s (Ruzaykin, Khalturin, 1974) this corresponds to a Q of about 300-500, which agrees with known data on surface waves (Smit, 1975).

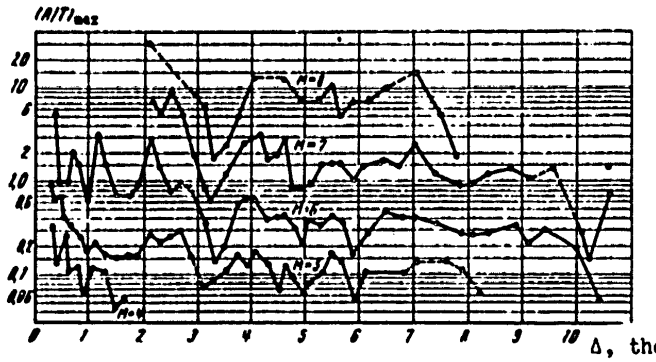

Fig. 14. Family of curves of change in $(A/T)_{max}$ in a P_V wave with distance for five values of M_{LH} (SK equipment); the white circles are averages, and black circles are isolated values.

TABLE 1

Average values of coefficient b in regression $m = bM_{LH} + a$

Distance ranges, km	Magnitude M_{LH}			
	4-5	5-6	6-7	7-8
200-2,000	0.39	0.68	—	—
2,000-5,000	—	0.58	0.64	0.66
5,000-7,000	—	0.50	0.62	0.72
7,000-10,000	—	—	0.60	—

Analysis of calibration curves of longitudinal P_Y waves obtained on medium-period equipment SK (Fig. 14) shows that in general the parallelism of the $(A/T)_{max}$ curves for different amplitude intervals is not violated. The average values of the step between these curves or the regression coefficient in the equation $m = bM_{LH} + a$ for different distance ranges are summarized in Table 1.

The data of Table 1 show that only for the amplitude range $M_{LH} = 4\text{-}5$ and the distance range of 200-2,000 km is the regression coefficient appreciably different from the average value of 0.63 found without consideration of this anomalously low value. A scale step equal to 0.63 was obtained by B. Gutenberg (1963) in a world-wide summary. At the same time, including the estimate of the coefficient b for $M_{LH} = 4\text{-}5$ in the average reduces the scale step to 0.57. This value in turn is close to the estimate recommended by the Committee on Earthquake Magnitudes at Zurich on 3 October 1976.

It is suggested that two branches of the calibration curve be used for calibrating earthquakes on distances up to 1000 km: one with respect to Pn waves, and the other with respect to Pg waves. This will appreciably expand the dynamic range of calibration on such distances.

For comparison with the calibration curve of the North Tyan'-Shan' group of stations in Fig. 13*a*, calibration curves of the YeSSN service are presented (shown by the light line) and the Talgar station for the SK channel (broken line). Note that the calibration curve of the YeSSN service is extremely smoothed out and cannot account for regional peculiarities that are rather well differentiated on the North Tyan'-Shan' data.

Fig. 13*б* juxtaposes calibration curves with respect to longitudinal waves obtained on North Tyan'-Shan' stations on two types of equipment: medium-period (solid line) and short-period (broken line). It is clear that the calibration curve obtained from data of the SKM-3M channel is considerably complicated by fine details. At the same time, it clearly shows the major elements of the calibration curve for the medium-period equipment SK (SKD-0). Taking the detail of the SKM-3M curve as excessive and noting that it is an average of 0.3 log unit away from the SK curve, we can recommend the calibration curve for the SK channel with a correction of 0.3 for calibrating earthquakes from data of the SKM-3M channel.

Fig. 13a shows calibration curves for S and Lg waves. In plotting them as a function of the value of M_{LH} an identical scale step is obtained that is equal to 0.60 log unit. However, wave damping in the distance range from 200 to 2500 km differs appreciably. For the Sn(S) wave, damping on the average takes place according to the law $\Delta^{-1.8}$. For Lg waves this law takes the form $\Delta^{-1.6}$, which agrees on the average with damping of the Rayleigh wave, as was shown above.

It is interesting that attenuation of the Lg wave differs somewhat for distances $\Delta > 1000$ and $\Delta < 1000$ km. In fact, if expression (***) is used to approximate the amplitude curve of the Lg wave, assuming that it is related to higher modes of surface waves propagating with minimum group velocity, then the best agreement of the theoretical curve with experimental data is observed for $\gamma = 0.20$ when $\Delta < 1000$, and $\gamma = 0.13$ when $\Delta > 1000$ km. Taking into consideration that T is approximately 3 s, V = 3.57 km/s for $\Delta < 1000$ km and V = 3.65 km/s for $\Delta > 1000$ km, we get for the first case a Q of approximately 160, and for the second case a Q of approximately 250. Such a simplified estimate allows us to assume that the Lg wave recorded at distances $\Delta > 1000$ km propagates in a relatively high-Q medium.

TABLE 2.

Values of calibration functions $Q_M(\Delta)$ for longitudinal Pg and P_V waves from from shallow (H < 60 km) earthquakes

Δ, км	Pg	Pv	Δ, км	Pv	Δ, км	Pv	Δ, км	Pv
200	4,85	5,05	3300	7,18	6400	6,90	9500	6,86
300	5,14	5,80	3400	7,08	6500	6,90	9600	6,89
400	5,36	5,94	3500	6,98	6600	6,90	9700	6,92
500	5,54	6,06	3600	6,88	6700	6,90	9800	6,98
600	5,70	6,18	3700	6,78	6800	6,90	9900	7,06
700	5,87	6,32	3800	6,70	6900	6,90	10000	7,20
800	6,00	6,44	3900	6,70	7000	6,84	10100	7,41
900	6,10	6,45	4000	6,70	7100	6,84	10200	7,64
1000	6,22	6,22	4100	6,70	7200	6,84	10300	7,86
1100	—	6,32	4200	6,70	7300	6,86	10400	7,74
1200	—	6,42	4300	6,70	7400	6,90	10500	7,58
1300	—	6,46	4400	6,70	7500	6,96	10600	7,40
1400	—	6,50	4500	6,70	7600	7,01	10700	7,28
1500	—	6,53	4600	6,70	7700	7,02	10800	7,29
1600	—	6,55	4700	6,82	7800	7,02	10900	7,30
1700	—	6,59	4800	6,92	7900	7,02	11000	7,35
1800	—	6,63	4900	7,05	8000	6,98		
1900	—	6,63	5000	6,97	8100	6,90		
2000	—	6,40	5100	6,86	8200	6,88		
2100	—	6,36	5200	6,85	8300	6,85		
2200	—	6,39	5300	6,85	8400	6,82		
2300	—	6,40	5400	6,85	8500	6,80		
2400	—	6,41	5500	6,78	8600	6,82		
2500	—	6,42	5600	6,77	8700	6,85		
2600	—	6,40	5700	6,90	8800	6,90		
2700	—	6,38	5800	7,02	8900	7,01		
2800	—	6,42	5900	7,08	9000	7,14		
2900	—	6,57	6000	7,00	9100	7,12		
3000	—	6,70	6100	6,94	9200	6,88		
3100	—	6,90	6200	6,90	9300	6,82		
3200	—	7,08	6300	6,90	9400	6,83		

TABLE 3

Calibration functions $Q_M(\Delta)$ for transverse Sn and S waves and Lg waves of shallow earthquakes from measurements of $(A/T)_{max}$ on the single most intense component

Δ, km	Lg	Sn	Δ, km	S	Δ, km	S	Δ, km	S
200	4,34	4,80	3200	6,87	6200	6,82	9200	7,16
300	4,57	5,20	3300	6,92	6300	6,80	9300	7,10
400	4,78	5,40	3400	6,86	6400	6,76	9400	7,03
500	4,96	5,58	3500	6,82	6500	6,66	9500	7,00
600	5,15	5,73	3600	6,75	6600	6,61	9600	7,00
700	5,30	5,86	3700	6,68	6700	6,69	9700	7,02
800	5,42	6,00	3800	6,64	6800	6,77	9800	7,06
900	5,50	6,14	3900	6,64	6900	6,81	9900	7,09
1000	5,55	6,23	4000	6,70	7000	6,80	10000	7,13
1100	5,55	6,26	4100	6,73	7100	6,76	10100	7,18
1200	5,56	6,30	4200	6,86	7200	6,78	10200	7,25
1300	5,60	6,31	4300	7,00	7300	6,83	10300	7,33
1400	5,67	6,31	4400	6,96	7400	6,93	10400	7,42
1500	5,73	6,40	4500	6,86	7500	6,97	10500	7,52
1600	5,80	6,54	4600	6,78	7600	7,02		
1700	5,86	6,62	4700	6,82	7700	7,04		
1800	5,90	6,62	4800	6,95	7800	7,07		
1900	5,94	6,60	4900	7,02	7900	7,10		
2000	6,00	6,48	5000	7,00	8000	7,10		
2100	6,05	6,30	5100	6,96	8100	7,08		
2200	6,12	6,29	5200	6,95	8200	7,07		
2300	6,20	6,38	5300	6,95	8300	7,06		
2400	6,28	6,44	5400	6,93	8400	7,07		
2500	6,38	6,48	5500	6,92	8500	7,11		
2600	6,50	6,53	5600	6,94	8600	7,16		
2700	—	6,56	5700	7,03	8700	7,19		
2800	—	6,60	5800	7,08	8800	7,21		
2900	—	6,64	5900	7,02	8900	7,22		
3000	—	6,70	6000	6,94	9000	7,22		
3100	—	6,77	6100	6,87	9100	7,22		

In comparing the morphological peculiarities of calibration curves for longitudinal and transver waves given in Fig. 13*a* and *e* one can note a considerable similarity of both average tendencies and a number of details, such as agreement of the minima of curves in the vicinity of 3300, 4300, 4900, 5800 and 9000 km, and of the maxima in the vicinity of 4000, 5600, 6600 and 9600 km. At the same time, there are some discrepancies in the behavior of the curves at distances of from 1000 to 3000 km. This may serve as an indirect indication of asymmetry of the elastic profile of the earth with respect to longitudinal and transverse waves.

In comparing the calibration curve for S waves obtained on stations of the Northern Tyan'-Shan' with the SH curve used in the YeSSN service (Vanek et al., 1962) we are convinced that the use of the regional calibration curve will improve the convergence of amplitude calibration with respect to transverse waves on the whole.

Table 2 gives the values of calibration functions $Q_M(\Delta)$ for longitudinal Py and Pg waves from shallow earthquakes obtained from stations of the Northern Tyan'-Shan', and Table 3 gives these functions for transverse waves and Lg waves obtained on the North Tyan'-Shan' station group.

It should be noted that in recent years there has been considerable interest in using a series of seismic waves for calibrating purposes that have not been traditionally used in amplitude calibration (Bacer, 1967; Evernden, 1967; Nuttli, 1972; Street, 1976; Zoltan et al., 1975). It is to be hoped that the calibration functions found in our work for a series of body and surface waves will help to expand the possibilities of calibrating seismic sources and considerably improve the reliability of magnitude determinations.

2. Calibration curves of waves that have passed through the core

PKP waves have not been widely used as yet in magnitude classification of earthquakes. At the same time, the use of waves of this type would enable us to include processing of data for earthquakes more than 12,000 km away.

The analysis done in the preceding chapter showed that differentiation of some branches of PKP waves is very uncertain, and therefore the construction of magnitude calibration curves should be done with respect to two groups of waves. In one group we have included the clearly differentiated AB branch (PKP_2), and in the other -- the DF and GH branches considered together. We will use the convention of designating the aggregate of these two groups of branches as the PKP_1 group.

In constructing the magnitude scale it is necessary to solve the following problems:

1) proving the validity of the basic principle of construction of magnitude scales -- parallelism of amplitude curves for earthquakes of different energies;

2) evaluating the relation between the given scale and known scales that have been plotted with respect to other types of waves.

The time intervals in which the amplitudes of seismic waves were measured were chosen in accordance with the plotted hodograph.

On the section up to 15,000 km the maxima of the PKP waves lie no further than 10 s beyond the first entry. On the 15,000-16,000 km section where waves of the GH branch can sometimes be seen in the first entries, to avoid errors the interval of measurements was increased to 15 s after the first entry regardless of which branch these entries belong to. Beyond the zone of interference, the interval of measurements in the first group of waves (the DF and GH branches) is bounded by the instant of entry of the PKP_2 (AB) branch.

For the PKP_2 branch, the time interval in which amplitude maxima is observed is somewhat greater than for waves of the first group, and averages 20 s after the first entry of the PKP_2 group.

Data processing was done separately for the two differentiated groups. The A/T values were reduced to the level of $m_b = 5.5$, and were then averaged in

hundred-kilometer intervals of epicentral distance. The resultant curve was the basis for a calibration curve in units of the U. S. magnitude scale. To check satisfaction of the basic principles of construction of magnitude scales, a comparison was made of the deviations of the reduced A/T values from the average curve on the one hand, and the magnitudes of the corresponding shocks on the other hand. Such comparisons were made in different ranges of epicentral distances. No relation was observed between A/T deviations and magnitude or epicentral distance.

The measurements were made on seismograms obtained on standard channels. The materials were processed in such a way that the level of the amplitude curves corresponded to a magnitude evaluation of 5.5 in m_b scale units. To reduce the calibration curves plotted from type PKP waves in accordance with the m_{PV}^{SKM} scale, an empirical curve relating the m_b and m_{PV}^{SKM} scales was used (Fig. 15). Let us note that close to the value $m_b = 5.5$, scaling of

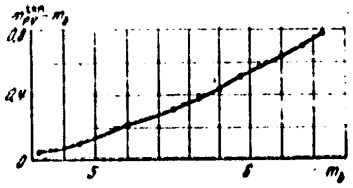

Fig. 15. Relation between the m_b (United States) and m_{PV}^{SKM} (Comprehensive Seismological Expedition) magnitude scales

the magnitudes to convert from one scale to the other takes place with minimum errors since the formulas obtained by different authors close to the value $m_b = 5.5$ yield practically identical results.

Besides, for earthquakes with normal focus depth we had magnitude estimates in units of the M_{LH} scale (about 50 cases). These estimates were also converted according to known formulas (Antonova et al., 1968; "Magnitude and Energy Classification of Earthquakes" 1974) to units of the M_{PV}^{SKM} scale.

For some earthquakes, our station network simultaneously recorded waves of the P and PKP types (about 40 cases). This enabled a direct comparison of the A/T values for PKP waves with m_{PV}^{SKM} magnitude estimates.

The differences in the calibration curve tie-in level found by the three methods did not exceed 0.1 magnitude unit. Estimates according to the constructed magnitude scales that we will designate $m_{PKP_1}^{SKM}$ and $m_{PKP_2}^{SKM}$ coincide on the average with the m_{PV}^{SKM} scale.

The accuracy of separate determination of magnitude by scales for PKP waves is approximately the same as for P waves. Increased regional variability of magnitude deviations is observed only close to the minimum of the calibration function. This error can be eliminated by introducing regional magnitude corrections. The calibration function is given in Tables 4 and 5 and on Fig. 16, where data from reference sources are shown for comparison.

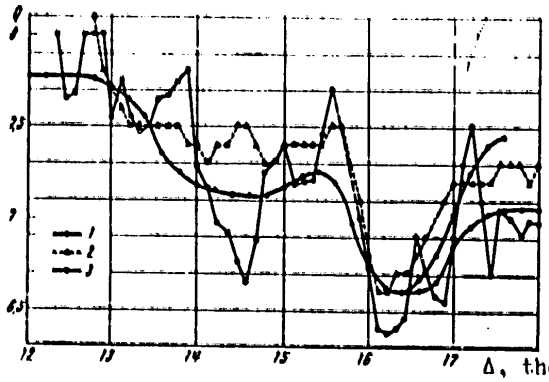

Fig. 16. Calibration curves for PKP waves: 1--according to data of the Comprehensive Seismological Expedition; the upper branch corresponds to the PKP_1 group, the lower -- to PKP_2; 2--according to data of I. V. Gorbunova and N. V. Shatornaya (1976); 3--according to data of S. Miyamura (1974)

TABLE 4

Magnitude calibration curve for PKP_1 waves

Δ, thous. km*	Q_M	Δ, thous. km*	Q_M	Δ, thous. km*	Q_M
12,0	7,80	13,9	7,20	15,8	7,00
12,1	7,80	14,0	7,20	15,9	6,80
12,2	7,80	14,1	7,15	16,0	6,75
12,3	7,80	14,2	7,15	16,1	6,70
12,4	7,80	14,3	7,15	16,2	6,80
12,5	7,80	14,4	7,10	16,3	6,80
12,6	7,80	14,5	7,10	16,4	6,80
12,7	7,75	14,6	7,10	16,5	6,80
12,8	7,75	14,7	7,10	16,6	6,85
12,9	7,75	14,8	7,10	16,7	6,70
13,0	7,70	14,9	7,15	16,8	6,80
13,1	7,70	15,0	7,20	16,9	6,90
13,2	7,65	15,1	7,20	17,0	7,0
13,3	7,60	15,2	7,25	17,1	7,15
13,4	7,55	15,3	7,25	17,2	7,25
13,5	7,45	15,4	7,25	17,3	7,35
13,6	7,35	15,5	7,25	17,4	7,40
13,7	7,30	15,6	7,20	17,5	7,45
13,8	7,25	15,7	7,10	17,6	7,45

*Δ, thous. km

TABLE 5

Calibration function Q_M for PKP_2 waves

*Δ, thous. km	Q_M	*Δ, thous. km	Q_M	*Δ, thous. km	Q_M
16,5	6,6	17,0	6,85	17,5	7,05
16,6	6,6	17,1	6,90	17,6	7,05
16,7	6,6	17,2	6,95	17,7	7,05
16,8	6,65	17,3	7,00	17,8	7,05
16,9	6,75	17,4	7,00	17,9	7,05
				18,0	7,05

*Δ, thous. km

Discussion of the Results

Investigation of the travel times and amplitudes of body waves, phase velocities of surface waves and free oscillations of the earth has given an idea of the layered structure of the earth and enabled construction of a radially inhomogeneous and spherically symmetric model. At the same time, many known facts cannot be explained within the framework of a radially inhomogeneous model and require expansion of the class of models of the earth that account for both radial and lateral inhomogeneity of the structure of the earth.

Experimental investigation of the horizontal inhomogeneity of the earth requires the development of detailed cross-sectional and areal seismologic systems that in accordance with the degree of detail of the investigation should be oriented toward some characteristic scale of inhomogeneity of structure. To do this, it is necessary to establish a hierarchy of natural scales of inhomogeneities of the structure of the earth's interior and the relation between these scales and the scales of variations in parameters of the wave field.

To detect and study the scale effects that determine the regional variability of elements of the wave field, it is necessary to introduce a number of new morphological characteristics of the field and to develop relatively simple and effective techniques for data analysis.

In the first part of the monograph on the basis of experimental data about the patterns of propagation of seismic waves in an inhomogeneous earth it is shown how the major elements of the wave field are related to the nature of distribution and the scale of variation of velocities of propagation of seismic waves and the absorbing properties of the medium.

The main procedural technique used to analyze regional variability of the characteristics of body and surface waves is to separate the observed wave fields into two main components: the average field (background) and the deviations from the average -- fluctuations. Simple and comparatively

effective techniques are proposed for analyzing the statistical structure of fluctuations. Characteristic examples are given to show the actual possibilities of methods that have been developed for studying the scale effects in manifestation of inhomogeneities of the structure in the pattern of fluctuations of wave field patterns.

It is shown that to analyze the structure of fluctuations of the wave field parameters, such statistical characteristics as functions of coherence, correlation and structure functions have great possibilities. A summary curve for the correlation ratio as a function of epicentral distance in the range of 10 km to 12,000 km is plotted from the data for P wave pulse shape correlation found in different parts of the world. Analysis of these data shows that by using a spatial correlation function in essentially different geological-tectonic regions of the earth one can distinguish the scales of fluctuations in parameters of the wave field that are typical of these regions, and put them into correspondence with the scales of inhomogeneities of the medium.

Spatial structure functions are especially convenient for evaluating the spatial scales of inhomogeneities in structure from the nature of fluctuations in wave field patterns. They were calculated for fluctuations in the travel time of the P wave for the LASA group and 20 USGS stations located in the continental region, and also for a group of seismic stations in California in the zone of transition from continent to ocean, and for a system of seismic stations in other territories of the United States and Canada. A spatial structure function of fluctuations in the logarithm of the amplitude of a longitudinal wave is plotted from station data on the territory of the United States. The resultant data are compared with the structure function of thickness of the earth's crust in the territory of the LASA group and with the system of velocity profiles of the crust and upper mantle of six regions of the United States and Canada. A direct relation is established between the structure function of wave field elements and horizontal inhomogeneities of the structure of the crust and mantle.

A structure function of fluctuations in the times of arrival of the PcP wave is plotted for a system of world-wide seismic stations from data of registration of the LONG SHOT underground nuclear explosion. It is shown that by using structure functions, horizontal inhomogeneities can be traced to great depths, including in the region of transition from the lower mantle to the outer core.

It is also shown that use of the system of regionally differentiated curves of Pn, Pg, P, Sn, S, Lg and R waves can appreciably extend the dynamic range and the range of epicentral distances in solving the problem of estimating the magnitudes of seismic sources.

II. REGIONAL PECULIARITIES OF SEISMIC WAVES AND STRUCTURE OF THE UPPER MANTLE IN CENTRAL ASIA

The second part of the monograph presents the results of years of research done in the central part of the Asiatic continent. A major place is given to investigation of the structure of the upper mantle in the Pamir-Baykal region, where seismologic profile observations were made in 1961-1963 (Lukk, Nersesov, 1965; Nersesov, Rautian, 1964). In subsequent years, additional data have been obtained that have enabled more detailed analysis of the internal structure of the upper mantle within the limits of this region.

The territory of Central Asia between Pamir and Baykal includes a series of tectonic structures that comprise the eastern branch of the Ural-Mongolian geosynclinal folded region: Tyan'-Shan', Kazakhstan, Mongolia, Altay and Pribaykal'ye.

Ye. N. Altukhov et al. (1974) feel that these relatively "widely aged folded zones can be unified into three groups that have similarity of development and structure." In this connection it is hypothetically assumed that the regional structures can be systematized according to the types of the earth's crust that made up the folded base of Archean age for the "primary and regenerated geosynclines" that have developed since the Lower Proterozoic and later. Fig. 17 gives a diagram of the major structural elements of the eastern part of the Ural-Mongolian folded zone (Altukhov et al., 1974).

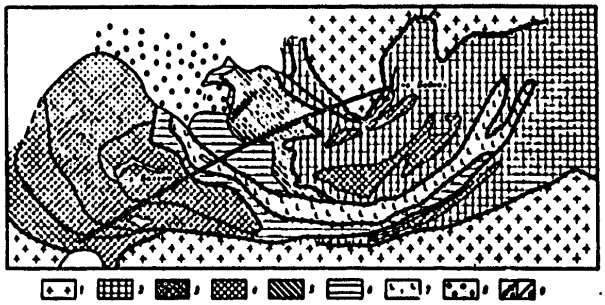

Fig. 17. Major structural elements of the eastern part of the Ural-Mongolian zone (Altukhov et al., 1974): 1--ancient platforms and massifs; 2-4--folded systems that have developed on a crust of continental type (Kazakhstan-Tyan' Shan', Sayan-Baykal, Khingan-Gobi); 2--primary geosynclines; 3, 4--regenerated geosynclines (3--early Caledonian, 4--Hercynian); 5, 6--folded system that has developed on a crust of transition type (Mongol-Altay), primary geosynclines; 5--early Caledonian, 6--Hercynian; 7--folded system that has developed on a crust of oceanic type (Zaysan Gobi, Hercynian); 8--sheath of the West Siberian Plate; 9--zones of fractures; a--along boundaries of folded systems; b--along boundaries of geosynclinal zones of different ages. The double line shows the Pamir-Baykal profile.

It is considered a characteristic feature of the folded systems that belong to the first group, including the Sayan-Baykal, Kazakhstan-Tyan' Shan' and Khingan-Gobi systems, that the folded zones of this group were formed on a basement with a continental type of crust "with a thick granite-Gneiss layer of Archean age." The primary geosynclinal systems of Proterozoic-reefogenic age comprise the framework of the Siberian and Chinese platforms and mainly represent structures of the Sayan-Baykal folded system. The regenerated geosynclines showed up mainly within the limits of the Kazakhstan-Tyan' Shan' system: the Kokchetav-North Tyan' Shan' geosyncline of the Caledonian Era, and the Zhungar-Balkhash and South Tyan' Shan' geosynclines of the Hercynian.

Belonging to the third type of folded systems that were formed on a basement with oceanic type of crust (without a sialic layer) is the Zaysan-Gobi folded region that "extends for more than 2000 km in a continuous strip 150 200 km wide from Semipalatinsk on the west through the Zaysan-Ulengur cauldron, along the southwestern slopes of Mongolian Altay, across Gobi Altay to the lowlands of the Eastern Gobi."

Thus Ye. N. Altukhov et al. assume that during the evolution of the earth's crust in the Ural-Mongolian zone, the Archean granite-metamorphic layer of crust from the Lower Proterozoic and later period was converted by successive geosynclinal cycles to a new type of crust. The Baykal-Sayan and the Kazakhstan-Tyan'Shan' folded systems with continental type of crust were formed in the process of the primary geosynclinal cycle in the Proterozoic and the regenerative cycle in the Caledonian and Hercynian epochs. A crust of intermediate type was formed within the limits of the Mongolian-Altay folded system in the Lower-Upper Paleozoic epoch. It is assumed that the growth of the crust took place from the edges of the system toward the center. In the Ordovician-Silurian, as a consequence of disintegration and "stretching of the crust nearly from the axial part of the Ural-Mongolian belt the Zaysan-Gobi system arose with a crust of oceanic type."

The given pattern of evolution of the crust of the Ural-Mongolian belt is to a certain extent hypothetical. The extent to which such a treatment is realistic may depend directly on the possibility of explaining a number of facts discovered in recent years by geology, geophysics and geochemistry.

It seems that some of the assumptions stated by geologists on the basis of generalization of various data relative to the origin and tectonic structure of the eastern part of the Ural-Mongolian folded region (Altukhov et al., 1974; Zaytsev et al., 1974; Zonenshtayn, 1974, Shul'ts 1974) may be confirmed to some extent by the results of seismologic studies presented in our monograph.

Chapter 1. Spectral Characteristics of P, Pg and Lg Waves

Investigation of the structure of the upper mantle is based mainly on the travel times of body waves, the phase velocities of surface waves, and on data about free oscillations of the earth. The use of dynamic characteristics of seismic waves for these purposes opens up new possibilities (Azbel' et al., 1966; Yanovskaya et al., 1964). Of greatest promise is the consideration of

spectral amplitude curves (Volkov, Yanovskaya, 1974). However, so far this question has not been given adequate attention. We know of only an extremely small number of papers in which satisfactory data would have been found on the spectral amplitude curves of different phases of body and surface waves (Malinovskaya, 1971; Archambeau et al., 1969). So much the more deserving of interest are the data on amplitude curves of different frequencies found by the Comprehensive Seismological Expedition as a result of more than a decade of observations using the ChISS frequency-selective seismic stations (Zapol'skiy, 1971).

1. Amplitude curves of different frequencies

The Materials Processed. Recordings of earthquakes by a seven-channel ChISS station located in Talgar were used for experimental investigation of the general structure of seismic waves in the range of epicentral distances from 500 to 3500 km. For the sake of brevity, this distance range is sometimes called the intermediate zone. The average frequencies f of the registration channels of the station were 0.35, 0.7, 1.4, 2.8, 5.6, 11 and 22 Hz. Data of about 800 earthquakes were processed in all.

Information on earthquakes (time at the focus, coordinates, depth, magnitude and class) were taken from the seismic bulletins of the USSR and the United States, and also from data of regional networks (Baykal, Altay and North Tyan' Shan'). Most of the earthquakes in the zone up to 1000 km have a value of K from class 9 to 11, and in the zone beyond 1000 km, the magnitude M is from 4 to 5.5.

The entire aggregate of epicenters of the earthquakes was divided into four directions. In accordance with the location of the epicenters relative to the Talgar station these directions were termed: Northeast, East, South and West, designated from here on for brevity by NE, E, S and W. The epicentral distances within each direction with varying detail covered the range from 200-300 to 3000-3500 km. The distribution of the number of epicenters by directions is shown in Table 6.

TABLE 6

Data on the number of earthquakes as a function of distance interval and direction

Δ, km	NE	E	S	W
200-1000	59	153	60	—
1000-3000	108	127	130	132

The Northeast direction is formed by the epicenters of Zaysan, Altay, Sayan, Pribaykal'ye and Trans-Baykal. The East -- by earthquakes of Dzhungaria, Northwest China, Mongolia. Comprising the South direction are the epicenters

of Kashgaria, Pakistan, Nepal, India and the Bay of Bengal. In the West direction are South Tyan' Shan', Pamir, the Tadzhik Depression, Kopet-Dag, Iran and the Caucasus.

Measurement and Processing Methods. In each of the four directions, spectral amplitude curves were plotted for the major wave groups reliably differentiated in the intermediate zone: Pn, P, Pg, S and Lg. The hodograph compiled by I. L. Nersesov and T. G. Rautian (1964) was used in data analysis. Maximum amplitudes were measured in intervals lasting 10-15 s for longitudinal waves, and 15-20 s for S and Lg waves.

Due to strong absorption, high frequencies could not be followed throughout the distance range. For instance the recordings on the seventh channel ($\bar{f}$ = 22 Hz) were made at distances up to 300 km, on the sixth ($\bar{f}$ = 11 Hz) -- up to 500-700 km, on the fifth ($\bar{f}$ = 5.6 Hz) -- up to 800-1000 km. The amplitude curves for the four low-frequency channels could be followed throughout the interval of investigated distances.

The single-station method was used in data processing. The amplitude curves were plotted from recordings of many earthquakes with epicentral distances covering the range of interest. Intensity estimates were known for all these earthquakes -- either the energy class K (at distances up to 1000 km) from observations of regional networks, or the magnitude M determined from surface waves (at distances beyond 1000 km). It is important that these estimates do not depend on the behavior of the body waves in the intermediate zone.

If we have an estimate of earthquake intensity M_i or K_i and we know how the spectral amplitudes A(f) depend on M or K (Nurmagambetov et al., 1975), we can normalize the measured amplitudes, reducing them to a fixed value of M_0 or K_0. It was such normalized amplitudes that were used to plot the amplitude curves.

All measured spectral amplitudes were reduced to the reference class $K_0 = 10$ or to the reference magnitude $M_0 = 5$. Normalization was done by the formulas

$$A(f, K_0) = A(f, K_i) \cdot 10^{\beta_K(f)(K_0 - K_i)}$$

or

$$A(f, M_0) = A(f, M_i) \cdot 10^{\beta_M(f)(M_0 - M_i)}.$$

Values of functions $\beta(f)$ for average frequencies of a ChISS station obtained experimentally (Nurmagambetov et al., 1976) are summarized in Table 7.

The function $\beta(f)$ was taken as the same for different waves and regions. The values of β_K and β_M are related by the formula

$$\beta_K = 0.64\,\beta_M,$$

implied by the energy relation between the M and K scales that is valid within the limits of the dynamic range of the earthquakes used (Zapol'skiy et al., 1974).

TABLE 7

Values of $\beta(\bar{f})$ for channels of a ChISS station

(1) Параметр	1	2	3	4	5	6
(2) $\bar{f}$, Гц	0,85	0,70	1,40	2,80	5,60	11,00
β_K	0,64	0,62	0,59	0,54	0,50	0,46
β_M	1,00	0,96	0,91	0,84	0,78	0,72

KEY: 1--Parameter
2-- $\bar{f}$, Hz

Since the amplitudes were normalized to $K_0 = 10$ in the near zone (up to 1000 km) and to $M_0 = 5$ in the far zone, in comparing the amplitude curves summarizing the data for the entire distance interval (from 200 to 3000 km), the curves of the near zone were shifed by an amount proportional to β_K until they coincided with the curve of the far zone on the section of coverage. Since β depends on frequency, this shift was different for different recording channels.

Thus in plotting the spectral amplitude curves we used normalized values of the maximum amplitudes of wave groups Pn, P, Pg, Sn, S and Lg.

Graphs for the dependence of maximum amplitudes on distance were plotted from six frequency channels for each wave group. The experimental values (from 60 to 250 points) were averaged, and a smoothed curve was drawn through the centers of gravity of the individual distance intervals. The method is described in detail in another work (Antonova et al., 1968). As a result, families of spectral amplitude curves were obtained for each direction by wave groups.

Shown on graphs plotted from recordings of the ChISS station at Talgar are amplitude curves for approximately the same azimuths according to data of wide-band instruments of the general type SK for six stations located in Northern Tyan' Shan'. Graphs for the ratios of amplitudes of Pg and Pn waves as a function of epicentral distance are plotted for each direction.

Let us go on to a detailed examination of the amplitude curves.

Spectral amplitude curves of Pn and P waves for the four directions are shown in Fig. 18. Characteristic peculiarities of all curves are: uniform drop in the interval from 250 to 350-400 km, increase in intensity at about 350-400 km, and a second spike at 500-600 km that shows up more reliably in all directions, and then a section of strong decline from 600 to 800-1000 km.

The structure of the amplitude curve of the Pn wave on the section up to 1000 km is the most unstable in comparison with all the wave groups considered. The amplitude curves are characterized by strong oscillations that

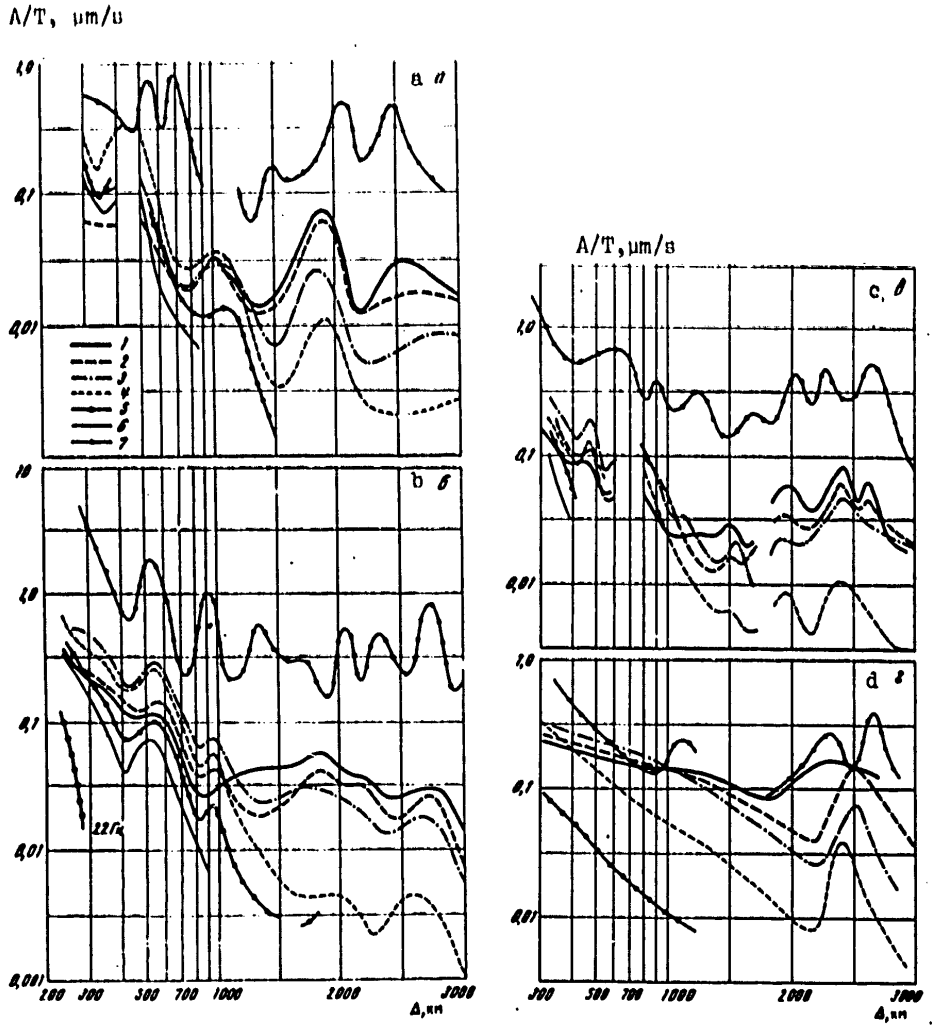

Fig. 18. Spectral amplitude curves of P and Pn Waves for Northeast (a), East (b), South (c) and West (d) directions: 1--average channel frequency 0.35 Hz; 2--0.7; 3--1.4; 4--2.8; 5--5.6; 6--11 Hz; 7--from recordings of wide-band SK equipment

are difficult to distinguish with the methods used for the observations and data processing. As an example, we give a version of possible approximation of experimental data for the spectral amplitudes of Pn waves for the South direction (Fig. 19).

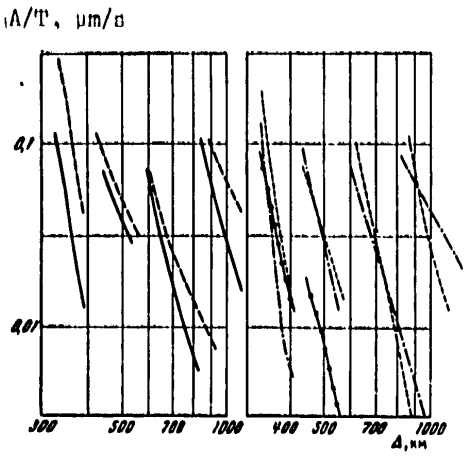

Fig. 19. An example of possible approximation of experimental values of the spectral amplitudes of a Pn wave on the 300-1000 km section for each direction: channels are separated; see Fig. 18 for designation of curves

One can clearly distinguish three sharp spikes of intensity at 400, 600 and 800-900 km, where the amplitude differentials reach one and a half orders of magnitude. An example of another technique for averaging experimental data is shown by the curves for the West direction (see Fig. 18d) that are plotted with strong smoothing, resulting in revelation of the most "long-period" component of the attenuation curve and total filtering of the "short-period" (oscillating) component.

The given two versions of averaging show the inhomogeneity of structure of of the spectral amplitude curves in the near zone.

Let us continue the examination of curves for all directions (Fig. 18). The frequency-selective nature of attenuation on the section up to 800 km shows up weakly. The curves of the first four channels (frequencies from 0.35 to 3 Hz) are nearly parallel, the attenuation curve of the fifth channel (5.5 Hz) has a somewhat greater slope, and it is only the curve of the sixth channel (11 Hz) that is appreciably steeper. The most pronounced differences in the behavior of spectral curves of different frequencies are observed on the 800-1000 km section. At a distance of 600-800 km the amplitudes on the fifth and sixth channels (5-10 Hz) are approximately equal to the amplitudes on the first and second channels (0.35-0.7 Hz); at distances of 1300-1500 km they become 20-30 times lower.

From a comparison of curves of different directions on the section up to 1000 km it is clear that as there is a change from NE to E, and then toward W and S there is a reduction in the slope of the curves and displacement of the position of extrema toward greater distances.

On curves for directions NE and E near 1000 km, oscillation is observed with a minimum at 800-850 km and a maximum at 950-1050 km. This feature shows up very weakly on curves for directions S and W.

At distances greater than 1000-1500 km the general attenuation of amplitudes decreases sharply, the curves flatten out, reaching a minimum at distances of about 1500 km, which is clearly distinguished on curves of directions NE, E and S. Apparently for the West direction the minimum is shifted toward 2000-2200 km.

Further on a maximum is observed that is most pronounced on curves of directions NE and W, where its "amplitude" reaches 0.7-0.9 log unit. For directions E and S, the "amplitude" of the spike is lower: 0.3-0.4 log unit. The position of the maximum of the amplitude curve gradually shifts from 1800 km to 2400 km with a change from directions NE and E to S and W. This maximum has a complex structure and can be resolved into two maxima located at distances of about 2000 and 2500 km.

Unfortunately, it has been nearly impossible to determine the spectral structure of this spike, i. e. to trace stable differences in the behavior of different frequencies. The curves of frequencies from 0.35 to 2.8 Hz behave about the same, and the higher frequencies disappear at distances greater than 1500 km.

For a quantitative description of regional differences we introduce several parameters that characterize the major features of the amplitude curves: $l_i$min. or $l_i$max. -- the position (in km) of the extrema of the curves; n_i -- the logarithmic steepness of the slope (negative exponent of the approximating power function) within the limits of a certain distance interval; δ_i -- the "amplitude" of the maximum of the curve (in log units); and the characteristics of level -- the value of the ratio A/T (in μm/s) at a certain distance. We will determine the values of these parameters for three frequency intervals: 0.35-0.7, 1.4-2.8 and 5.6-11 Hz, that we will designate for brevity by the values of the average frequencies -- 0.5, 2 and 8 Hz. All values of the parameters for the amplitude curves of P and Pn waves as well as Pg waves are summarized in Table 8. The unreliable determinations of parameters are enclosed in parentheses.

The amplitude curves of Pg waves are shown in Fig. 20. These curves also show a characteristic oscillatory structure; however it shows up much more weakly than in Pn waves. Two sections of monotonic fall-off in amplitude are observed: the first from 250 to 350-500 km, and the second from 500-600 to 800-1000 km. These two sections are separated by an oscillation that shows up clearly on curves of directions NE and E, and to a much lesser extent on curves for S and W.

On curves for directions NE, E and S one can distinguish a minimum located at distances of 340, 420 and 450 km respectively, and a maximum -- at distances of 400, 500 and 520 km. The average values of logarithmic steepness

TABLE 8

Values of parameters of spectral amplitude curves of Pn, P waves and Pg waves for four directions of propagation and three average frequencies: 0.5, 2, 8 Hz

(1) Параметр	Δ, км	СВ ≈NE			В ≈E			ЮВ≈S			З ≈W		
		0,5	2	8	0,5	2	8	0,5	2	8	0,5	2	8
Pn and P waves													
η_h	250—400	—	4,5	5	1,7	2,2	3,5	(3)	3,0	4,5	(0,6)	1,8	3,0
l_1 мин. (2)	300—450	—	340	360	450	420	400	420	420	—	—	—	—
l_1 макс (3)	400—600	—	450	—	550	540	510	470	480	—	—	—	—
η_h	500—800	4,0	6,5	8,0	4,5	5,0	5,5	3,5	5,0	—	0,6	1,6	2,0
A/T	800	20	25	10	35	60	15	70	90	—	150	100	20
A/T	1500	13	5	1	35	12	3	20	10	—	100	50	—
l_2 мин. (2)	1300—1500	1350	1500	—	1350	1300	—	1300	1400	—	—	—	—
l_2 макс (3)	1700—2000	1900	1870	—	1850	1700	—	2000	1950	—	—	—	—
δ_1 макс (3)	1700—2000	0,7	0,5	—	0,3	0,1	—	0,45	0,35	—	—	—	—
l_3 макс (3)	2400—2700	2500	2700	—	2500	2700	—	2700	2800	—	2450	2450	—
δ_3 макс (3)	2400—2700	0,25	0,15	—	0,15	0,20	—	0,35	0,40	—	0,40	0,55	—
Pg wave													
η_1	250—500	2,5—5	5	6	(2)	3,2	3,7	3—5	3,0	6,0	(3,3)	1,7	3,0
η_2	500—800	7,5	9	10	5,3	4,5	5	(4,2)	5	—	3,3	2,8	(3,0)

KEY: 1--Parameter; 2--min; 3--max

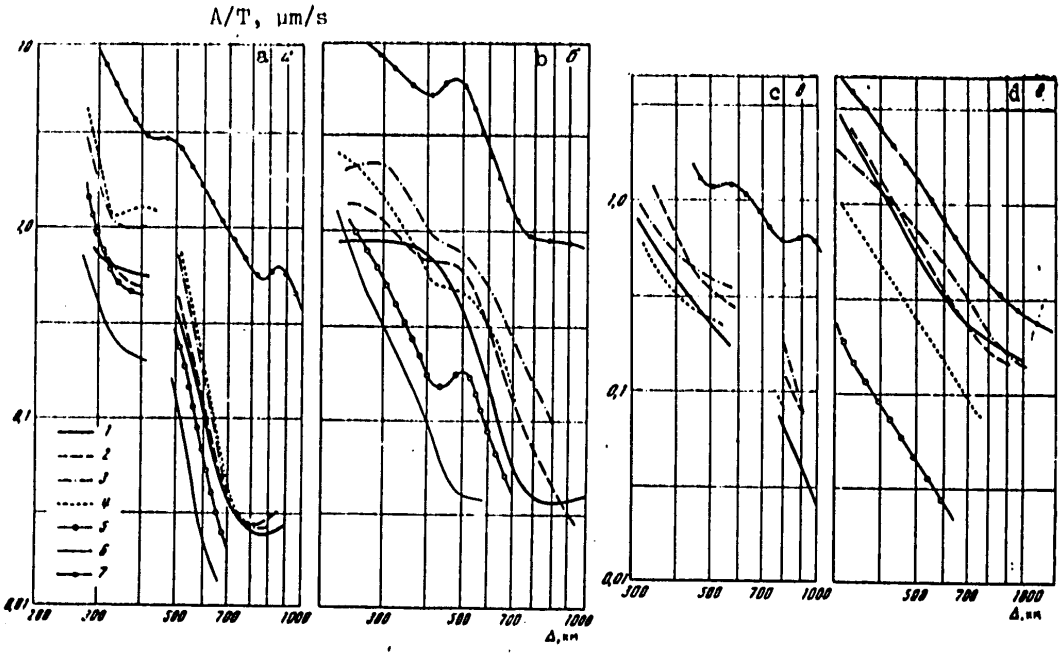

Fig. 20. Spectral amplitude curves of Pg waves of the Northeast (a), East (b), South (c) and West (d) directions; see Fig. 18 for designation of curves

n_1 and n_2 of these two sections of the amplitude curves are given in Table 8. The Pg waves dump out very strongly (approximately as Δ^{-3}-Δ^{-5} within the limits of the first section, and still more strongly within the limits of the second section). The extent of attenuation weakens with a transition from direction NE to E and then from S to W. The spectrally selective nature of attenuation is weakly expressed, so that general damping cannot be attributed to the effect of absorption. A comparison of the Pg and Pn waves with respect to level shows us that at a distance of 300 km they differ by a factor of 5-15 on frequencies of about 1 Hz, and by a factor of 3-4 on frequencies of 3-6 Hz.

From a comparison of the amplitude curves of Pg and Pn waves with respect to shape, we see that the exponent of the approximating power function for Pg waves is about two units higher than for Pn waves. Particularly deserving of attention is the coincidence of positions (with respect to the distance axis) of the extrema of the amplitude curves of both types of waves. For instance their minima coincide and come at 340-420 km for the directions NE and E respectively. Similarly coincident are the positions of the next maximum: at 400-450 and 500-520 km for the given directions. For convenience in comparing the spectral amplitudes of Pg and Pn waves, graphs were

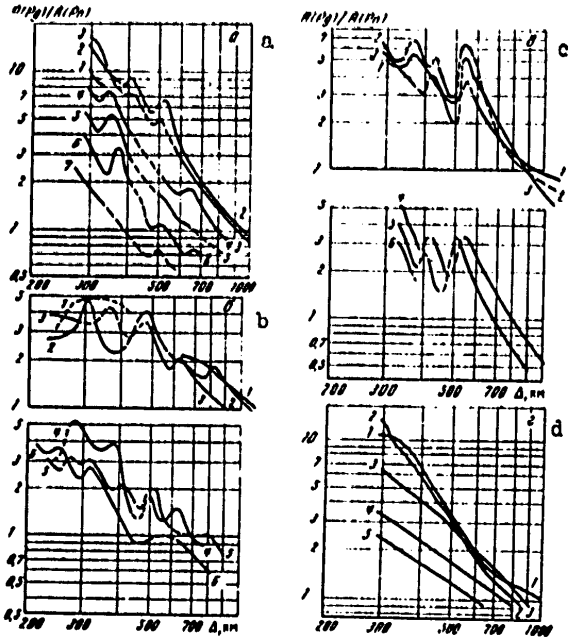

Fig. 21. Amplitude ratio of Pg and Pn waves as a function of epicentral distance for the Northeast (a), East (b), South (c) and West (d) directions; the curve numbers correspond to the conventional designations in Fig. 18a

plotted for the change with distance in the ratio of their amplitudes with respect to each direction (Fig. 21). These graphs also have an oscillatory structure that to a considerable extent copies (with reverse sign) the oscillation of amplitude curves of Pn waves.

The graphs of the amplitude ratio enable one to readily determine the limiting distances to which the Pg group dominates on the recording, i. e. how much it exceeds the Pn wave in amplitude. They show the interval of tracking of the Pg group in different frequency ranges. The values of these distances are summarized in Table 9. It can be seen from this table that the interval of tracking of the Pg wave decreases with increasing frequency -- from 1000 km for a frequency of 0.35-0.7 Hz to 400 km for a frequency of 22 Hz.

TABLE 9

Values of epicentral distances (km)
at which amplitudes of Pn and Pg waves are equal

(1) Направление распространения	(2) Частота канала, Гц						
	0,35	0,7	1,4	2,8	5,6	11	22
(3) СВ	—	950	900	780	650	540	300
(4) В	1150	1100	900	680	650	550	—
(5) Ю	1000	870	850	780	700	—	—
(6) З	1050	870	840	760	610	—	—
(7) Среднее	1070	910	890	750	650	550	(400)

KEY: 1--Direction of propagation
2--Channel frequency, Hz
3--NE
4--E
5--S
6--W
7--Average

Another quantitative characteristic of these graphs is their logarithmic steepness n_1 within the limits of certain distance intervals. The values of this parameter with respect to each distance and for all frequencies are summarized in Table 10. The differences in steepness of the ratio of amplitudes of Pg and Pn waves with respect to directions are slight. But it can be noted that the highest steepnesses are observed for the directions NE and long distances in direction S, while the lowest steepness is shown by W.

Of importance in understanding the nature of the Pg wave is the way that the slope of the graphs depends on frequency. Table 10 shows that the effect of absorption is about the same for both types of waves.

Amplitude curves of S waves are shown in Fig. 22. The Sn and S waves are the weakest among the groups of waves considered. In many instances it is almost impossible to distinguish them on recordings. It should be noted that the Sn waves in general are poorly observed over the entire territory of the southeast USSR. Besides, additional difficulties are caused by the

TABLE 10

Average values of the logarithmic steepness n of the ratios of amplitudes of Pg and Pn waves

(1) Направление распространения	(2) Интервал расстояний, км	(3) Частота канала, Гц						
		0,35	0,7	1,4	2,8	5,6	11	22
(4) СВ	300—700	—	2,4	2,6	2,0	1,9	2,0	2,4
(5) В	450—900	1,5	1,6	1,6	1,6	1,2	1,4	—
(6) Ю	300—500	(1,1)	1,2	1,6	2,0	2,0	—	—
(6) Ю	500—900	(2,2)	(3,0)	3,2	3,0	3,3	—	—
(7) З	300—700	2,8	2,8	1,7	1,4	1,2	—	—
(8) Среднее		1,9	2,2	2,1	2,0	1,9	(1,7)	—

KEY: 1--Direction of propagation
2--Distance interval, km
3--Channel frequency, Hz
4--NE
5--E
6--S
7--W
8--Average

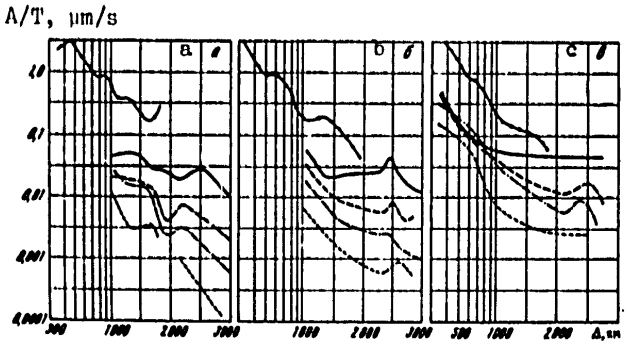

Fig. 22. Spectral amplitude curves of S waves of East (a), South (b) and West (c) directions; see Fig. 18a for designations of curves

use of recordings of the vertical component on which these waves show up much more poorly than on the horizontal components. For cases where the S wave does not have clear entries, and the recordings show only some increase in amplitudes, measurements are made within a time segment differentiated in accordance with the hodograph. The resultant amplitude curves of Sn waves are less reliable than the curves of other types of waves.

For East and South directions, the amplitude of the Sn waves of epicentral distances up to 1000 km was not measured because of their very low intensity. And for the Northeast direction it was impossible in general to distinguish these waves within the limits of the entire investigated interval of epicentral distances. The amplitude curve of this direction was not plotted.

Let us take up the characteristic of spectral amplitude curves in more detail.

On the section up to 1000 km according to data of recordings by wide-band GK instruments the general slope of the curves for the three directions is approximately constant: they decline in inverse proportion to the cube of the distance. A relative maximum can be distinguished in the interval of 450-600 km, i. e. in the same region as for P waves. A second, less pronounced maximum can be seen at distances of 800-900 km.

At greater distances the decline of the curves decreases somewhat, and close to 1500-2000 km a relative minimum is observed, followed by a maximum at distances of 2200-2500 km. On the 1500-3000 km segment of the spectral curves of the West direction the level is approximately 1.8-2 times as high as in other directions.

One can judge the spectrally selective nature of attenuation of S waves at distances from 300 to 700 km only from curves of the West direction. Their parallelism shows that the spectrum of S waves remains practically unchanged. In the distance range from 1000 km to 2000-2500 km one can see an appreciable frequency dependence of attenuation: damping increases strongly with an increase in frequency.

Amplitude curves of Lg waves are shown in Fig. 23. They also have an oscillatory structure, though much less pronounced than for longitudinal waves. Curves of the West direction are monotonic, and have no oscillations at distances up to 1000 km. Several characteristic sections can be distinguished on the amplitude curves.

The initial section up to distances of 350, 400 and 550 km for directions NE, E and S respectively is characterized by relatively weak damping, and the logarithmic steepness n_1 shows little frequency dependence.

Within the limits of distances Δl_1 of 400-800 km a spike appears on the curves that is most strongly pronounced for the NE direction. With a transition to other directions the "amplitude" of the spike decreases, and the interval Δl_1 itself shifts toward greater distances: 350-450 km for NE, 400-550 km for E and 550-800 km for S.

On section Δl_2 the amplitude curves decline monotonically, being well approximated by a power-law function with exponent n_2 approximately equal to 5-7. Section Δl_2 occupies the distance intervals of 500-800, 600-1200, 800-1500 and 700-1500 km for the curves of directions NE, E, S and W respectively. The degree of damping n_2 gradually decreases with a transition from the Northeast direction to the West.

In the distance interval from 800 to 1500-2000 km, the frequency selective nature of attenuation shows up strongly. For the directions NE and E the spectral curves of frequencies 0.35 and 2.8 Hz approximately coincide in level at a distance of 500 km; at 1500 km they differ by 1.5-2 orders.

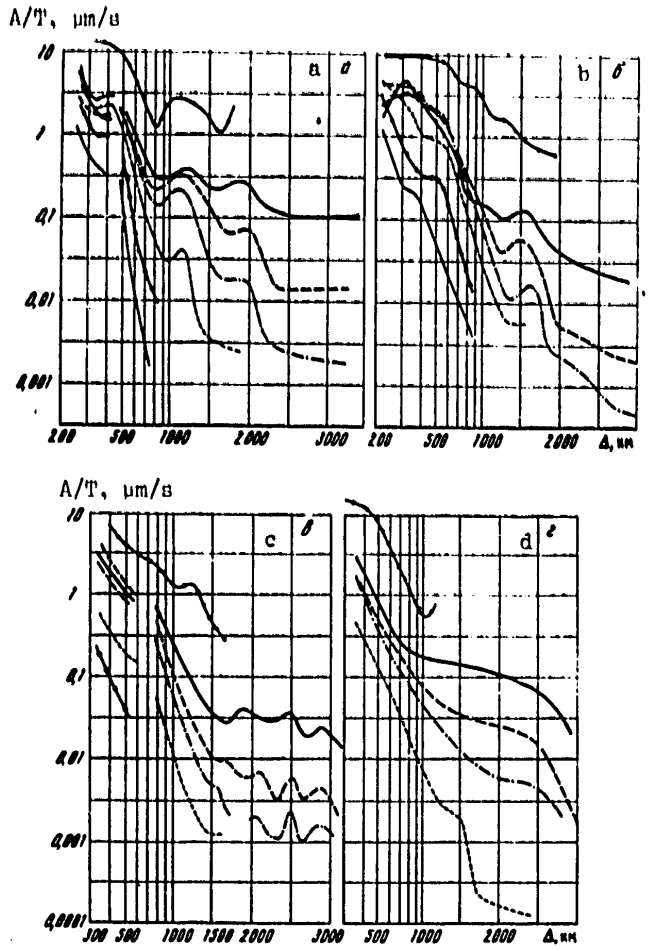

Fig. 23. Spectral amplitude curves of Lg waves of Northeast (a), East (b), South (c) and West (d) directions; see Fig. 18a for designations of curves

Section Δl_2 terminates with the next oscillation of the amplitude curves, which shows up most clearly for the NE direction. The position of the minimum l_3^{min} and the maximum l_3^{max} gradually shifts toward greater distances with an increase in the azimuth of the direction into the epicentral region. The "amplitude" of the oscillation also decreases at the same time.

For the South and West directions in the distance interval of 2000-2500 km one can distinguish a relative increase of intensity -- l_4^{max}.

Table 11 gives the parameters of spectral amplitude curves of Lg waves.

TABLE 11

Parameters of spectral amplitude curves of Lg waves for four directions of propagation and three frequencies: 0.5, 2, 8 Hz

(1) Параметр	(2) Расстояние, км	СВ=NE			В=E			ЮВ=S			З=W		
		0,5	2	8	0,5	2	8	0,5	2	8	0,5	2	8
η_1	300—600	2,5	5	4	—	2	4,5	2,7	3,0	4,0	3,6	3,6	—
η_2	500—1000	4,5	6,5	11	5,0	6,5	6,5	5,5	6,5	—	(2,5)	(3,3)	—
A/T	800	250	100	3	300	200	14	500	100	—	120	20	—
A/T	1500	200	10	—	100	10	—	20	2	—	80	5	—
l_0 мин (3)	—	850	900	—	1250	1350	—	1600	1500	—	—	—	—
l_0 макс (4)	—	1100	1150	—	1500	1600	—	2000	2000	—	—	—	—
l_0 макс (4)	—	1900	1900	—	—	—	—	2500	2500	—	—	—	—

Note: unreliable data are shown in parentheses

KEY: 1--Parameter
2--Distance, km
3--min
4--max

The general level of amplitudes of waves of the Lg group at distances of up to 1000 km is approximately the same for all directions considered. An exception is the West direction for which the amplitude level is 1.5-2 times lower. In the interval of 1500-2000 km the greatest intensity of Lg waves is typical of the Northeast direction, while minimum intensity is typical of the South direction, which is due to the sharp increase of amplitudes within the limits of the northern border of the Tibetan plateau. This effect will be examined in detail below.

Scattering of individual experimental values of A/T relative to the amplitude curves depending on frequency, wave type and epicentral distance is shown in Table 12. Frequency dependence of σ is not noted.

TABLE 12

Values of standard deviations σ (log units) of individual measurements of spectral amplitude curves as a function of frequency and type of wave

(1) Усреднение по всем типам волн		(2) Усреднение по всем частотам		
(3) $\bar{f}$, Гц	σ	(4) Волна	σ	Δ, км
0,35	0,34	*Pn*	0,38	200—1000
0,70	0,32	*Pg*	0,30	
1,40	0,31	*Lg*	0,29	
2,80	0,31	*Pn* и *P*	0,32	1000—3000
5,60	0,31	*S*	0,34	
11,00	0,33	*Lg*	0,33	

Note: The overall average of the standard deviation of an individual measurement is 0.32.

KEY: 1--Averaging with respect to wave types
2--Averaging with respect to frequencies
3--$\bar{f}$, Hz
4--Wave

An examination of the dependence of σ on wave type and distance shows that up to 1000 km the Lg wave has the minimum scatter, and the Pn wave-- the maximum. Beyond 1000 km in the Northeast direction the Pn waves are more stable, while scattering for the Lg wave group rises sharply: σ increases from 0.30 to 0.40; in the South direction the value of σ for Lg waves is low. This can apparently be attributed to the fact that the measurements here properly apply not to the Lg wave, but to the "background of oscillations," which is formed as a result of repeated scattering of the longitudinal and transverse waves that form the P-code and S-code.

The code waves diffuse the energy of seismic oscillations and level out the inhomogeneity of radiation that is associated both with large inhomogeneities of structure and with the mechanism of the focus; therefore these waves are characterized by low scatter of individual measurements.

The direction dependence of σ shows up rather noticeably. For instance at distances up to 1000 km σ increases with a transition from the Northeast direction to the South, and at distances beyond 1000 km σ increases with a transition from the South direction to the Northeast. This is apparently due to the fact that distances of the order of 1000 km to the south of Talgar correspond to exit of the seismic ray beyond the limits of the mountain system of the Tibetan Himalayas, onto the Hindustan Platform, where the structure of the crust and mantle is more uniform, whereas in directions toward the east and northeast the seismic rays remain within the limits of large mountain systems and the inhomogeneities of structure that are associated with them.

Apparently we can treat the quantity σ as an estimate of convergence of magnitudes with respect to corresponding waves if the amplitude curves that we have plotted are used as calibration curves. An analysis of the spread of the data leads us to the conclusion that in order to increase the accuracy of magnitude determinations, a calibration curve should be used on distances up to 1000 km that is plotted from Lg or Pg waves, and at distances beyond 1000 km -- from the P wave. An appreciable improvement in accuracy can be realized both by using several types of waves and by simultaneous use of recordings of several frequency selective channels.

Comparison of the Parameters of the Wave Pattern with Respect to Different Directions.

Typical of recordings of the Northeast direction are intense phases of Pg and Lg waves with a clear entry and a steep leading edge; the Pn waves are the weakest. The considerable differences in the amplitudes of the initial and subsequent parts of the recording in weak earth tremors frequently leads to loss of the true first entries. In such cases, the subsequent waves in the Pn group or even in the Pg group are mistakenly taken as the first entries. This happens most often at distances of 400 700 km.

On amplitude curves of three types of waves -- Pn, Pg and Lg -- the intensity spike at a distance of 350-450 km is most pronounced in comparison with other

directions, and in the 500-1000 km interval these waves damp out more strongly than in other directions.

Within the distance interval of 800-1300 km the longitudinal wave group is extremely insignificant, the amplitudes are very low, 2-4 times lower than in other directions. The greatest spike of P wave amplitudes is noted at a distance of about 2000 km. The entries of all waves (in the interval up to 1000 km) show the highest frequencies in their spectral makeup in comparison with other directions.

Showing up most poorly in this direction are S waves, which could be distinguished only in rare instances at distances beyond 1500 km.

The amplitude curves of the East direction have much in common with the curves for the Northeast. The first spike on the Pn, Pg and Lg curves was shifted here to 400-550 km, and its "amplitude" was noticeably decreased. Curves of these three types of waves are much more wekaly damped. At distances of 800-1300 km the Pn group is more compact, the maximum amplitude usually gravitating toward the initial part of the group. In general the amplitudes of the main groups of waves at these distances (in the shadow zone) are noticeably higher than on recordings of the NE direction. The 20-degree spike (distance about 2000 km) is almost unexpressed for this direction.

All waves are somewhat lower-frequency with respect to their spectral composition at distances up to 1000 km. On some recordings of this direction the phases of Sn and S waves could be distinguished. The amplitude curves of Lg waves have a maximum at 1600 km, after which their intensity decreases sharply.

The South direction is characterized by clear entries of waves of the P group within the limits of the entire tracking interval, by low intensity of the high-frequency components (above 2.8 Hz) in the spectra of the major wave types, and a pronounced 20-degree spike for longitudinal waves.

West direction: the longitudinal waves are most intense; transverse waves can be distinguished that become stable at distances of more than 1500 km. The Lg wave group shows up here most poorly: there are no clear entries, the amplitude is 3-4 times lower than for the NE and E directions.

The amplitudes of the main groups of waves on the average damp out more weakly than in other directions.

The lowest-frequency are the Pg and Lg waves.

Characteristic Features of Amplitude Curves of Main Wave Groups.

The parameters of the spectral amplitude curves for different directions of propagation are summarized in tables 8, 9, 10 and 11.

1. The spectral amplitude curves of Pn, Pg, S and Lg waves have an oscillatory structure that is most strongly pronounced in the Pn group, and more weakly pronounced in the Lg group. The positions of the principal extrema on the distance axis approximately coincide for all wave groups. One can distinguish several sections of comparatively monotonic change in amplitudes separated by maxima and minima.

2. The first section of the curve is from 200-250 to 350-500 km. Damping of amplitudes is moderate. In the distance interval of 350-450 km a minimum shows up that is replaced by a maximum at 450-550 km. The amplitudes of the various frequencies within the limits of this section damp out practically identically. Apparently the oscillatory structure of the Pn waves on this section is more complicated, and spikes occur at 350, 500 and 600 km.

3. The second section of the curve is from 500 to 800-1000 km for longitudinal waves, and up to 1200-1500 km for Lg waves (South and West directions). Within the limits of this section, waves of all types experience the strongest damping, and its frequency selective nature shows up here most clearly.

4. The Pg wave is 5-15 times more intense than the Pn wave on frequencies of 0.3-2 Hz and at distances of 300-400 km. With increasing distance this ratio decreases noticeably, approximately as Δ^{-2}. Pg waves predominate in the group of longitudinal waves up to distances of 800-1000 km on frequencies of 0.3-2 Hz and up to distances of 500-700 km on frequencies of 3-10 Hz.

5. The Lg wave is predominant on recordings up to 1500-2000 km (and further for lower frequencies). For the Northeast direction in the distance interval of 800-2000 km on frequencies of 0.35-0.7 Hz the Lg wave is 8-15 times as intense as longitudinal waves. This ratio decreases with increasing frequency and with a change to other dierctions.

6. Major features of amplitude curves in the interval from 700 to 1600 km: oscillation with minimum at 700-900 km and maximum at 900-1100 km is typical of the amplitude curves of Pn waves and to a lesser extent of Lg waves; a minimum can be seen at about 1400-1600 km, after which the attenuation of amplitudes (particularly for longitudinal waves) abates noticeably -- the curves flatten out, and frequency differences in damping decrease.

7. At distances of about 2000 and 2500 km, intense maxima are noted on the amplitude curves, most clearly for longitudinal waves, and weakly pronounced for Lg waves.

2. Spectra of principal waves

This section gives experimental data on the shape of the spectra of the principal waves -- Pn, Pg, S, Lg -- and their variation with distance as a function of the azimuth of the direction of propagation. Regional differences of the spectra are demonstrated that arise both during the formation of seismic waves and during propagation. The distances are determined for the most considerable changes in spectra.

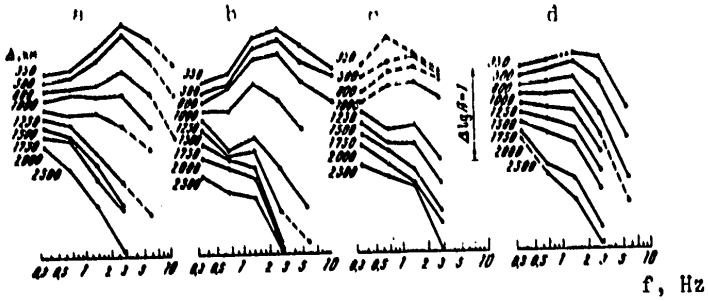

Fig. 24. Change with distance in the spectral shape of Pn and P waves (Talgar station) for the Northeast (a), East (b), South (c) and West (d) directions

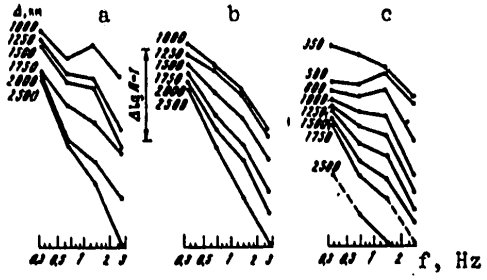

Fig. 25. Change with distance in the spectral shape of S waves (Talgar station) for the East (a), South (b) and West directions

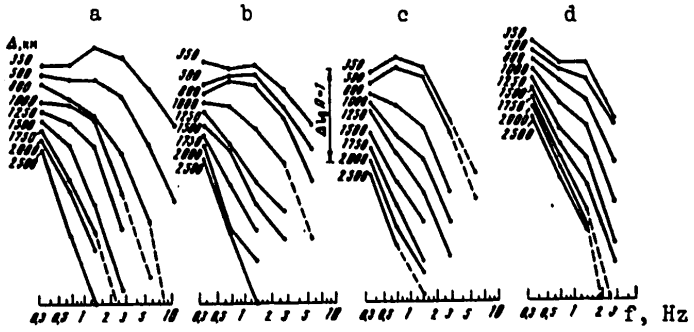

Fig. 26. Change with distance in the spectral shape of Lg waves (Talgar station) for the Northeast (a), East (b), South (c) and West (d) directions

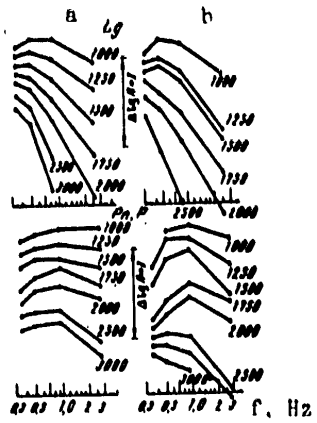

Fig. 27. Change with distance in the spectral shape of Lg and Pn, P waves (Temporary station) for East (a) and Southwest (b) directions

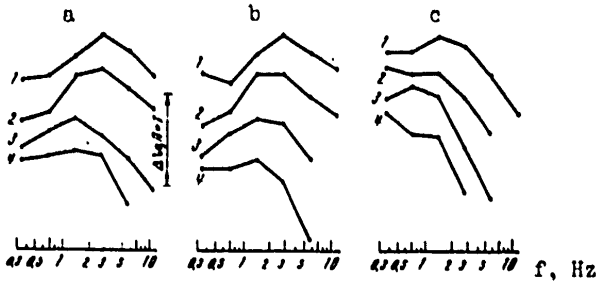

Fig. 28. Comparison of spectral shape (Talgar station) of Pn (a), Pg (b) and Lg (c) waves for the Northeast (1), East (2), South (3) and West (4) directions at an apicentral distance of 300 km

The amplitude curves given in the preceding section constitute the basis for consideration of the spectral characteristics of the waves. Here we will study the "cross sections" of the amplitude curves that enable comparison of the spectral shape of the principal waves without reference to their level.

Fig. 24, 25, 26 show families of spectra of Pn, S and Lg waves for certain values of epicentral distances from 350 to 2500 km and various directions of propagation of waves relative to Talgar station. The experimental materials used are described in section 1 of this chapter. The spectra are normalized to M = 5, and their level is arbitrary.

Fig. 27 shows similar families of spectra for Pn and Lg waves plotted from data of Temporary station for two azimuthal directions, the first coinciding approximately with Norhteast and East, and the second -- with West as taken for Talgar station.

The spectra of Pn waves are shown on Fig. 24. Their shape is influenced by two main factors: systematic differences in the shape of earthquake spectra with different directions, which show up on the initial tracking stage; difference in the nature of variation of the spectra with distance for the directions of propagation considered.

First let us consider the differences associated with the azimuths of directions that are illustrated by the selections of ChISS spectra given in Fig. 28. Here we compare the spectra of Pn, Pg and Lg waves of four azimuthal directions at a fixed distance of 300 km. We can see that the spectra of directions NE and E are considerably higher in frequency than the S and W spectra. This also shows up in the position of the maximum of the spectra (which is at a frequency of 2.8 Hz for two directions and at 1.4 Hz for the other two) and in the steepness of its slopes. For instance the ratio of the amplitude on a frequency of 2.8 Hz to that on 0.7 Hz for the first two directions is equal to approximately three, while these amplitudes are equal for the second pair of azimuths.

TABLE 13

Parameters of the spectra of principal waves in different directions for distances of 350 and 800 km

(1) Тип волны	(2) Параметр	СВ=NE		В=E		ЮВ=S		З=W	
		350	800	350	800	350	800	350	800
Pn	f_{max}	2,8	2,8	2,8	2,8	1,4	1,4	1,4	1,4
	$\gamma(0,35/0,7)$	−0,04	−0,02	−0,10	−0,17	−0,30	−0,20	−0,06	0
	$\gamma(0,7/2,8)$	−0,50	−0,18	−0,50	−0,36	0,07	0,15	0	0,40
	$\gamma(1,4/5,6)$	−0,09	0,04	0,09	0,15	0,45	—	0,60	1,10
Pg	f_{max}	2,8	2,8	2,8	1,4	1,4	1,4	1,4	1,4
	$\gamma(0,35/0,7)$	0,10	−0,11	−0,16	−0,14	−0,28	−0,20	0	0
	$\gamma(0,7/2,8)$	−0,56	−0,10	−0,49	−0,14	−0,10	0,07	0,13	0,45
	$\gamma(1,4/5,6)$	0	0,30	0,23	0,53	0,44	0,97	0,87	1,33
Lg	f_{max}	1,4	0,35	1,4	0,7	0,7	<0,35	<0,35	<0,35
	$\gamma(0,35/0,7)$	0	0,17	0,07	0,12	0,17	0,13	0,23	0,23
	$\gamma(0,7/2,8)$	−0,10	0,60	0,23	0,40	0,65	0,92	0,62	0,77
	$\gamma(1,4/5,6)$	0,47	1,15	0,65	1,07	1,10	—	—	—

KEY: 1--Type of wave
2--Parameter

Data on the parameters of spectra of different directions for two distances (350 and 800 km) are summarized in Table 13. The parameters shown are f_{max} -- the position of the maximum of the ChISS spectrum, and $\gamma(f_i/f_j)$-- the logarithm of the ratio of amplitudes on two frequencies.

Fig. 24 and 28 and Table 13 imply that the spectra of Pn waves in directions NE and E differ from each other insignificantly. The same can be said about the spectra of the other two directions: S and W. The differences in the parameter γ within each pair do not exceed 0.2 log unit, whereas between pairs these differences amount to 0.5-0.6 log unit on the average.

Let us examine the other peculiarity of the spectra. For all types of waves the amplitude of the 0.35 Hz frequency is anomalously high on near distances for NE and E. The spectra of Pn waves show how the noted low-frequency slope is interrupted by a rise in amplitude on the 0.7-3.5 Hz section, even though under conditions of absence of the effect of absorption one should expect constant steepness of the low-frequency slope.

Turning to the nature of the change in spectra with distance, we see that the strongest damping of high frequencies occurs in the 800-1500 km distance interval. The spectral shape changes insignificantly both preceding and following this section.

The most graphic representation of this pattern is given by graphs of the change in spectral ratios with distance (Fig. 29). Let us note that oscillations of graphs of $\gamma(\Delta)$ are confined to the same intervals of epicentral distances where oscillations were noted in the amplitude curves described in detail in the preceding section.

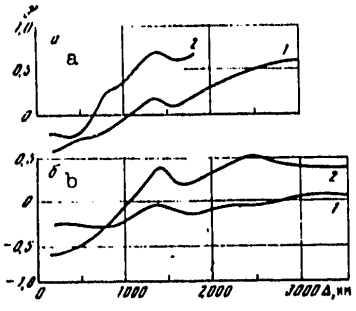

Fig. 29. Graph of the change with distance in the spectral ratios γ (ChISS Temporary station) of frequencies 0.47 and 0.9 Hz (1) and frequencies 0.9 and 0.25 Hz (2) for Lg (a) and P (b) waves

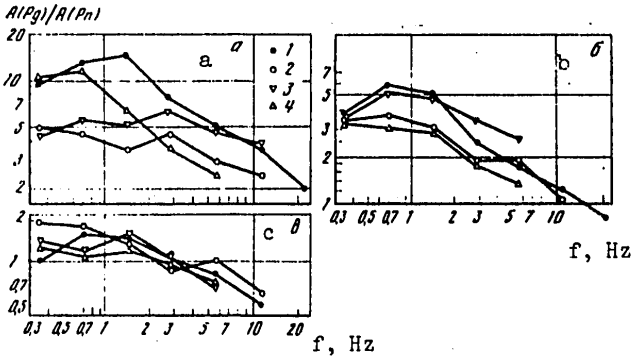

Fig. 30. Ratio of spectral amplitudes of Pg and Pn waves for epicentral distances of 300 (a), 500 (b) and 800 (c) km for the Northeast (1), East (2), South (3) and West (4) directions

The spectra of Pg waves differ considerably from those of Pn waves in their relative low-frequency nature. Typical spectra of Pg waves can be seen in Fig. 28b, where they are shown for a distance of 300 km with respect to all four directions. The spectra of the Pg waves steadily repeat the amplitude differences that we found previously for Pn waves.

A more objective idea is given by the ratios of spectral amplitudes of these two waves (Fig. 30); the graphs are plotted for three values of the epicentral

distance (300, 500 and 800 km) and four directions of propagation. The values of the ratios were calculated from direct measurements of the amplitudes of these waves rather than with respect to amplitude curves or spectra.

Let us consider the graph for 300 km in more detail (see Fig. 28b). At this distance one begins to track the Pg wave. From recordings of the Talgar station this wave is distinguished from distances of 250-280 km. By 300 km the Pg wave is usually delayed relative to the first entry by no more than 2 s. It can be assumed that at this distance the conditions of propagation have not yet had any appreciable influence on the spectrum of the Pg wave.

Detailed studies of the spectra of local earthquakes undertaken by us previously on materials of the Talgar ChISS station showed that the spectrum of the Pn wave inherits the spectral peculiarities of the direct $\overline{P}$ wave propagating in the earth's crust. This gives us a basis for assuming that the difference spectra shown in Fig. 30a can be interpreted as the frequency response of the mechanism of formation of the Pg wave.

The amplitude differences of this response are quite considerable. For instance the greatest relative intensity of the Pg wave is noted for earthquakes of the Northeast and West directions for which the ratio of amplitudes of Pg to Pn is equal to 10-15 on a frequency lower than 1 Hz. The ratio of these waves begins to decrease from a frequency of 1.4 Hz in the NE direction, and from 0.7 Hz in the West, and is inversely proportional to frequency with exponent 0.7-0.8.

For directions S and E the frequency dependence is much less pronounced. In the frequency range of 0.3-3 Hz the wave ratio is approximately constant and equal to 4-6. For higher frequencies the ratio decreases weakly: in inverse proportion to frequency to a power of 0.3-0.4.

With increasing distance the azimuthal differences damp out, and at 800 km (Fig. 30c) they become insignificant.

The spectra of S waves are shown on Fig. 25 for three directions of propagation. Of all the investigated types of waves, the data on transverse waves are the least reliable and representative. Therefore let us deal with them briefly.

Just as for longitudinal waves, the highest-frequency spectra are those of the East direction. The spectra of the West and South directions are appreciably lower-frequency ones. For directions E, S and W the ratio of amplitudes of the frequencies 0.7 and 2.8 Hz at a distance of 1000 km is 0.22, 0.70 and 0.68 log unit respectively. By a distance of 1500-2000 km the differences in spectra of different directions abate.

For the spectra of transverse waves of the East direction the effect of the increase in amplitude on a frequency of 0.35 Hz is observed to a still greater extent than for longitudinal waves.

The spectra of S waves show a more stable change with distance than longitudinal waves. An appreciable change in the spectra takes place in a more extended interval: from 800-1000 to 2000-2500 km. The principal oscillations are confined to 2000 and 2500 km.

The spectra of Lg waves as a function of distance are shown in Fig. 26 and 27 for the Talgar and Temporary stations.

The amplitude differences of the spectra of Lg waves that show up at short distances repeat the peculiarities of the spectra of longitudinal waves. The spectra of the NE direction are the highest-frequency. With an increase in azimuth one notes a considerable increase in low-frequency components of the spectrum. For instance Table 13 shows that the maximum differences in the ratio of amplitudes of frequencies of 0.7 and 2.8 Hz reach 0.7-0.8 log u. The maximum of the spectrum of directions NE and E is at a frequency of 1.4 Hz, and for the West direction -- at frequencies lower than 0.35 Hz. These estimates apply to epicentral distances of 350 km.

Anomalously high amplitudes of the 0.35 Hz frequency can be seen on the spectra at short distances for all directions except the South.

Now let us examine the change with distance in the spectrum of Lg waves. Fig. 29 shows a graph of the distance dependence of spectral ratios as plotted from data of the Temporary ChISS station. The plot of the graph repeats the main peculiarities noted previously for other types of waves.

In the interval from 200-250 to 500-700 km the spectrum of Lg waves changes more weakly than at greater distances. The strongest changes take place on the section between 600-800 and 1300-1400 km. At distances of 1300-1700 km the oscillation shows up clearly, after which the regular change in spectral shape with distance abates noticeably.

In conclusion let us repeat the main peculiarities of spectra of different waves and their change with distance.

In comparing the spectra of different azimuths of propagation for all waves, one trend shows up: the spectra become lower-frequency as the azimuth increases, i. e. with a transition from the NE direction to S. For Pg and Lg waves these differences show up even on the initial tracking stage, and consequently they are due to a greater extent to the mechanism of formation than to the conditions of propagation.

The patterns of change in spectra with distance are most graphically described by curves for the dependence of spectral ratios on distance. These graphs show several distance intervals within which the changes in spectral shape of all waves are approximately uniform. In the initial part (from 200-300 to 500-700 km) spectral changes are insignificant. In the next distance interval (from 500-800 to 1300-1700 km) the strongest change in spectra occurs with principal damping on higher frequencies. Between 1300 and 2000 km

an interval of the opposite change in spectra can be distinguished, i. e. stronger damping of lower frequencies. This shows up as oscillation on graphs of the distance dependence of spectral ratios. The next oscillation, with a lower "amplitude," is noted at distances of 2000-2500 km.

At distances greater than 1500-2000 km there is practically no systematic component in the change with distance in the spectra of longitudinal waves for frequencies lower than 3 Hz. At these distances the spectral shape of P waves on the average is the same as in the teleseismic zone. The spectra of S waves and especially Lg waves continue to change, but noticeably more weakly than at shorter distances.

At distances up to 800-1000 km the amplitudes on a frequency of 0.35 Hz are anomalously high for the spectra of all types of waves (especially S and Lg waves). This effect is characteristic to a greater extent of recordings in the NE and E directions.

The spectra of P and Lg waves at Temporary station are appreciably higher-frequency spectra than on Talgar station. However, the general patterns of change in the spectra with distance and the distance intervals with characteristic changes of spectra for both stations are the same.

Chapter 2. Differentiation of Large Horizontal Inhomogeneities with Respect to the Characteristics of P, Lg and Rg Waves

In this chapter an investigation is made of the spatial structure of the azimuthal differences of amplitude curves and the spectra of seismic waves described in the preceding chapter. It is shown that these differences are formed chiefly on certain sections of the paths of propagation of seismic rays when they cross certain geological boundaries or structures.

The principal form of representation of experimental data is by spatial constructions: comparison of amplitude and spectral characteristics on different paths, mapping of these characteristics, localization of sections of abrupt changes in the kinematic and dynamic parameters of seismic waves.

In section 1 an investigation is made of the spatial distribution of the spectral characteristics of longitudinal waves from remote earthquakes. It is shown that regional differences in the value of this parameter are statistically significant. A description is given of the spectral characteristics of P waves as distributed for earthquakes of the major seismically active zones of the earth, and in more detail for Central Asia. The region of the most minimal values of spectral parameters is confined to the Tibetan massif, and a region of somewhat higher values -- to the Persian Plateau. They are interpreted as regions of elevated absorption of seismic waves in the upper mantle.

Lg and Rg interference waves are registered only in the case where the entire path of the seismic ray traverses a crust of continental type. Consequently

by comparing the intensity of these waves on different propagation routes one can localize the blocks in which there is no "granite" layer, or other appreciable changes are noted in the structure of the earth's crust.

In sections 2 and 3, an investigation is made of the peculiarities of propagation of these waves on different paths that cross Central Asia and the adjoining territories. From observations of the system of stations, the boundaries are localized at which a change in the intensity of Lg waves occurs. These waves disappear completely in those cases where the paths of the seismic rays even partly intersect the Tibetan massif. On the boundaries of this massif, sharp changes are also noted in the parameters of a train of Rg surface waves.

1. Mapping of spectral characteristics of P waves

In this section an analysis is made of the results of mapping of the spectral characteristics of individual earthquakes done with respect to observations in the intermediate and teleseismic zones. The regional differences found in the spectral characteristics of P waves are interpreted as a manifestation of horizontal inhomogeneities of the absorbing properties of the upper mantle in the vicinity of the focus.

Spectral Characteristics of Remote Earthquakes and Absorbing Properties of the Upper Mantle. The experimental data presented below and the results obtained by other authors (Tsujiura, 1969) show the stability of regional differences in the spectral composition of longitudinal waves according to observations at remote stations. The spatial degree of ordering of the spectral differences can be attributed either to the particulars of focal radiation or to horizontal inhomogeneities of absorbing properties of the medium along the paths of the seismic rays.

We assume that the particulars of the focus, which are definitely important in formation of the spectral composition of an individual earthquake, may not be predominant in a set of earthquakes over an extensive territory. Experience in studying the spectral particulars of focal radiation of local earth tremors of a number of regions (Molnar et al., 1976; Hanks, Wyss, 1972; Thatcher, Hanks, 1973; Tucker, Brune, 1973) has shown that within the limits of each region there is a considerable variety of spectral characteristics, primarily of the angular frequencies, that is due to the difference in the mechanisms of foci and to variations in the stress field. Spatial ordering of spectral parameters is noted only for quite small epicentral zones. For extensive global seismically active regions, no systematic deviations of the spectral composition are noted in observations at small distances. Therefore we assume that the spectral differences observed in the teleseismic zone are formed mainly on the path of the seismic ray.

It has been established that the greatest distortions are introduced into the signal spectrum when a seismic ray crosses the low-Q layer associated with the

asthenosphere. Many researchers have detected considerable regional differences in the absorbing properties of this layer. Apparently it is the mosaic nature of the absorbing properties of the upper mantle that determines the great variety of steepness of the high-frequency slope of the spectra of remote earthquakes.

The presence of the asthenospheric layer has an effect both in the region of the epicenter and in the vicinity of the station. For a tectonically homogeneous region, the influence of the asthenospheric layer in the vicinity of the exit of the rays can be taken as identical in registration of earthquakes at a single station from different azimuths. Use of a system of observations from several stations almost completely eliminates this influence.

Thus we assume that the observed differences in the high-frequency slope of the spectra of remote earthquakes reflect mainly horizontal inhomogeneity of the absorbing properties of the upper mantle in the vicinity of the focus (with consideration of drift of the seismic ray). Spatial mapping of the peculiarities of the high-frequency part of the spectrum (with reference of these peculiarities to the epicenter) will reveal the regional differences of absorbing properties of the upper mantle in seismically active regions.

The Materials and Technique Used. About a thousand recordings of earthquakes of the territory of Central Asia and adjacent territories, recorded at ChISS stations (Garm, Talgar and Temporary) were processed. Besides, about 700 recordings of earthquakes from different epicentral regions of the earth were processed at these same stations. The magnitudes of the earthquakes were from 4.5 to 5.5.

The spectral ratio of amplitudes for channels with average frequencies of 2.5 and 0.7 Hz or 2.5 and 0.35 Hz was determined from the seismograms. The value of this parameter calculated from each recording was mapped, i. e. it was assigned to the epicenter of an earthquake. Maps were then constructed for an intermediate smoothing stage in which the average values of the parameter were calculated for a group of 5-10 closely spaced earthquakes. On the next smoothing stage the values of the parameters (the averages for large regions) were calculated, or maps of isolines of the parameter γ were constructed.

Zoning of the Earth by Spectral Peculiarities of Remote Earthquakes. On the first stage to determine the stability and scale of regional differences of the spectral composition of P waves an examination was made of the materials of the teleseismic zone, where the conditions of observations are more favorable for detecting the investigated effect than in the intermediate zone.

As is known (Antonova et al., 1968; Carpenter et al., 1967) in the teleseismic zone the distance factor can be disregarded, the seismic signal is simple in shape, and consequently the measurements of the maximum amplitudes are more unambiguous.

The experimental data on remote earthquakes that were used were obtained at Temporary station. Materials of the Garm and Talgar stations were utilized only in part.

More than 700 recordings of remote earthquakes from all major seismically active zones of the earth were processed. The logarithm of the amplitude ratio on frequencies of 2.5 and 0.5 Hz was taken as the characteristic of the spectrum.

The average values of this parameter for thirty epicentral territories are shown on the map in Fig. 31. It can be seen that the spectrum does not depend on epicentral distance. Earthquakes in relatively near regions -- Tibet, Iran, the Tyan' Shan'-Pamir chain -- are comparatively low-frequency.

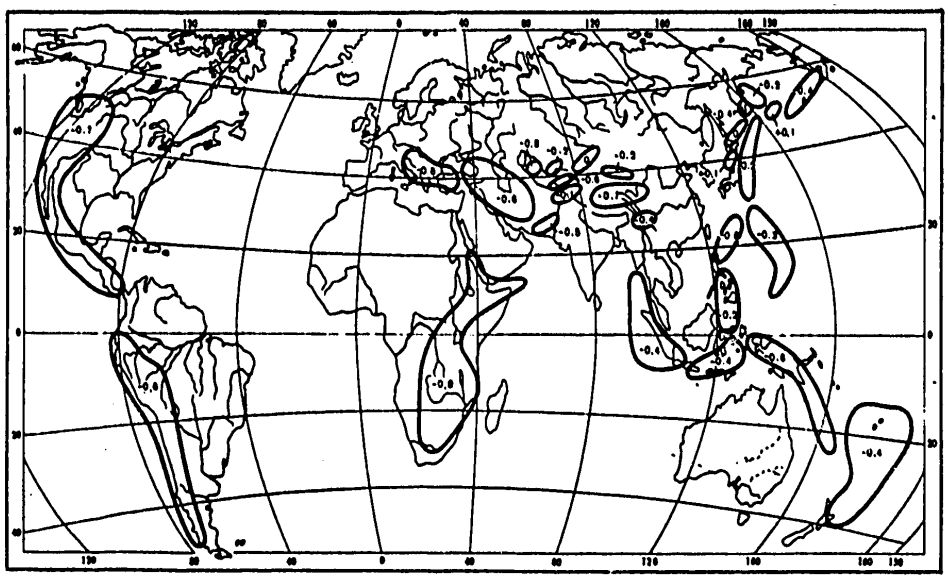

Fig. 31. Map of the spectral ratio γ(2.5 Hz/0.5 Hz) for the major seismically active zones of the earth (from data of the Temporary ChISS station)

In examining the map, we can see certain patterns in the spatial distribution of values of the parameter. All seismically active zones of the earth were classified into four groups differing in the parameter γ by 0.20-0.25 (i. e. by 50-80%).

The first, highest-frequency group, included earthquakes of the Aleutians, the Kuril-Kamchatka arc and Japan. The average value of the parameter γ for these territories is 0.16 log unit.

The earthquakes of Soviet Middle Asia and the part of Central Asia situated to the north of Tibet are also high-frequency. Here the average value of the parameter is 0.20. But these regions are located rather close to the recording station (distance 1000-2000 km), which may explain the high-frequency nature of the earthquakes.

The earthquakes of Indonesia and the Philippines, for which the average parameter is 0.33, make up the next group.

Still lower-frequency are the recordings of earthquakes of the Alpine belt -- the Mediterranean, Turkey, the Caucasus and Iran -- where the parameter averages 0.55. About the same values of the parameter are typical of earthquakes of South America and the continuation of the Indonesian belt to the east -- New Guinea, the Solomon Islands, the Fiji territory.

The lowest-frequency group is comprised by earthquakes of Tibet ($\gamma = -0.70$), North and Central America ($\gamma = -0.72$), South and East Africa ($\gamma = -0.82$).

The differences of the parameter between adjacent groups are significant since there were from 20 to 100 earthquakes in each regional sample, the average value of the standard deviation of an individual measurement within a sample being 0.25 log unit.

Analogous zoning, but with respect to a smaller number of epicentral regions, was also done from recordings of remote earthquakes at Garm and Talgar stations. Joint examination of the materials of the three stations showed a systematic influence, common to all zones, introduced into the spectrum by station conditions. In comparison with the Garm station, the spectra of the Temporary station were on the average more high-frequency, while those of Talgar station were more low-frequency.

The relative spectral differences of the epicentral regions were retained with respect to the recordings of the three stations as well. For instance the highest-frequency spectra were those of Northern Japan, the Aleutians and Indonesia. The spectra of the Mediterranean, South America and New Guinea occupy an intermediate position. The spectra of North America, Tibet, the Arabian Peninsula and South Africa are definitely low-frequency.

Of course one should not overestimate the generality of these data. The stations that were used are situated comparatively close together (average distance about 1000 km). It is possible that observations on completely different azimuths of propagation of rays, especially for seismically active zones, that extend along oceanic archipelagoes, will show other tendencies.

The spatial structure of the spectral parameter was studied in more detail for the northern and northwestern part of the Pacific arc of seismicity. The results of mapping of this region with respect to the parameter γ on the intermediate averaging stage are shown in Fig. 32. Here the average value of the parameter is shown for each group of epicenters made up of 3-6 earthquakes.

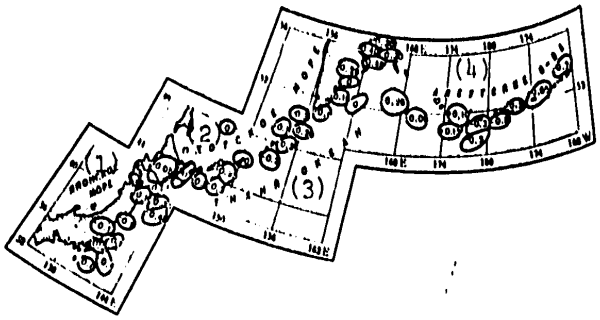

Fig. 32. Map of values of the spectral ratio γ(2.5 Hz/0.9 Hz) for the northern and northwestern parts of the Pacific Ocean seismically active belt (from data of the Temporary ChISS station)

KEY: 1--Sea of Japan 3--Pacific Ocean
2--Sea of Okhotsk 4--Aleutian Islands

On this map, one can clearly see the pattern of spatial distribution of the parameter γ. For instance for the Aleutian arc as one advances from east to west, the values of the parameter first increase from -0.7 to +0.15, i. e. the spectra become higher-frequency, and then they become lower-frequency once more, the parameter decreasing to -0.25.

For the Kuril-Kamchatka arc one notes a tencency for the parameter to increase with movement from the northeast to the southwest from -0.4 to +0.25. For Northern and Central Japan the patterns show up more weakly. Nevertheless two tendencies can be noted: concentration of high-frequency foci near the island of Hokkaido and intensification of the high-frequency character of earthquake spectra in the direction perpendicular to the axis of the trend of seismicity -- from a deep-water trench toward the continent.

To evaluate the statistical significance, we present the following data. The total number of epicenters with respect to which the values of the parameter were determined for the investigated part of the Pacific Ocean arc was 247, the average value of the parameter for the entire region was -0.17 log unit, the standard deviation of an individual measurement with respect to the entire region of investigation was -0.27 log unit, the standard deviation of an individual measurement within each group was -0.16 log unit. The difference of average values of the parameter for groups of earthquakes appreciably exceeds the standard deviation of an individual value.

The statistical significance of the results is also confirmed by the pattern of change in the value of the parameter γ along the Pacific Ocean arc.

Mapping of Spectral Parameters for the Central Part of the Asiatic Continent. Observations within the limits of this territory covered an interval of epicentral distances from 1000 to 4000 km. Here, in contrast to the

teleseismic zone, the influence of distance on the spectra of earthquakes becomes appreciable and the results of mapping should in principle reflect the patterns of change in the spectra for different directions. Such mapping will enable detection of regional differences in the values of the parameter γ not with respect to directions that are selected a priori, but will reveal their spatial structure.

The strong dependence of the spectra on distance impedes quantitative comparisons and estimates, making them possible only for regions that are located at different distances from the station. However, the actual situation is more favorable for quantitative comparisons of spectral parameters of different regions, since the spectra of longitudinal waves at distances greater than 1500 km change insignificantly, at least on frequencies lower than 2500 Hz. Most experimental data used in this division apply to distances in excess of 1500 km, while estimates of the steepness of the spectrum apply to frequencies lower than 2.5 Hz. All this has enabled us to apply to the intermediate zone as well the method of mapping spectral parameters already used above in the processing of observations in the teleseismic zone.

Estimates of the spectra of the same epicentral regions from data of different stations diverge more strongly in the intermediate zone than in the teleseismic zone, and it is difficult to make a quantitative comparison of maps plotted for the three stations. Nevertheless, even for these distances the results of the studies show coincidence of the position of regions of reduced and elevated values of the paraemter with respect to all three stations.

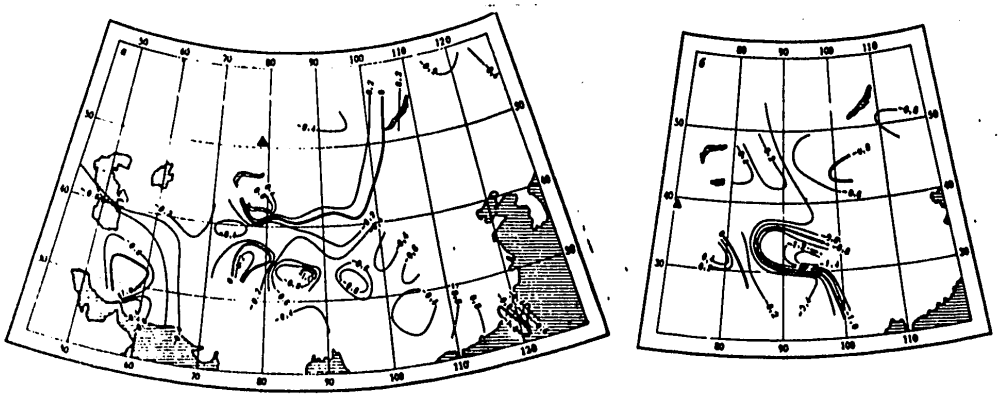

Fig. 33. Maps of isolines of values of the spectral ratio γ(2.5 Hz/0.5 Hz) for the central part of the Asiatic continent (from data of the ChISS stations of Temporary (a) and Garm (b))

Shown in Fig. 33 are maps of isolines of the spectral ratio γ for the central part of the Asiatic continent plotted from data of the Temporary and Garm stations. The region of minimum values of the parameter is confined to the

Tibetan plateau. According to the Garm data it is situated between 85-100° E long and 30-36° N lat., and according to data of Temporary station -- between 81-97° E long and 29-35° N lat. According to the data of Talgar station, the region of minimum values is less pronounced, and is situated between 84-100° E long and 29-35° N lat.

If consideration is taken of drift with respect to the directions of propagation of rays from the region of the minimum to the recording stations (for Garm toward the west-northwest, for Temporary toward the north, and for Talgar toward the northwest), the coincidence of the position of the differentiated minimum values with respect to the data of all three stations can be considered good.

Judging from the map of isolines, the maximum difference in values of the parameter within the limits of the region from its center toward the periphery is 0.6 log unit for Temporary station, and 1.0 log unit for Garm.

The number of determinations of the spectral ratio for territories inside Tibet and its framework (conventially taken as a strip 300 km wide) is 21 and 24 respectively for Temporary station, and 11 and 22 respectively for Garm station. The average values of the parameter inside and outside of Tibet are 0.75 and 0.35 log unit respectively according to Temporary, and 1.2 and 0.3 log unit respectively according to Garm. The value of the standard deviation of an individual determination from the average in all cases is equal to 0.2 log unit. The simplest analysis of these estimates confirms the statistical significance of the values found for γ in Tibet.

The few determinations of spectral ratios for Central Asia that have been made from recordings of ChISS stations at Novosibirsk and Bodon also show a minimum of the values of the parameter in the territory of Tibet.

Another region of minimum values of the parameter is located in the territory of the Persian plateau, approximately between 50 and 63° E long.

In more detailed zoning of the territory of Soviet Middle Asia from the data of Temporary station a strip of low-frequency earthquakes is distinguished that runs along the Tyan' Shan'-Pamir zone between 67 and 79° E long. Within the strip the average value of the parameter is minus 0.6, and along its periphery -- minus 0.2.

According to data of Garm and Talgar stations, a minimum is noted in the territory of Mongolia with a differential in values of the parameter between the center and the periphery that is equal to 0.4 log unit.

A region of high-frequency earthquakes is situated to the north and to the west of Tibet. These are the territories of Northwest China, Dzhungaria, Altay and Zaysan, Karakorum, the Hindu Kush and Kok-Shaal. However, the regions of maxima are not as pronounced as the regions of minima. The differential in values of the parameter γ between the center of the maximum and its periphery averages 0.4 log unit.

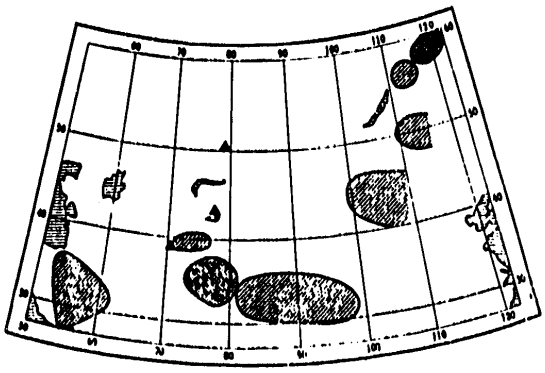

Fig. 34. Map diagram of the location of regions of elevated (light shading) and reduced (heavy shading) absorption for the central part of the Asiatic continent. Regions are shown that are repeated with respect to the data of the three stations -- Garm, Talgar and Temporary

The most general peculiarities that are steadily repeated in observations on the three stations are shown on the map diagram in Fig. 34. Regions of negative values of γ, i. e. elevated absorption, and positive values, i. e. relatively weak absorption, are distinguished.

The results, in particular for the regions of Tibet and Mongolia, agree well with independent determinations of the absorbing properties of the upper mantle within the limits of the investigated territory made by L. P. Vinnik and A. A. Godzikovskaya (1975).

2. Particulars of propagation of Lg waves on paths that cross Central Asia

The intensity of interference groups of waves of the Lg or Rg type depends considerably on the type of structure of the earth's crust on the path of propagation. If the path crosses even a small section with crust of oceanic type or transition type, this leads to sharp damping or even total disappearance of these waves. It is possible that other peculiarities in the structure of the earth's crust (disruption of the granite layer and the like) may also lead to effects of this kind. This is what makes it possible to use Lg and Rg waves as a simple and promising tool in studying the earth's crust.

In this section an examination is made of particulars of propagation of Lg waves on different routes that cross the central part of Asia. It is shown that Lg waves propagate over an appreciable part of the continent situated approximately to the north of the 35° parallel of north latitude. On routes that cross the Tibetan plateau these waves completely disappear. The study technique that is used reliably localizes large horizontal inhomogeneities in the structure of the crust, and possibly the upper mantle as well.

Region of Studies and the Materials Used. The intensity of Lg waves was studied on paths crossing Central Asia and the contiguous territories of China, Mongolia, the Soviet Union (Middle Asia, Kazakhstan, Siberia), India and in part Pakistan, Afganistan and Iran. The paths were within the territory bounded approximately by 75 and 125 E long and 20 and 55 N lat.

The particulars of propagation of Lg waves on routes crossing the Tibetan plateau were studied in more detail. This territory has received very little geophyscial study, even though information on its structure is extremely important for tectonic constructions and for an understanding of the mechanism of convergence and motion of tectonic plates. Therefore the dynamic peculiarities of propagation of Lg waves and the dispersion properties of surface waves are so far almost the only sources of information on the structure of the earth's crust within the borders of this mountain region.

Recordings of earthquakes on two groups of stations situated to the north and south of Central Asia were examined. Included in the northern group were the Soviet stations of Talgar (ТЛГ), Novosibirsk (НСБ), Bodon (БДН) situated 50 km to the east of Lake Baykal, and in part Garm (ГРМ). Included in the southern group were stations of the world-wide seismic network (WWSSN) situated in India and Southeast Asia: New Delhi (NDI), Chiangmai (CHG), Shillong (SHI), etc.

The four Soviet stations used ChISS seismograms in the frequency band from 4 to 0.05 Hz. The stations of the world-wide network used recordings of standard short-period and medium-period equipment. An analysis was made of several hundred recordings of earthquakes from different focal zones located both within the investigated region and on its outer border. The magnitudes of the earthquakes lay mainly in the range of 4.5-5.5. Epicentral distances were from 300 km to 3000-3500 km.

Regional Differences in the Intensity of Lg Waves. In most cases Lg waves have the maximum amplitude on earthquake recordings. This applies to the seismograms of short-period instruments or ChISS channels in the range from 0.5 to 3 s. The wave group as a rule has clear entries.

Particularly clear and intense entries of Lg waves are observed on recordings of the north group of stations for earthquakes of Altay, Sayan, Pribaykal'ye, Mongolia and Eastern Siberia. One of the most characteristic features of the dynamics of Lg waves in the investigated region is that this group of waves always predominates on the recording of all earthquakes of the eastern and northeastern azimuths of propagation (relative to the northern group of stations). For earthquakes of the western and southwestern azimuths of propagation, Lg waves are reliably observed and predominate on the recording only within the limits of the first 2000 km of the epicentral distance. After that their intensity gradually declines, and the spectrum shifts toward longer periods.

The Lg wave group shows up on all earthquakes situated to the east of the Caspian, to the north and northeast of the Persian plateau and to the north

of the Tibetan massif. Within the limits of the extensive territory conventionally bounded by the enumerated regions, Lg waves propagate without undergoing any appreciable changes. These estimates apply to routes of northeast, north and south (to the limits of Tibet) directions of propagation relative to stations located in the USSR (north group).

An exceptionally abrupt change in the amplitude of Lg waves is noted when paths of propagation cross the north border of the Tibetan massif. As long as the epicenters of earthquakes are to the north of this boundary, running approximately along 35° N lat, Lg waves are clearly apparent on the recordings of all northern stations and predominate in amplitude. On the recordings of earthquakes with epicenters located close to the northern border of the Tibetan massif, the Lg waves are noticeably attenuated, and are totally absent if the epicenters are 100 km or more to the south of this border.

For instance, for two earthquakes with approximately equal amplitude of P waves, but situated on different sides of the boundary with a distance of the order of 150-200 km between epicenters, the differences in intensity of the Lg waves may reach a factor of 100 or more. In this connection, on seismograms of the focus further to the south in the pair being compared, no wave groups at all can be distinguished at the place where one would expect the entry of Lg waves.

Everything that has been said here is illustrated by the set of recordings of earthquakes of two azimuths of propagation shown in Fig. 35 (Baykal and Tibet) obtained at Temporary station. The coordinates of the epicenters of these earthquakes are given in Table 14. It is apparent that on the recordings of the Baykal direction (Fig. 35a) the Lg waves can be confidently identified and predominate at all distances right up to 3000 km.

TABLE 14

Coordinates of epicenters of earthquakes with recordings shown in Fig. 35

(1) Байкальское направление			(2) Тибетское направление		
№ п/п	(3) φ° с.ш.	(4) λ° в.д.	№ п/п	(3) φ° с.ш.	(4) λ° в.д.
1	52,9	89,5	11	40,0	77,4
2	55,1	93,1	12	37,4	77,8
3	46,4	96,6	13	37,9	86,0
4	44,9	101,0	14	35,3	86,4
5	53,1	107,8	15	34,8	87,4
6	56,6	114,0	16	34,0	87,0
7	58,2	120,7	17	30,0	84,4
8	56,3	123,6	18	32,5	93,7
9	56,9	127,7	19	28,2	93,3
10	44,7	82,8			

KEY: 1--Baykal direction
2--Tibet direction
3--φ° N lat
4--λ° E long

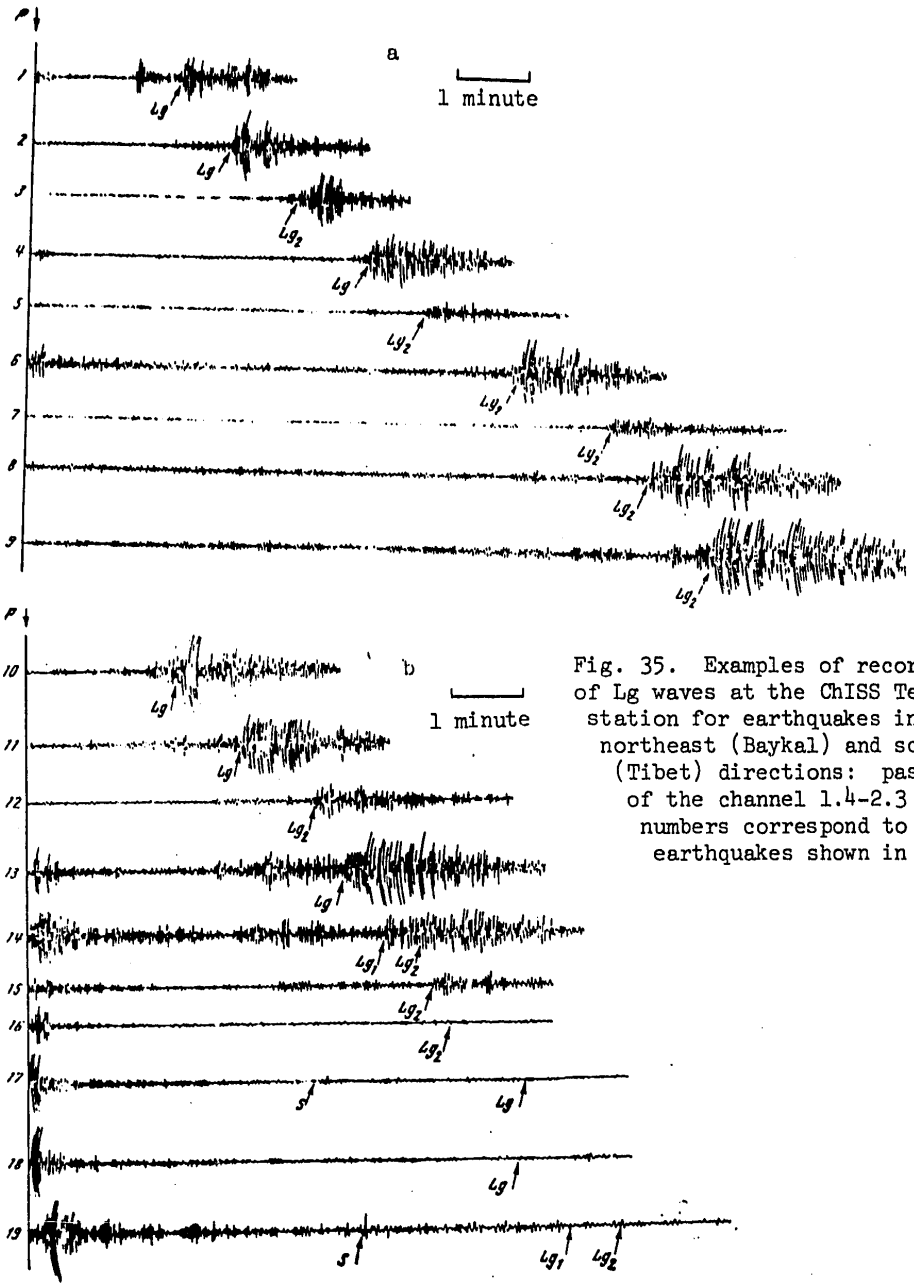

Fig. 35. Examples of recording of Lg waves at the ChISS Temporary station for earthquakes in the northeast (Baykal) and south (Tibet) directions: passband of the channel 1.4-2.3 s. The numbers correspond to the earthquakes shown in Table 14

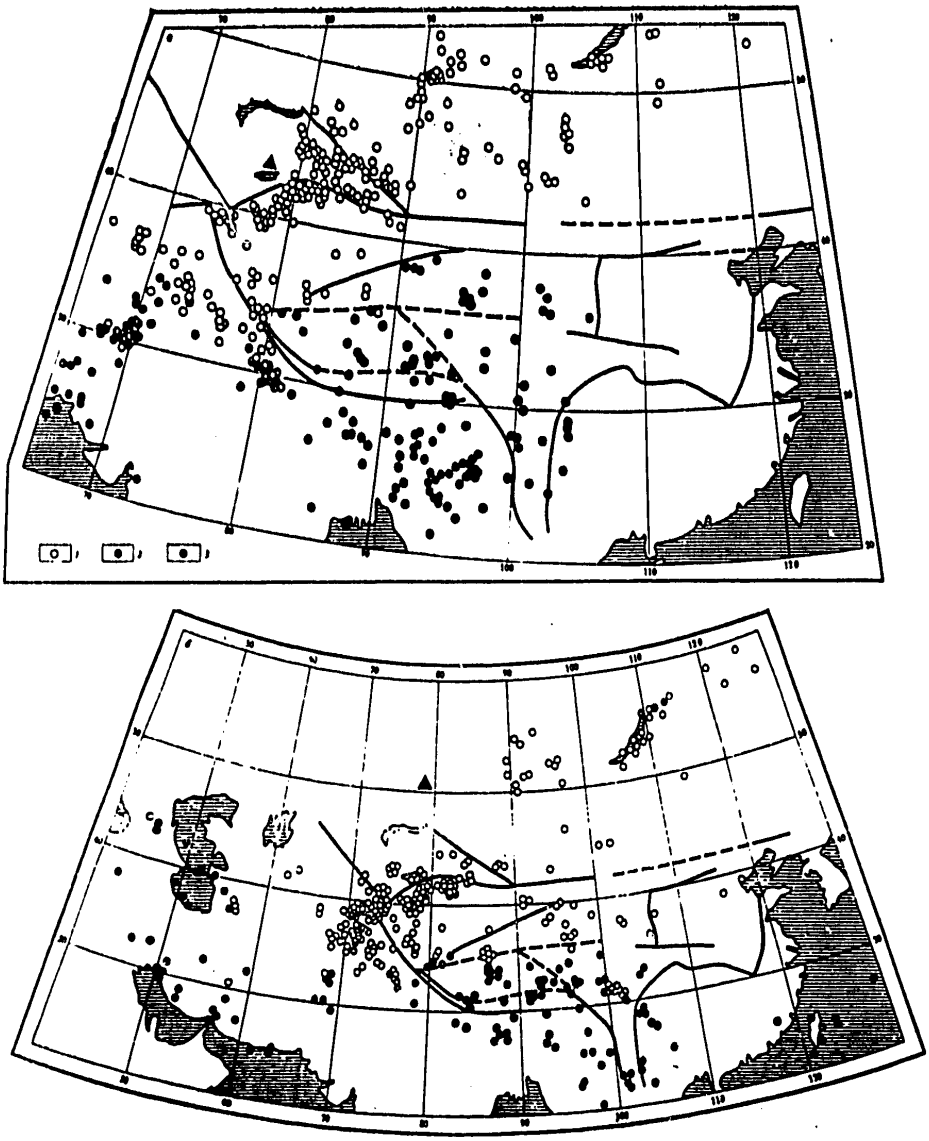

Fig. 36. Maps of epicenters of earthquakes showing qualitative evaluation of the relative intensity of Lg waves from recordings of Talgar (a) and Temporary (b) stations: 1--Lg waves predominate with respect to amplitude on the seismogram; 2--Lg waves have low amplitude; 3--Lg waves entirely absent; major fractures are shown by solid and broken lines.

An approximately similar pattern is observed on recordings of the Tibet direction (Fig. 35b) as long as the epicenters are to the north of the Tibetan massif (No 10-13). Epicenters situated directly on the boundary of the massif (recording No 14) are characterized by a noticeably attenuated Lg wave. A still sharper contrast is apparent between the recordings of earthquakes No 15 and No 16, located directly on the boundary of the massif and 90 km to the south respectively. On the recording of the south earthquake the Lg waves are totally absent. They cannot be seen at all either on earthquakes still further to the south (No 17-19).

Such strong difference in the intensity of Lg waves enabled us to use a simplified method of classifying recordings. All seismograms considered were broken down into three groups with respect to amplitude level. The first group included recordings with an intense Lg wave (of the type of No 1-12, Fig. 35a, b), in the second group the amplitude of the Lg waves is approximately equal to that of P waves or somewhat lower (type 13-15 on Fig. 35b), and the third group included no Lg waves at all (type No 16-19 on Fig. 35b).

The results of such sorting of the recordings obtained at the Talgar and Temporary stations are shown in Fig. 36 in the form of maps of the epicenters of the given earthquakes. The type of recording is arbitrarily assigned to the epicenter.

Unfortunately, such maps were constructed only for northern stations since we had little available experimental data on southern stations.

A comparison of the recordings of the same earthquake at different stations shows that the intensity of the Lg waves is practically independent of the source, but is determined by the location of the path. For some earthquakes for which we had recordings made at several stations, the positions of the epicenters are indicated together with the paths of the seismic rays corresponding to the system of observations (Fig. 37). Here we selected only those epicenters such that their position relative to the recording stations enabled more precise determination of the boundary where the Lg waves disappear. The prevailing system of observations does not permit an answer to the question of whether the disappearance of the Lg waves is connected with the influence of this geological boundary or these waves do not propagate within the limits of the territory of the Tibetan plateau.

Fig. 38 shows the amplitude graphs of Lg waves for two directions: Baykal and Tibet. On these graphs, plotted from data of the Talgar and Temporary stations, the shading shows the interval of epicentral distances that corresponds to the north boundary of Tibet. It can be seen that for the Tibetan direction in this region the amplitudes decrease by at least an order. Such an estimate is the lower limit of the change in amplitudes since on the earthquake recordings where the Lg waves were absent the phase amplitudes of scattered oscillations were measured on the section of existence of Lg waves that was isolated in accordance with the average hodograph.

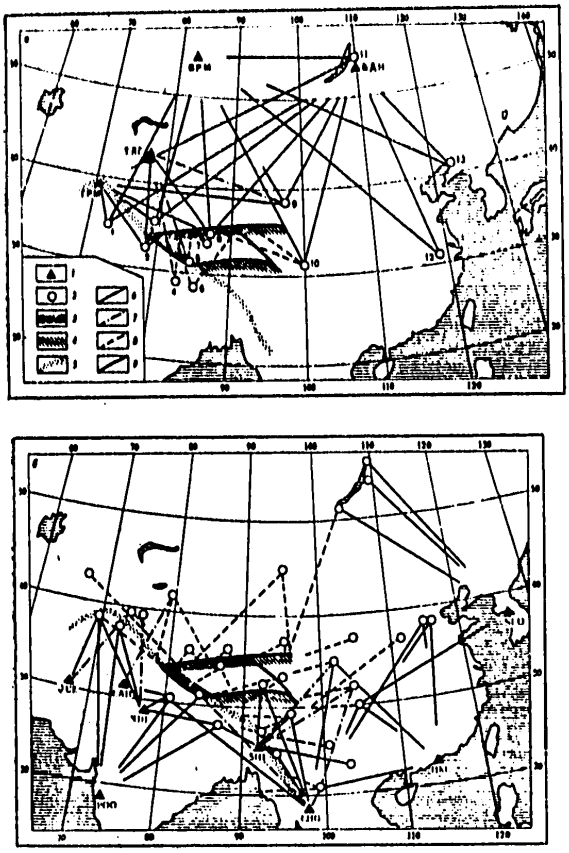

Fig. 37. Maps of epicenters and paths of propagation of Lg waves toward the northern (a) and southern (b) groups of stations: 1--seismic stations; 2--epicenters; 3--"sharp" boundaries that totally screen Lg waves with position fairly reliably determined; 4--the same boundaries drawn hypothetically; 5--"weak" boundaries where Lg waves are appreciably attenuated when they cross; 6--paths corresponding to recordings with intense entries of Lg waves; 7--paths with recordings of intermediate type; 8--paths corresponding to recordings with total absence of Lg waves; 9--deep-level breaks that outline the Tibetan massif according to the tectonic map of Eurasia

From the graphs of the Baykal direction we can see that the intensity of Lg waves changes weakly when they cross such a large tectonic structure as the Baykal rift zone.

The position of the boundaries that cause disappearance of Lg waves or that separate regions (blocks) that are "favorable" or "unfavorable" for the

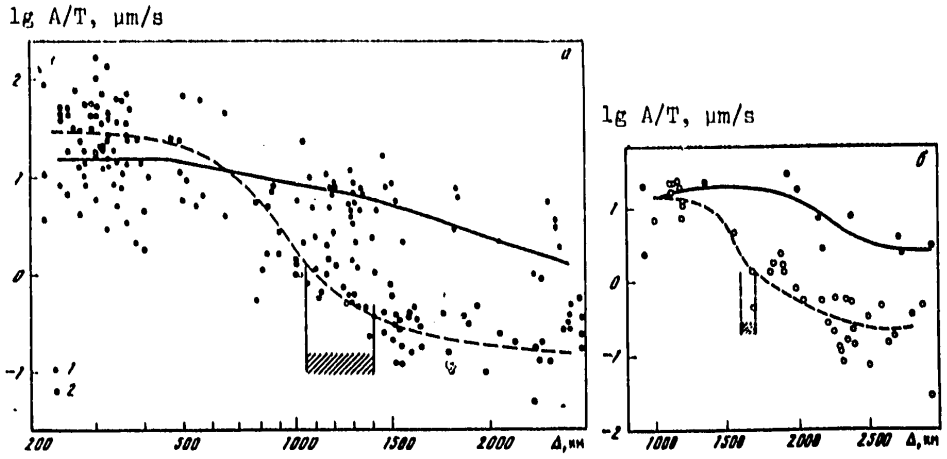

Fig. 38. Graphs of attenuation of the amplitudes of Lg waves according to the data of Talgar (a) and Temporary (b) stations for the Baykal (a) and Tibet (b) directions. The shading shows the distance interval that corresponds to the north boundary of the Tibetan plateau

propagation of Lg waves can be more precisely determined from analysis of the maps shown in Fig. 36 and 37. First let us consider the north boundary. This boundary passes approximately between points with coordinates 34° N lat and 78° E long, and 35.5° N lat and 90° E long. Its position with respect to latitude is most reliably determined with an error of less than 100 km. This is apparent from the maps (see Fig. 36) when a comparison is made of the intensity of the Lg waves from recordings of two closely spaced epicenters (No 8 and 9 on Fig. 37a). Analysis of all data confirms that the north boundary is the sharpest and its position is determined by the accuracy of calculation of the coordinates of the epicenters, which is apparently not high here, and according to our estimates amounts to 30-50 km, which is due to the unilateral location of the stations.

We cannot speak so confidently of the western and eastern ends of this boundary. For instance the west end is apparently at 78° E long, which is verified by the data of the maps (see Fig. 36) and the sharp difference in the intensity of Lg waves on paths going from epicenter No 2 toward the northern stations (see Fig. 37a).

The position of the eastern terminus of the boundary, according to data of different stations, is ambiguously determined. With respect to the recordings of Talgar station (see Fig. 36a) the boundary that separates the two types of paths goes along the parallel of 36° N lat and terminates at about 97-98° E long. The few determinations from recordings of the Novosibirsk station indicate that beyond the point with coordinates 36° N lat and

90° E long the boundary goes in the northeasterly direction to approximately 96° E long, coinciding with the deep-level break that bounds the Tibetan massif on the northeast. This hypothesis is also confirmed by data on the intensity of Lg waves on different routes according to the recordings of Bodon station.

The southwest and south boundaries of the block, which do not transmit Lg waves, are localized by recordings of the southern group of stations (see Fig. 37b) with less surety. On the section between 78 and 90° E long they apparently coincide with the system of deep-level breaks that separates the Tibetan massif from the Himalayas (the Karakorum break on the southwest and the "Indian suture" on the south). Further on this boundary goes off toward the southeast, apparently coinciding with the general trend of geological structures, but in view of the dearth of experimental data on the intensity of Lg waves, it can be only hypothetically drawn.

The effect of disappearance of Lg waves is observed, in addition to Tibet, on paths that cross the Zagros break zone separating the Iranian plateau from the Zagros Mountains. However, we have not examined this region in detail.

Along with the "sharp" boundaries, one can distinguish "weak" boundaries at which a reduction in amplitudes of Lg waves takes place. Such a boundary (Fig. 37) passes along the Hindu Kush-Karakorum arc, and its continuation to the southeast. Among the "weak" boundaries is the strip that coincides with the Kopetdag Foothill downwarp, and further to the east with the Herat break, and also the northwest border of the Indian shield (Beluchistan, the Sulaiman Range). Thus an investigation of the relative intensity of Lg waves on routes crossing Central Asia and the contiguous territory has shown the following.

Lg waves are reliably registered over the entire extensive territory of the Asiatic continent that is situated to the north of the Kopet-Dag and its continuation, Hindu Kush and the Tibetan plateau, and also on the territories of the Indian shield.

Lg waves are attenuated as they cross Pamir-Hindu Kush, the north border of the Indian shield, in propagation along Tyan' Shan'.

Lg waves are completely absent on recordings if the epicenter is located within the Tibetan massif, or the path of the ray even partly crosses this territory. Even 100-150 km of travel through Tibet is sufficient for total disappearance of these waves on recordings.

3. Regional differences in the characteristics of Rg waves

The Rg wave group in most instances is observed on seismograms simultaneously with Lg waves. The properties of both wave groups are to a great extent analogous. They propagate only on continental paths, have comparatively clear entries, their velocity is independent of distance.

In the intermediate distance zone under the conditions of the southeastern USSR, Rg waves usually predominate in amplitude through the entire train of surface waves, and have a group velocity of about 3 km/s (Ruzaykin, Khalturin, 1974). For earthquakes with magnitude of less than 5.5, this group is frequently the only one to be distinguished in a train of surface waves, especially at distances of up to 1500-2000 km.

The Rg wave group usually takes the form of a short train on the seismogram, consisting of several extrema without pronounced dispersion. The apparent period of the oscillations in the group is 8-12 s. The low-frequency character as well as the fact that other poorly identifiable surface waves follow this group make it difficult to distinguish Rg waves on seismograms. Therefore, parameters that characterize the entire train of surface waves were picked out as the object of measurements. In the great majority of cases they applied directly to the Rg group.

In this section we give the results of investigation of the parameters of a train of Rg surface waves -- its duration, shape of the envelope, time of onset of maximum amplitude -- observed on different paths crossing the Central part of the Eurasian continent. It is shown that the changes in these parameters with transition to more remote earthquakes take place in many instances abruptly rather than gradually. This made it possible to localize the territories responsible for such changes, and then to interpret them as large horizontal inhomogeneities in the structure of the earth's crust. The Tibetan plateau is the largest such inhomogeneity in the investigated region.

Moreover, to check the methods developed, the characteristics of the train of surface waves were studied on different paths corssing the Black Sea. According to data of several stations, we have reliably localized the deep-water part of the Black Sea Basin for which a crust of suboceanic or transitional type is typical.

Materials Used. Method of Measurements and Processing. The recordings of a channel with passband of 10-20 s of the Temporary ChISS station were used for studying the parameters of Rg waves. The data of a total of 300 earthquakes of Soviet Middle Asia, Siberia, Mongolia, China, India, Pakistan, Iran and the Caucasus were processed in all. The range of epicentral distances was from 600 km to 400-5000 km. The use of band filtration with magnification of the order of 15,000-20,000 enabled confident differentiation of trains of surface waves even for comparatively weak earthquakes with magnitude of 4.5-5.

The apparent periods of maximum amplitudes ranged from 7-9 s at the beginning of the tracking interval to 12-14 s at the end.

At distances up to 1500 km in all cases, and at greater distances in nearly all cases, the train of surface waves was simple in form and consisted of 3-4 extrema with a comparatively clear entry and very weakly expressed

dispersion. The group velocity was equal to approximately 3.0 km/s, varying over a range of 7-8% in different directions.

To describe kinematic peculiarities the parameter $t'_{max} = t_{max} - (\Delta/3.0)$ was used, where t_{max} is the time of onset of the maximum of amplitudes in the train of surface waves at epicentral distance of Δ km.

The form of the train was characterized by duration τ -- the time of existence on the seismogram of amplitudes of at least $1/3$ of the maximum.

The amplitude changes on the route were characterized by the magnitude correction $\Delta M = M_{st} - \bar{M}$, where M_{st} is calculated for the given station, and the average value of the magnitude $\bar{M}$ is determined with respect to the network of stations.

The further technique for representation of primary data was identical to that used in processing the materials of Lg waves. Curves were plotted for the parameters t'_{max} and τ as functions of distance for several directions of propagation, these parameters were mapped by assigning their values to epicenters, and the values of the parameters were compared on different paths crossing the investigated territory.

Changes in parameters with distance were considered for four directions of propagation relative to Temporary station: Northeast -- Altay, the Sayans, Pribaykal'ye, East Siberia, Kamchatka, the Aleutians; East -- Northwest China, Mongolia, Northeast China, Sakhalin, Southern Japan; South -- Northwest China, Tibet, South China, India, the Indian Ocean; Southwest -- Soviet Middle Asia, Afganistan, Pakistan, Iran, the Caucasus, Turkey.

The time of onset of the maximum amplitude t'_{max} reduced to a group velocity of 3.0 km/s is shown on Fig. 39 as a function of epicentral distance for the four directions of propagation relative to Temporary station.

It can be seen that on the graph of the Northeast direction (Fig. 39a) the velocities lie in a range of 3.0-3.2 km/s for the entire continental segment of the path within which the Rg group is distinguishable. At distances of more than 4000 km (beginning of oceanic routes) the times t'_{max} and accordingly the average group velocities increase sharply.

Typical of the East direction (Fig. 39b) is approximately constant time t'_{max}; group velocities are 2.9-3.1 km/s. The most remote earthquakes (Sakhalin, Southern Japan) are situated on routes with a continental type of crust.

For the South direction (Fig. 39c) the Rg group is reliably distinguishable only up to 1500 km, beyond which it disappears on all recordings for paths that cross the Tibetan plateau. On other routes in the same direction the Rg wave group gradually stretches out, the number of extrema increases. On Tibetan routes, recordings show up with large values of t'_{max}, while for other routes this quantity increases gradually. The average group velocities

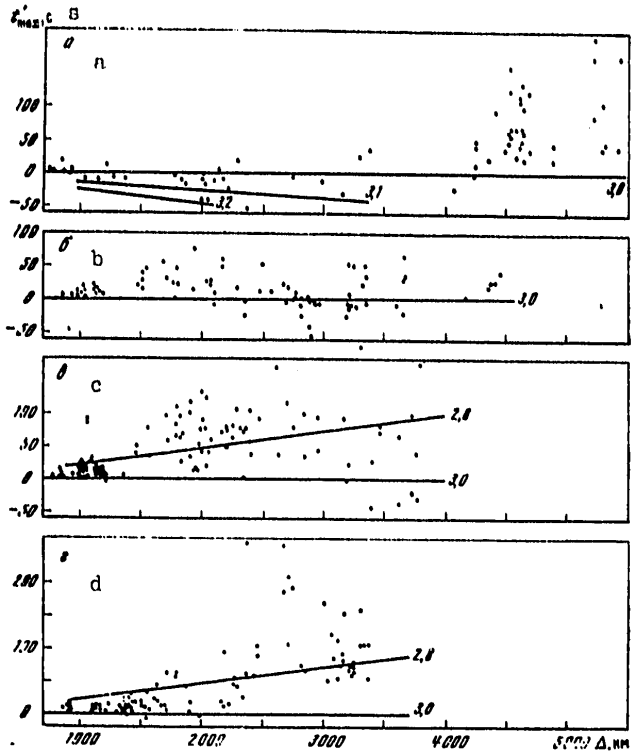

Fig. 39. Time of onset of maximum amplitude t'_{max} in a train of surface waves reduced to a group velocity of 3 km/s as a function of epicentral distance from data of the Temporary ChISS station (passband of the channel 10-20 s) for the Northeast (a), East (b), South (c) and Southwest (d) directions

lie in a range of 2.7-3.0 km/s, and are much lower for recordings from foci located inside Tibet (distances from 1600 to 220 km).

In the Southwest direction (Fig. 39d) up to distances of 1500-2000 km the group velocities are 2.8-3.0 km/s, and then they gradually decrease to 2.6-2.8 km/s with increasing distance. Crossing the Caspian leads to total transformation of the train of Rg waves; it is considerably stretched out, and the times of onset of maximum amplitude increase sharply to 150-300 s.

Duration of Recording of a Train of Surface Waves. Graphs of the change in duration with distance for three directions are shown in Fig. 40.

Typical of the East direction (Fig. 40a) is a weak change in duration: within the limits of the continental section of the path (up to 3700 km) it remains

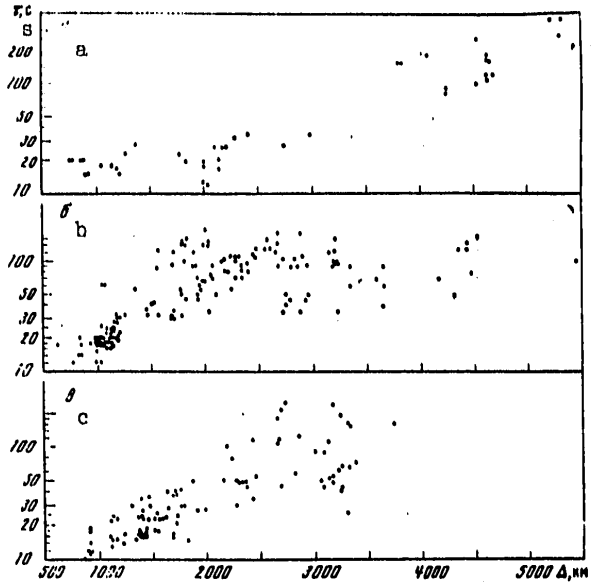

Fig. 40. Distance dependence of duration of a train of surface waves for the Northeast and East (a), South (b) and Southwest (c) directions

approximately equal to 15-30 s. For earthquakes from the territory of the Pacific Ocean the duration increases sharply to values of 100-300 s. The Rg group follows and retains its simple shape over the entire continental path. It is lacking in more remote earthquakes; a complex distended pattern of surface waves is observed.

In the South direction (Fig. 40b) the investigation of duration with distance follows another pattern. Here the train keeps its original form, and accordingly a short duration of the order of 12-30 s up to distances of about 1300 km. A bend then takes place in the train that is especially noticeable on recordings of earthquakes located within the Tibetan plateau. On these recordings the compact Rg group disappears, and a distended group of surface waves shows up at later times. The overall duration increases sharply and then changes but little, remaining within limits of 40-150 s.

In the Southwest direction (Fig. 40c) the duration increases approximately in proportion to the square of the distance. A sharp increase in duration -- up to 150-200 s -- takes place on the recordings of earthquakes on routes that have crossed the Caspian Sea.

The parameters of the train of surface waves t'_{max} and τ were mapped by the method described above as applied to the spectral parameters of longitudinal

waves. The value of a parameter was nominally assigned to an epicenter and intermediate averaging was then done with respect to 3-6 closely spaced epicenters. Maps of this stage of averaging of the parameters t'_{max} and τ are shown on Fig. 41. They illustrate the major trends in variation of parameters in different directions, and indicate the spatial confinement of points of greatest changes in the parameters (maximum values of the gradient).

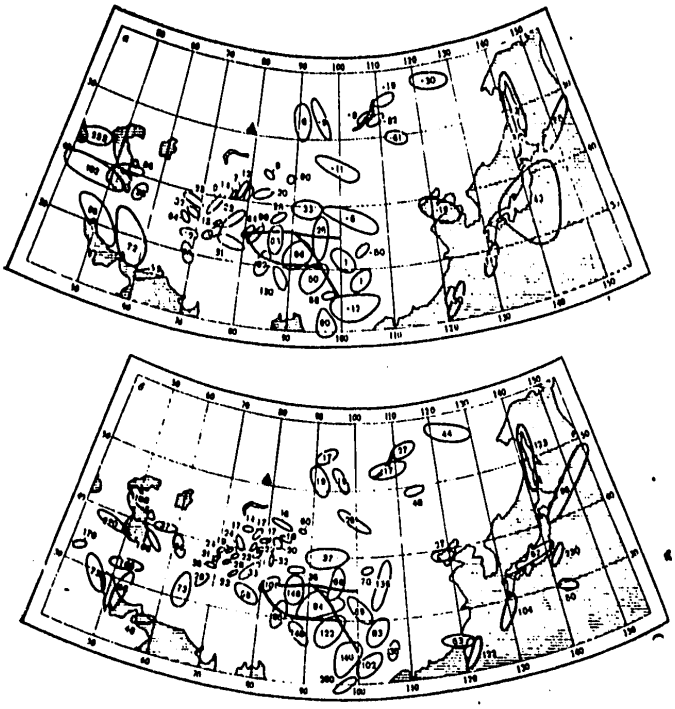

Fig. 41. Maps of the parameters t'_{max} (a) and τ (b) from data of the Temporary ChISS station

Within the limits of the transition zone from the Asiatic continent to the Pacific Ocean, abrupt changes in the parameters occur only where the routes cover a section of crust of oceanic type.

Among those territories with a maximum gradient is the Caspian Sea. On routes that cross or even graze the southern part of the Caspian Sea Basin (with crust of transitional type) the train is completely broken, resulting in an abrupt rise in the measured parameters.

Somewhat less of an increase in the values of the parameters also takes place when the Persian plateau is crossed.

A section of the strongest changes in the parameters of a train is situated on the territory of Central Asia, confined to the northern boundary of Tibet. For instance on recordings of earthquakes with epicenters to the north of Tibet within a strip approximately 500 km wide the values of the parameters t'_{max} and r are equal to 35 and 28 s; on the recordings of earthquakes situated inside Tibet, the values of the parameters increase right away to 80 and 125 s respectively. A comparison of the parameters of earthquakes close to the boundary of Tibet but on both sides of that boundary showed that the parameters change sharply rather than gradually.

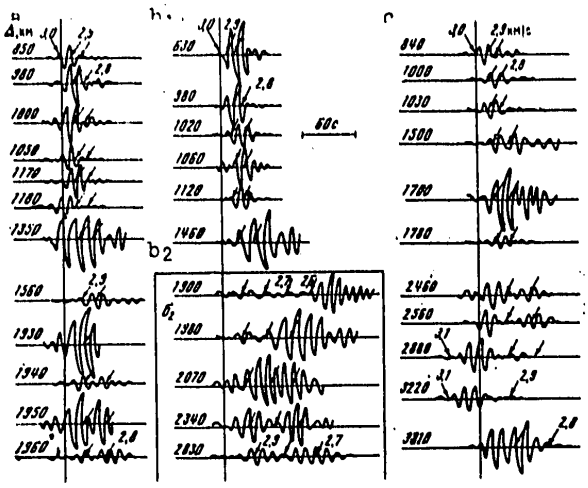

Fig. 42. Specimens of recordings of trains of surface waves for directions that pass to the west of Tibet (a), cross the Tibetan plateau (b) and pass to the east of Tibet (c). For the direction that crosses the Tibetan massif (b), we distinguish recordings from earthquakes located to the north of Tibet (b_1) and within Tibet (b_2). The vertical line corresponds to a group velocity of 3.0 km/s. The arrows indicate the times on the seismograms that correspond to group velocities of 3.1, 2.9, 2.8, 2.7 and 2.6 km/s. Temporary ChISS station, channel with passband of 10-20 s

The influence that the boundary of Tibet has on the shape of the recording of a train of surface waves is illustrated by the set of seismograms shown in Fig. 42. Shown here are specimens of the recording of a train of the Rg group for three comparatively narrow directions of propagation: a--for paths to the west of Tibet; b--for paths that cross Tibet, and c--for those going to the east of Tibet. A distinction is made between the recordings of earthquakes from epicenters located to the north of Tibet (b_1) and directly in the Tibetan massif (b_2).

Up to distances of 1500 km the shape of the train is approximately the same and comparatively simple in all directions. After crossing the northern

boundary of Tibet or its continuation (1600 km for the western sector, 1700 km for the Tibetan sector and 2000 km for the eastern), the shape changes noticeably, especially sharply on the recordings of earthquakes located inside the massif. The time of onset of the maximum amplitude of the train increased by 100 s relative to the velocity of 3.0 km/s, and the shape of the train was noticeably stretched out.

Gradually, with increasing epicentral distance in the South direction, the train is somewhat consolidated, and its shape becomes closer to that of the neighboring directions at the same distances.

Thus when the northern boundary of the Tibetan plateau is crossed there is a loss of the Rg phase and associated strong changes in both parameters of the train. These changes have the same scale as with a transition from paths of propagation along an oceanic type of crust to routes with a continental type.

Propagation of Surface Waves on Paths that Cross the Black Sea. As has already been stated, to evaluate the possibilities of the method and compare the scales of distortions that arise in a train of surface waves when horizontal inhomogeneities are crossed in the earth's crust, analogous work was done for the territory of the Black Sea Basin.

It is known (Balavadze, Mindeli, 1966; Neprochnov, 1962) that the deep-water part of the Black Sea is characterized by a crust of intermediate type in which there is no granite layer. The boundaries of this section and its structure have been independently studied by several geophysical methods with the maximum possible detail.

Seismologists have established (Savarenskiy, Val'dner, 1960; Sikharulidze, 1963) that Lg and Rg waves are totally screened by this part of the Black Sea Basin. The belt of active seismicity that passes to the south and west of the Black Sea, and the presence of a network of recording stations provide good conditions for "x-raying" the entire Black Sea area and adjacent territories by using Rg waves from seismic sources on different paths.

All this makes the region of the Black Sea an ideal testing ground for evaluating the possibilities of the method and quantitative comparisons of the scales of measurements of parameters here and in Tibet.

To study changes in the parameters of a train of surface waves on routes that cross the deep-water part of the Black Sea and pass outside of it, more than 300 recordings of 120 earthquakes on stations of Obninsk, Simferopol' and Bakuriani were processed. The parameters t'_{max} and τ were measured on seismograms of SK and SKD instruments. Besides, the magnitude correction ΔM was calculated for each recording.

The results of measurements in the form of maps of the intermediate stage of averaging are shown in Fig. 43. Given here for each of the three stations

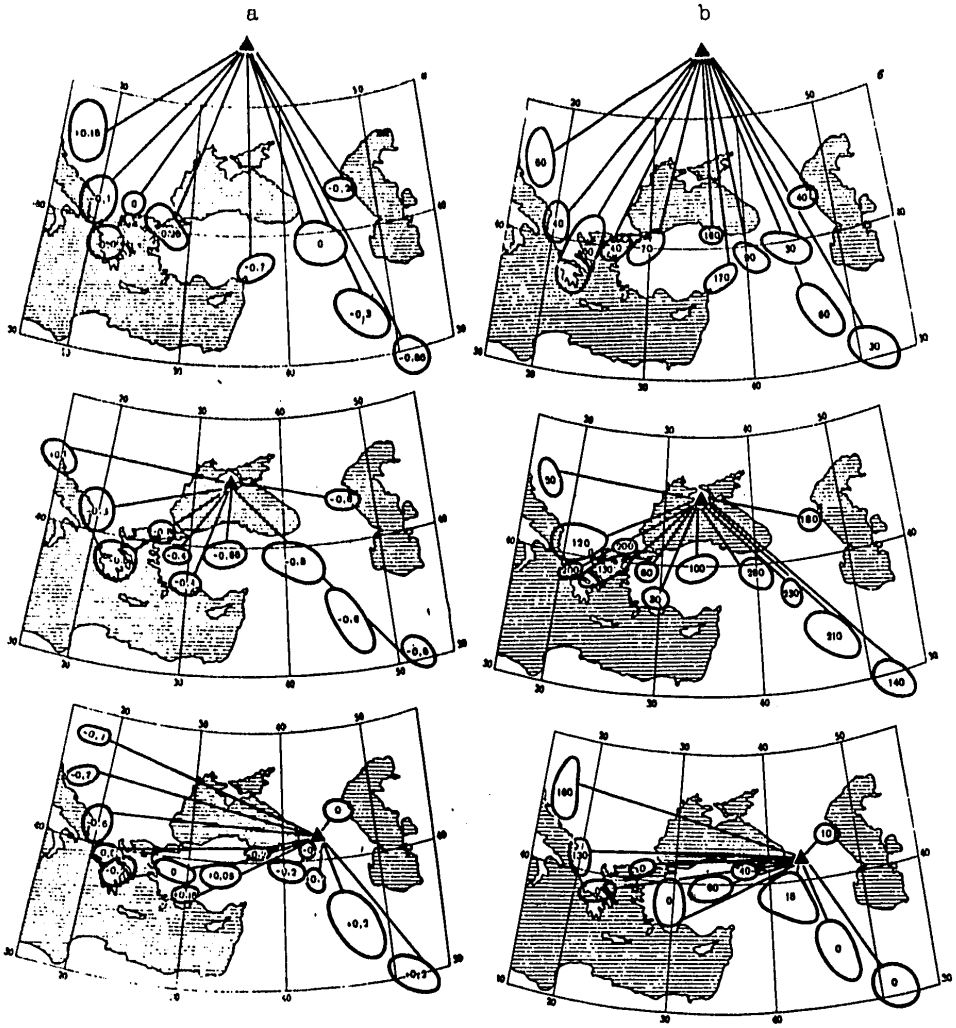

Fig. 43. Maps of values of the parameters ΔM (a), t'_{max} (b) and τ (c) [next page] according to data of stations at Obninsk (top), Simferopol' (center) and Bakuriani (bottom)

considered are maps of the magnitude deviation ΔM (Fig. 43a), the parameter t'_{max} (Fig. 43b) and the parameter τ (Fig. 43c).

One can readily see the effect of an abrupt increase in parameters t'_{max} and τ and a reduction in ΔM on paths that cross the deep-water part of the sea. The average values of all three parameters with respect to each station

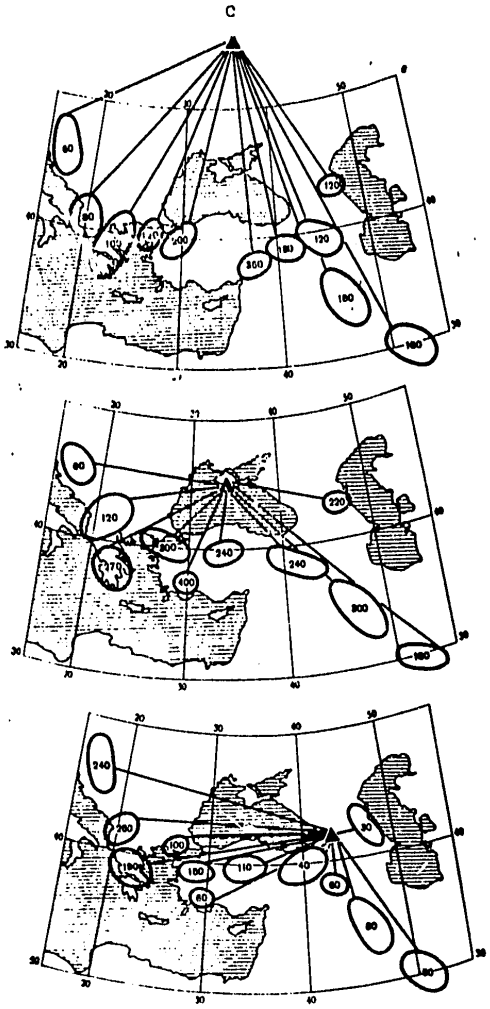

Fig. 43 (continued)

separately for routes that cross the deep-water basin and pass by it are summarized in Table 15 along with the standard deviations of the individual determinations of the parameters.

TABLE 15

Parameters of a train of surface waves for routes that cross the deep-water basin (1) and pass by it (2)

(1) Станция	ΔM		t'_{max}, с		τ, с	
	1	2	1	2	1	2
(2) Обнинск	−0,7	−0,15	140	50	250	110
(3) Симферополь	−0,7	−0,10	170	50	280	90
(4) Бакуриани	−0,6	0	150	15	250	90
(5) Среднее	−0,67	−0,08	150	40	200	100
σ	0,12	0,15	42	23	50	35

KEY: 1--Station
2--Obninsk
3--Simferopol'
4--Bakuriani
5--Average

Analysis of the data in the Table shows that crossing of the deep-water basin by the path of a seismic ray shows up in the following changes of parameters: reduction of the maximum amplitude of the train of surface waves by a factor of 4, increase in duration by a factor of 2.5, and in the parameter t'_{max} by a factor of 4.

The statistical significance of this effect cannot be doubted since the difference of the averages exceeds σ -- the standard deviation of an individual determination of the parameter -- by a factor of 4-5, assuming that the average value was determined from samples containing 20-25 individual determinations.

Comparison of the Influence that Large Inhomogeneities have on the Parameters of a Train of Surface Waves. An examination was made of the largest inhomogeneities of the earth's crust of the investigated territory whose influence on the parameters of the train was detected in analysis of seismologic materials. Surface waves experience strong distortions when they cross the Tibetan massif, the Caspian and Black seas, the Persian plateau and the transition zone from the continent to the ocean in the territory of the Kuril-Kamchatka arc.

The average values of the parameters of the train t'_{max} and τ were determined for the enumerated structures from the recordings of earthquakes with foci located on both sides of the structure within a 300-500 km strip. The first group (1) includes earthquakes whose routes cross the investigated structure; the paths of the second group (2) do not cross (Table 16).

The magnitude deviation ΔM was also determined for the Black Sea territory. The value of this parameter for the transition zone between the continent

and the ocean in the vicinity of the Kuril-Kamchatka arc is taken from the work of S. L. Solov'yev and V. B. Shein (1959).

TABLE 16

Parameters of a train of surface waves of groups of earthquakes with paths that cross (1) and do not cross (2) large structural elements

(1) Структурные элементы	T_{max}		τ		ΔM	
	1	2	1	2	1	2
(2) Каспийское море	190	45	230	45	—	—
(3) Черное море	150	40	260	100	—0,7	—0,1
(4) Персидское плато	90	50	110	40	—	—
(5) Тибетский массив	80	35	130	30	—	—
(6) Камчатка — Курилы	100	0	200	30	—0,5	0

KEY: 1--Structural elements
2--Caspian Sea
3--Black Sea
4--Persian Plateau
5--Tibetan Massif
6--Kamchatka-Kurils

Analysis of the data in the Table shows that all three structures where routes pass over a crust of oceanic or transitional types -- the Black and Caspian seas, and also the transition zone between the continent and the ocean -- distort the train of surface waves to an approximately equal extent. Somewhat lesser distortions take place with crossing of the Tibetan massif, and still smaller -- when the Persian plateau is crossed.

Thus "x-raying" of extensive and varied territories by Lg and Rg waves has demonstrated the feasibility of distinguishing and localizing the largest inhomogeneities in the structure of the earth's crust, and possibly the upper mantle. The developed technique can be used primarily for studying the position of boundaries of continental plates in little investigated regions or localizing sections of the earth's crust characterized by the absence of a "granite" layer.

Chapter 3. Particulars of the Structure of the Upper Mantle in Central Asia

1. Structure of the upper mantle along the Baykal--Pamir profile

The structure of the upper mantle of the territory of Central Asia was studied on the basis of seismographic materials obtained on the profile of Pamir-Baykal seismic stations (Nersesov, Rautian, 1964). Observations on this profile were begun in 1961 and completed in mid 1963. In 1962 the number of stations reached 54.

Earlier, on the basis of a detailed study of the deep-focus zone of Pamir-Hindu Kush earthquakes, the structure of the upper mantle in this territory had been studied to depths of the order of 800 km (Lukk, Nersesov, 1965).

Later on, the materials of observations on the Pamir-Baykal profile were processed on the basis of methods developed at the computing center of the Siberian Department of the Soviet Academy of Sciences for numerical solution of inverse three-dimensional kinematic problems (Alekseyev et al., 1969, 1971). The results gave a general idea of the structure of the upper mantle in the central part of the profile.

This section gives results of a more complete analysis of the structure of the upper mantle based on the use of profile data on the kinematic characteristics of first and subsequent entries as well as spectral dynamic characteristics of longitudinal waves from the materials of the Talgar ChISS station. In the process of interpretation, experimental hodographs were compared with theoretical hodographs calculated by M. V. Alekseyeva for a number of cross sections of the upper mantle. The authors are sincerely grateful to her for furnishing these materials.

TABLE 17

List of the earthquakes used in constructing graphs for the Pamir-Baykal profile

(1) Дата	(2) Время в очаге			(6) Координаты эпицентров		(9) Глубина, км	(10) Энергетический класс K (10^K Дж)
	(3) ч	(4) мин	(5) с	(7) с.ш.	(8) в.д.		
Soviet Middle Asia and Kazakhstan							
23.VIII.1961	04	12	36,5	38°33'	68°33'	20	13,0
21.IX.1961	05	00	08,0	40 20	70 13	15—20	12,3
03.XII.1961	09	32	55,0	41 38	75 08	5—15	10,0
31.I.1962	00	05	53,0	38 38	70 07	5—10	13,4
28.III.1962	13	36	23,0	46 06	82 32	5—10	12,6
26.IV.1962	03	11	35,6	44 43	78 45	5	12,4
09.V.1962	12	12	20,0	36 36	68 30	5	13,0
Altay and the Sayans							
21.V.1961	01	05	57,0	46°29	85°30	5—20	10,4
20.XI.1961	04	03	47,0	50 40	92 45	5—20	13,0
13.IV.1962	18	36	03,0	49 37	87 30	5—20	12,7
22.I.1962	07	26	41,0	52 22	100 25	5—20	13,2
Pribaykal'ye							
28.X.1961	22	45	08,0	53°35	108°50	0—33	13,0
23.XI.1961	01	11	43,0	55 53	109 53	0—33	13,0
11.I.1962	14	16	27,2	54 30	111 00	0—33	11,4

KEY: 1--Date
2--Time at focus
3--hours
4--minutes
5--seconds
6--Coordinates of epicenters
7--N lat
8--E long
9--Depth, km
10--Energy class K (10^K J)

The seismograms of earthquakes with data summarized in Table 17 were used for the kinematic constructions. The earthquake materials were supplemented

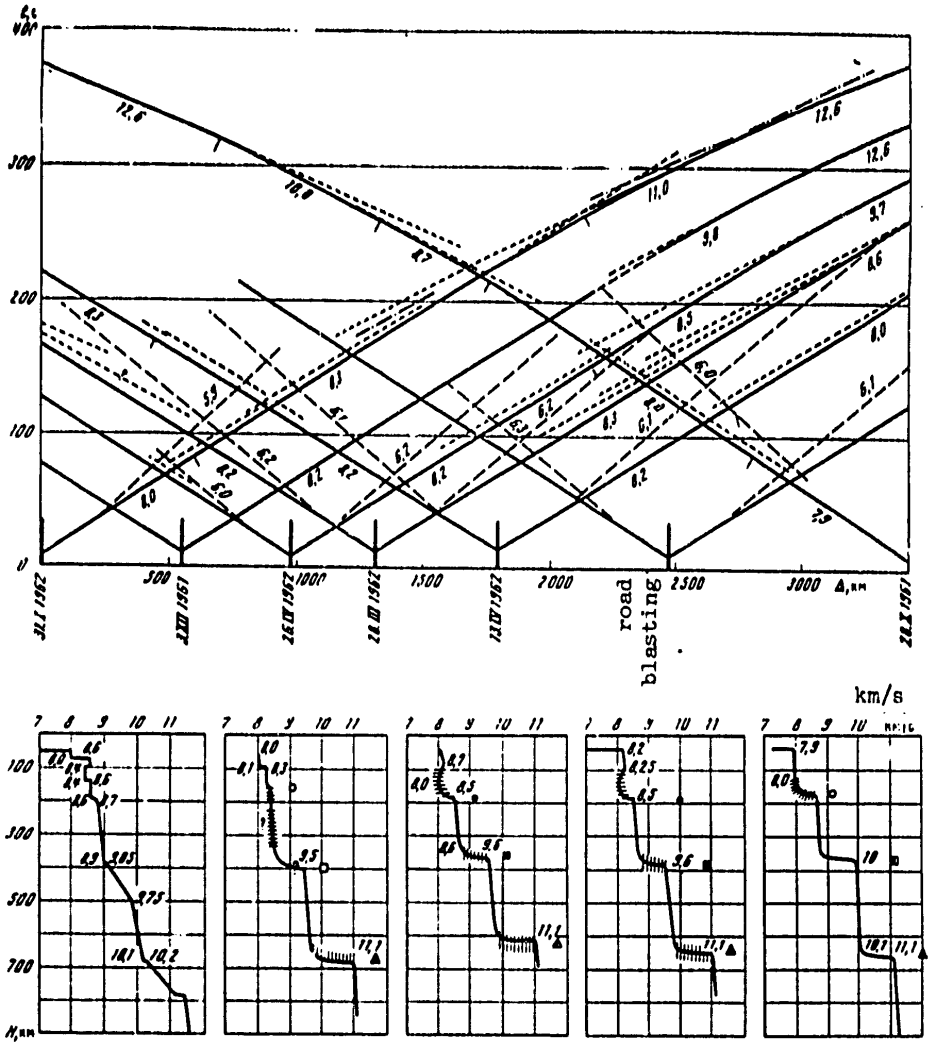

Fig. 44. Diagram of hodographs of longitudinal waves on the Pamir-Baykal profile: solid lines--first entries; dashed lines--Pg waves; dotted lines--reflected waves for the loop section. Shown below are the velocity profiles of the upper mantle for the corresponding sections of the profile, plotted on the basis of interpretation of hodographs and spectral amplitude curves. See Fig. 45 for symbols. The shading shows the regions of ambiguous determination of depth and velocity

by seismograms of three comparatively large explosions (600-700 metric tons) in the Eastern Sayans set off in late 1961 and early 1962 in construction of the Abakan-Tayshet Railroad.

The hodographs of the earthquakes and explosions were plotted in a scheme of contrary and overtaking systems along a profile with overall extent of about 3500 km as shown in Fig. 44. The entire system of hodographs was tied in with respect to first entries at mutual points with reduction of the foci of earthquakes to the earth's surface. The accuracy of this coordination was ±1.5 s, and can be taken as satisfactory considering the great extent of the profile, the displacement of the epicenters with relation to the profile and inexact knowledge of the depths of the earthquake foci.

The hodographs of two earthquakes -- 31.I.1962 in the Vakhsh Mountains on the southwest of the profile, and 28.X.1961 in the northeast direction in the vicinity of Eastern Pribaykal'ye -- were the reference base for the entire system of observations. A comparison of these two hodographs with the standard of E. Herrin's commission (1968) shows that in the northeast direction (from Pamir to Baykal) at distances up to 3000 km the experimental hodograph is more high-velocity, and in the opposite direction contrariwise, less high-velocity.

Thus the general tendency of the structure of the upper mantle in the east is characterized by lower velocities, and on the west -- by higher velocities.

For epicentral distances that correspond to the position of the interface at a depth of about 700 km, both hodographs have about the same velocities. At the same time, waves that are tracked in the second entries and are associated with this interface are better distinguishable on the eastern branch of the hodograph and more weakly distinguishable on the western branch, which may indicate a difference in the sharpness of this interface in the territories of Soviet Middle Asia and the Sayans.

Subsequent entries associated with a 400 km interface are also identically expressed on both hodographs. For the eastern direction the reflected waves (or loop sections of the hodographs) are observed in fragments, and for the western direction -- they are clearly tracked at a great distance. A comparison of the experimental hodographs of second entries with theory for the interfaces at depths of 400 and 700 km shows disagreement in the times of delay of the second entries relative to the first. According to the experimental data these delays are shorter.

In the western direction the velocity of longitudinal waves of the initial part of the hodograph (earthquake of 28.X.1961) in the first entries has a value of 7.9 km/s, and does not increase to 8.0 km/s until a distance of the order of 1000 km. In the vicinity of 2000 km the velocity increases abruptly from 8.7 to 10.0 km/s, and then at a distance of 2800 km -- to 12.6 km/s.

The contrary hodograph (earthquake of 31.I.1972) has considerably different velocities. Up to approximately 600 km the velocity of longitudinal waves

is about 8.0 km/s. Then it increases to about 8.3 km/s and gradually rises to values of 8.4-8.5 km/s. At about 2200 km the velocity of longitudinal waves increases abruptly from 9.6 to 11.0 km/s and at 2800 km reaches values of 12.6 km/s.

The contrary-overtaking hodograph from the earthquake of 26.IV.1962 in the eastern direction has a velocity of longitudinal waves of 8.1 km/s in the first entries in the intial part, which gradually increases to 8.5 km/s with a jump to 9.7 km/s at about 2000 km. The hodographs of the central part of the profile (earthquakes 28.III.1962 and 13.IV.1962) are higher-velocity in the initial part; here the velocity lies in a range of 8.2-8.3 km/s. The hodograph of road blasting in the territory of the Eastern Sayans is a lower-velocity hodograph, the velocity in the first entries being 8.0 km/s.

In the western direction the velocities of the first entries for the explosions in the initial part of the hodograph have a value of 8.0 km/s. For the earthquake from the territory of the Sayans (13.IV.1962) the velocity is higher, and comes to 8.3 km/s. The more easterly earthquake (28.III.1962) shows a change in velocity of the first entries in the western direction from 8.0-8.1 to 8.2-8.3 km/s.

Of definite interest is the behavior of longitudinal Pg interference waves, since they give some idea of the average velocity of longitudinal waves in the crust. On the eastern end of the profile their average velocity is close to 6.0 km/s, and they are tracked to a greater extent than on the west. In the vicinity of the Western Sayans and Altay the velocity of these waves increases to 6.2-6.3 km/s. Such a velocity is typical of all of Kazakhstan as well. Within the limits of Soviet Middle Asia the velocity of Pg waves ranges from 6.0 to 6.3 km/s. In comparison with the western direction a general tendency is observed toward a reduction in the intervals over which longitudinal interference waves can be tracked.

A general examination of the wave pattern done with the use of data on the dynamics of longitudinal waves obtained with the use of the ChISS station at Talgar gives us a basis for some remarks on trends in the structure of the crust and mantle in the territories that are crossed by the Pamir-Baykal profile. In the preceding chapter a detailed examination was made of the spectral amplitude curves of Pn, Pg, Sn and Lg waves (Fig. 18, 20, 22, 23).

The average velocity in the earth's crust in Pribaykal'ye and the Eastern Sayans is close to 6.0 km/s. The upper part of the mantle from the underside of the crust and down to 100-130 km has a weak gradient and is characterized by velocities from 7.9 to 8.0 km/s. In this connection, difficulties arise in evaluating the existence of the low-velocity layer that is usually associated with the asthenosphere. In any event, it can be assumed that if it occurs, it is very faint.

The interface at 400 km is evidently upheaved, and should not be deeper than 360 km. This interface is clearly expressed and is characterized by a sharp

gradient. Below this interface, the velocity approaches 10 km/s. A deeper boundary (700 km division) is located in the 640-660 km interval and is not very clearly expressed. It probably has a weak gradient.

In the vicinity of the transiton from the Western Sayans to Altay the crust has an average velocity of 6.2-6.3 km/s. Beneath the underside of the crust the mantle becomes more high-velocity. An abrupt decline in amplitudes of seismic oscillations (Fig. 18a) according to data of the Talgar ChISS station in the distance range from 700 to 1700 km, and the presence of a small increase in amplitudes at a distance of about 1000 km show the existence of an asthenospheric layer of reduced velocity, and beyond it -- an interface.

A clear boundary is distinguished at a depth of the order of 360 km. Associated with this boundary is a sharp amplitude spike observed at a distance of 1800 km. The deeper 700 km interface is much more weakly expressed. In this territory it is at a depth of 650-700 km.

A comparison of mantle velocity data for depths ranging from 350 to 630 km in the territories of Pribaykal'ye, Kazakhstan and Altay shows that the velocities in this interval are higher in the east than in the west: 10 and 9.6 km/s respectively. Thus in the eastern section of the profile the lower velocity in the upper part of the cross section is compensated by higher-velocity low levels.

The presence of an amplitude spike on the amplitude curves of the Northeast direction (Fig. 18a, b) at distances of the order of 450 km, and a branch that can be tracked on the hodograph at the same distances of a weak reflected wave with short delay with respect to the first entries indicate an inhomogeneity in the topmost levels of the mantle at depths of the order of 80-90 km. It can be assumed that there is a boundary of low rigidity at this depth. Territorially, this inhomogeneity is confiend to the section of the profile between Lake Balkhash and the boundary of the Northern Tyan'-Shan'.

In the environs of Northern Tyan'-Shan' the earth's crust has an average velocity close to that observed in Kazakhstan -- 6.3 km/s. Further toward the southwest the average velocity in the crust decreases to 6.0 km/s. In the first entries, deep longitudinal waves have a velocity of 8.1-8.3 km/s. These velocities are close to those observed for the territory of Kazakhstan; however, in contrast to the northeast direction (recalling that the azimuth is read from Talgar station), the amplitude curves are situated considerably higher with respect to level, and they have no characteristic spikes. This circumstance, as well as the absence of pronounced waves or loops in the hodograph show that the low-velocity channel in the Middle-Asiatic direction is poorly expressed.

The poor show of the 20-degree spike on the curves leads us to assume that the deep-level boundary close to 400 km is also less pronounced. The 700 km boundary in this region can be much better tracked on the amplitude and kinematic curves of reflected waves (Fig. 18c, d).

A much higher-velocity cross section is typical of the southern part of the profile -- the region of the Pamir-Hindu Kush earthquakes (Lukk, Nersesov, 1965). Here the main difference between the deep-level cross section and those examined previously is observed in the upper levels of the mantle to a depth of 400 km. The high-velocity cross section of the mantle to the south of Pamir is confirmed by research of Indian seismologists as well.

In evaluating the peculiarities of the structure of the mantle of Soviet Middle Asia as a whole we can note that it is apparently transitional between the high-velocity upper mantle of Pamir (with poorly expressed deep-level interfaces) and the mantle of Kazakhstan. It is quite significant that the asthenospheric channel in Soviet Middle Asia is much more poorly expressed than in the territory of Eastern Kazakhstan. It is a triking fact that the presence of the low-velocity channel in the asthenosphere of Kazakhstan is accompanied by somewhat of an increase in velocity at a relatively greater depth (down to 400 km), while in Soviet Middle Asia the absence and weak expression of this channel is associated with somewhat of a reduction in velocity at these depths.

Unfortunately, the available material does not permit detection of clear boundaries of division of the upper mantle among the individual noted blocks. We can only present a few considerations. The boundary between the mountainous Pamir block and the central part of Soviet Middle Asia runs in the zone of the Darvaz-Karakul' break zone (Vinnik, Lukk, 1975). The transition from the Middle Asia type of mantle to the Kazakhstan type is noted in the region of the northern spurs of the Trans-Ili Mountains on the border of the Ili Basin. The boundary between the Sayans proper and Altay is quite pronounced. In deep-level structure, these two regions differ considerably. Besides the materials that we have used, confirmation of the existence of this boundary is to be found in the results of study of Lg waves (Nersesov, Rautian, 1964). The pattern of change in velocities in the upper mantle for the territories crossed by the profile is shown in Fig. 44.

The principles governing the relation between the spectral amplitude curves and kinematic curves lead to a number of considerations of a more general nature for the eastern and southern directions (see Fig. 18b, c). In the eastern direction (western territories of China) the spectral curves have a poorly expressed amplitude spike associated with a depth of 360-400 km. Apparently this boundary is fuzzy, which is also confirmed by the relative spectral width of this spike: the low-frequency components of the ChISS spectrum come close together. The spike at 25° is located at a comparatively great distance, and is more pronounced on the high-frequency components, which indicates that it is associated with a rather sharp boundary at depths of around 700 km.

A comparison of the eastern and northeastern directions shows that considerable changes take place in the structure of the upper mantle to the south of the profile: the low-velocity asthenospheric channel dies out; the 400 km boundary loses clarity and rigidity, and its depth apparently

increases; the sharpness of the boundary of the upper mantle at a depth of 700 km increases somewhat, the boundary itself also becoming somewhat deeper as compared with the northeast. New data agree with the particulars of the structure of the eastern part of the given territory found previously as a result of processing of the materials of observations on the Pamir-Baykal profile (Bugayevskiy et al., 1971).

It can be assumed that the enumerated considerable changes in the structure of the mantle occur between Altay and Northern Dzhungaria both within the borders of the USSR and in China.

In the southern direction (see Fig. 18c) oriented from Talgar mainly toward Tibet and the northern provinces of India, the deep-level cross section also changes considerably. The low-velocity channel again begins to be tracked, although weakly, and the presence of a small spike in amplitudes at distances of about 1500 km indicates either that its depth increases to approximately 200 km, or that the nature of the boundary itself changes. The 400 km boundary in this region is weakly expressed. It is characterized by narrowing of the spectrum of the reflected wave, which is evidence of a strong gradient. In addition, the lower boundary of the upper mantle is much more clearly expressed than for previously examined directions. The two-humped nature of the amplitude curve is an indication of the complexity of this boundary, and the configuration of the first maximum confirms a tendency to increase. In comparing the southern direction with the southwest direction considered above, one can note an increase in expression of the lower boundary of the mantle, as well as less rigidity, which shows up in narrowing of the spectrum of waves reflected from it.

The use of the spectral curves of longitudinal waves obtained at Garm station and at Temporary station situated in Northeastern Kazakhstan to study general patterns of structure provides additional information on the structure of the mantle within the limits of the southern and southwestern sections, and also on the eastern continuation of the profile. All available data are shown in the diagram on Fig. 45.

The shading on the diagram shows regions of development of mountain structures. A number of interesting conclusions derived from the given data. The prairie regions of Kazakhstan are characterized by a higher-velocity crust and the presence of a low-velocity channel in the upper part of the mantle. Also striking is the circumstance that an asthenospheric channel can be noted both in the vicinity of the Tarim plate and in the western parts of Soviet Middle Asia. In the mountain regions of Asia and the Sayans, the channel is lacking or poorly expressed. It shows up again in the territories of the Tadzhik-Afgan depression and is weakly pronounced in Northeast India between the Hindu Kush and Himalayan mountain systems. The 400 km boundary is less well pronounced in the mountain regions than in the platform areas. More stable is the lower boundary of the upper mantle, which can be clearly traced in the prairie regions of Soviet Middle Asia, the foothills of the Tibetan plateau and the intermountain regions of Altay and the Eastern Sayans.

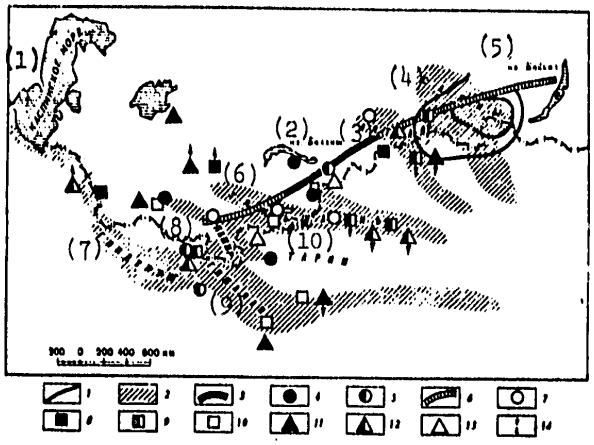

Fig. 45. General nature of deep-level boundaries of the upper mantle in Central Asia: symbols--1--isolines of regions of reduced velocities of the upper mantle according to G. N. Bugayevskiy et al. (1971); 2--mountain systems; 3--region of tracking of the mantle channel along the Pamir-Baykal profile; 4--regions of differentiation of the mantle channel from spectral amplitude curves; 5--points that are weakly tracked; 6, 7--sections of the profile and points that are poorly tracked; 8--regions that are well tracked for the 400 km boundary; 9, 10--points that are weakly (9) and poorly (10) tracked; 1--regions in which the 700 km boundary is well tracked; 12, 13--points that are weakly (12) and poorly (13) tracked; 14--tendency for depression or elevation of the corresponding boundary

KEY:
1--Caspian Sea
2--Lake Balkhash
3--Altay
4--Sayans
5--Lake Baykal
6--Tyan'-Shan'
7--Hindu Kush
8--Pamir
9--Himalayas
10--Tarim

One observes a general tendency toward an increase in the depth of the lower boundary in the eastern regions of the investigated territory and an elevation of this boundary in the western regions. An analogous tendency is tracked for the 400 km boundary as well.

Data that have been obtained give grounds for some considerations on the peculiarities of seismically active regions. From the standpoint of the relation between seismically active regions and the deep-level structure, they are typified by the absence or weak expression of the low-velocity asthenospheric channel and reduced velocities of the longitudinal waves in the upper part of the mantle. The reduced velocities of longitudinal waves in the crust of these regions can apparently be related to the existence of a layer of reduced velocities in the crust. This channel is lacking in

non-seismic regions (Belyayevskiy, 1974). The latter assumption needs more careful verification; however, extensive experimental material on the structure of the crust in non-seismic regions shows that the crustal channel has not been distinguished in these regions.

The 400 km boundary is more poorly expressed in seismically active regions than in non-seismic regions. Of course, the notion "poorly" is a qualitative one, but nevertheless it can be stated that sharpness of the boundary falls off, it becomes "higher-gradient" or more complicated in structure. The detailed investigation of this boundary in seismically active regions can probably give significant information on the degree of seismic danger of individual regions of seismically active territories. It is also striking that the deeper mantle boundary at 700 km is more poorly expressed in regions of elevated seismic danger.

We can assume that the elevated mobility of the upper mantle of seismically active regions, the difference in the temperature conditions of stable platform structures and active sections of the earth's crust are causes of nonuniform structure of the upper mantle of these regions.

Thus we arrive at the conviction that analysis of the general patterns of the structure of the upper mantle in the regions of Central Asia enables us to formulate the question of distinguishing sections of increased seismic danger on the basis of the seismological characteristics of the crust and upper mantle.

2. Evaluation of absorbing properties of the medium

Absorption and Scattering of Transverse Waves in the Lithosphere. An important peculiarity of near and intermediate epicentral distances is the formation of numerous secondary waves that arise in the upper layers of the earth as a result of reflections, refractions, exchange, conversion at boundaries, interference in layers distinguishable by acoustic impedance, and scattering on small inhomogeneities. The number of such waves is very great, and their superposition is conducive to the formation of an exceptionally complicated and prolonged seismic recording. The propagation of seismic waves in such a case is very close in its nature to the process of diffusion of seismic energy in the plane layer close to the earth's surface.

The idea that the flow of seismic energy at a great remove from a spherical source may be described by a diffusion equation was suggested earlier (Wesley, 1965) and found application in the investigation of the internal structure of the moon (Dainty et al., 1974) and in such a field of physics as acoustics (Ponomareva, 1969).

According to J. Wesley (1965) the expression for the energy flux density E in a narrow frequency band can be found as a result of solving the following differential equation

$$\partial E/\partial(\omega t) = (L^2/4)\nabla^2 E - E/Q - \pi L^2 B\delta(t)\delta(r).$$

J. Wesley's solution takes the form

$$E' = (B/t)\exp\left(-\frac{r^2}{L^2\omega t} - \frac{\omega t}{Q}\right). \qquad (*)$$

Here ω is angular frequency; r is epicentral distance; t is time; Q is the mechanical quality factor of the medium; B is the spectral function of the source; L is a parameter with dimensions of length that can be referred to the mean free path of the wave, to the effective size of a scattering inhomogeneity or to the size of the region that takes an appreciable part in the process of energy transfer.

The expression (*) can be used to evaluate parameters of absorption and scattering in the surface layer of the earth as dependent on available experimental data. For instance J. Wesley (1965) used for these purposes the relation between the apparent period on seismograms of explosions on the one hand, and time of registration and epicentral distance on the other. In our case it is convenient to use the envelopes of ChISS recordings at fixed distances from the source and the relation between epicentral distance and the logarithm of the ratio of amplitudes of the envelopes of two frequency components of ChISS recordings calculated for a fixed time. The logarithm of the ratio of closest frequency components of ChISS recordings is called the spectral ratio γ (Khalturin, 1971; Pasechnik, 1970):

$$\gamma_{ij} = \ln(A_i/A_j)/\ln(T_i/T_j), \qquad (**)$$

where A_i, A_j, T_i, T_j are the amplitudes and periods respectively of the i-th and j-th components of the ChISS spectrum. More detailed information on the ChISS spectrum can be found in the work of P. Molnar et al. (1976).

Within the framework of our materials it can be assumed that $(T_i/T_j) \approx 0.7$ since ChISS stations have a filter setting of an octave with respect to frequency. Taking the square root of (*) and substituting the result in (**) we get

$$\gamma_{ij} = c\lg(A_i/A_j) = c\left[\frac{r^2}{4\pi L^2 t}(T_j - T_i) + \frac{\pi t}{Q}(T_j^{-1} - T_i^{-1})\right] + \text{const},$$

where c = const.

Of interest is the special case r/t = V = const. Then

$$\gamma_{ij} = c(T_j - T_i)\left(\frac{V}{4\pi L^2} - \frac{\pi}{VQT_iT_j}\right)r + \text{const}, \qquad (***)$$

or

$$\gamma_{ij} = ar + b,$$

where

$$a = c(T_j - T_i)\left(\frac{V}{4\pi L^2} - \frac{\pi}{VQT_iT_j}\right); \quad b = \text{const}.$$

As we can see, the spectral ratio γ_{ij} is a linear function of the epicentral distance, which is apparently true within the first hundred km. Table 18 summarizes estimates of the coefficient a of linear regression for several pairs of frequency components found by the method of least squares for spectral ratios within the limits of sections of seismograms beginning with the first entry of an S wave.

TABLE 18

Average estimates of regression coefficient a

Ratio of frequency components (Hz)	Regression coefficient $a \cdot 10^{-5}$, km^{-1}
0.35/0.7	3.9
0.7/1.4	5.2
1.4/2.8	7.8
2.8/5.6	10.4

The ChISS station (Talgar) registers the velocity of displacements of the soil and therefore to approximate the envelope of the recording of each frequency component Wesley (1965) used the expression

$$A = \frac{A_0}{f^{1/4}}[(\rho^2+1)^{1/4}+1]\exp\left\{\ln\tau - \frac{5}{2}\tau - \frac{1}{2}[(\rho^2+1)^{1/2}-1]\left(\tau+\frac{1}{\tau}\right)\right\},$$

where

$$\rho = r/L^2Q;\ \tau = \ln(t/t_0);\ t_0 = r/V;\ A = \text{const.}$$

The approximation was done by selecting the theoretical envelope that best coincides with the experimental envelope plotted in coordinates $\ln A_i$ and $\ln(t/t_0)$, where time t is counted from the time at the source. An example of matching of the theoretical envelope is shown in Fig. 46a. Matching of the envelopes of ChISS recordings was done with respect to the parameter $LQ^{1/2}$. Estimates of the parameter $LQ^{1/2}$ are summarized in Table 19.

TABLE 19

Estimates of parameter $LQ^{1/2}$ from data of envelopes of ChISS recordings (Talgar)

Average frequency of channel (Hz)	Range of the parameter $LQ^{1/2}$
0.35	130-160
0.7	130-150
1.4	80-100
2.8	60-65
5.6	40

The use of equations (**) and (***) enables us to plot a nomogram (Fig. 46b) to evaluate the reciprocal relation between frequency ω, quality factor Q and the effective size L of the scattering inhomogeneity. By using the data of tables 18 and 19 we get estimates of L and Q as functions of frequency, as is shown in Fig. 46c. It was assumed in doing this that the velocity $V = 4$ km/s corresponds to the average velocity of transverse waves of the lithosphere within the limits of the investigated territory. Given in Fig. 46c for comparison are estimates that we obtained for data of the SKM-3M

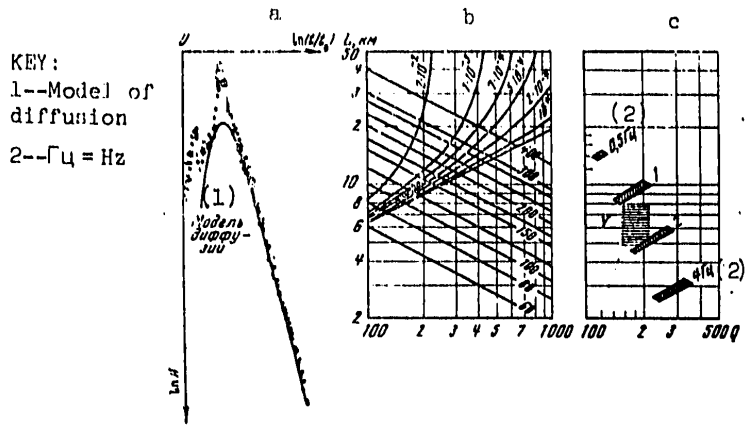

Fig. 46. Matching of the theoretical envelope of a ChISS seismogram and estimate of the ratio between parameters of absorption Q and distance L for S waves: a--example of approximation of experimental data; b--nomogram for the 0.7-1.4 Hz frequency band (average frequency 1.0 Hz); $LQ^{-\frac{1}{2}}$ scale from 60 to 400, scale of the coefficient of linear regression from 10^{-4} to $2 \cdot 10^{-3}$. Shaded region in confidence limits (on the 0.9 level) of the matching parameters $LQ^{-\frac{1}{2}}$ and coefficient of linear regression; c--summary of estimates of L and Q for average frequencies 0.5, 1.0, 2.0 and 4.0 Hz. V is the region of estimates from our data (SKM-3M channel) and from J. Wesley's data (1965)

channel in analogous arrangement to J. Wesley's (1965), and also Wesley's own estimates. Agreement of the results can be considered satisfactory.

The regions of solutions for different frequency components form a regular sequence in coordinates of lg L and lg Q, showing a linear relation between quality factor Q and frequency ω. The quality factor increases with frequency approximately as the cube root of frequency. A rise in frequency, as was to be expected, is accompanied by a reduction in the effective size L of inhomogeneities of the medium that take a significant part in transfer of seismic energy.

Absorption of Longitudinal Waves in the Mantle. Let us evaluate the absorbing properties of the mantle in accordance with a simplified scheme (Sato, Espinoza, 1967; Teng, 1968). We will assume that the hodograph and the cross section of velocity are known for longitudinal waves in a spherically symmetric earth. We will also assume that radiation at the source is isotropic, and that any possible relation between Q and frequency can be disregarded in an octave frequency band. Within the framework of these assumptions we can use the data we have derived from spectral ratios γ_{ij} (Fig. 47) to evaluate the change in Q with depth:

$$\gamma_{ij} = \pi (f_i - f_j) \sum_{k=1}^{N} \frac{t_k(\Delta)}{Q_k},$$

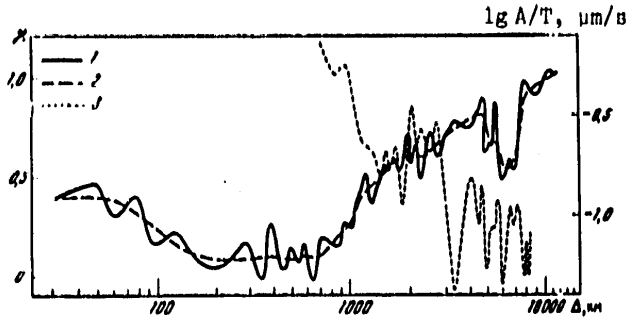

Fig. 47. Spectral ratio γ of ChISS components 0.7-1.4 Hz and amplitudes for the SKM-3M channel as functions of epicentral distance for the Pamir-Baykal direction: 1--initial data for $\gamma(\Delta)$; 2--averaged data for $\gamma(\Delta)$; 3--amplitude curve of A/T

where f_i, f_j are the average frequencies of the ChISS channels; $t_k(\Delta)$ is the travel time of the wave along a ray in the k-th spherical layer of the earth; Q_k is the average value of the quality factor in the k-th layer.

Moreover, we take as the average value of the quality factor in the earth's crust $Q = 420$-450, bearing in mind that

$$Q_P = \frac{3}{4}\left(\frac{V_P}{V_S}\right)^2 Q_S$$

and $Q_S \approx 180$-190 for $f = 1$ Hz.

The method of calculation (Teng, 1968) consists in inverting the matrix T of travel times ΔT and solving the matrix equation

$$q = T^{-1}g,$$

where Q is the sought vector $(1/Q_1, 1/Q_2, \ldots, 1/Q_n)$, g is the vector $(\gamma_1, \gamma_2, \ldots, \gamma_n)$, T is the matrix

$$\begin{vmatrix} \Delta t_1^1 & \Delta t_2^1 & \Delta t_3^1 & \ldots & \Delta t_m^1 \\ \Delta t_1^2 & \Delta t_2^2 & \Delta t_3^2 & \ldots & \Delta t_m^2 \\ \ldots & \ldots & \ldots & \ldots & \ldots \\ \Delta t_1^N & \Delta t_2^N & \Delta t_3^N & \ldots & \Delta t_m^N \end{vmatrix};$$

Δt_k^i is the travel time of a P wave along the i-th ray in the k-th layer.

An algorithm proposed by V. P. Valyus (1971) was used to calculate the t_k^i. The initial data were the hodograph and velocity cross section with respect to the Pamir-Baykal profile described in the preceding section, and also the data found by L. P. Vinnik and A. V. Nikolayev (1970). The spectral ratios γ_{ij} are obtained from materials of registration of earthquakes by the Talgar and Temporary ChISS stations in the northeast direction coincident with the direction of the profile.

Analysis of the γ_{ij} data shown on Fig. 47 shows that several characteristic sections can be observed in the behavior of the average line. The first

section, up to 60-70 km, is characterized by an approximately constant value of γ_{ij} and is apparently related to the the influence chiefly of the upper layers of the earth's crust. The second section, from 70 to 150 km, is associated with a relative reduction in the values of γ_{ij} by approximately 0.3 lg unit. The section from 150 to 700 km is associated with the very lowest values of γ_{ij}, apparently due to the influence of the lower layers of the earth's crust and the lithosphere. The next section from 700 to 1500 km is characterized by a steep rise in the graph of γ_{ij} by approximately 0.45 log unit, after which a gently sloping section is observed, coinciding in position with the 20-degree feature. In the distance range from about 2500 to 4700 km an increase is observed in the values of γ_{ij} by approximately 0.2 log unit. Then a sharp drop is observed that reaches the lowest value at a distance of 6000-6500 km. The amplitude of this minimum is about 0.3 log unit. At a distance of about 7000 km a steep rise begins in the graph of γ_{ij}, flattening out somewhat at a distance of about 8000 km.

Note should be taken of the oscillatory structure of the initial curve of γ_{ij}, the main spikes being confined to characteristic sections of the smoothed line. The strongest oscillations are observed in regions of relative declines in the function of the spectral ratio as well as in its transitional sections. In our opinion it is quite characteristic that there are two relative minima on the initial curve for γ (see Fig. 47) that are confined to distances of 4800-5300 km and 5800-7500 km. If the data of spectral ratios are compared with the amplitude curve of a longitudinal wave shown on Fig. 47 (for greater detail see Part I), one can see that there is an inverse relation between the two curves. Corresponding to the general decline of the A/T curve is a general rise in the γ curve, and corresponding to relative rises in the A/T curve are flat sections and relative minima on the γ curve.

Apparently the observed relation is not accidental since the data were obtained for a single frequency band: γ -- from materials of a ChISS station (0.7 and 1.4 Hz channels), A/T from SKM-3M materials (frequency band about 0.7-2.0 Hz). This relation shows that a drop in amplitude of a P wave is accompanied by attenuation of its high-frequency components.

With respect to the distance range beyond 65°, it is assumed that the spectrum of a P wave may be influenced by the PcP wave, which is delayed in arrival by less than 30 s at these distances. In our case such an influence, if significant in general at these distances from the source, may show up at a remove of 80° or more since in deriving the data on γ the measurements were made in a time interval equal to 10 s. Moreover, special consideration was given here to the time interval from 10 to 20 s, and it was established that on this section the spectral ratios have appreciably greater values.

In the inversion of the spectral ratios, indirect use was made of their relation to the A/T amplitude curve. We point out the usefulness of such an operation, bearing in mind the results of inversion of amplitude curves to the cross section of mechanical Q as undertaken by K. Veith and G. Clawson

(1972). Also used in an indirect way were the spectral amplitude curves of P waves considered above; the usefulness of these curves was pointed out by T. B. Yanovskaya et al. (1964) and also by B. Kennett (1975). In particular, these authors turned their attention to the significant way that the characteristic elements of spectral amplitude curves are related to the position of the low-Q section and to the absolute value of Q.

In addition to the indirect criteria of consistency of the results of inverting γ to the cross section of Q, use was made of average quantitative estimates of Q that are known for the mantle as a whole (Zharkov et al., 1974; Kanamory, 1967 a, b, c, d; Teng, 1968) and also for the crust and upper mantle of the investigated region (Vinnik, 1976; Zhadin, Dergachev, 1973; Khalturin, 1971; Khalturin, Urusova, 1962).

As has already been pointed out, we have taken the value Q = 420-450 as the average estimate for the crust. There are grounds for assuming (Zhadin, Dergachev, 1973) that the lower and upper layers of the crust have quality factors appreciably different from this average. To analyze this hypothesis, we use the data of A. Nurmagambetov (1974) and the inversion equation (Sato, Espinoza, 1967)

$$\frac{1}{Q(r)} = \frac{2}{\pi} V \frac{d}{dr}\left(\frac{r}{V}\right)\left|\int_0^{\Delta_r} \frac{(dI_0/d\Delta)\,d\Delta}{V p^2 - q^2}\right|,$$

where p is the parameter of a ray, V is the velocity of a P wave, Δ_r is the epicentral distance at exit of the ray that has radius of penetration r, $q = p(\Delta_r)$, $dI_0/d\Delta$ is the derivative of the damping function of a P wave in a medium with velocity V(r) and quality factor Q(r). In agreement with Dergachev (1975) we approximate the velocity cross section of the crust in the investigated region by the exponential law

$$V = V_0 e^{kH},$$

where V_0 is the initial velocity of the P wave, and H is depth from the surface of the earth.

For A. Nurmagambetov's data, the derivative $dI_0/d\Delta$ can be represented as

$$\frac{dI_0}{d\Delta} \approx \frac{(n_1 - n_2)\lg(\Delta_2/\Delta_1)}{(\Delta_2 - \Delta_1)\delta\omega \lg e}.$$

Here n_1 and n_2 are the coefficients of attenuation of ChISS components of the P wave in the distance range from Δ_1 to Δ_2, $\delta\omega$ is the difference in angular frequencies of the two ChISS channels.

The average value of the quality factor of the layer bounded from below by the tip of the seismic ray with exit at distance Δ_2 is evaluated in accordance with A. A. Dergachev (1975) by $Q_{av} = A^{-1}B^{-1}$, where

$$A = \frac{2V_0}{\cos(k\Delta_2/2)}; \quad B = \frac{(n_1 - n_2)\lg(\Delta_2/\Delta_1)}{(\Delta_2 - \Delta_1)\delta\omega \lg e}$$

Taking $V_0 = 4.0$ km/s and $V_{50} = 8.1$ km/s, we get k = 0.0144. Using the data for $f_1 = 0.8$ and $f_2 = 1.5$ Hz from Table 4 in A. Nurmagambetov's work (1975) we find that when $\Delta_2 = 100$ km, $A = 12.8$, $B = 2.58 \cdot 10^{-3}$, $Q_{av} \approx 30$. The calculated estimate

must be referred to the very upper layer of the crust that has a thickness of no more than 4-5 km.

The estimates of the quality factor obtained by V. I. Khalturin (1971) for the territory of the Northern Tyan'-Shan' from observations at distances of 100-200 km for frequencies close to 1 Hz do not exceed values of Q = 350, and apparently correspond to depths of 15-30 km. Thus it can be expected that appreciably higher values of Q will correspond to the bottoms of the crust and the asthenosphere.

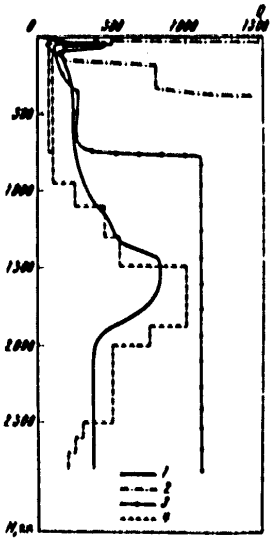

Fig. 48. Cross sections of mechanical quality factor Q of the crust and mantle: 1--our model; 2-- the model of C. Archambeau et al. (1969); 3--K. Veith and G. Clawson (1972); 4--T. Teng (1976)

Shown in Fig. 48 is the Q(H) cross section found by inversion of γ data with observance of the following limitations: the average values of the quality factor in the crust must be of the order of 450, and throughout the mantle -- of the order of 400-600 (Kanamory, 1967 a, b, c, d; Kovach, Anderson, 1964). For purposes of comparison of results, Fig. 48 shows relations for Q as a function of depth H according to the data of C. Archambeau et al. (1969), K. Veith and G. Clawson (1972) and T. Teng (1968). From the set of models of the distribution of quality factor with depth, these were chosen for the reason that they were derived by similar techniques for inversion of amplitude data.

Analysis of the relations for quality factor as a function of depth that are shown in Fig. 48 shows that all models are in satisfactory agreement with one another only in the region of the upper 150 km layer. The most contrasty differences are observed for the model obtained by C. Archambeau et al. (1969) for the territory of the United States. In constructing the model, data were used on spectral amplitude curves from two explosions along four profiles. In this model, values of Q = 8000 were found at depths from 1000 to 1700 km, which is apparently excessive, and cannot be matched with the latest data on free oscillations of the earth (Zharkov et al., 1974) and surface waves (Kanamory, 1970).

A comparison of the resultant model of Q(H) with that of K. Veith and G. Clawson (1972) shows that they agree satisfactorily down to depths of the order of 700 km. For greater depths the data of K. Weith and G. Clawson rise abruptly to a value of 1100 and remain constant right down to 2800 km. For their calculations these authors used data on the velocity cross section and amplitude measurements for a frequency f = 1 Hz obtained by E. Herrin (1968).

Characteristic features of this model are two relative minima in the region from 150 to 300 km, and from 650 to 750 km, and an abrupt rise in the vicinity of 760-770 km. As noted by the authors themselves, the increase in Q may, in particular, be a consequence of the weak increase of velocity in E. Herrin's model. At the same time, they note that that an increase of Q and V in this region is entirely possible. Moreover, it is suggested that the decline in the region of 350-650 km might be entirely due to the monotonic increase of velocity in E. Herrin's model in this region. With respect to the evaluation of quality factor for the lower mantle, the authors feel that the available data permit only an estimate of the average, equal to 1100, relative to which the individual determinations fluctuate.

The greatest agreement is observed between the model of Q found in this book and T. Teng's model (1968). T. Teng's model is based on relatively low-frequency data of stations of the world-wide WWSSN netowrk found for two deep-focus South American earthquakes. T. Teng used a method of inverting the spectral ratio to the Q cross section by successive approximations, utilizing two computational schemes with considerably different initial approximations. In the first scheme, the initial variant was taken as the simplest model of a three-layer mantle: low-, intermediate- and high-Q layers. In the second scheme, the initial approximation was a model close to the MM8 model (Anderson et al., 1965). The final result of selection was the model shown in Fig. 48. A characteristic feature of this model is first of all the relatively low Q in the layer from 36 to 950 km, where it is equal to 75-100. Moreover, an important detail of the cross section is a relative maximum of the Q in the 1500-1875 km region and the considerable reduction of the Q in the region of transition from the lower mantle to the outer core, from 2000 to 2800 km, which has recently been confirmed by data of free oscillations of the earth (Zharkov et al., 1974).

Let us note that our Q model has nearly identical cross sectional details, particularly in the vicinity of transition from the upper to the lower mantle and then to the outer core. On the whole, the model is in agreement in the region of the upper mantle as well. In our model, the upper mantle is somewhat higher-Q, particularly below the 400 km interface. At the same time, in the resultant model the region of the asthenosphere is much more clearly delineated by a relative reduction in Q.

If T. Teng's model of the mechanical quality factor of the mantle (Teng, 1968) is taken as the average world-wide model of an anomalous mantle in activated regions, our model can be classified as one of an essentially normal mantle of platform regions, or at least as the model of the mantle of a weakly activated region.

Discussion of the Results

The second part of this monograph has presented a detailed analysis of the particulars of propagation of seismic waves over an extensive territory of Central Asia. Major emphasis has been placed on problems of the mutual

relation between peculiarities of the internal structure of the crust and upper mantle of the territory on the one hand, and the kinematic and dynamic characteristics of fundamental seismic waves on the other.

It was shown in Chapter 1 that amplitude curves of different frequencies and the spectra of different types of waves are a comparatively precise tool in solving problems of outlining and delineating regions of the crust and mantle with considerably anomalous properties. These characteristics were successfully used in Chapter 2 for mapping individual blocks of the crust and mantle. It was shown in particular that from a number of dynamic properties of fundamental types of waves one can outline boundaries of what are apparently essentially dissimilar blocks: Tibet and the Tarim platform, Tarim and Tyan'-Shan', Dzhungaria, the Balkhash region and Northern Tyan'-Shan', Dzhungaria and Altay, Altay and the Sayans.

In Chapter 3 a detailed analysis was made of the internal structure of the territories crossed by the Pamir-Baykal seismologic profile. Regular alternation of crust and mantle of platform and activated types is demonstrated as a result. For instance at the southeast end of the profile in the territory of Pamir one notes a high-frequency type of upper mantle with poorly defined deep-level boundaries; as one moves in the northeastern direction within the limits of the Tyan'-Shan' and adjacent territories of Kazakhstan there is a characteristic transition to a different crust-mantle block, This block differs from the preceding one in an overall reduction of velocity throughout the cross section, and more pronounced major interfaces, whose depth is somewhat reduced. Further on toward the northeast a block can be distinguished with still more elevated boundaries of major physicochemical interfaces with velocity increasing on the average through the cross section, and the presence of a pronounced low-velocity layer. With consideration of the drift of seismic rays, the given block of the mantle is assigned to a region with axial part coincident with the position of the Zaysan-Gobi folded zone.

The next crust-mantle block is distinguished within the limits of the Mongolian-Altay folded zone. It is differentiated from the previous one by a relatively weakly expressed asthenospheric layer and increasing thickness of the upper mantle on the average. The velocity characteristics remained as before on the average.

On the northeast end of the profile in the vicinity of the Sayans still another crust-mantle block is noted in which a characteristic feature is redistribution of velocity characteristics along the entire cross section: in the upper part the velocities decreased considerably, while in the lower part they increased. The position of interfaces with respect to depth is close to that of the preceding type of cross section.

For the northeastern direction of the profile, a cross section of the mechanical quality factor of the medium was constructed for the crust and mantle that for the first time gives an idea of the distribution of absorbing properties of the medium to a depth of 2800 km in Central Asia.

On the whole, in evaluating the results presented in the second part of the monograph, it should be emphasized that this is the first time that such a detailed analysis of seismological materials has been made for the territory of Central Asia. It is to be hoped that this will enable a still sounder interpretation of the data of other geological-geophysical methods.

III. MANIFESTATION OF INHOMOGENEITIES OF STRUCTURE IN FLUCTUATIONS OF THE CHARACTERISTICS OF LONGITUDINAL WAVES

The detailed spatial structure of P waves has been comparatively little investigated. This is due in part to a lack of sufficiently dense systems of seismic observations, and in part to the fact that seismology uses mainly averaged characteristics of travel times and amplitudes of seismic waves from which the coordinates of the focus and energy of earthquakes are determined. In doing this, major emphasis is placed on the stable deterministic characteristics of the wave field: average station corrections, systematic changes of amplitude, travel time and apparent velocity. So far, little attention has been given to the structure of small-scale fluctuations of travel times and amplitudes: intervals of spatial correlation and the relation between fluctuations of various parameters have remained practically unstudied.

The first data on the structure of fluctuations of amplitudes and travel time of the P wave were obtained from deep seismic sounding (Galkin et al., 1970; Nikolayev, Tregub, 1969). A detailed study of the spatial structure of fluctuations in travel time from seismic observations was done only from data of the LASA group (Aki, 1973) and from the North Tyan'-Shan' group of stations (Nersesov et al., 1972; Sedova, 1974).

Systematic differences of the parameters of seismic waves carry information on the difference of deterministic components of the inner structure of the investigated regions; random fluctuations of these parameters carry information on the nature of inhomogeneities. The detail of investigation of inhomogeneities with respect to fluctuations in the parameters of seismic waves depends on the density of the network of observations, the nature of the experimental material and the method of processing it.

This section gives the results of a number of studies by the KSE [Kompleksnaya seysmologicheskaya ekspeditsiya Instituta fiziki Zemli: Comprehensive Seismological Expedition of the Institute of Physics of the Earth] based on data obtained chiefly by expeditionary stations deployed in various years in a number of territories of the Soviet Union.

The greatest dimensions of the network of seismological stations of which materials were used in studying the fluctuations of parameters of longitudinal waves were determined by the area of the Soviet Union, and reached an area of 2000 x 8000 km. The network included 16 stations situated in different territories of the Soviet Union.

For more detailed studies, regional networks of stations were used with the following dimensions: Northern Tyan'-Shan' -- 200 x 400 km; Central Tyan'-Shan' -- 100 x 250 km; Northern Kazakhstan -- 150 x 250 km; Garm -- 50 x 100 km.

The most detailed studies were done on specially created compact groups of temporary expeditionary stations of the KSE. For instance in the Zeysk group the maximum distances between them were about 2 km. Selected groups of stations were deployed in such a way as to represent territories with different geological structures. The Northern Tyan'-Shan' group was placed on the junction between mountain and prairie sections, while the Central Tyan'-Shan' group was situated in the center of one of the largest mountain formations; the Northern Kazakhstan network of stations was placed within the limits of the Kazakh folded region; the Western group of stations was located on the European platform; the Garm network -- in the region of conjunction of two colossal tectonic systems -- Tyan'-Shan' and Pamir, etc.

Chapter 1. Fluctuations of Amplitudes and Travel Times

1. Presentation of experimental material and methods of processing it

The seismological experimental material from the different groups of stations differs in quantity and quality. The temporary groups of field stations sometimes were operated for the duration of a single field season, and therefore for such groups many epicentral regions are not represented due to lack of data. Depending on the amount and uniformity of the material, the earthquakes were grouped by epicentral zones in different ways. For instance in studying fluctuations of seismic oscillations, all earthquakes of Indonesia on the Northern Kazakhstan group of stations were considered jointly, while for the aggregate of stations deployed over the entire territory of the USSR, earthquakes of the Banda region of the sea were considered separately. Earthquakes of Alaska, the Aleutians, Kuril-Kamchatka and other zones were grouped differently for different sets of stations.

Let us introduce a number of symbols and definitions. The symbol e will denote a set of earthquakes of one epicentral region; a--a set of epicentral regions; S--a set of seismic stations; angle brackets <> denote the operation of statistical averaging; δ--deviations from the mean. A subscript will indicate the parameter of averaging, e. g. $\langle\rangle_e$ denotes averaging of data with respect to all earthquakes of a given region, and δ_e will mean deviation from the calculated mean.

To study the inhomogeneity of a medium one can use not only the fluctuations of amplitudes and travel times themselves, but also the correlations between these fluctuations. Actually, similar fluctuations should be observed for closely spaced stations. In the limit when the instruments are located on the same pedestal their readings should be identical.

For the sake of convenience in calculations and representation of results, the absolute values of differences $|\delta \lg A_i - \delta \lg A_j| = \delta\delta \lg A_{ij}$ and

$|\delta t_i - \delta t_j| = \delta\delta t_{i,j}$ are calculated with respect to each pair of stations (i,j). For the sake of brevity we will call these quantities the second differences. If the values of $\delta\delta \lg A_{i,j}$ are considered as a function of the distance between the corresponding stations $\Delta_{i,j}$, we get a representation of the results in a form that is close in content to the reciprocal structure function. The difference is that in this instance the absolute values of differences are used rather than their squares. In a similar way one can find the second differences with respect to regions and plot their values as a function of the average distance between regions.

2. Variations of magnitude deviations for the system of stations deployed over the entire territory of the USSR

We begin our analysis of fluctuations in amplitudes with the system of stations representing the entire territory of the USSR (Fig. 49). From the data of this system, the deviations of magnitudes δm were calculated for 492 earthquakes of eight regions (Table 20).

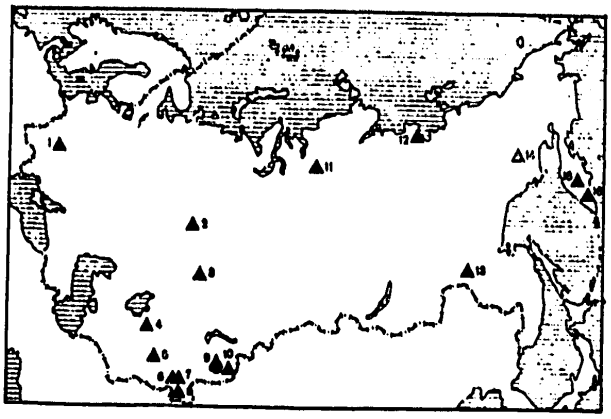

Fig. 49. Diagram of deployment of seismic stations

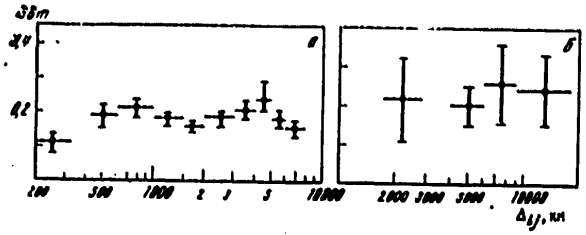

Fig. 50. Average values of the second differences of magnitudes δδm for seismic stations (a) and epicentral regions (b) from observations at stations deployed over the entire territory of the USSR: the horizontal lines show the interval of averaging; the vertical lines show the 70% confidence interval of the average values.

TABLE 20

Deviations of magnitudes for seismic stations deployed over the entire territory of the USSR

Epicentral regions	seismic stations															
	1	2	3	4	5	6	7	8	9	10	11	12	13	14	15	16
China	—	−0,01	−0,11	−0,09	−0,15	0,23	0,20	0,22	0,19	0,25	−0,03	−0,20	−0,09	−0,26	0,15	0,00
Indochina	0,00	−0,15	−0,01	0,04	−0,06	−0,12	−0,11	0,00	0,11	0,21	0,13	0,25	−0,01	−0,15	0,08	−0,08
Indonesia	0,17	0,20	0,11	0,21	0,18	0,27	0,31	0,25	0,07	0,06	−0,02	—	0,09	0,20	0,09	0,17
Banda Sea	—	−0,19	0,08	0,14	0,42	0,19	0,21	−0,01	0,22	−0,03	−0,31	−0,25	—	0,03	−0,18	0,02
Australia	—	—	−0,35	0,18	0,06	−0,58	−0,63	−0,54	−0,20	−0,08	0,39	0,39	−0,05	0,13	−0,21	0,08
India	−0,06	−0,03	−0,01	−0,27	−0,14	0,02	0,11	0,04	−0,01	0,09	−0,09	−0,08	0,39	−0,18	−0,04	−0,16
Red Sea	0,17	0,20	0,17	−0,11	−0,05	0,02	0,08	0,14	−0,13	−0,06	−0,07	−0,10	−0,02	0,19	0,15	0,01
Africa	−0,25	—	0,03	−0,14	−0,25	−0,01	−0,15	−0,09	−0,09	−0,46	—	—	−0,28	—	—	—

Let us examine the dependences of the second differences $\delta\delta m$ on the distance between stations. To do this, we refer to the graph shown in Fig. 50. It is clear from this graph that the second differences $\delta\delta m$ increase with distance between stations, reaching a maximum in the 600-1000 km interval. On the basis of the analogy between the function of second differences and the structure function, the position of this maximum on the Δ_{ij} axis can be interpreted as half the spatial dimension of the characteristic inhomogeneities, which agrees with the next minimum of the function in the 1500-2000 km interval. The second maximum of the given graph is observed in the vicinity of Δ_{ij} = 4000-5000 km.

3. Amplitude fluctuations on the North Tyan'-Shan' station group

For stations of the North Tyan'-Shan' network (Fig. 51) the second differences of logarithms of the P wave were considered. The processing technique here was somewhat different in connection with the fact that in the case of short distances between stations there was no need to introduce a correction into the epicentral distance and average values of the logarithm of the amplitude for each earthquake were determined as the arithmetical means, while the fluctuations were determined as the deviations from these means.

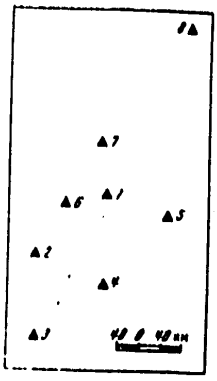

Fig. 51. Diagram of location of stations of the North Tyan'-Shan' group

In this way the errors associated with individual peculiarities of separate earthquakes were sharply reduced.

The mean values of fluctuations in amplitudes are summarized in Table 21. The experimental data were selected with respect to the quality and nature of the P wave recording; obligatory requirements were clarity of the first entry, pulse shape of the wave and a considerable, at least tenfold, excess in amplitude over the microseismic background. Altogether, 89 earthquakes were selected with $M \geq 5.75$.

The individual error of measurements of the maximum amplitude of oscillations in our procedure is about 0.04 log unit. Each value in the table is the result of averaging of the data of 5-15 earthquakes. Thanks to this, the relative error is reduced by a factor of $\sqrt{n}$ (n is the number of measurements), and hence the error of each tabulated value becomes no greater than 0.02. Let us note that this is considerably less than the variations $\langle\delta \lg A\rangle_e$. The average station values $\langle\langle\delta \lg A\rangle_e\rangle_S$ lie in the interval from -0.06 to 0.04, and the average values with respect to epicentral regions $\langle\langle\delta \lg A\rangle_e\rangle_\alpha$ lie in the interval from -0.13 to 0.06.

In accordance with the previously introduced definition, the quantities $\langle\langle\delta \lg A\rangle_e\rangle_S$ should be equal to zero since for each individual earthquake $\langle\delta \lg A\rangle_S = 0$. The difference of this quantity from zero that is observed in

TABLE 21

Average values of the fluctuations of amplitudes $\delta \lg A$ of a P wave on North Tyan'-Shan' stations

(1) Эпицентральные районы	(9) Сейсмические станции 1	2	3	4	5	6	7	8	$\langle(\overline{\delta \lg A})_\alpha\rangle_S$	$\langle\sigma_{\delta S}\rangle_\alpha$
(2) о-в Кадьяк	−0,01	−0,18	0,15	−0,03	0,01	0,01	−0,03	−0,03	−0,02	0,09
(3) Алеуты, Командоры	−0,10	−0,00	0,17	0,05	0,16	0,12	−0,03	0,05	0,03	0,13
(4) Курилы, Охотское море	0,18	−0,21	−0,20	0,01	0,01	0,11	0,12	−0,02	−0,06	0,15
(5) Японские острова	−0,03	0,07	0,15	−0,04	−0,02	0,10	0,04	0,08	0,04	0,11
(6) Индонезия	−0,15	−0,21	−0,01	−0,03	0,16	−0,03	0,18	0,12	0	0,14
(7) Европа и Северная Африка	−0,05	−0,11	−0,03	0,14	0,14	−0,20	−0,09	0,03	−0,03	0,13
(8) Исландия, Гренландия, Баффинова Земля	0,11	−0,10	0,17	0,18	−0,09	0,12	−0,03	−0,10	0,02	0,14
$\langle(\delta \lg A)_\alpha\rangle_s$	−0,08	−0,13	0,05	0,04	0,06	0,03	0,02	0		
$\langle\sigma_{\delta s}\rangle_s$	0,10	0,10	0,10	0,09	0,10	0,14	0,09	0,08		

KEY:
1--Epicentral regions
2--Kodiak Island
3--Aleutians, Komandors
4--Kurils, Sea of Okhotsk
5--Japanese Islands
6--Indonesia
7--Europe and North Africa
8--Iceland, Greenland, Baffin Island
9--Seismic stations

reality is probably due to the fact that individual averaging operations were done both with respect to insufficient data and with respect to appreciably different stations. The confidence interval for each average is equal to $\sigma/\sqrt{n}$ where n is the number of terms. Thus the values of averages with respect to epicentral regions do not exceed the confidence interval, and their values are not statistically significant. At the same time, the difference of mean square deviations is significant. In fact $\langle\sigma_{\delta S}\rangle_\alpha$ exceeds $\langle\sigma_{\delta\alpha}\rangle_S$, i. e. the fluctuations associated with differences of seismological conditions close to observation points are more pronounced than those associated with individual peculiarities of epicentral regions. No clear correlation occurs between separate pairs of columns and lines in Table 21.

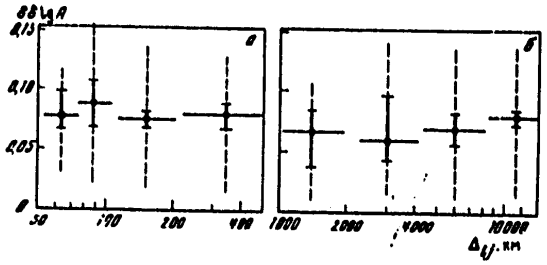

Fig. 52. Average values of second differences $\delta\delta \lg A$ for seismic stations (a) and epicentral regions (b) from observations on North Tyan'-Shan' stations. Horizontal lines show intervals of averaging, vertical lines show the 70% confidence interval of averages; the broken line shows the 70% confidence interval of an individual measurement.

Shown in Fig. 52 are the average values of the second differences $\delta\delta \lg A_{ij}$ as a function of Δ_{ij} determined for stations and epicentral regions respectively. The interval of variation of average values is small, and the confidence of their relative location is low. The confidence interval is most cases is greater than the observed variations. Nevertheless the graphs presented in Fig. 52 show some regularities.

In Fig. 52a, one notes a reduction in values of $\delta\delta \lg A$ with a transition from the distance range of 75-100 km to 55-75 km; this begins a decline in the graph that by definition must be at the coordinate origin. From this we conclude that the interval of spatial correlation of amplitudes in the vicinity of the seismic stations is about 50 km. The local reduction of $\delta\delta \lg A$ in the 110-200 km interval and the following slight increase are characteristic elements that show fluctuations of the spatial dimension of 110-200 km in the field of amplitudes.

Elements of the form of the graph of second differences that are similar to those considered can be seen as well for the epicentral regions in Fig. 52b. In fact, a reduction of $\delta\delta \lg A$ is observed in the distance interval of 2200-4000 km, and a relative increase can be seen on both sides of this interval. Apparently a drop in the graph to the zero value should occur when $\Delta_{ij} < 1000$ km. On the basis of the resultant data it is difficult to judge the interval of spatial correlation of amplitude fluctuations, but one can assume a characteristic scale of such fluctuations of 2200-4000 km.

Bearing in mind the small and commensurate values of the minima noted in Fig. 52a, b one can assume that they are genetically related. This relation consists in the fact that the 2200-4000 km scale of fluctuations in the amplitudes that is inherent in the relative location of earthquakes shows up in the fluctuations of amplitudes that have a characteristic dimension of 110-200 km and that are inherent in the same relative location of seismic stations.

4. Magnitude deviations on stations of the Central Tyan'-Shan' group

For the Central Tyan'-Shan' network (Fig. 53) data on magnitude deviations were analyzed as a function of the distance between stations. The data averaged by stations and by epicentral regions are shown in tables 22 and 23 as well as in Fig. 54.

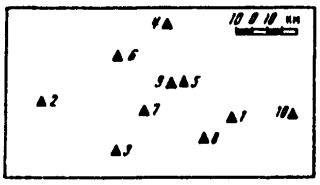

Fig. 53. Diagram of location of stations of the Central Tyan'-Shan' group

TABLE 22

Deviations of magnitudes from the average group value on Central Tyan'-Shan' stations, averaged by epicentral regions

Station	Δm	Station	Δm
1	0.046	6	-0.104
2	-0.023	7	-0.062
3	0.208	8	0.036
4	0.055	9	-0.124
5	-0.007	10	-0.058

TABLE 23

Deviations of magnitudes from the average for different epicentral regions with respect to the group of stations of Central Tyan'-Shan'

Regions	Δm	Regions	Δm
Alaska	0.03	India	-0.54
The Aleutians	0.14	The Persian Gulf	-0.03
Mongolia	0.17	Iran, Iraq	-0.05
Japan	0.11	The Red Sea	-0.30
Ryukyu Retto	0.02	Turkey	0.19
The Philippines	-0.02	The Mediterranean Sea	0.22
Indonesia	0.00	The Greenland Sea	0.05
Hindu Kush	-0.17		

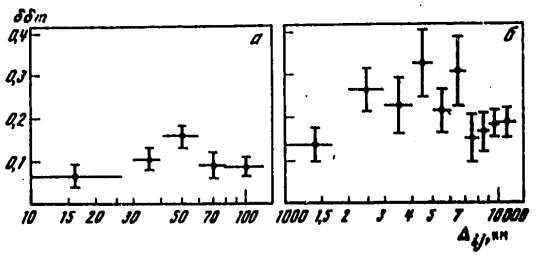

Fig. 54. Average values of second differences of magnitudes δδm for seismic stations (a) and epicentral regions (b) from observations on the Central Tyan'-Shan' group. See Fig. 52 for explanation

Analysis of these data shows a more contrasty manifestation of characteristic scales of fluctuations of the intensity of P waves that were noted previously on other groups of stations. As a matter of fact a reduction in correlatedness of magnitude deviations with increasing distance between stations is observed in the 40-50 km interval. With increasing Δ_{ij} one also notes a

maximum in the interval of 50-60 km and a new rise in the reciprocal relation between magnitude fluctuations that reaches an extremum for $\Delta_{ij} > 80$ km.

In plotting the graph of magnitude deviations as a function of distance between epicentral regions, the relatively large number of such regions enabled us to narrow the intervals of averaging and to increase detail on the graph (Fig. 54b). Here one can also observe good agreement with the data of other station groups: the first maximum is in the interval of 2000-3000 km, the first minimum -- in the interval of 3000-4000 km; the second, and most intense maximum is in the interval of 4000-5000 km, and is replaced by a minimum in the interval of 5000-6000 km. The maximum that can be distinguished from materials of the stations of the Central Tyan'-Shan' network in the interval of 6000-7000 km cannot be distinguished on other groups of stations due to shortage of data. The most remote minimum to be noted on the Central Tyan'-Shan' comes in the 7000-8000 km interval. Attention should be called to the fact that the interdependence of fluctuations of amplitude deviations at this distance is nearly the same as in the interval of 1000-2000 km.

5. Fluctuations of intensity of the P wave from materials of the North Kazakhstan group of stations

The relative placement of the seismic stations that make up the North Kazakhstan group is shown in Fig. 55. Data on fluctuations of intensity of the P wave are represented by amplitude deviations for 145 earthquakes of 16 epicentral regions, and are summarized in Table 24.

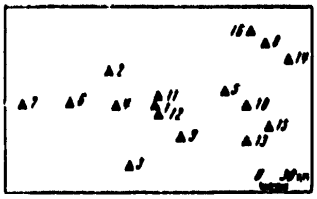

Fig. 55. Diagram of deployment of stations of the North Kazakhstan group

The second differences $\delta\delta \lg A_{ij}$ were calculated from the average values of amplitude fluctuations, and graphs were plotted for the way that they depend on the distance between corresponding stations (Fig. 56a). Just as for the North Tyan'-Shan' stations, the interval of spatial correlation of fluctuations of amplitudes is 50-80 km. The minimum on the graph in the 120-150 km interval also agrees with the data of other groups of stations.

Shown in Fig. 56b are the second differences of the logarithms of amplitudes as a function of the distances between epicentral regions. Since the dimensions of the regions are being compared with the distances between regions, the oscillations on the graph are strongly smoothed out. Nevertheless, there can be no doubt about the minimum in the interval of 5000-7000 km.

TABLE 24

Average values of fluctuations of amplitudes of P waves on North Kazakhstan Stations

(2)	(1) 1	2	3	4	5	6	7	8	9	10	11	12	13	14	15	16
(3) Аляска	−0,08	0,15	−0,06	0,03	−0,06	−0,12	0,17	0,10	0,11	0,02	−0,02	−0,03	0,00	0,01	0,07	−0,02
(4) Алеуты	−0,01	0,34	0,10	−0,03	−0,22	−0,15	—	0,02	0,04	0,04	−0,06	0,02	0,02	0,14	0,06	−0,02
(5) Япония	−0,04	0,23	0,08	−0,03	−0,06	−0,07	—	−0,03	0,02	−0,01	−0,06	−0,11	0,09	—	0,02	—
(6) Индонезия	0,00	−0,15	−0,02	0,15	−0,01	−0,06	—	0,10	−0,01	−0,07	−0,25	0,00	0,14	−0,02	0,18	−0,06
(7) Курилы	0,03	−0,12	0,16	−0,34	−0,07	−0,09	0,20	0,13	−0,09	0,01	−0,04	−0,05	−0,02	—	0,07	0,09
(8) Камчатка	0,07	−0,20	—	0,20	−0,10	−0,02	—	0,17	−0,09	0,06	0,01	0,06	−0,12	0,21	0,10	−0,20
(9) Китай	0,02	—	0,06	−0,12	—	0,04	−0,23	−0,02	−0,03	−0,09	−0,01	0,07	0,06	0,02	−0,15	−0,01
(10) Индия	−0,06	—	—	−0,04	−0,08	−0,11	—	0,16	−0,03	−0,10	−0,10	0,02	0,00	—	0,23	0,20
(11) Индокитай	0,17	—	—	−0,09	0,00	0,04	—	−0,04	−0,23	0,07	0,15	0,06	−0,01	−0,19	−0,26	−0,27
(12) Тайвань	−0,07	—	−0,01	−0,07	−0,04	−0,02	—	−0,12	0,12	−0,11	−0,28	0,06	0,18	—	0,29	−0,22
(13) Соломоновы о-ва	0,06	—	—	—	−0,16	—	—	−0,07	0,13	−0,25	0,06	0,01	0,04	−0,09	0,12	−0,16
(14) Северная Атлантика	0,18	0,06	−0,06	−0,07	−0,09	−0,02	—	−0,18	−0,07	−0,12	0,06	0,09	0,00	−0,03	0,18	−0,21
(15) Чили	−0,04	−0,07	0,00	0,06	0,03	0,02	−0,11	−0,03	0,23	−0,09	−0,25	−0,05	0,06	0,19	0,21	0,07
(16) Средиземное море	−0,07	—	—	—	0,26	—	—	0,04	0,22	0,07	−0,18	0,00	−0,04	0,18	0,11	0,03
(17) Океания	−0,06	0,11	0,10	−0,12	−0,01	−0,10	—	0,14	0,11	−0,26	−0,10	−0,09	0,18	0,16	−0,04	0,06
(18) Арктика	0,06	—	—	—	—	—	—	0,12	−0,23	0,04	−0,14	0,06	0,01	—	0,06	−0,07

KEY:
1--Seismic stations
2--Epicentral regions
3--Alaska
4--The Aleutians
5--Japan
6--Indonesia
7--The Kurils
8--Kamchatka
9--China
10--India
11--Indochina
12--Taiwan
13--The Solomon Islands
14--The North Atlantic
15--Chili
16--The Mediterranean Sea
17--Oceania
18--The Arctic

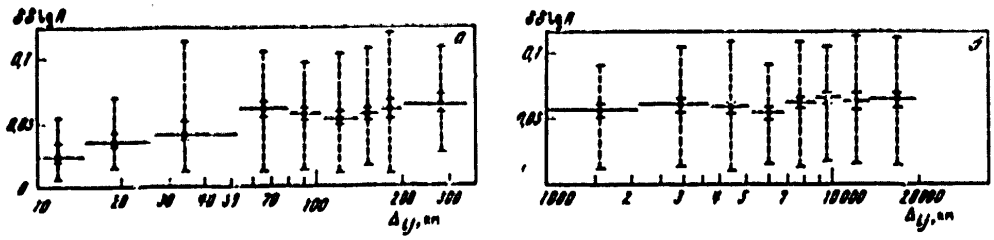

Fig. 56. Average values of the second differences $\delta\delta \lg A$ for seismic stations (a) and epicentral regions (b) from observations on stations of North Kazakhstan. See Fig. 52 for explanation

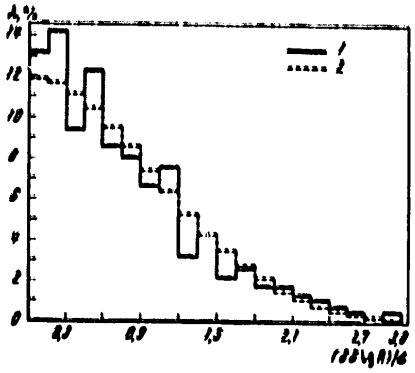

Fig. 57. Distribution of second differences $\delta\delta \lg A$ for the group of stations in North Kazakhstan: 1--Experimental; 2--theoretical normal for $\sigma = 0.08$ log unit

Of definite interest is the question of the distribution of second defferences of intensity of the P wave. For this purpose the experimental distribution of deviations of the logarithms of amplitudes was plotted for $\Delta_{ij} > 40$ km (Fig. 57). The experimental distribution was compared with a number of theoretical distributions. Best agreement is observed with the normal distribution when $\sigma = 0.08$ log unit, which is shown for clarity in Fig. 57.

6. Variations of travel times on stations deployed over the entire territory of the USSR and in the North Tyan'-Shan' group

The same second-difference procedure as used for the logarithms of amplitudes was applied to the travel times of the P wave. These data are less reliable because of the microseismic interference on the seismographic recordings, and the related difficulties in distinguishing the first entries of the P wave.

We begin our analysis of fluctuations in travel times with an examination of materials of the system of stations deployed over the entire territory of the USSR (see Fig. 49). The average deviations of travel times for the 16 stations with respect to 8 epicentral regions are summarized in Table 25. The second differences of travel times (Fig. 58) increase with increasing distance between stations and reach a maximum in the interval of 350-600 km. At distances of 600-1200 km a shallow relative minimum is observed which is then replaced by a sharp maximum in the interval of 1200-2000 km. Further on there is a minimum situated in the interval of 2200-4000 km.

In interpreting the extrema of the second-difference functions by analogy with the structure function we can assume that inherent in deviations of the travel times of P waves within the limits of the USSR and adjacent regions are characteristic scales of fluctuations of the order of 1000 and 3000 km.

TABLE 25

Average deviations of the travel time δt (s) of a P wave for the system of stations deployed over the entire territory of the USSR

	Seismic stations															
	1	3	2	4	5	6	7	8	9	10	11	12	13	14	15	16
China	0,0	2,1	—1,1	0,4	0,6	1,8	1,6	1,4	0,2	—1,2	—1,8	2,3	2,7	1,8	3,2	3,3
Indochina	—1,8	—2,1	—1,4	—1,7	—1,9	—1,0	—0,8	—0,6	0,4	—1,2	—0,5	—	—1,5	—2,0	0,1	—1,4
Banda Sea	—1,1	—	—1,7	—	—	—2,0	—1,1	—0,8	—1,4	—	—	—	—3,2	—1,6	—1,9	—3,8
Australia	—0,6	—2,0	—1,5	0,1	0,1	0,0	—0,1	—1,3	0,4	—0,6	—3,0	0,6	—	1,8	—2,2	—1,0
India	—	—	—1,1	—1,7	—1,7	—3,0	—2,8	—3,3	—1,2	—1,8	—3,4	—3,5	—1,8	—1,8	—1,5	—
Red Sea	—0,3	—0,9	—0,9	—0,3	—0,1	—1,3	—0,6	—0,2	0,4	—0,9	—2,0	—1,0	—	0,0	—1,8	—2,1
Africa	0,4	—0,3	1,7	1,4	1,3	3,8	1,8	4,8	2,4	3,2	2,1	1,1	1,2	3,2	—	—
	—2,3	—	0,3	—	—	—2,3	—	—2,2	—1,2	—	—	—	—	—	—	—

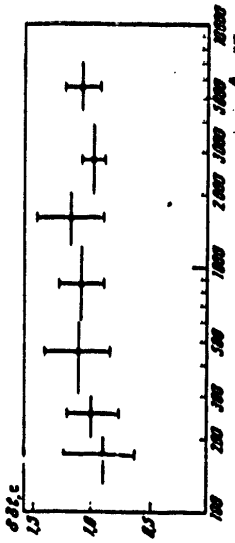

Fig. 58. Average values of second differences of travel times δδt (s) for the system of stations deployed over the entire territory of the USSR. See Fig. 52 for explanation

In calculating the fluctuations of travel times on stations of the North Tyan'-Shan' group each earthquake had its own straight-line hodograph that best approximated the observed data. The use of such hodographs has certain advantages and disadvantages. An advantage is that in this case the fluctuations are independent of the changes in apparent velocity that characterize large-scale anomalies of the hodograph. The linear dimensions of such an anomaly are comparable to or greater than those of the station group; the measured fluctuations of times characterize only the "fine" structure of the wave field. It should be borne in mind that in isolated cases the makeup of the group was changed (shifts of stations, lack of recordings), and this must have had an effect both on the parameters of the straight-line hodograph and on the values of fluctuations in travel times.

The fluctuations of travel times δt are made up of two main parts: the station anomaly that depends on the structure of the medium directly beneath the station and is calculable as the average of all measured deviations of travel times, and the individual fluctuations relative to this average.

The station anomaly can be calculated in different ways, depending on the earthquake sample with respect to which averaging is done.

First let us consider the results of averaging of station fluctuations with respect to separate epicentral regions $\langle \delta t \rangle_e$. These data are given in Table 26. The average values of fluctuations with respect to all stations for each region $\langle\langle \delta t \rangle_e \rangle_S$, as implied by our method of determining fluctuations, should be close to zero, and therefore slight corrections have been made in the columns of Table 26 so that $\langle\langle \delta t \rangle_e \rangle_S = 0$.

TABLE 26

Average values of deviation (s) from the straight-line hodograph $\langle \delta t \rangle_e$ of the P wave on stations of the North Tyan'-Shan' group

(2) Эпицентральные районы	(1) Сейсмические станции 1	2	3	4	5	6	7	8	$\langle \sigma_e^2 \rangle_S$
(3) О-в Кадьяк	−0,13	0,08	−0,41	−1,31	0,57	0,02	−0,8[illegible]	2,90	1,40
(4) Алеуты, Командоры	0,27	−0,73	−0,55	0,20	1,08	0,68	−2,72	1,56	1,34
(5) Курилы, Охотское море	−1,51	−0,13	−0,01	1,65	0,20	0,62	−1,65	0,83	1,13
(6) Японские острова	−0,93	−0,48	−1,28	−0,16	0,68	−0,16	0,98	1,27	0,93
(7) Индонезия	−0,37	−0,26	−2,19	2,11	−0,48	−0,01	−2,25	2,45	1,93
(8) Европа и Северная Африка	0,11	0,87	−1,58	1,72	−0,29	−0,18	−0,29	−0,11	1,03
(9) Исландия, Гренландия, Баффинова Земля	−1,74	1,09	1,88	−1,11	−1,28	0,97	−0,28	0,52	1,21
$\langle\langle \delta t \rangle_e \rangle_S$	0,81	0,07	−0,78	0,61	0,07	0,28	−1,02	1,36	
$\langle \sigma_m^2 \rangle_S$	0,25	0,48	1,40	1,55	0,97	0,58	1,18	1,18	

KEY:
1--Seismic stations
2--Epicentral regions
3--Kodiak Island
4--Aleutians, Komandors
5--Kurils, Sea of Okhotsk
6--Japanese Islands
7--Indonesia
8--Europe and North Africa
9--Iceland, Greenland, Baffin Island

A striking peculiarity of the fluctuations is the wide range of variations in $\langle \delta t \rangle_e$ from -2.72 to +3.11, considerable differences being noted in isolated cases on the same station for adjacent regions (for instance for station 7 and regions IV and V the difference is 3.21 s). The differences of average station fluctuations $\langle\langle \delta t \rangle_e \rangle_\alpha$ are considerable: from -1.02 to +1.38. These values characterize the inhomogeneity of the upper part of the cross section beneath the seismic stations. If consideration is taken of the fact that all stations are located on crystalline rocks, and inhomogeneity occurs only within the limits of the earth's crust, which is about 45 km thick, the contrast in velocity fluctuations should be about 10%. A prreciable differences of the mean square deviations $\sigma_{e\alpha}$ (from 0.25 to 1.55) characterize the strong contrast between inhomogeneities of the crust and those of the mantle, the latter not being part of the upper cross section. The presence of these inhomogeneities shows up with greatest contrast in the data of station 4. If it is assumed that the characteristic vertical and horizontal size of these inhomogeneities is the same, and equal to approximately 100 km, then the fluctuations of velocity must average 10-12%, and the maximum deviations -- up to 15-20%. On the other hand, if such anomalies are impossible, we must assume that their vertical dimension is appreciably greater than the horizontal.

Shown in Fig. 59 are the second differences of the travel time $\delta\delta t_{ij}$.

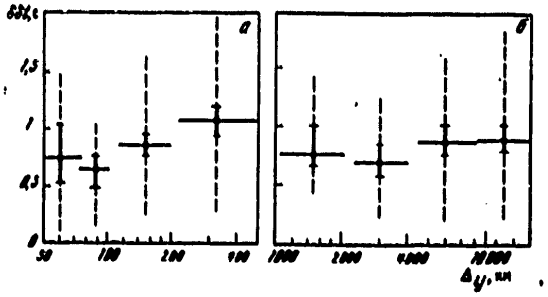

Fig. 59. Average values of second differences of travel times δδt for seismic stations (a) and epicentral distances (b) from observations on the North Tyan'-Shan' group. See Fig. 52 for explanation

The structure of the graphs and the behavior of the average δδt are very similar to what was noted in Fig. 52 for the second differences of the logarithms of amplitudes. The elements of the graph of δδt have been shifted to the left with respect to the data for δδ lg A. The interval of correlation of fluctuations of travel time is less than the fluctuations of amplitudes, and therefore the inflection and decline of the graph of δδt that correspond to the graph of δδ lg A have been pushed off to the left out of the figure.

Let us note that in wave propagation in media with random inhomogeneities the intervals of correlation of fluctuations of amplitudes must be greater than the fluctuations in travel times.

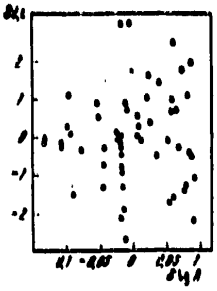

Fig. 60. Correlation of fluctuations in the amplitudes and travel times of P waves from data of the North Tyan'-Shan' station group

Similarity in the behavior of graphs of $\delta\delta \lg A$ and $\delta\delta t$ is also a rather convincing sign of statistical significance of the results.

The correlation of fluctuations in amplitudes and travel times is illustrated by Fig. 60 plotted from data of the North Tyan'-Shan' group of stations. We can readily see that there is practically no correlation. This result is important for judging the nature of inhomogeneities of the upper part of the cross section that determine the average station anomalies of amplitude and travel time: velocity inhomogeneities of the upper part of the medium that cover points of observation should generate weakly correlated functions $\delta \lg A$ and δt that are characterized by a correlation coefficient of 0.4 in the case of low-contrast anomalies of velocity (Chernov, 1975). Thus the lack of correlation can be interpreted as comparative homogeneity of the very top of the cross section, about a 10 km layer. Then the average station anomalies should be considered as the result of inhomogeneities that are situated more deeply, right down to the underside of the earth's crust. Anomalies of amplitudes may be generated both by velocity inhomogeneities and by the inhomogeneities of absorbing properties. Such inhomogeneities with dimensions of 50-100 km and average Q of about 300 should be characterized by variations of Q ranging from 150 to 400.

Chapter 2. Investigation of Fluctuations in the Shape of a P Wave Recording

1. Study of the shape of the recording of a P wave on stations situated in different territories of the Soviet Union

This study is based on calculating the coefficients of correlation between seismic signals registered by different seismic stations. The initial sections of the seismograms that contained the recording of the P wave were quantized. The seismograms that were used to study the spatial structure of the P wave were obtained on 55 seismic stations situated in different regions of the USSR, and in part included data used in studying the fluctuations of amplitudes and travel time described in the preceding chapter.

In selecting the material, consideration was given to the following peculiarities of seismic recordings: the pulse shape of the initial part of the recording, i. e. those sources that had short-term action and were

characterized by simplicity of the shape of the first wave and its comparatively wide-band spectrum; sufficient intensity of the recording -- on three stations as a minimum; maximum peak-to-peak amplitude of the first pulse on the seismogram of at least 10 mm; clear entries.

Three-component recordings of 51 earthquakes with magnitude $M > 5$ were used with epicenters removed by a distance of 30-80° from the stations. The foci of the earthquakes were situated in different regions of the earth: in the western part of the Pacific Ocean belt, in Indonesia, in the Mediterranean Sea, in the North Atlantic and in the Arctic Ocean.

The X-component corresponding to the direction toward the source was predetermined from the horizontal components of each recording N-S and W-E. In this way the vertical and radial X-component of the P wave recording were subjected to subsequent correlation analysis.

The shape of the recording is analyzed by comparing recordings of the P wave from one source on different stations. A quantitative measure of the degree of resemblance of shape is the correlation coefficient K_{ij} of the recordings of the i-th and j-th seismic stations determined from the formula

$$K_{ij} = \frac{\int P_i(t) P_j(t)\,dt}{\left[\int P_i^2(t)\,dt \int P_j^2(t)\,dt\right]^{1/2}}.$$

Since $K_{ij} = K_{ji}$ the entire set of correlation coefficients for n earthquakes can be represented as a symmetric matrix containing n - 1 rows and columns.

The value of the correlation coefficient for a pair of similar functions such as the recordings of remote earthquakes is a maximum with the proper coincidence of the first entries. In reality, there is no firm certainty that the beginning of coding of the recording coincides with the first entry. Possible errors reach a quarter of the predominant period.

In order to keep the errors associated with uncertain determination of the beginning of readout from "spoiling" the maximum value of K_{ij}, the signals were "synchronized" by calculating the correlation coefficients for several relative locations. The maximum shift of one signal relative to another was equal to ±0.4 s, which enabled calculation of nine values of the correlation coefficient for each pair of recordings in the case of a 0.1 s displacement step equal to the quantization step.

In other words, in the "synchronization" process the section of the correlation of two signals in the vicinity of their first arrivals is calculated. After that, only the maximum value of the function on this section was used.

Since there were comparatively few data of joint observations on individual pairs of stations, they were processed all together rather than being separated by epicentral regions. It was established as a result of such an analysis that stability of the shape of the vertical component is higher on

the average than the radial component. This shows up in the fact that high values of the correlation coefficient K ≥ 0.7 appear for the vertical component comparatively more often than for the horizontal component.

Of interest is an examination of the correlations both within groups of seismic stations and between separate groups. It has been established that the groups of stations of the European part of the USSR and Soviet Middle Asia are characterized by a relatively high level of internal correlation. These groups are unequally related with each other: the Middle Asia stations show good correlation with Northern Caucasus stations, while those of the European part of the nation show good correlation with both of these groups. The Yakut stations correlate well with all regional groups of stations. It is not possible to trace the nature of the correlation for other groups of stations due to insufficient data.

Thus relatively high correlation of the vertical component of the P wave recording is noted both within separate groups (European, Middle Asian) and between remotely spaced stations. At the same time, in many instances weak correlation is observed between comparatively close stations. With regard to the spatial correlation of the X-component it can be stated that the nature of the correlation dependences is basically the same as for the vertical component. At the same time, the vertical components correlate with each other more strongly on the whole than do the radial components.

The distortion of signal shape that shows up in impairment of its correlation with another, reference signal, may be attributed to several causes. In particular to scattering of seismic energy when the wave passes through a region that contains inhomogeneities that are contrasty and small compared with a wavelength, as well as to the distorting effect of the contrasty relief of buried and surface boundaries.

High correlation of the shape of a P wave may show up at distances of several thousand kilometres between stations if the deep interior of the earth introduces weak distortions, i. e. if it is comparatively uniform; moreover, it is important that the signals radiated by the source in different directions have a similar shape, even though they may differ appreciably in amplitude.

A reduction of correlation is usually caused by the screening action of sections of the medium in which minor inhomogeneities are strongly developed. The dimensions of these sections amount to several hundred kilometres, while the average distances between them are considerably greater -- thousands of kilometres.

Having made a detailed analysis of the spatial structure of the P wave, it is of interest to evaluate the principal scale effects of fluctuations of waveshape and to relate them to the inhomogeneity of the structure of the earth's interior.

2. Investigation of detailed structure of the shape of the P wave

The detailed structure of the longitudinal wave was studied from the data of observations on dense systems of seismic stations: North Tyan'-Shan', North Kazakhstan, European, Central Tyan'-Shan', Garm and Zeysk. These groups of stations operated at different times, the number of stations and their relative location in the group also changed, and therefore the study was based on initial data differing in detail.

The data of only the vertical component of the recording are considered here. The method of data preparation and calculations of the correlation coefficients is described in the preceding section.

The North Tyan'-Shan' Group of Stations. The recordings of 89 earthquakes were used, the same ones that were used to study the structure of fluctuations of amplitudes and travel time. A matrix of correlation coefficients K_{ij} was calculated for each earthquake; the values of the matrix were rather high on the average, exceeding a level of 0.5. The matrices of average values of the correlation coefficients $\langle K_{ij} \rangle_e$ were found from the correlation matrices of individual earthquakes corresponding to a single epicentral region; they are given in Table 27. Although each element of these matrices characterizes data relating to two stations, the individual characteristic of the shape of the P wave on individual stations can be found by averaging the $\langle K_{ij} \rangle_e$ with respect to all pairs that contain the given station i. The resultant values of $\langle\langle K \rangle_e \rangle_{Si}$ are presented in Table 28.

TABLE 27

Averaged matrices of the coefficients of correlation of the shape of the initial shape of the recording from materials of stations of North Tyan'-Shan'

	2	3	4	5	6	7	8
1	0,52	0,61	0,65	0,58	0,53	0,58	0,62
2		0,68	0,51	0,63	0,58	0,64	0,63
3			0,71	0,79	0,76	0,80	0,69
4				0,76	0,70	0,32	0,71
5					0,71	0,58	0,77
6						0,64	0,71
7	(1) [illegible]						0,65

	2	3	4	5	6	7	8
1	0,54	0,65	0,62	0,68	0,60	0,56	0,49
2		0,62	0,44	0,49	0,60	0,74	0,68
3			0,52	0,62	0,75	0,63	0,68
4				0,65	0,57	0,43	0,55
5					0,67	0,67	0,70
6						0,61	0,78
7	(2) Алеутск., Командорск.						0,63

	2	3	4	5	6	7	8
1	0,57	0,32	0,53	0,60	0,56	0,57	0,47
2		0,52	0,47	0,53	0,56	0,41	0,61
3			0,44	0,53	0,58	0,39	0,51
4				0,62	0,62	0,58	0,58
5					0,67	0,61	0,51
6						0,53	0,62
7	(3) Курилы, Охотское море						0,58

	2	3	4	5	6	7	8
1	0,44	0,58	0,65	0,64	0,60	0,51	0,65
2		0,69	0,51	0,64	0,69	0,58	0,51
3			0,42	0,79	0,78	0,78	0,66
4				0,67	0,62	0,48	0,62
5					0,70	0,67	0,77
6						0,71	0,68
7	(4) Японские острова						0,74

	2	3	4	5	6	7	8
1	0,54	0,53	0,50	0,54	0,54	0,58	0,47
2		0,48	0,50	0,43	0,37	0,61	0,36
3			0,65	0,54	0,67	0,69	0,62
4				0,53	0,59	0,48	0,51
5					0,66	0,57	0,58
6						0,67	0,53
7	(5) Индонезия						0,82

	2	3	4	5	6	7	8
1	0,46	0,33	0,40	0,50	0,48	0,42	0,39
2		0,54	0,54	0,45	0,46	0,56	0,48
3			0,37	0,53	0,78	0,49	0,59
4				0,58	0,57	0,51	0,56
5					0,56	0,61	0,71
6						0,53	0,56
7	(6) Европа, Северная Африка						0,61

	2	3	4	5	6	7	8
1	0,79	0,44	0,88	0,46	0,57	0,54	0,70
2		0,59	0,34	0,62	0,51	0,60	0,41
3			0,60	0,77	0,80	0,47	0,68
4				0,67	0,67	0,44	0,48
5					0,81	0,50	0,57
6						0,43	0,70
7	(7) Исландия, Гренландия, Баффинова Земля						0,74

KEY: 1--Kodiak Island
2--Aleutains, Komandors
3--Kurils, Sea of Okhotsk
4--Japanese Islands
5--Indonesia
6--Europe, North Africa
7--Iceland, Greenland, Baffin Island

TABLE 28

Average values of the coefficients of correlation of the shape of a P wave recording for stations of Northern Tyan'-Shan'

(1)	(2) Сейсмические станции								
	1	2	3	4	5	6	7	8	9
(3) О-в Кадьяк	0,58	0,60	0,69	0,65	0,69	0,66	0,60	0,68	0,61
(4) Алеуты, Командоры	0,59	0,59	0,64	0,54	0,64	0,65	0,62	0,65	0,62
(5) Курилы, Охотское море	0,54	0,50	0,43	0,55	0,58	0,52	0,53	0,47	0,52
(6) Японские острова	0,56	0,58	0,67	0,57	0,70	0,66	0,64	0,66	0,64
(7) Индонезия	0,53	0,53	0,61	0,53	0,57	0,61	0,63	0,57	0,57
(8) Европа, Северная Африка	0,43	0,50	0,55	0,53	0,56	0,56	0,53	0,56	0,53
(9) Исландия, Гренландия, Баффинова Земля	0,57	0,50	0,65	0,61	0,59	0,60	0,56	0,61	0,59
(10) Среднее	0,55	0,54	0,60	0,57	0,62	0,61	0,59	0,60	

KEY:
1--Epicentral regions
2--Seismic stations
3--Kodiak Island
4--Aleutians, Komandors
5--Kurils, Sea of Okhotsk
6--Japanese Islands
7--Indonesia
8--Europe, North Africa
9--Iceland, Greenland, Baffin Island
10--Average

The average values of the coefficients calculated from the rows of the table are the station characteristics, while those calculated from the columns are the averaged characteristics of the given earthquake sample for a specific epicentral region. The average values of the coefficients of correlation of the shape of the recording of a P wave for stations of Northern Tyan'-Shan' vary from 0.43 to 0.70. Since each value is found by averaging at least 50 individual estimates, differences greater than 0.02 should be taken as significant.

For each seismic station the values of the coefficients are varied as a function of the azimuth to the epicentral region, the amount of the variation reaching 0.2. For each of the seven regions the values of the coefficients change little as a function of the position of the recording station, and variations remain within limits of 0.1. This means that the change in spatial stability of the shape of the P wave is related primarily to the position of the epicentral region, and depends comparatively little on the individual peculiarities of the seismic stations. Let us note that the differences in frequency responses of the recording channels should show up in variations of the average values of the coefficients with respect to different pairs of stations for separate epicentral regions. The comparatively slight values of these variations show that the effect of the difference in spatial stability of the P wave from different epicentral regions is reliably detected on the background of variations that may be possibly associated with some non-identity of equipment characteristics.

The appreciable influence that the region of location of the source has on the spatial structure of the shape of the longitudinal wave shows up in comparatively weak similarity of the correlation matrices for different regions.

TABLE 29

Correlation of matrices of the coefficients of correlation of the shape of the recording of a P wave for all epicentral regions

Эпицентральные районы	I	II	III	IV	V	VI	VII
I	1	0,28	−0,09	0,32	0,30	0,57	0,006
II		1	−0,30	0,54	0,40	0,44	0,25
III			1	0,002	0,03	0,02	−0,1
IV				1	0,42	0,38	0,48
V					1	0,44	0,36
VI						1	0,21
VII							1

Эпицентральные районы = Epicentral regions

Note: Roman numerals denote I--Kodiak Island
II--Aleutians, Komandors
III--Kurils, Sea of Okhotsk
IV--Japanese Islands
V--Indonesia
VI--Europe, North Africa
VII--Iceland, Greenland, Baffin Island

To find a quantitative measure of similarity of matrices of $\langle K \rangle_e$, we correlated them with each other, getting the seventh-order matrix shown in Table 29. In correlating the matrices, they were all converted to numerical series, the values of each series being referred to a zero average. Twenty-one correlation coefficients were calculated, of which three are negative, but have low absolute values. The positive values of the coefficients range in absolute value from 0.02 to 0.57.

Thus each value in Table 29 was calculated from two series containing 21 terms apiece; the mean square error of the result close to zero is ±0.3, and on the 0.4 level -- from 0.1 to 0.5. Therefore values exceeding +0.4 and -0.3 have a considerable difference from the background. A comparatively high correlation is observed in the initial matrices for remote territories of Alaska and the Mediterranean. No dependence of the degree of correlation on distance between epicentral regions is observed.

Let us consider the way that the correlation coefficient $\langle K \rangle_e$ depends on the distance Δ_{ij} between pairs of seismic stations i and j and on their position relative to the source. In doing this we separate all data into two parts corresponding to longitudinal and transverse correlations. In the first case the source is in line with the stations, and in the second -- in the direction perpendicular to the line joining the stations.

Shown in Fig. 61 are data obtained in our observations on North Tyan'-Shan' stations and also in observations by G. M. Tsibul'chik in the Sayans (1968) and by V. Din in North America (1965). All these data were obtained by

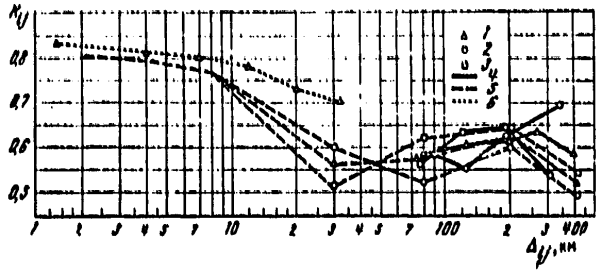

Fig. 61. Coefficients of correlation of the shape of the recording as a function of the distance between stations: 1--correlations with respect to all directions; 2--longitudinal correlation; 3--transverse correlation; 4--our data from stations of the North Tyan'-Shan' group; 5--data of V. Din (1965); 6--data of G. M. Tsibul'chik (1968)

short-period vertical instruments. The observations in the Sayans are characterized by short distances between stations from 1 to 30 km. The data on correlation are not differentiated with respect to the position of stations relative to the direction to the source. The level of correlation falls off uniformly with increasing Δ_{ij} from 0.85 to 0.70.

V. Din's data relate to a wide range of distances from 2 to 400 km. The graphs of $K(\Delta_{ij})$ have a characteristic shape: as Δ_{ij} increases one first observes a drop, then a rise and once again a drop to an asymptotic value of $K_{ij} \approx 0.5$ when $\Delta_{ij} = 400$ km. Din's curve is situated considerably lower than Tsibul'chik's as a consequence of the difference in the length of the signals being correlated: 20 s for V. Din, and 3 s for G. M. Tsibul'chik.

It is important to note that the graph of longitudinal correlation is as it were the graph of transverse correlation stretched out in the Δ_{ij} scale.

The same characteristic features can be seen as well on our graphs in the interval of $\Delta_{ij} = 70$-400 km. At $\Delta_{ij} = 120$-190 km a maximum K is observed that can be identified with the corresponding maximum of the Din curve: the minimum of transverse correlation is at $\Delta_{ij} \leq 70$ km. Corresponding characteristics of an element of the curve of longitudinal correlation are noted at $\Delta_{ij} \geq 340$ km (maximum) and at $\Delta_{ij} = 125$ km (minimum). Thus our data show general similarity to those of V. Din as expressed in the identical structure of the graphs of $K(\Delta_{ij})$ and their close levels at extremum values. This peculiarity of the spatial change of shape of the longitudinal wave is probably a consequence of similarity in the structure of inhomogeneities of the earth in different regions. Let us examine this problem in more detail.

The differences in the intervals of longitudinal and transverse correlation indicate that the horizontal inhomogeneities that distort the waveshape lie at such depths that their upper edges are below the open surface. In this connection, the "shadows" of inhomogeneities that are projected by seismic rays onto the surface of the earth are stretched out in the source-

inhomogeneity direction. Let us note that in the given case when remote earthquakes are used we see longitudinal correlation with respect to some intermediate direction closer to the wave front rather than in pure form, i. e. along the rays. Therefore the true longitudinal correlation of the shape must extend to still greater distances.

The interval of transverse correlation of amplitude and phase of a plane wave is close to the characteristic dimension of anomalies of the field of velocities of elastic waves (Chernov, 1958). This statement can be applied to waveshape as well since the latter is determined by the ratio of amplitudes of separate extrema and by their position in time from the initial part of the seismic recording.

Let us define the interval of correlation of shape as the distance at which the first minimum is observed on the curve of $K(\Delta_{ij})$. Taking into consideration that the wave front in the region of exit to seismic stations has a low slope, we conclude that the characteristic scale of a horizontal inhomogeneity in the vicinity of North Tyan'-Shan' is no more than 70 km; extrapolation of the graph of $K(\Delta_{ij})$ toward low values of Δ_{ij} to a level of $K_{ij} = 0.5$ (the same as the level of the minimum on Din's curve) gives a value of about 50 km for the interval of correlation of inhomogeneities. In North America (region of the Tonto Forest group) the corresponding dimension is 30 km.

The North Kazakhstan Group of Stations. In the given case a more complicated technique was used for studying the shape of the P wave from remote earthquakes. The similarity of shape was studied in three frequency ranges: up to 1 Hz, from 1 to 1.5 Hz and from 1.5 to 3 Hz; to do this, three numerical filters were introduced into the program for calculating the correlation coefficients, and as a result of filtration, three signals -- $P_1(t)$, $P_2(t)$ and $P_3(t)$ -- characterizing clearly bounded spectra, were derived from each signal P(t).

The correlation coefficients were calculated for two groups of earthquakes in intervals of epicentral distances of 3000 km < Δ < 10,000 km and Δ>10,000 km; the latter interval corresponds to registration of the PKP wave.

For the first group of earthquakes the coefficients of correlation of shape were calculated as well from wide-band recordings -- from 0.5 to 3 Hz (Fig. 62).

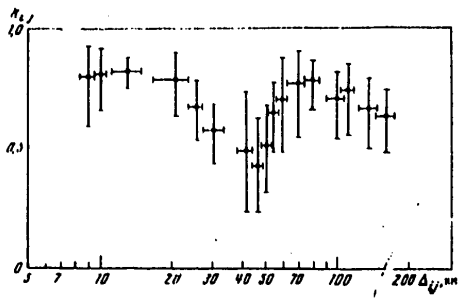

Fig. 62. Correlation coefficient for shape of recording as a function of the distance between stations of the North Kazakhstan group from wide-band (0.5-3 Hz) recordings. See Fig. 52 for explanation

The data of each group were plotted separately for three frequency ranges in the form of the average values of the correlation coefficient as a function of the distance between stations Δ_{ij} and are shown in Fig. 63. The individual values were averaged over the distance intervals Δ_{ij} that are shown by the horizontal lines. The solid vertical line shows the 70% confidence interval for evaluation of the average, and the broken line -- for the individual values.

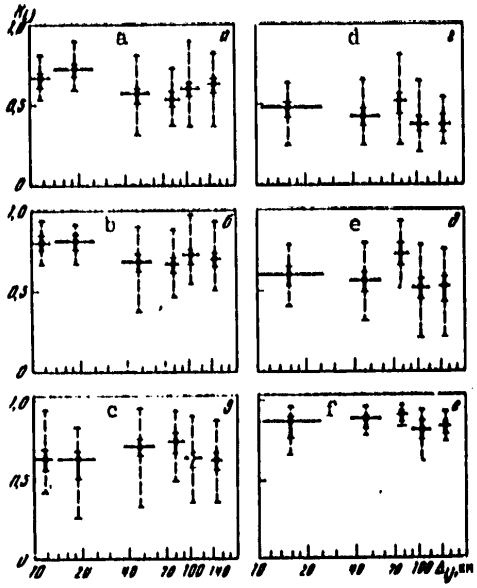

Fig. 63. Coefficient of correlation of the shape of a recording as a function of distance between stations of the North Kazakhstan group: a, b, c--for the interval of epicentral distances of $3000 < \Delta < 10{,}000$ km, P wave; d, e, f--for the interval of epicentral distances $\Delta > 10{,}000$ km, PKP wave; a, d--frequency interval of 1.5-3 Hz; b, e--1-1.5 Hz; c, f--less than 1 Hz. See Fig. 52 for explanation

For earthquakes from the teleseismic region $3000 < \Delta < 10{,}000$ km good spatial stability of shape is observed in all the investigated frequency ranges. For frequency bands of 1.5-3.0 Hz and 1-1.5 Hz the graphs have identical behavior, but on a higher level in the latter case. The decline in the correlation coefficient with an increase in Δ_{ij} up to 30-60 km should be attributed to the characteristic inhomogeneity of structure in the locality of the stations of the North Kazakhstan group. There is a striking feature in behavior of the correlation coefficient in the frequency interval below 1 Hz within the limits of this same range of epicentral distances: comparatively high correlation of long-period components of the recording at distances of more than 30 km between stations.

Comparing the results with data of other authors (see Fig. 5 and 61), we are convinced that the general nature of the spatial structure of the P wave coincides for essentially different regions of the earth. Actually, as we can see from Fig. 63, the correlation of signals at points of registration decreases with increasing distance between them. At the same time, following a relative minimum in the correlation of signals at distances of the order of 50-70 km (for frequencies of 1-1.5 Hz and distances of $3000 < \Delta < 10{,}000$ km) one observes a comparatively strong increase in correlation at distances about twice as great.

Attention should also be given to the change in positions of the minimum and maximum of the drop and spike in signal correlation as dependent on frequency and wave type.

We can attempt to explain the indicated peculiarities in the behavior of $K(\Delta_{ij})$ on the basis of the following concepts. When a P wave propagates in a medium with inhomogeneities that are randomly distributed, fluctuations are observed simultaneously in the amplitude and phase of the wave. This fact may be due to the superposition of waves formed on inhomogeneities of the medium on the primary P wave. As a result of such superposition, fluctuations arise in the form of a train of oscillations of the P wave that are registered at the beginning of the recording. Gradual attenuation of correlatedness of signals with an increase in the relative distance between stations characterizes increasing disparity of the parameters of inhomogeneities in the structure of the medium directly beneath the stations. The observed minima and maxima of correlation of signals are associated with the effect of the most pronounced inhomogeneities, which are probably fairly extended and abrupt rises and drops in contrasty seismic boundaries.

The greatest contribution to the formation of the wave registered on the open surface is made by a certain region of the interface beneath the station with effective dimensions that can be represented by an ellipse with semimajor axis equal to

$$R_1 \approx \frac{1}{\sin\psi}\sqrt{\frac{VTH}{\sin\psi}},$$

where V is the velocity of the wave, T is the period of the wave, H is the average depth of the interface, ψ is the angle of incidence of the wave on the interface or the angle of inclination of the interface in the case of normal incidence of the wave (Fig. 64).

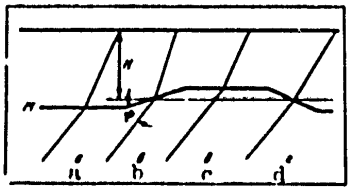

Fig. 64. Diagram of the influence that the relief of boundary M has on propagation of a P wave: a, b, c, d--sections of boundary M; ψ--angle of incidence of the wave on the boundary

Obviously the nature of the action of boundary M on the parameters of a P wave will be considerably different for cases where the ellipse with semimajor axis R_1 covers sections a, b, c and d respectively. This will show up in the behavior of the correlation coefficient for the corresponding pairs of registered signals. According to available information (Vol'kovskiy, 1973) the shape of the relief of boundary M in Northern Kazakhstan where the group of seismic stations was located corresponds to the diagram shown in Fig. 64. Let us carry out simple calculations that will give quantitative estimates of the possible fluctuations in waveshape. We will assume that the average depth of occurrence of boundary M is $H = 50$ km, and the velocity of a wave is $V = 8$ km/s, $T = 1$ s, $\psi = 50^\circ$. For such conditions the effective dimensions of the medium that plays an essential part in formation of the P wave train are determined by the quantity $2R_1 \approx 60$ km.

This means that for average characteristic dimensions of undulations of boundary M of the order of 60 km the coefficient of correlation for a P wave with period of 1 s may have a sharp drop (minimum) in the interval of distances between stations of 50-70 km, and a rise (maximum) at distances of the order of 120 km.

Analogous constructions can be done for evaluating the influence of the basement boundary, which occurs at an average depth of 5 km with velocity of horizontal wave propagation of about 6 km/s, $2R_1 \approx 12$ km, which also agrees with the behavior of the function of spatial correlation of waveshape.

At the same time, according to the considerations presented above, the positions of the relative maximum and minimum of the function of spatial correlation should shift with increasing period of the wave toward greater values of relative distances between stations of registration, which is probably just what happens in reality.

A close relation between the correlation of shape and frequency is also observed for PKP waves recorded at distances of more than 10,000 km from the source. It should be noted that the spatial stability of the recording increases with a reduction in frequency: for the low-frequency range one observes the highest values of the correlation coefficients. This is apparently due to two circumstances. In the first place the PKP wave approaches the group of seismic stations practically from below, and therefore the section of its path through the upper part of the medium that is characterized by increased inhomogeneity is shorter than for the P wave. In the second place, the predominating periods of the P wave are longer than for the PKP wave, and therefore the major part of the energy of the signal is concentrated in the frequency band below 1 Hz; in the processing system used, the signal-to-error ratio of the measurements of experimental data was comparatively low.

An examination of the average level of spatial correlation within identical bands (see Fig. 63) shows that some reduction of correlation with increasing

epicentral distance is observed for the interval of 1.5-3 Hz; for the interval of 1-1.5 Hz the level of correlation is in a range of 0.5-0.8, being appreciably higher for the teleseismic region than for the intermediate zone and the distant zone (PKP wave). In the frequency interval below 1 Hz a regular increase is observed in the spatial correlation of the first wave with an increase in epicentral distance.

A common typical feature of all graphs is also a weakly expressed rise in the region of $\Delta_{ij} \approx 10$ km, which in all probability is associated with the appearance of inhomogeneities situated in the very topmost layer of the earth's crust.

The Central Tyan'-Shan' Group of Stations. The transverse spatial correlation of the shape of the P wave was estimated from recordings of 37 earthquakes from different epicentral regions. For each earthquake, in accordance with the method described above, the matrix of the correlation coefficient was calculated for the shape of the signal recorded on the vertical component. The interval of relative distances between recording stations varied from 2 to 30 km. The epicentral distances ranged from 3000 to 9000 km.

Shown in Fig. 65a is the dependence of the correlation coefficient on the distance between seismic stations, and in Fig. 65b -- on the distance between the epicenters of earthquakes.

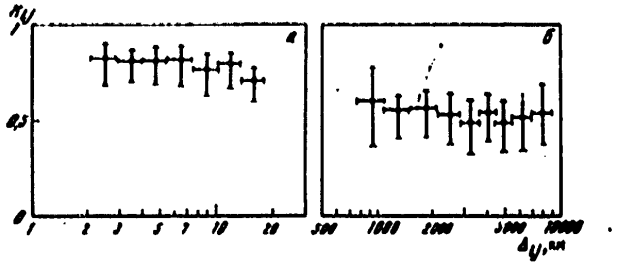

Fig. 65. Dependence of the coefficient of correlation of shape on the distance between stations (a) and between epicenters (b) from observations on the Central Tyan'-Shan' group. See Fig. 52 for explanation

For the function of spatial correlation as related to the distance between epicenters of earthquakes, spikes and drops in correlation of the shape of the P wave are noted at distances of 1500, 3500 and 5000 km. The general form of the relation and the location of the characteristic peculiarities agree well with the data on other regions of the world (see Fig. 5), as well as with the data on fluctuations of the amplitudes and travel times of the P wave that are given in the preceding chapter.

The correlation function for the shape of the P wave as dependent on the distance between seismic stations, just as in the preceding cases, shows a

tendency toward gradual attenuation with increasing relative distance between stations. Moreover, a comparatively clear minimum in correlation is observed in the vicinity of 8-11 km. It can be assumed that this minimum on Fig. 65a arises under the influence of undulations of a sharp seismic interface in the uppermost part of the earth's crust, and the nature of the overall decline in correlation is a manifestation of the patterns of distribution of inhomogeneities in the crust and mantle like what is noted in other station groups.

The Garm Station Group. The dependence of the correlation coefficient on the relative distance between seismic stations (Fig. 66) is found from the data of 18 earthquakes with epicenters situated chiefly in the seismically active regions of the Pacific Ocean belt. The distance between recording stations did not exceed 25 km.

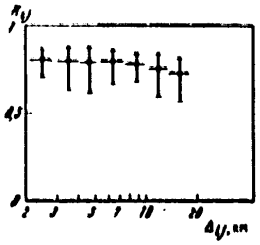

Fig. 66. Dependence of the coefficient of correlation of shape on distance between stations from observations on the Garm group. See Fig. 52 for explanation

Comparing the data of the Garm group with the data of stations of Central Tyan'-Shan;, we are convinced of their identity. The decline in correlation of the shape of the P wave is somewhat weaker in the 12 km region, which may be due to a less sharply pronounced boudary that is tracked in the upper part of the earth's crust.

The European Station Group. To evaluate the spatial correlation of the shape of the P wave, recordings of 33 earthquakes from different epicentral regions were used. The matrices of the correlation coefficients were calculated for each earthquake, as in the other cases. The distances between the recording stations varied from 3 to 100 km. The epicentral distances were 3500-10,000 km. The resultant data are shown in Fig. 67 in the form of relations for the correlation coefficient as a function of the relative distance between stations (Fig. 67a) and the relative distance between the epicenters of earthquakes (Fig. 67b).

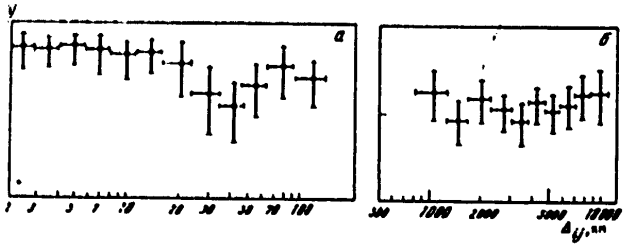

Fig. 67. Dependence of the coefficient of correlation of shape on distance between stations (a) and between epicenters (b) from observations of the European group. See Fig. 52 for explanation.

Analysis of the resultant data shown (Fig. 67a) that in the locality of stations of the European group just as in the vicinity of the North Kazakhstan station group the decline in correlation of shape of the P wave is most pronounced in the region of 50-60 km, as is the rise noted in the region close to 100 km. The drop in the function of spatial correlation in the vicinity of 10-12 km that is noted in other regions is practically unexpressed in this case.

In this connection we may assume that in the locality of the European group of stations by analogy with the region of North Kazakhstan there are probably variations in the dpeth of occurrence of the Mohorovičić discontinuity, which according to the data in the literature (Belyayevskiy, 1974; Pavlenkova, 1973) is situated here at an average depth of 40-45 km.

The graph shown in Fig. 67b for the coefficient of correlation of shape of the P wave as a function of the distances between epicenters demonstrates the same stable coordination of drops and spikes in correlation that is observed in other regions. Against the background of a general decline in the function of spatial correlation that asymptotically approaches a level of 0.5, one observes relative minima of correlation for relative distances of 1500, 3500, 5000 and 9000 km and correlation spikes at 2000, 4000 and 8000 km.

The Zeysk Station Group. Data on the Zeysk group of stations were found as a result of processing recordings of 16 earthquakes of the Pacific Ocean belt. Epicentral distances are 3000-6000 km. The relative distances between stations varied from 2 to 20 km. The results of calculations of the correlation matrices are shown in Fig. 68 in the form of the dependence on distance between seismic stations.

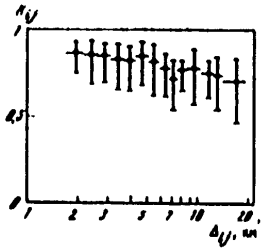

Fig. 68. Dependence of the coefficient of correlation of shape on the distance between stations in the Zeysk group. See Fig. 52 for explanation

Analysis of these data shows that in the locality of the Zeysk station group one observes two relative minima of correlation confined to relative distances of 4 and 7 km.

The overall decline in the relation $K(\Delta_{ij})$ toward 20 km takes place more intensively than in the regions considered previously. It can be assumed that the relative minimum in the function of spatial correlation that is distinguished in the regions of the North Kazakhstan and European groups of stations in the vicinity of 50-60 km will show up here at somewhat closer relative distances.

Discussion of the Results

The third part of the monograph has presented experimental data on the spatial structure of fluctuations in the characteristics of a longitudinal wave. The authors set themselves the problem of evaluating the characteristic scales of major structural elements of the wave field and showing their relation to corresponding inhomogeneities in the inner structure of the depths of the earth.

To get data on the ratio of typical scales of elements of the wave field, information was used on deviations from the average (standard) values of amplitudes, travel times and the shape of the longitudinal wave as provided by deep seismic sounding on temporary expeditionary stations in different tectonic provinces of the Soviet Union.

The main procedural technique on which the study of the fine structure of the P wave is based, consists in evaluating the stability of deviations from average fluctuations of kinematic and dynamic parameters of the wave field as a function of the relative distances between recording stations or between the epicentral regions of earthquakes.

Conventional methods of statistical processing of experimental data were used for quantitative evaluation of the stability of deviations. In particular, extensive use is made of correlation and structure functions.

As a result of the studies it was found that the spatial structure of fluctuations of such elements of the wave field as amplitude, travel time and shape of the longitudinal wave have distinct characteristic scales. The concept of scale in the given instance is arbitrary, and has the following conceptual significance. The depths of the earth are characterized by such a structure that in the selection of a pair of recording stations or a pair of seismic sources on the average one will observe an increase or reduction in the deviation of wave parameters from certain standard values if the relative distances between corresponding pairs satisfy the observed spatial scales. Table 30 summarizes data on the spatial scales of elevated and reduced values on the average in fluctuations in the parameters of a longitudinal wave. Fig. 69 summarizes experimental data on the spatial correlation of the shape of the longitudinal wave.

It is rather difficult to give an unambiguous quantitative interpretation of the scales differentiated for the fluctuations in parameters of the P wave and to draw specific conclusions on the structure of the depths of the earth. At the same time, the resultant data give such clear evidence that the coincidence of the characteristic scales of fluctuations of elements of the wave field that are distinguished in different tectonic provinces is not accidental, that we must accept at least their qualitative relation to inhomogeneities of the internal structure of the earth.

TABLE 30

Characteristic spatial scales of elevated (max) and depressed (min) values of deviations from average (standard) fluctuations of the amplitude $\delta\delta \lg A$ and travel times $\delta\delta t$, and also in the values of the coefficient of correlation K_{ij} of longitudinal waveshape

(2) По данным групп станций КСЭ	(1) Пространственные масштабы (км)					
	$\delta\delta t$		$\delta\delta \lg A$		K_{ij}	
	max	min	max	min	max	min
(3) По взаимным расстояниям между станциями						
(4) Вся территория СССР	350—600 1200—2000	600—1200 2200—4000	600—1000 4000—5000	1500—2000 >8000	—	—
(5) Европейская часть СССР	—	—	—	—	~100	10—12
(6) Северный Казахстан	—	—	50—80	120—150	100—140	50—60 8—10
(7) Северный Тянь-Шань	300—500	80—100	75—100	55—75 100—200	120—190	50—70 <70
(8) Центральный Тянь-Шань	—	—	50—60 >80	45—50 60—80	—	10—12
(9) Гармский район	—	—	—	—	—	10—12
(10) Зейский район	—	—	—	—	—	4—7
(11) По взаимным расстояниям между эпицентральными районами						
(4) Вся территория СССР	—	—	2000—3000 7000—9000	4000—6000	—	—
(5) Европейская часть СССР	—	—	—	—	~3000 ~4000 ~8000	~1500 ~3500 ~5000
(6) Северный Казахстан	—	—	—	5000—7000	—	—
(7) Северный Тянь-Шань	8000—10 000	3000	1700—2000 4000—5000	~1000 2200—4000	—	—
(8) Центральный Тянь-Шань	—	—	2000—3000 4000—5000 6000—7000	3000—4000 5000—6000 7000—8000	~3000 ~4000	~1500 ~3500 ~5000

KEY: 1--Spatial scales, km
2--from data of the KSE station group
3--with respect to the relative distances between stations
4--Entire territory of the USSR
5--European part of the USSR
6--Northern Kazakhstan
7--Northern Tyan'-Shan'
8--Central Tyan'-Shan'
9--Garm region
10--Zeysk region
11--with respect to relative distances between epicentral regions

In the first part of the monograph we already discussed the fact that the distribution of physicochemical properties of the depths of the earth is characterized primarily by radial inhomogeneity. The most contrasty changes are associated with zones of juncture of the sedimentary sheath with the consolidated crust, the region of contact between the lithosphere and the

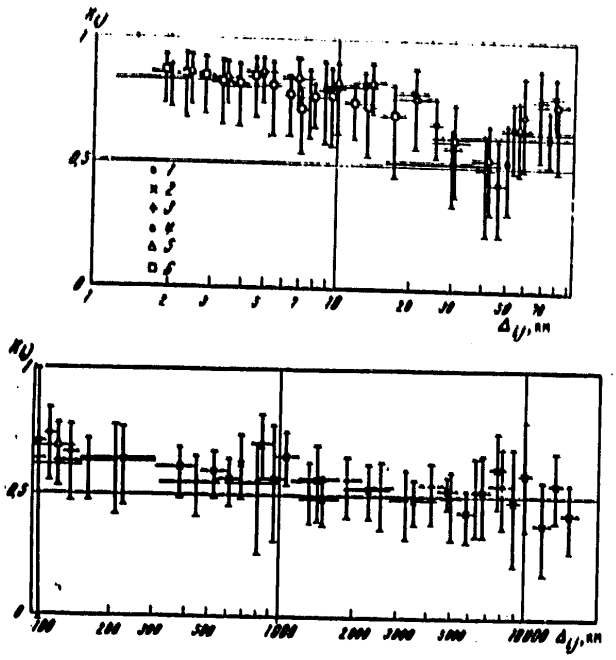

Fig. 69. Summary of data on spatial correlation of pulse shape of a P wave: 1--from the work of V. Din (1965); 2--B. Jansson and E. Husebye (1968); 3--stations of Central Tyan'-Shan'; 4--Northern Kazakhstan; 5--the European part of the USSR; 6--the Zeysk group. See Fig. 52 for explanation

asthenosphere, the transitional region between the asthenosphere and upper mantle, the region of juncture between the lower mantle and outer core and the boundary between the inner and outer core. Hence the radial distribution of physicochemical properties emerges as the most contrasty inhomogeneity of structure of the depths of the earth on a global scale.

The horizontal changes in radial inhomogeneity that are largest in scale correspond to regions of the earth of the ocean-continent type. In this connection, the considerable changes in structure of the interior of the earth are associated with the outer shells: the lithosphere, the asthenosphere and the transitional zone (The Upper Mantle, 1975; Nature of the Solid Earth, 1975). Horizontal variations in the structure of the inner shells at present are hypothetical to a certain extent.

Showing up with greatest contrast are horizontal variations of radial inhomogeneity on the regional and local scales that are associated with variability of the physicochemical properties of the lithosphere and asthenosphere. At present they can be studied by methods of seismological profiling and deep

seismic sounding. Regional and local scales of inhomogeneous structure of the depths of the earth are the least of those that can be distinguished in analysis of the experimental materials obtained by the KSE.

Obviously the detail of investigation of the inhomogeneous structure depends both on the resolving capacity of the system of observations and on the detail of analysis of the wave pattern. It can be assumed that the detail of our analysis for the case of the densest groups of stations of the KSE permits differentiating an inhomogeneity of the medium with linear dimnesions of at least 3-5 km. Therefore from here on we will consider only those details of the wave field that considerably surpass the detail of our plots with respect to the region of tracking.

The least of the distinguished spatial scales of fluctuations in parameters of the P wave is 10-12 km. As Table 30 shows, this scale is obtained from data of fluctuations in the shape of the P waves on the densest groups of stations of the KSE. The given scale is expressed with rather high contrast and is regionally stable. The proposals introduced in Chapter 2 imply that this scale is determined by inhomogeneity of the structure of the very topmost part of the earth's crust bounded by the surface of the consolidated basement. Consideration should also be taken of the fact that in interpreting the fluctuations of parameters of the P wave in terms of inhomogeneous structure it is important to make a joint analysis of data on variation of velocities and the geometry of seismic boundaries. Frequently the examination of the geometry of the interfaces alone may not reveal the causes of fluctuations in parameters of the P wave on the given scale.

Inhomogeneity of structure may show up entirely in the change (variation) of velocity along a boundary that is geometrically not expressed (Puzyrev et al., 1975).

The next typical scale of fluctuations of parameters of the P wave, equal to 45-60 km, can be assumed to be caused by inhomogeneity of the lower part of the earth's crust and the lithosphere, and as in the preceding case is likewise a consequence of spatial variation of geometric, velocity, and inelastic characteristics of media. This scale of inhomogeneities shows up with greatest contrast in fluctuations of the parameters of the longitudinal wave: amplitude, travel time and pulse shape. Particular attention should be given to the fact that the spatial scale of fluctuations of the order of 45-60 km is one of the most contrasty, and is distinguished within the limits of all investigated territories. Therefore we can expect its occurrence in both continental and oceanic regions. At the same time, with a transition from a continental to an oceanic type of lithosphere this scale is probably transformed to a scale of the order of 12-45 km.

A spatial scale of 100-200 km is distinguished from data of fluctuations in the amplitude and shape of the P wave, and is apparently due to the influence of inhomogeneous structure of the lithosphere, the zone of its juncture with the asthenosphere, and even the asthenosphere itself. The comparatively wide

limiting boundaries of the scale of fluctuations show that it can be stipulated specifically in each local region.

Consider for example the data on second differences of amplitudes $\delta\delta \lg A$ found in North Kazakhstan (see Fig. 56). First we look at the relation between $\delta\delta \lg A$ and distance between stations (see Fig. 56a). It can be assumed that the minimum of values of $\delta\delta \lg A$ is associated with a 120 km characteristic scale of horizontal inhomogeneities in the locality of the station group. The contribution of these inhomogeneities to fluctuations of amplitudes is $\sigma\delta\delta \lg A \sim 0.2$, i. e. the "signa" interval reaches about 7% of the average value of fluctuations in the amplitude of the P wave, which shows comparatively high contrast of inhomogeneities of this scale.

Consider now the way that the second differences of the logarithm of the amplitude depend on the distance between epicentral regions. The outward similarity of the graphs in Fig. 56a and b is striking. There are grounds for assuming that they have an intimate genetic relation. As a matter of fact, both relations were found from the same data. If we imagine a ray diagram for each such system of observations, it will be clear that there is a fan of rays that converges in the locality of the recording stations and diverges toward the epicentral regions. The first plot was constructed with the use of fans of rays converging toward each separate station, and the second -- with the use of fans converging toward each separate epicentral region. Thus in both cases the same processing scheme is used; however, the proportions of the resultant relations are determined by the relation between the regions of location of the stations and epicenters.

It can be assumed that the characteristic minima on both plots are genetically related and that the ratio of the characteristic scales is thus $\sim 6000/120 \approx 50$. Since the epicentral distances average 6000 km, a rough estimate can be made of the depth of occurrence of inhomogeneities that correspond to the differentiated characteristic scales of fluctuations. By dividing an "average" ray joining the epicentral regions and group of stations in the ratio of 1/50, we find that the inhomogeneities are situated at a remove of about 120 km along the ray from the group of stations, or at a depth of about 100-110 km. At such a depth of occurrence of inhomogeneities it can be expected that the dimensions of the region that essentially determines the fluctuations in shape of the P wave pulse correspond to $2R_1 \approx 60$ km.

If the relations for the second differences $\delta\delta \lg A$ for the North Tyan'-Shan' station group are analyzed in a similar way, it turns out that the inhomogeneities beneath this group are at a remove of $\sim 6000/(3000/200) \approx 400$ km along the ray, or at a depth of 370-380 km. In this case the characteristic dimension of inhomogeneities is $2R_1 \approx 120$ km.

As was shown in the second part of the monograph, within the limits of Northern Tyan'-Shan' the phase transition (350-400 km) (Nature of the Solid Earth, 1975) is at a depth of 370-390 km.

Thus it can be assumed that a spatial scale of 120-200 km in fluctuations of the parameters of the P wave is associated with inhomogeneities of the region of physicochemical phase transitions in the upper mantle.

The spatial scales of fluctuations in parameters of the P wave that exceed the dimensions of regional networks of stations are determined from mixed correlation and structure functions since it was difficult to match up a sufficient number of pairs of stations that satisfy the construction of purely transverse or purely longitudinal functions. The same thing applies to the data on epicentral regions. This circumstance impedes the determination of the nature of the differentiated characteristic scales.

It can be expected that consistency of the spatial scales of fluctuations of phase, amplitude and pulse shape of the P wave provides the basis for hypothetical notions on correspondence of the spatial scales of inhomogeneities of the structure and fluctuations of the parameters of the wave field.

The spatial scale of fluctuations of the P wave of about 4000 km are distinguished with the greatest assurance. It seems that the scale is a manifestation of a structural element of radial inhomogeneity in the upper mantle that is associated with a phase transition at a depth of about 680 km. For an average relative distance between stations and epicentral regions of about 6000 km it should be expected that the corresponding spatial scale of fluctuations in the parameters of P waves according to data of epicentral regions will be observed at distances of the order of 7000-9000 km. Such a scale is indeed observed for the Central Tyan'-Shan' stations over the entire territory of the USSR. These data confirm the relation between the the spatial scale of fluctuations in the parameters of the P wave and inhomogeneity of the structure of the transitional zone of the upper mantle in the vicinity of the 680 km boundary.

Thus analysis of data on the spatial scales of fluctuations of amplitude, travel time and shape of the P wave as differentiated from materials obtained by the KSE on groups of seismic stations shows their genetic mutual relation with inhomogeneities in the structure of the lithosphere, asthenosphere and the transitional zone of the upper mantle of the earth. As a result we can speak with assurance of the fact that horizontal variations in the radial inhomogeneity of the earth are confined to regions with the most contrasty physicochemical transitions: along the Mohorovičić discontinuity and the zone of transition between the lithosphere and the asthenosphere, in the region of juncture between the asthenosphere and the transitional zone of the upper mantle and at the bottom of the transitional zone.

IV. RELATION BETWEEN THE AMPLITUDE PECULIARITIES OF SEISMIC WAVES AND GEOLOGICAL-GEOPHYSICAL FIELDS

The variations of amplitudes of recorded seismic signals may be caused by various factors associated with the internal structure of the earth and distributed along the entire path of a seismic ray. These factors can be

arbitrarily divided into three groups. In the first place the amplitude of a recording may be influenced by geological surface conditions in the locality of registration: the composition of the rocks on which the seismic receiver is mounted, their cracks, physical properties, thickness of layers and geometry of the interface and the like. In the second place, the structure of the lower part of the earth's crust may have a certain influence, in particular, the depth, inclination and clarity of manifestation of the Mohorovičić discontinuity. In the third place the dynamic characteristics of seismic waves may be influenced by horizontal variations in the structure of the earth's mantle. The very existence of these variations shows up in seismological, electromagnetic and gravimetric studies. However, investigations of this type have been undertaken for only a small number of territories.

Data on the geological and tectonic structure of the earth's crust give a general idea of the physical properties of rocks and the spatial structure of inhomogeneities. The most appreciable changes in the seismic parameters of the medium -- the velocities of waves and inelastic characteristics -- are observed in zones of tectonic ruptures and breaks. These zones frequently have a considerable width comparable with the lengths of seismic waves, and a large horizontal extent (up to several hundred kilometres) and go to a depth of several tens of kilometres.

The relation between the dynamic characteristics of seismic waves on the one hand and geological and geophysical fields on the other has been poorly studied so far. Given below is a comparison of the magnitude corrections of seismic stations with anomalies of the gravitational and magnetic fields, as well as the position of seismic stations relative to the zones of tectonic breaks.

Chapter 1. Investigation of the Way that Amplitude Peculiarities of Seismic Waves are Related to Gravitational and Magnetic Anomalies of the Territory of the USSR

1. General information on gravitational anomalies

The anomalous gravitational field is the sum of the gravitational influences of anomalous (i. e. differing from certain standard) masses distributed in the body of the earth. The greatest contribution to the observed anomalies of the force of gravity is made by the influence of dense inhomogeneities of the upper part of the cross section (the earth's crust). The influence of the earth's crust on the gravitational field is eliminated to a great extent by introducing topographic-isostatic reduction. The isostatic anomalies of the force of gravity that are obtained as a result are associated with disruptions of isostatic equilibrium (on the average this equilibrium holds to an accuracy of at least 90%) (Lyustikh, 1957) and with inhomogeneities of the crust not taken into consideration in introducing the reduction, as well as with the influence of density inhomogeneities in the mantle. The results of numerous studies of isostatic anomalies show that the anomalies that are associated with disruptions of isostasy and density inhomogeneities of the

crust have a pronounced local nature with respect to area. On the other hand, isostatic anomalies that are large with respect to the area occupied cannot be associated with disruptions of isostatic equilibrium of the lithosphere since such disruptions will recover very quickly (on the geological time scale) because of the low viscosity of the asthenosphere.

In this connection the asthenosphere is understood to mean the layer of reduced viscosity in the mantle of the earth whose existence is deduced from the advent of isostatic equilibrium in regions of current and recent glaciations (Artyushkov, 1970) as well as in other regions of abrupt change in the external loading on the earth's crust (Artyushkov, 1971). The asthenospheric layer is usually identified with a layer characterized by relatively low velocities of seismic waves -- a seismic waveguide (Gutenberg, 1963).

The anomalous masses situated below the asthenosphere may exist for a long time, and large regional anomalies of the gravitational field are associated with them.

These anomalies can be distinguished from isostatic anomalies through the corresponding transformations of the field.

A map of regional isostatic anomalies in the force of gravity of the USSR has been obtained by averaging isostatic anomalies of the force of gravity over squares of 550 x 550 km. Such averaging practically eliminates the gravitational influence of masses located down to depths of several tens of km. Thus the regional anomalies shown on the map are due to masses distributed in the mantle of the earth. Among these anomalies, planetary and zonal anomalies can be distinguished. The planetary anomalies cover areas of tens of millions of square kilometres. Sections of three such anomalies extend into the territory of the USSR. The first of these covers the European part of the nation. This is a region of positive values covering all of Europe, the North Atlantic and Africa. The second planetary anomaly covers a considerable territory of the asiatic part of the USSR, and then extends across Northern China and India into the central regions of the Indian Ocean. The third planetary anomaly within the borders of the USSR covers the eastern regions of the nation -- from Chukotka to Primor'ye [the Maritime Provinces]. This anomaly is part of a region of positive values that can be traced in the peripheral areas of the Pacific Ocean zone.

Against the background of the enumerated extensive planetary anomalies one can distinguish regions of smaller area of relative maxima and minima with characteristic dimensions of the order of a thousand kilometres. Such anomalies are called zonal.

There is a difference of opinion on the nature of zonal and planetary anomalies and on the depths of occurrence of the bodies that cause them. Estimates made by V. N. Strakhov and M. Ye. Artem'yev (1971) showed that sources of zonal anomalies are situated at depths of about 150-200 km. It can be assumed that they are associated with a change in the depths to the

underside of the asthenosphere or with density inhomogeneities directly beneath this boundary. The shape of the planetary anomalies is such that the masses causing them may either be located at any depths in the mantle of the earth, or they may be caused by even slight perturbations on the boundary of the earth's core. Gravimetric data alone are insufficient to determine their nature. However, there are grounds for assuming that the planetary anomalies or considerable parts of them are associated with depths in the mantle that are not very great. This is shown by the correlation of the values of anomalies with heat flux from the depths of the earth: elevated heat fluxes gravitate toward zones of gravitational minima. The results of electromagnetic studies done in the southern regions of Siberia show that in regions of negative regional anomalies one observes an elevation in the boundary of the conductive layer located in the upper mantle. This is apparently due to the higher temperature of the depths in these regions. The Asiatic region of negative anomalies coincides spatially with the so-called zone of neotectonic activation. According to the views that have become popular in recent years, there are large-scale convective movements in the depths of the earth. It can be assumed that the planetary minima of the gravitational field are associated with regions where anomalously heated masses of deep-level material of comparatively low density rise to the surface of the earth.

Seismological research (Antonova et al., 1968) has shown that there is a region in southern Pribaykal'ye that is characterized by low values of the velocities of seismic waves in the upper mantle. This region is situated close to the axial part of a planetary gravitational minimum.

Thus there are grounds for thinking that negative planetary anomalies are associated with low-density, and hence low-velocity masses located at comparatively shallow depths in the earth's mantle.

We do not yet have data for any kind of estimate of the factors capable of producing anomalies in the propagation of seismic oscillations. However, it can be assumed from general geological-geophysical considerations that the uppermost levels of the mantle are most inhomogeneous, and it is these inhomogeneities that must distort the parameters of seismic waves. The anomalous sections of the mantle to a considerable extent are reflected by regional anomalies of the gravitational field.

2. Investigation of the relation between gravitational and magnitude anomalies on the territory of the USSR

Seismic waves from remote sources have nearly vertical angles of emergence, and therefore magnitude corrections will be primarily influenced by the differences in the structure of the upper mantle in a comparatively small vicinity of the recording stations.

These considerations were the basis in seeking the correlation between magnitude corrections Δm and regional gravitational anomalies Δg.

In accordance with the nature of variation in the gravitational field the influence that the structure of the upper mantle has on values of Δm (if it exists) should change fairly smoothly. There is no doubt that local geological peculiarities of an individual station can strongly distort the influence of depth factors. These local perturbations may to some extent be suppressed by calculating the average values of amplitude corrections Δm within the limits of certain territories. The dimensions of such territories were determined in accordance with the actual relative location of stations unified into groups, and the characteristic peculiarities of the field of regional gravitational anomalies. The stations of observations were associated into 18 groups.

The number of stations in the groups is different: from two to fifteen. Eight isolated stations were considered separately. Data on the gravitational field of the territory of the USSR were taken from a map with scale of 1:10 000 000.

It is difficult to make a predetermination of which parameters of the gravitational and seismic fields are most closely interrelated. In and of itself the magnitude deviation depends to a considerable extent not only on the structure of the medium in the vicinity of the seismic station, but also on the conditions of propagation of seismic energy on the entire route from the focus to the seismic receiver. Magnitude deviations differ considerably for different epicentral regions. To reduce this influence, magnitude deviations were considered for earthquakes only from the northeast direction.

The values of the gradient of anomalies to a certain extent reflect the variability of properties of the mantle, and therefore it is advisable to attempt to correlate the station values of Δm with the values of the derivative of the gravitational field or the absolute value of the horizontal gradient of the field in the directions to the epicenters of earthquakes.

On the basis of analysis of relations for Δm as a function of the values of the anomalies Δg, the horizontal derivative (change of the field in the direction to the source within the limits of a base of 150 and 300 km) and the modulus of the derivative, it can be confidently stated that the values of Δm are not related to the values of horizontal gradients (K = 0.1). A very weak relation is noted between the values of Δm and the absolute values of the derivative (K = 0.3).

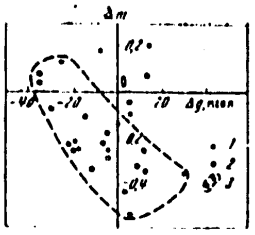

Fig. 70 Relation between the magnitude correction Δm and the smoothed value of the isostatic anomaly of the force of gravity Δg for the territory of the USSR: 1--individual seismic station; 2--group of stations; 3--region of values for stations of Siberia, Asia and the Caucasus; мгал = mgal

Fig. 70 shows the relation between the average values of Δm and the smoothed values of isostatic anomalies of the force of gravity Δg in the localities of an individual station or groups. As one can see from Fig. 70, a tendency is observed toward a reduction in the amplitude corrections with increasing values of Δg. The coefficient of correlation between Δm and Δg for groups of stations is equal to 0.55. It should be noted that if we eliminate the stations situated in the European part of the USSR from consideration, the coefficient of correlation increases to 0.81.

Thus the average values of Δm for groups of stations situated in Asia and the Caucasus are closely correlated with the values of anomalies of the gravitational field due to density inhomogeneities in the mantle of the earth.

Fig. 70 also shows the values of Δm and Δg for isolated stations. Some of them satisfy the general relation found for the groups, but a number of points deviate strongly. The coefficient of correlations between Δm and Δg calculated jointly for groups and individual stations (all values being taken with identical weight) was equal to 0.2. However, the closeness of the relation between the quantities Δm and Δg in the given case is worsened only by stations situated in the European part of the USSR. If we eliminate from consideration both the groups and the individual stations of this region, the correlation coefficient is equal to 0.75.

Thus for extensive regions of Siberia, the Far East, Soviet Middle Asia, Kazakhstan, the Urals and the Caucasus, where 16 groups of stations and 5 individual stations were located, a fairly pronounced relation is observed between Δm and Δg. Consequently the distortion of the seismic signal may intensify with increasing intensity of negative anomalies.

Within the limits of the investigated territory this might be associated with the presence of a comparatively extensive anomaly with anomalously low density in the mantle, and probably one that has anomalously low velocity of seismic wave propagation.

Of undoubted interest is the question of why the observed relation is disrupted for stations situated in the European part of the nation. Apparently the stations in the European part of the USSR are too far away from seismic sources located in the northeast, and earthquakes of other regions should be used to get good results.

An analysis of the dynamics of the P wave as presented in the preceding sections gives grounds for suggesting that the disruption of the relation between Δm and Δg in the given case could be related to the influence of inhomogeneity of the mantle of the earth. In particular, data on the structural analysis of magnitude deviations and their relation to the distance between seismic stations (see Fig. 50a) or to the distance between regions of seismic sources (see Fig. 50b) do not contradict the suggestion that the upper mantle beneath the European part of the nation, while it does not differ in density from the mantle in other regions that have a similar regional gravity field, does differ in conditions of seismic wave transmission.

For a more detailed study of the relation between seismic fields and other geophysical fields, an examination was made of data obtained in a number of regions of Soviet Middle Asia and Kazakhstan. These regions on the one hand have been well studied by geophysical methods, and on the other hand, fairly varied geological-geophysical conditions are observed in these regions: thickness of the earth's crust, seismic wave velocities, close proximity of high-seismicity and aseismic areas. It is in these regions that we have the densest network of seismic stations, which has provided fairly reliable results. For the regions of Soviet Middle Asia and Kazakhstan that are bounded on the north by the 47-th parallel, on the west by the 62-d meridian, and on the south and east by the national border, we had data on gravitational anomalies in the Fay reduction averaged over a grid of 10' x 15'. Such detail corresponds to a geophysical map scale of 1:2 500 000. These data were converted to maps of isostatic anomalies of the force of gravity Δg_{isost} and their gradients $\text{grad}\,\Delta g_{isost}$.

We had the material of 40 seismic stations to correlate magnitude deviations with the parameters of geophysical fields within the limits of the investigated territory.

Comparison of the magnitude corrections with gravitational and magnetic anomalies requires solution of the problem of choosing the size of the area for which the average characteristics of the fields are taken since this size is related to the scale of the investigated inhomogeneities and the interval of depths on which they are situated. Since we did not know of any a priori concepts of the nature of the relation between Δm and the geophysical parameters of the medium, we considered "point" values of the fields $\Delta g_{isost}(1)$, $\text{grad}\,\Delta g_{isost}(1)$ and $\Delta T_a(1)$ corresponding to the averages for a small vicinity of the seismic station -- 10 x 10 km, and also $\Delta g_{isost}(3)$, $\text{grad}\,\Delta g_{isost}(3)$, $\Delta T_a(3)$, $\Delta T_a(8)$ that correspond to areas of averaging of 30 x 30 and 80 x 80 km.

The unsmoothed value of the anomalies feels the influence of all anomalous masses (gravitational or magnetic), while the smoothed values are free of the influence of anomalous masses situated in the upper part of the earth's crust and having small predominant dimensions. Averaging with respect to an area of 30 x 30 km corresponds to scaling of an anomalous field into the upper half-space to a height of 10 km with an appreciable reduction in the contribution of anomalies with linear size not exceeding 10 km.

The magnitude of the gradient of the anomaly in the force of gravity $\text{grad}\,\Delta g_{isost}$ is an indication of the dynamic state of the earth's crust; high values correspond to regions that participate in active tectonic movements and may be characterized by anomalous elastic and absorptive properties.

To compare the magnitude correction Δm with the investigated characteristics of the gravitational field, the correlation graphs shown in Fig. 71 and 72 were plotted. Data corresponding to seismic stations of the North Tyan'-Shan', Central Tyan'-Shan', Garm and Pamir-Afgan groups are shown by different signs.

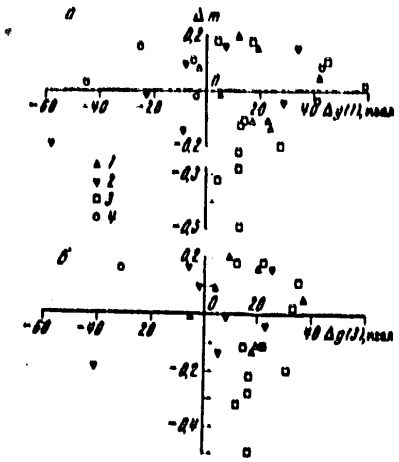

Fig. 71. Relation between amplitude correction Δm and isostatic anomaly of the force of gravity Δg for regions of Soviet Middle Asia and Kazakhstan: a--value of Δg(1) at the "point" of observation, average for an area of 10 x 10 km; b--value of Δg(3), average for an area of 30 x 30 km; 1--North Tyan'-Shan' group; 2--Central Tyan'-Shan' group; 3--Garm group, 4--Pamir-Afgan group; mean = mgal

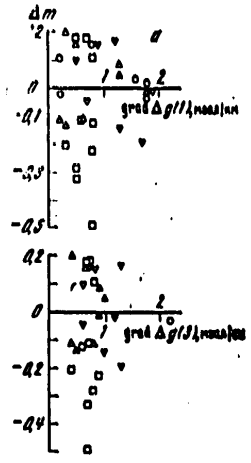

Fig. 72. Relation between the magnitude correction Δm and the gradient of isostatic anomaly of the force of gravity grad Δg for regions of Soviet Middle Asia and Kazakhstan: a--value of grad Δg(1), average for an area of 10 x 10 km; b--value of grad Δg(3), average for an area of 30 x 30 km. See Fig. 71 for the arbitrary signs

The given relations for Δm and Δg are characterized by a nearly total lack of system in the location of points. A lack of any relations is observed both in the overall position of all points and in the position of points for different groups of stations.

The absence of a system that is observed in the position of individual points shows up as well in the relative location of the differentiated groups. At the same time, the average magnitude corrections with respect to the groups of stations correlate well with the averaged isostatic anomalies.

3. Investigation of the relation between magnetic and magnitude anomalies

Magnetic field anomalies ΔT_a characterize the overall inhomogeneity of magnetization of the rocks of the consolidated layer of the earth's crust and sedimentary deposits. Corresponding to the anomalies are surface outcroppings of magmatic rocks, zones of tectonic fractures, and differences in the petrographic composition of rocks. The enumerated characteristics, which are reflected in the anomalies of the magnetic field, are also closely related to the seismic parameters of the medium. Therefore we can expect that the

structure of magnetic anomalies will contain certain information on the possible peculiarities of dynamic characteristics of seismic waves, and specifically on magnitude corrections.

To determine the relation between the values of ΔT_a and magnitude corrections on seismic stations a map of the anomalous magnetic field of the USSR in ΔT_a isolines was used in a scale of 1:5 000 000 made in 1963. To characterize the local structure of ΔT_a the area within a radius of 50 km around the seismic station was examined. Two quantitative parameters were studied as well as one qualitative parameter. The first quantitative parameter was the average value of the ΔT_a field within a 50 km neighborhood of the station, and the second was variation of the anomaly $\delta\Delta T_a$ within the same region, i. e. the difference between the maximum and minimum values. The qualitative parameter was the characteristic dimension of the local anomaly. The following three gradations of dimensions were set: large anomalies -- more than 100 km across; medium anomalies -- from 25 to 100 km; small anomalies -- less than 25 km.

The data of 59 seismic stations were used. The results of comparison of the correction Δm with anomalies ΔT_a and $\delta\Delta T_a$ are shown in Fig. 73. The position of the points shows that the values of Δm are practically independent of ΔT_a and $\delta\Delta T_a$. This negative has at any rate the practical value that it shows the existing relationship between the nature of the wave field and the structure of the medium: the average characteristics of the structure of the medium weakly influence the dynamics of waves. This result is particularly interesting in connection with the fact that the magnitude corrections correlate well with just the average values of the anomalous gravitational field in the isostatic reduction.

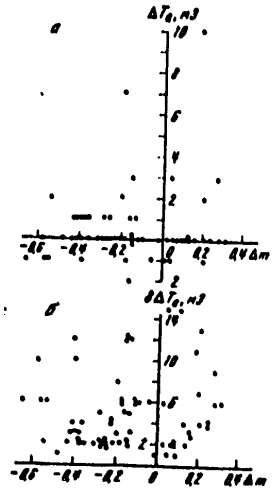

Fig. 73. Relation between the magnitude correction Δm and magnetic field anomaly: a--anomalies ΔT_a; b--variations $\delta\Delta T_a$ мЭ = millioersteds

A comparison of the values of Δm for stations located in regions that are characterized by large, medium and small dimensions of magnetic anomalies shows that for regions of "large" anomalies the average value of Δm is: +0.06 ± 0.05; for "medium" anomalies: -0.01 ± 0.05; for "small" anomalies: -0.11 ± 0.06. Large-scale inhomogeneities of the medium and the corresponding ΔT_a are related to anomalous magnetic masses located in the lower parts of the earth's crust or in the very top of the mantle*. Consequently the homogeneity of the upper mantle and the consolidated crust impede the damping of seismic waves which shows up in negative magnitude corrections. Let us note that distribution of the value of Δm within the investigated groups is characterized by mean square values of 0.24-0.26. Therefore the forecast of magnetic field anomalies with respect to the scale of inhomogeneity is uncertain (more qualitative than quantitative); nevertheless it is useful to account for this relation for decision making in controversial situations.

For regions of Soviet Middle Asia and Kazakhstan we had data on magnetic field anomalies ΔT_a averaged over a grid of 10' x 15', i. e. corresponding to a scale on geophysical maps of 1:2 500 000. Just as for the gravitational field, no relation was observed between the seismic and magnetic field.

An exception is the graph for Δm, ΔT_a, where a linear relation is observed for points corresponding to North Tyan'-Shan' stations; the correlation coefficient is equal to -0.7. However, this relation is based on the data of only eight seismic stations, and therefore the confidence interval of the reduced estimate at the 95% level of significance is from -0.10 to -0.95, from which it can be assumed that the peculiarity under discussion came up fortuitously.

One of the reasons for a lack of connection between Δm and the investigated geophysical fields (both gravitational and magnetic) is that in the case of comparatively short epicentral distances, up to 2000 km, seismic waves go from the source to the receivers through the upper mantle. The latter is characterized by considerable inhomogeneities of the velocities of seismic waves and absorbing properties, and therefore the observed magnitude corrections reflect the influence of all inhomogeneities that lie on the path of propagation of the wave, whereas the geophysical anomalies characterize only local inhomogeneities close to observation points. The influence of these inhomogeneities on the amplitude peculiarities of seismic waves that traverse the greater part of the path in the very inhomogeneous top of the upper mantle is appreciably weaker than for waves that go through the appreciably more homogeneous lower mantle. Thus the geological-geophysical characteristics of the medium permit a more certain prediction of the effect of an anomalous change in the amplitudes of seismic waves only from remote sources (Δ ~ 7,000-10,000 km), i. e. for cases where a considerable part of the path of propagation falls to the lower mantle.

---

*At temperatures in excess of 700°C rocks are completely nonmagnetic. Anomalies of the magnetic field can be related only to the topmost layer of 40 km.

Chapter 2. Investigation of the Relation Between Amplitude Anomalies and Geological Conditions

1. Influence that general features of geological structure have on the level of amplitudes of seismic waves

Geological conditions in the vicinity of a station may have an appreciable influence on the size of the magnetic correction Δm. Apparently it is the influence of local geological conditions that is responsible for the fact that in some cases the Δm differ by 0.4-0.5 for stations separated by a few kilometres.

A whole complex of detailed geological studies in the vicinity of each station is required to determine the way that the amplitude of a recording of seismic signals depends on the peculiarities of geological conditions. It would be necessary to study the way that the value of Δm is influenced by the thickness and makeup of loose deposits, the ground water level, anisotropy of the physical properties of rocks of the basement and the sedimentary sheath, relief of the basement, the thickness of the earth's crust and the inclinations of its boundaries, the petrographic composition of the basement rock, the presence of deep breaks and tectonic fractures, the type of geological structures that the rocks belong to and so forth.

Let us try to evaluate the influence of the most general geological and tectonic conditions on the values of Δm. Most stations were located in territories where fairly ancient crystalline rocks (Paleozoic or older) crop out on the surface. Such are the stations located on the south of the European part, within the borders of Kazakhstan, in the Urals, in Trans-Baykal, on the Kola Peninsula and in the vicinity of Noril'sk. It should be noted that all these stations are characterized by values of Δm from -0.1 to -0.6, i. e. they are quite favorable for registration of seismic signals. An exception is observed in all the stations on the south of the European part, where the values of Δm are about +0.20.

A second group of stations is situated within the limits of ancient platforms with a thick cover of sedimentary rocks. Such are the stations in the vicinity of Moscow, Kirov, Riga, on the south of the Ukraine, in the vicinity of Mirnyy and Yakutsk. The values of the magnitude corrections on these stations vary over a wide range, and in some instances there are sharp differences between stations located only a few kilometres apart. In this connection it is quite difficult to extrapolate the values of Δm to other territories.

Let us distinguish the stations that fall within the limits of so-called "tectonic activation." These are stations that are situated in Tyan'-Shan', Altay, Kuzbass, the Western and Eastern Sayans, and in Pribaykal'ye. The values of Δm here have a range from -0.40 to +0.30. An increase is observed in the values of Δm in the easterly direction. The region of tectonic activation is characterized by a differentiated relief, alternation of

surface outcroppings of rocks of the folded foundation and sedimentary basins. No systematic peculiarities could be found in the relation between the values of Δm and geological conditions in the vicinity of the stations.

Finally, a number of stations are situated within the limits or on the boundary of the zone of the Meso-Cenozoic geosynclinal region. Such are the stations in the Carpathians and Trans-Carpathia, in Trans-Caucasia, South Turkmenia, on Chukotka, within the limits of the Tadzhik Depression and on the Pamirs. These stations also differ strongly in values of Δm. For instance in the Caucasus, in Turkmenia and on Chukotka the values of Δm are negative, while in the Tadzhik Depression and the Pamirs they have positive values.

Thus the general features of geological structure in the vicinity of a station do not determine the particulars of the nature of registration of seismic signals in explicit form. Apparently to determine the influence of geological conditions we need to do incomparably more thorough, detailed and comprehensive research on the geology and geophysics of the station locality.

2. Influence that breaks have on the parameters of seismic waves

More obvious was the influence of breaks on the shape and amplitude level of seismic signals recorded on stations situated in direct proximity to these breaks. For seismic waves the fault zone may be a shield on the one hand that reflects part of the wave energy, and on the other hand may be an inhomogeneity with anomalously high absorbing properties.

As experimental material, we used recordings of 40 remote earthquakes from three epicentral zones: Aleutian, Japanese and Indonesian. The recording was done by standard seismic channels of the SK-3M seismic receiver. Signal amplitudes were measured from recordings of the vertical component.

The amplitude of the maximum phase was selected as the parameter characterizing the dynamics of the longitudinal wave of a remote earthquake. This choice is dictated by the fact that the maximum phase of the P wave corresponds fairly well to the maximum of the spectrum of oscillations and is the most stable in comparison with other phases of the given wave group when the frequency response of the recording channel is used (Antonova et al., 1968; Paschenik, 1970).

Three major factors influence the amplitudes of remote earthquakes: conditions at the focus (energy, depth, directionality of radiation, etc.), the elastic parameters of the medium through which the waves pass, and the geological-geophysical environment close to the recording station.

Consideration of the influences of the first two factors on the amplitude of the seismic signal was taken care of by calibrating the recordings of closely spaced stations with respect to a single station taken as the reference; the ratio $a_i = A_i/A_{st}$ is calculated, where A_i is the amplitude on the i-th station, and A_{st} is the amplitude on the reference station.

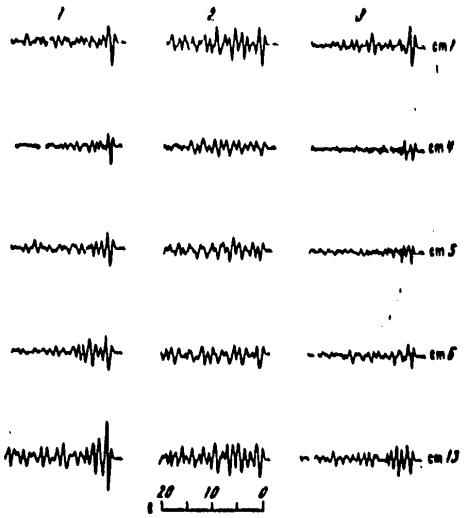

Fig. 74. Recordings of remote earthquakes on seismic stations of the Garm group: 1--Aleutians, 21.II.1968, $t_0 = 19^h08^m$; 2--Japan, 01.V.1968, $t_0 = 08^h43^m$; 3--Indonesia, 23.II.1968, $t_0 = 16^h14^m$; cm = station number

Taken as the reference was station 1 (see Fig. 76) which is located in relatively quiet geological conditions and is fairly remote from tectonic fractures. Besides, on this station one observes a comparatively stable simple pulse shape of the first wave group for the given recordings of Japanese, Aleutian and Indonesian earthquakes (Fig. 74).

The nature of the influence of fault zones on the amplitude of a registered remote earthquake signal was studied from pairs of earthquakes; Aleutian earthquakes were taken as the reference. This is explained by the fact that in comparison with Japanese and Indonesian zones, the Aleutian zone has higher seismicity, i. e. practically every month there is a tremor there that is clearly recorded on the Garm station group. In the second place, this zone is very stable with respect to the amplitude parameter α_i.

The stability of the parameter α_i was studied as follows. Spatial constancy of the quantities α_i was verified. To do this, pairs of earthquakes were selected with close apparent periods of the recording of oscillations, and the ratio of amplitudes of like phases $\alpha_i^1 = \alpha_i^1/\alpha_i^2$ was examined. The paired earthquakes were selected within the limits of a strictly bounded time segment not exceeding three days. This limitation is explained first of all by possible equipment instability in time, which had to be excluded as much as possible.

As a result of an examination of about fifty independent earthquakes it is apparent that the value of α_i^1 for every i-th station is fairly stable, and

In fact the average value $\bar{a}_i$ for each station is close to unity, while the average scatter of individual values does not exceed 15%.

Change in Pulse Shape of a Remote Earthquake as a Function of the Azimuth to the Epicenter. Preliminary visual analysis of recordings of remote earthquakes allows us to draw the qualitative conclusion that for some stations the pulse shape of a longitudinal wave is distorted with a change in the azimuth to the epicenter. Fig. 74 shows an example of a recording of three earthquakes from different epicentral zones. It is apparent that the shape of the recording of the Aleutian earthquake has the same clear pulse form on all stations, and differs only in maximum amplitudes. For the Japanese earthquake this clarity of the first wave group is disrupted on stations 4 and 5. For the Aleutian earthquake, the ratios of amplitudes of subsequent oscillations to the maximum amplitudes A_{max} were less than unity; for the Japanese earthquake these ratios became greater than unity.

With respect to the recordings of the Indonesian earthquake the clarity of the first wave train is disrupted on stations 6 and 13. For the Aleutian earthquake on these stations the measure of distinctness of the pulse A/A_{max} was less than 1.0, being in a range of 0.35-0.80; for the Indonesian earthquake the value of A/A_{max} is in a range of 0.60-1.60.

The pulse shape on station 1 does not undergo any appreciable changes. The value of A/A_{max} here for all earthquakes is less than 1.0, and is in a range of 0.30-0.60.

In the investigated time period (February - May, 1968) the frequency responses on the stations were rigidly standardized. This enabled comparison of the recordings shown in Fig. 74 not only with respect to shape, but also with respect to amplitudes for the three azimuths (Fig. 75). As we can see, the different azimuths are characterized by different values of the reference recordings normalized with respect to amplitudes.

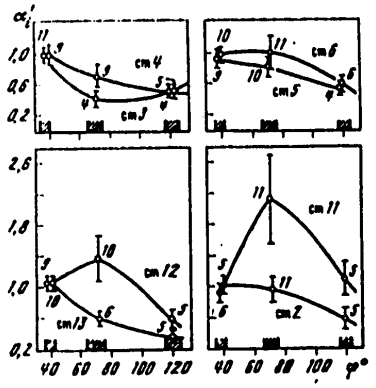

Fig. 75. Graphs of the dependence of relative amplitude a_i' on the azimuth to the epicentral zone. The shading indicates azimuth intervals of about 40° (Aleutians), 70° (Japan) and 120° (Indonesia). cm = station number

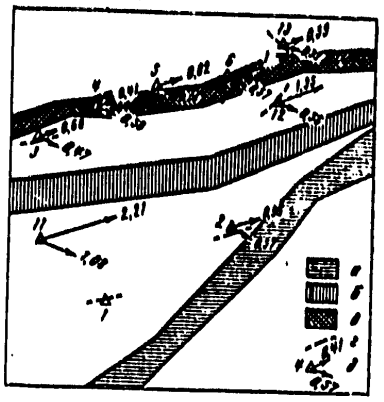

Fig. 76. Tectonic diagram of the Garm region. Zones of breaks: а--Karakul'; б--Petrovsk; в--Surkhobsk; г--fragments of Quaternary breaks; д--seismic stations with values of azimuthal sensitivity

Quantitative Evaluation of Change in the Amplitude Parameter as a Function of Azimuth. Graphs were plotted for each station for the average $\bar{a}_i$ as a function of the average azimuth ϕ° to the epicentral zone. These relations are shown in Fig. 75. Given for each average value of a_i on the graph is the scatter of the individual values of the data in the form of "whiskers," and the number of pairs of earthquakes from which the relative amplitudes a_i were determined.

The value of $\bar{a}_i(\phi)$ is a measure of the azimuthal amplitude sensitivity of the i-th station with respect to the direction of the average azimuth ϕ°. At seismic stations 3, 4 and 13 this parameter varies in the following way: it decreases by a factor of 1.7-2.4 for earthquakes of Japan, and by a factor of 1.7-3.0 for the earthquakes from Indonesia.

Stations 2, 5 and 6 "feel" the Japanese earthquakes about the same as the Aleutian ones; their sensitivity in the Indonesian direction is 1.7 times less. Stations 11 and 12 show exceptionally high sensitivity to Japanese earthquakes, exceeding their sensitivity to Aleutian earthquakes by a factor of 2.1 and 1.4. The sensitivity of the 11-th station to Indonesia is the same as for the Aleutians, while for the 12-th station it is less by a factor of 1.8.

Influence of Breaks on the Amplitude Level of Signals. Before examining the relation between the position of breaks relative to the station and the direction of arrival of waves with the amplitude sensitivity of each station, let us turn to the tectonic scheme of the Garm region.

Fairly complete data on the geological structure and tectonics of the region are to be had in the work of M. V. Gzovskiy et al. (1960). We have taken as our basis the tectonic diagram presented in this work (Fig. 76).

The Garm region is an alpine structure comprised of two structural stages and broken up into individual blocks (structural steps) by deep tectonic breaks that intersect the earth's crust.

Three steeply falling zones of deep-level breaks are distinguished: Karakul', Petrovsk and Surkhobsk.

In addition to the deep-level breaks, faults of the Quaternary Era are distinguished that are shown in fragments on the diagram according to data taken from the map of recent movements of the earth's crust in the Garm region compiled by V. K. Kuchay.

Fig. 76 shows only those faults that are situated no more than 5 km from the seismic stations.

On the tectonic diagram the magnitudes of azimuthal sensitivity $\tilde{a}_i^!(\phi)$ for each station are shown by vectors. It can be seen from the size of the vectors that the earthquakes with rays crossing nearby fault zones are "felt" more poorly by the stations. An exception is station 3 for which the directional sensitivity was lower than expected. This can be explained by the fact that the Surkhobsk fault zone in the vicinity of station 3 is much wider than shown on the tectonic diagram (see Fig. 76), and the boundary of the zone passes to the south of the station.

This hypothesis is confirmed by data on recent movements of the earth's crust from the results of geodetic observations to the south of station 3 that show vertical displacements of the earth's crust, although such displacements have not been observed to the north (Enman, Sambireva, 1971).

The influence of Quaternary breaks is also felt by stations 12 (Petrovsk zone), and 2 (Karakul' zone): the amplitudes of Indonesian earthquakes at the given stations are 1.8 times lower.

The way that the reduction in amplitude of the recordings of remote earthquakes is related to the position of the station relative to tectonic breaks can be explained in the following way. The boundaries of the fault zones are formed by surface breaks; therefore within the limits of the zone itself that is filled with crushed rocks the amplitude of the signal must decrease, and reflections from the surfaces of faults may increase the amplitude, focusing it in the recording area. The ratio of these opposed effects is associated with the seismic wavelength and its path within the limits of the fault zone (width of the zone).

An unstable value of amplitudes is also noted on stations situated directly on Quaternary breaks. For instance on station 13 the signal of Aleutian earthquakes is 1.5-2.5 times as strong as at the other stations. Japanese earthquakes give recordings here that are 1.5-2.0 times weaker than Aleutian earthquakes. The same instability of behavior is noted at station 12 situated on a Quaternary fault.

An analysis of the amplitudes of P waves on stations of the Garm group showed that the fault zones have a considerable effect on the spatial structure of the wave field. This influence can be seen in distortion of

the pulse shape and in the considerable fluctuations of the amplitudes of seismic waves. The latter may have two possible causes. The first is the reflection of seismic waves from the boundaries of fault zones and the absorption of their energy due to propagation through the fault zones. As a result of the action of these factors the amplitudes of the first phases of the P wave are reduced, while those of the subsequent phases are distorted by interference. The second possible cause is the waveguide properties of the fault zones. These zones are comparatively thin steeply falling layers with reduced velocity. The difference of velocity from the values typical of the surrounding medium decreases with depth, and at depths of 10-12 km disappears completely, the fault is "healed." The amplitudes of seismic waves incident on this waveguide increase as the surface is approached as a consequence of a gradual reduction in elastic moduli.

In cases where the seismic rays are parallel to the fault plane, favorable conditions arise for propagation of waves in the waveguide fault zone, and one notes an increase in amplitude level on the surface as compared with closely spaced stations. This mechanism is well explained by the increase in amplitudes of Japanese earthquakes on the 11-th station.

Thus the given analysis shows that in selecting the points of location of sensitive stations in regions with complicated tectonic conditions it is necessary to do detailed research that will establish the spatial block structure of the amplitudes of seismic waves. In doing this it should be taken into consideration that the strongest deviations from average values are observed close to fault zones.

The formation of the seismic wave field is determined mainly by the elastic and dissipative properties of the earth's interior. At present these properties have been inadequately studied, and therefore it is difficult to carry out a detailed calculation of the kinematic and dynamic characteristics of the wave field. At the same time, a practically important problem -- localization of the horizontal inhomogeneity of acoustic properties in the depths of the earth -- is completely solvable by using supplemental geophysical information.

As has been shown, there are certain correlations between the physical parameters of matter in the depths of the earth; therefore, the magnetic and gravitational fields for instance may be used to get information on the elastic properties of the medium, and consequently to predict the dynamic peculiarities of seismic waves.

The most characteristic peculiarities of seismic waves, that are associated with inhomogeneities of the structure of the lower part of the crust and the upper mantle, show up with fairly good contrast in isostatic anomalies of the gravitational field and in the nature of the block structure of the anomalous magnetic field. At the same time, small-scale changes in the dynamic characteristics of the seismic waves are intimately related to the inhomogeneity of the very top part of the cross section, which is expressed

in a change in thickness of sedimentary deposits, zones of tectonic breaks and other peculiarities of the geological structure.

Conclusion

Ten years have passed since publication of the Comprehensive Seismological Expedition's monograph "Fundamental Experimental Patterns of the Dynamics of Seismic Waves" (Antonova et al., 1968). During this time the expedition has obtained new extensive experimental material on which the present monograph is based. A comparison of two periods separated by a decade gives an idea of the direction of development of experimental seismological research from analysis of general (average) patterns of seismic waves to the study of comparatively fine details of kinematic and dynamic characteristics and evaluation of inhomogeneities of the earth's structure.

The main purpose of this work has been the investigation of the mutual relation between inhomogeneities of the earth's structure and fluctuations of the wave field. The solution of this problem has been made possible by the development of dense systems of seismic observations.

The study of the complicated space-time structure of the wave field has required strong schematization: a rough hierarchy of spatial scales has been introduced, the field itself has been represented as the sum of components of different scales in a background-fluctuation relation with each other.

The components of the field are separated by geological criteria and methods of space-frequency filtration.

The morphology of the fluctuations is constructed on the basis of the characteristics of a random field. Despite the fact that such an approach had been suggested fairly long ago, there has been no unified system of quantitative description of the seismic wave field up until now. The system described here is formulated on the basis of the traditions of research of former years (Antonova et al., 1968; Nersesov, Rautian, 1964; Nersesov et al., 1972; Nikolayev, 1972); it is fairly complete and universal: any detail of the wave field is subject to schematization and division into parts, each part makes its own contribution to the quantitative description of the corresponding spatial scale. This technique is applicable both to analysis of the simple characteristics of seismic waves -- amplitudes, travel times, and to analysis of fairly complicated parameters such as those of polarization, energies in certain frequency bands and so forth.

The results are in many instances the first of their kind. From our standpoint the main significance of these results is that they provided new geological and geophysical information on the medium and in this way proved the competence of the research technique used. This gives us the impetus for recommending that seismologists use our method extensively under conditions of the widest scales and systems of observations.

Naturally in the course of research the method will undergo certain changes; nevertheless the results found in various regions of the globe can be compared, unified and perfected.

This work has established the fundamental rough spatial characteristics of the structure of the seismic wave field and horizontal inhomogeneities; the first, as yet approximate, features of distribution of horizontal inhomogeneities of various scales in the earth have been established. The refinement of these features, the investigation of unstudied regions of the earth, improvement of the reliability and detail of information -- all this is a matter for the future. The authors hope that future experimental seismic studies of the interior of the earth will take the path of development of the methods presented in this book.

REFERENCES

1. I. Ya. Azbel', V. I. Keylis-Borok, T. B. Yanovskaya, "A Method of Joint Interpretation of Hodographs and Amplitude Curves in the Study of the Upper Mantle" in the book: "Mashinnaya interpretatsiya seysmicheskikh voln" [Machine Interpretation of Seismic Waves], No 2, Moscow, Nauka, 1966.

2. K. Aki, I. L. Nersesov, A. V. Nikolayev et al., "Time Changes in the Fluctuations of Amplitudes and Travel Times of a Teleseismic P Wave on the Garm, California, LASA and NORSAR Groups" in the book: "Sovetsko-amerikanskiye issledovaniya po prognozu zemletryaseniy" [Soviet-U. S. Research on Earthquake Prediction], Vol 1, Dushanbe, Donish, 1976.

3. A. S. Alekseyev, M. M. Lavrent'yev, R. G. Mukhometov, V. G. Romanov, "A Numerical Method of Solving the Three-Dimensional Inverse Kinematic Problem" in the book: "Matematicheskiye problemy geofiziki" [Mathematical Problems of Geophysics], No 1, Novosibirsk, Computing Center, Siberian Department of the Academy of Sciences USSR, 1969.

4. A. S. Alekseyev, M. M. Lavrent'yev, R. G. Mukhometov et al., "A Numerical Method of Determining the Structure of the Upper Mantle of the Earth" in the book: "Matematicheskiye problemy geofiziki," No II, Novosibirsk, Computing Center, Siberian Department of the Academy of Sciences USSR, 1971.

5. Ye. N. Altukhov, K. L. Volochkovich, B. N. Krasil'nikov, A. D. Smirnov, "Experience in Standardizing the Folded Systems of the Ural-Mongolian Belt with Consideration of the Structure of Their Basement" in the book: "Tektonika Uralo-Mongol'skogo skladchatogo poyasa" [Tectonics of the Rual-Mongolian Folded Belt], Moscow, Nauka, 1974.

6. L. V. Antonova, F. F. Aptikayev, R. I. Kurochkina et al., "Osnovnyye eksperimental'nyye zakonomernosti dinamiki seysmicheskikh voln" [Fundamental Experimental Patterns of the Dynamics of Seismic Waves], Moscow, Nauka, 1968.

7. Z. I. Aranovich, ed., "Apparatura i metodika seysmometricheskikh nablyudeniy v SSSR" [Methods and Equipment for Seismotechnical Observations], Moscow, Nauka, 1974.

8. Z. I. Aranovich, N. A. Vvedenskaya, I. Ye. Gubin et al., "Instruktsiya o poryadke proizvodstva i obrabotki nablyudeniy na seysmicheskikh stantsiyakh Yedinoy sistemy seysmicheskikh nablyudeniy SSSR" [Instructions on the Order for Carrying out and Processing Observations on Seismic Stations of the Unified System of Seismic Observations of the USSR], Moscow, Institute of Physics of the Earth, Academy of Sciences USSR, 1966.

9. M. Ye. Artem'yev, "Planetary and Zonal Inhomogeneities of the Upper Mantle and Their Relation to Peculiarities of Regional Tectonics" in the book: "Svyaz' poverkhnostnykh struktur zemnoy kory s glubinnymi" [The Relation Between Surface Structures of the Earth's Crust and Deep-Level Structures], Kiev, "Naukova dumka," 1971.

10. Ye. V. Artyushkov, "Layer of Reduced Viscosity in the Upper Mantle of the Earth and Phenomena that are Related to it," BYULLETEN' MOSKOVSKOGO OBSCHESTVA ISPYTATELEY PRIRODY, OTDELENIYE GEOLOGII, 1970, No 2.

11. B. K. Balavadze, P. Sh. Mindeli, "Principal Results of Geophysical Studies of the Structure of the Earth's Crust in the Black Sea Basin" in the book: "Stroyeniye Chernomorskoy vpadiny" [Structure of the Black Sea Basin], Moscow, Nauka, 1966.

12. N. A. Belyayevskiy, "Zemnaya kora v predelakh territorii SSSR" [The Earth's Crust Within the Borders of the USSR], Moscow, Nauka, 1974.

13. G. N. Bugayevskiy, I. L. Nersesov, V. A. Rogozhina, "Horizontal Inhomogeneities of the Upper Mantle in Central Asia," IZVESTIYA AKADEMII NAUK SSSR, SERIYA GEOFIZICHESKAYA, 1971, No 6.

14. V. P. Valyus, "Algorithm for Rapid Calculation of Refracted Waves" in the book: "Algoritmy interpretatsii seysmicheskikh dannykh" [Algorithms for Interpretation of Seismic Data], No 5, Moscow, Nauka, 1971.

15. I. Vanek, A. Zatopek, V. Karnik et al., "Standardization of the Scale of Magnitudes," IZVESTIYA AKADEMII NAUK SSSR, SERIYA GEOFIZICHESKAYA, 1962, No 2.

16. A. Ritsema, ed., "Verkhnyaya mantiya" [The Upper Mantle], Moscow, Mir, 1975.

17. L. P. Vinnik, "Issledovaniya mantii Zemli seysmicheskimi metodami" [Studies of the Mantle of the Earth by Seismic Methods], Moscow, Nauka, 1976.

18. L. P. Vinnik, A. A. Godzikovskaya, "Lateral Variations of Absorption in the Upper Mantle Beneath Asia," IZVESTIYA AKADEMII NAUK SSSR, FIZIKA ZEMLI, 1975, No 1.

19. L. P. Vinnik, A. A. Lukk, "Tectonic Interpretation of the Deep-Level Structure of the Pamirs," IZVESTIYA AKADEMII NAUK SSSR, GEOTEKTONIKA, 1975, No 5.

20. L. P. Vinnik, A. V. Nikolayev, "Velocity Cross Section of the Lower Mantle from Direct Measurements of dt/dΔ," IZVESTIYA AKADEMII NAUK SSSR, FIZIKA ZEMLI, 1970, No 11.

21. I. Ye. Volkov, T. B. Yanovskaya, "On Determining the Velocity and Quality Factor in the Upper Mantle from Amplitude Curves" in the book: "Mashinnyy analiz tsifrovykh seysmicheskikh dannykh. Vychislitel'naya seysmologiya" [Machine Analysis of Digital Seismic Data. Computational Seismology], No 7, Moscow, Nauka, 1974.

22. I. S. Vol'vovskiy, "Seysmicheskiye issledovaniya zemnoy kory v SSSR" [Seismic Studies of the Earth's Crust in the USSR], Moscow, Nedra, 1973.

23. I. N. Galkin, A. V. Nikolayev, Ye. A. Starshinova, "Fluctuations of Wave Characteristics and Minor Inhomogeneity of the Earth's Crust," IZVESTIYA AKADEMII NAUK SSSR, FIZIKA ZEMLI, 1970, No 11.

24. M. V. Gzovskiy, V. N. Krestnikov, N. N. Leonov, et al., "Map of Most Recent Tectonic Movements of Soviet Middle Asia," IZVESTIYA AKADEMII NAUK SSSR, SERIYA GEOFIZICHESKAYA, 1960, No 8.

25. I. V. Gorbunova, N. V. Shatornaya, "Calibration Curve for Determining the Magnitude of Earthquakes from PKPIKP Waves," IZVESTIYA AKADEMII NAUK SSSR, FIZIKA ZEMLI, 1976, No 7.

26. B. Gutenberg, "Fizika zemnykh nedr" [Physics of the Depths of the Earth], Moscow, IL, 1963.

27. A. A. Dergachev, "Evaluating the Q of the Earth's Crust at Tuva" in the book: "Voprosy seysmichnosti Sibiri" [Problems of Seismicity of Siberia], part 1, Novosibirsk, Institute of Geology and Geophysics, Siberian Department of the Academy of Sciences USSR, 1972.

28. V. Din, "Correction of P Waves and Group Adjustment," "Trudy Instituta inzhenerov elektroniki i radiotekhniki" [Proceedings of the Institute of Engineers of Electronics and Radio Engineering], No 12, 1965.

29. V. V. Zhadik, A. A. Dergachev, "Measurements of the Quality Factor of the Earth's Crust from Recordings of Microtremors," IZVESTIYA AKADEMII NAUK SSSR, FIZIKA ZEMLI, 1973, No 2.

30. V. N. Zharkov, L. N. Dorofeyeva, V. M. Dorofeyev, V. M. Lyubimov, "Zone of Reduced Values of the Dissipative Function in the Shell on the Boundary with the Core," DOKLADY AKADEMII NAUK SSSR, 1974, Vol 214, No 4.

31. N. S. Zaytsev, L. P. Zonenshtayn, N. G. Markova et al., "Tectonics of Mongolia" in the book: "Tektonika Uralo-Mongol'skogo skladchatogo poyasa," Moscow, Nauka, 1974.

32. K. K. Zapol'skiy, "ChISS Frequency-Selective Seismic Stations" in the book: "Eksperimental'naya seysmologiya" [Experimental Seismology], Moscow, Nauka, 1971.

33. K. K. Zapol'skiy, I. L. Nersesov, T. G. Rautian, V. I. Khalturin, "Physical Principles of Magnitude Classification of Earthquakes" in the book: "Magnituda i energeticheskaya klassifikatsiya zemletryaseniy" [Magnitude and Energy Classification of Earthquakes], Vol 1, MSSSS, Academy of Sciences USSR, 1974.

34. L. P. Zonenshtayn, "Model of Development of the Geosynclinal Process" in the book: "Tektonika Uralo-Mongol'skogo skladchatogo poyasa," Moscow, Nauka, 1974.

35. "Local Structure of Turbulence in an Incompressible Liquid at Very High Reynolds Numbers," DOKLADY AKADEMII NAUK SSSR, 1941, No 30.

36. A. A. Lukk, I. L. Nersesov, "Structure of the Upper Part of the Earth's Mantle from Observations on Earthquakes with Intermediate Depth of the Focus," DOKLADY AKADEMII NAUK SSSR, 1965, Vol 162, No 3.

37. Ye. N. Lyustikh, "Isostasy and Isostatic Hypotheses," "Trudy Geofizicheskogo instituta Akademii Nauk SSSR" [Proceedings of the Geophysics Institute, Academy of Sciences USSR], 1957, No 38.

38. "Magnituda i energeticheskaya klassifikatsiya zemletryasneniy," collection of articles, Vol 1, 2, Moscow, MSSSS, Academy of Sciences USSR, 1974.

39. L. N. Malinovskaya, "Spectral Amplitude Curves of P Waves" in the book: "Algoritmy interpretatsii seysmicheskikh dannykh. Vychislitel'naya seysmologiya," No 5, Moscow, Nauka, 1971.

40. P. Molnar, T. G. Rautian, V. I. Khalturin, "Experience in Studying the Spectra of Local Earthquakes of the Garm Region" in the book: "Sovetsko-amerikanskiye issledovaniya po prognozu zemletryasneniy," Vol 1, Dushanbe, Donish, 1976.

41. Yu. P. Neprochnov, "Results of Deep Seismic Sounding on the Black Sea" in the book: "GSZ v SSSR" [Deep Seismic Sounding in the USSR], Moscow, Gostekhizdat, 1962.

42. I. L. Nersesov, T. G. Rautian, "Kinematics and Dynamics of Seismic Waves at Distances up to 3500 km from the Epicenter" in the book: "Eksperimental'naya seysmika" [Experimental Seismics], Moscow, Nauka, 1964.

43. I. L. Nersesov, A. V. Nikolayev, Ye. N. Sedova, "The Nature of Horizontal Inhomogeneity of the Mantle of the Earth from Seismic Data," DOKLADY AKADEMII NAUK SSSR, 1972, Vol 207, No 4.

44. A. V. Nikolayev, "Seysmika neodnorodnykh i mutnykh sred" [Seismics of Inhomogeneous and Turbid Media], Moscow, Nedra, 1972.

45. A. V. Nikolayev, F. S. Tregub, "Results of Investigation of a Statistical Model of the Earth's Crust," DOKLADY AKADEMII NAUK SSSR, 1969, Vol 189, No 6.

46. A. Nurmagambetov, "Damping of Seismic Waves and Energy Classification of Earthquakes from Observations by ChISS Equipment" in the book: "Magnituda i energeticheskaya klassifikatsiya zemletryasneniy," Vol 2, Moscow, MSSSS, Academy of Sciences USSR, 1974.

47. A. Nurmagambetov, T. G. Rautian, V. I. Khalturin et al., "Dependence of the Spectra of Seismic Oscillations on the Energy of Earthquakes" in the book: "Voprosy kolichestvennoy otsenki seysmicheskoy opasnosti" [Problems of Quantitative Evaluation of Seismic Danger], Moscow, Nauka, 1975.

48. N. I. Pavlenkova, "Volnovyye polya i model' zemnoy kory" [Wave Fields and a Model of the Earth's Crust], Kiev, "Naukova dumka," 1973.

49. I. P. Pasechnik, "Kharakteristika seysmicheskikh voln pri yadernykh vzryvakh i zemletryasneniyakh" [Characteristics of Seismic Waves in the Case of Nuclear Explosions and Earthquakes], Moscow, Nauka, 1970.

50. K. S. Ponomareva, "On Propagation of Diffusion Sound," UCHENYYE ZAPISKI KURSKOGO PEDAGOGICHESKOGO INSTITUTA, 1969, No 54.

51. F. Press, "Internal Structure of the Earth from Data of Theoretical Models" in the book: "Priroda tverdoy Zemli" [Nature of the Solid Earth], Moscow, Mir, 1975.

52. "Priroda tverdoy Zemli," Moscow, Mir, 1975.

53. N. N. Puzyrev, S. V. Krylov, B. P. Mashen'kin, "Metodika rekognostsirovochnykh glubinnykh seysmicheskikh issledovaniy" [Methods of Reconnaissance Deep-Level Seismic Studies], Novosibirsk, Nauka, 1975.

54. A. I. Ruzaykin, V. I. Khalturin, "Hodograph of the Maximum Phase of a Rayleigh Wave at Distances up to 3500 km" in the book: "Magnituda i energeticheskaya klassifikatsiya zemletryasneniy," Vol 2, Moscow, MSSSS, Academy of Sciences USSR, 1974.

55. Ye. F. Savarenskiy, N. G. Val'dner, "Lg and Rg Waves of Earthquakes of the Black Sea Basin, and Some Considerations on Their Nature" in the book: "Seysmicheskiye issledovaniya" [Seismic Research], No 4, Moscow, Academy of Sciences USSR, 1960.

56. Ye. N. Sedova, "Spatial Structure of a P Wave and Horizontal Inhomogeneity of the Crust and Mantle," IZVESTIYA AKADEMII NAUK SSSR, FIZIKA ZEMLI, 1974, No 12.

57. D. I. Sikharulidze, "The Nature of Lg and Rg Waves and Investigation of the Structure of the Earth's Crust," "Trudy Instituta geofiziki AN GSSR" [Proceedings of the Institute of Geophysics, Academy of Sciences of the Georgian SSR], 1963, Vol 21.

58. S. Smit, "Nonideal Elasticity" in the book: "Verkhnyaya mantiya" [The Upper Mantle], Moscow, Mir, 1975.

59. S. L. Solov'yev, V. B. Shein, "Intensity of an Earthquake from Data of Far Eastern and Continental Stations of the USSR" IZVESTIYA AKADEMII NAUK SSSR, SERIYA GEOFIZICHESKAYA, 1959, No 9.

60. V. I. Khalturin, N. B. Urusova, "Evaluation of the Absorption of Longitudinal and Transverse Waves from Observations on Local Earthquakes," "Trudy Instituta fiziki Zemli Akademii Nauk SSSR" [Proceedings of the Institute of Physics of the Earth, Academy of Sciences USSR], 1962, No 25.

61. V. I. Khalturin, "Absorption of Seismic Waves in the Earth's Crust of Northern Tyan'-Shan'" in the book: "Eksperimental'naya seysmologiya," Moscow, Nauka, 1971.

62. G. M. Tsibul'chik, "Nekotoryye chislennyye metody analiza struktury seysmogramm i opredeleniya srednikh kharakteristik zemnoy kory" [Some Numerical Methods of Analyzing the Structure of Seismograms and Determining the Average Characteristics of the Earth's Crust], Candidate's Dissertation, Novosibirsk, Institute of Geology and Geophysics, Siberian Department, Academy of Sciences USSR, 1968.

63. L. A. Chernov, "Rasprostraneniye voln so sluchaynymi neodnorodnostyami" [Propagation of Waves with Random Inhomogeneities], Moscow, Academy of Sciences USSR, 1958.

64. L. A. Chernov, "Volny v sluchayno-neodnorodnykh sredakh" [Waves in Randomly Inhomogeneous Media], Moscow, Nauka, 1975.

65. S. S. Shul'ts, "Formation of the Continental Crust of Paleozoic Folded Belts and Their Present Structure" in the book: "Tektonika Uralo-Mongol'skogo skladchatogo poyasa," Moscow, Nauka, 1974.

66. V. B. Enman, T. G. Simbireva, "Vertical Shifts on the Nimich Proving Grounds, and the Mechanism of Foci of Nearby Earthquakes," "Tezisy dokladov Vsesoyuznogo soveshchaniya po sovremennym dvizheniyam zemnoy kory" [Abstracts of Reports to the All-Union Conference on Recent Movements of the Earth's Crust], Alma-Ata, 1971.

67. T. B. Yanovskaya, G. V. Golikova, Yu. A. Surkov, "Amplitude Curves of P Waves" in the book: "Voprosy dinamicheskoy teorii rasprostraneniya seysmicheskikh voln" [Problems of the Dynamic Theory of Seismic Wave Propagation], No 7, Leningrad, Leningrad State University, 1964.

68. T. B. Yanovskaya, "Some Data on Seismic Waves in the Earth's Core" in the book: "Algoritmy interpretatsii seysmicheskikh dannykh," No 5, Moscow, Nauka, 1971.

69. R. D. Adams, E. R. Engdahl, "P-Wave Velocities in the Earth's Core: an Interim Report," PHYS. EARTH AND PLANET. INTERIORS, 1974, Vol 9, No 1.

70. K. Aki, "Scattering of P-Waves Under the Montana LASA," J. GEOPHYS. RES., 1973, Vol 78, No 8.

71. D. L. Anderson, A. Ben-Menahem, C. B. Archambeau, "Attenuation of Seismic Energy in the Upper Mantle," J. GEOPHYS. RES., 1965, Vol 70, No 6.

72. E. V. Artyushkov, "Rheological Properties of the Crust and Upper Mantle According to Data on Isostatic Movements," J. GEOPHYS. RES., 1971, Vol 77, No 5.

73. C. B. Archambeau, E. A. Flinn, D. G. Lambert, "Fine Structure of the Upper Mantle," J. GEOPHYS. RES., 1969, Vol 74, No 25.

74. R. G. Bacer, "Preliminary Study for Determining Magnitude from Lg," EARTHQUAKE NOTES SEISMOL. SOC. AMERICA, 1967, Vol 38, March-June.

75. B. A. Bolt, "Estimation of PKP Travel Times," BULL. SEISMOL. SOC. AMERICA, 1968, Vol 58, No 4.

76. I. Capon, R. J. Greenfield, R. J. Kolker, R. T. Lacoss, "Short-Period Signal Processing Results for the Large-Aperture Seismic Array," GEOPHYSICS, 1968, Vol 33, No 3.

77. D. S. Carder, D. W. Gordon, J. N. Jordan, "Analysis of Surface-Foci Travel Times," BULL. SEISMOL. SOC. AMERICA, 1966, Vol 56, No 4.

78. E. K. Carpenter, P. P. Marshall, A. Douglas, "The Amplitude-Distance Curve for Short-Period Teleseismic P-Waves," GEOPHYS. J., 1967, Vol 13, No 1-3.

79. M. A. Chinnery, M. N. Toksöz, "P-Wave Velocities in the Mantle Below 700 km," BULL. SEISMOL. SOC. AMERICA, 1967, Vol 57, No 2.

80. M. A. Chinnery, "Velocity Anomalies in the Lower Mantle," PHYS. EARTH AND PLANET. INTERIORS, 1969, Vol 2, No 1.

81. J. Cleary, "Analysis of the Amplitudes of Short-Period P-Waves Recorded by Long-Range Seismic Measurement Stations in the Distance Range of 30° to 120°," J. GEOPHYS. RES., 1967, Vol 72, No 18.

82. D. J. Corbishley, "Multiple-Array Measurements of the P-Wave Travel-Time Derivative," GEOPHYS. J. ROY. ASTRON. SOC., 1970, Vol 17, No 1.

83. A. M. Dainty, M. N. Toksöz, K. R. Anderson et al., "Seismic Scattering and Shallow Structure of the Moon in Oceanus Procellarum," MOON, 1974, Vol 9, No 1/2.

84. S. K. Dey-Sarkar, R. A. Wiggins, "Upper Mantle Structure in Western Canada," J. GEOPHYS. RES., 1976, Vol 81, No 1-2.

85. A. M. Dziewonski, R. A. Haddon, "The Radius of the Core-Mantle Boundary Inferred from Travel Time and Free Oscillation Data: a Critical Review," PHYS. EARTH AND PLANET. INTERIORS, 1974, Vol 9, No 1.

86. J. F. Evernden, "Magnitude Determinations at Regional and Near-Regional Distances in the United States," BULL. SEISMOL. SOC. AMERICA, 1967, Vol 57, No 4.

87. B. Gutenberg, C. F. Richter, "Magnitude and Energy of Earthquakes," ANN. GEOL., Rome, 1956, Vol 9, No 1.

88. A. L. Hales, J. Cleary, J. Roberts, "Velocity Distribution in the Lower Mantle," BULL. SEISMOL. SOC. AMERICA, 1968, Vol 58, No 6.

89. T. C. Hanks, M. Wyss, "The Use of Body-Wave Psectra in the Determination of Seismic-Source Parameters," BULL. SEISMOL. SOC. AMERICA, 1972, Vol 62, No 2.

90. H. S. Hasegawa, "Short-Period P-Code Characteristics in the Eastern Canadian Shield," BULL. SEISMOL. SOC. AMERICA, 1970, Vol 60, No 3.

91. E. Herrin, "Introduction to 1968 Seismological Tables for P-Phases," BULL. SEISMOL. SOC. AMERICA, 1968, Vol 58, No 4.

92. H. M. Iyer, I. H. Healy, "Teleseismic Residuals at the LASA-USGS Extended Array and Their Interpretation in Terms of Crust and Upper Mantle Structure," J. GEOPHYS. RES., 1972, Vol 77, No 8.

93. B. Jansson, E. S. Husebye, "Application of Array Data Processing Techniques to a Network of Ordinary Seismograph Stations," PURE AND APPL. GEOPHYS., 1968, Vol 69, No 11.

94. L. R. Johnson, "Array Measurement of P-Velocities in the Upper Mantle," J. GEOPHYS. RES., 1967, Vol 72, No 24.

95. L. R. Johnson, "Array Measurements of P-Velocities in the Lower Mantle," BULL. SEISMOL. SOC. AMERICA, 1969, Vol 59, No 2.

96. K. L. Kaila, D. Sarkar, "P-Wave Amplitude Variation with Epicentral Distance and the Magnitude Relations," BULL. SEISMOL. SOC. AMERICA, 1975, Vol 65, No 4.

97. H. Kanamory, "Attenuation of P-Waves in the Upper and Lower Mantle," BULL. EARTHQUAKE RES. INST. TOKYO UNIV., 1967a, Vol 45, pt. 2.

98. H. Kanamory, "Upper Mantle Structure from Apparent Velocities of P-Waves Recorded at Wakayama Micro-Earthquake Observatory," BULL. EARTHQUAKE RES. INST. TOKYO UNIV., 1967b, Vol 45, pt. 3.

99. H. Kanamory, "Spectrum of P and PcP in Relation to the Mantle-Core Boundary and Attenuation in the Mantle," J. GEOPHYS. RES., 1967c, Vol 72, No 2.

100. H. Kanamory, "Spectrum of Short-Period Core Phases in Relation to the Attenuation in the Mantle," J. GEOPHYS. RES., 1967d, Vol 72, No 8.

101. H. Kanamory, "Velocity and Q of Mantle Waves," PHYS. EARTH AND PLANET. INTERIORS, 1970, Vol 2, No 4.

102. B. L. N. Kennett, "The Effects of Attenuation on Seismograms," BULL. SEISMOL. SOC. AMERICA, 1975, Vol 65, No 6.

103. R. L. Kovach, L. D. Anderson, "Attenuation of Shear Waves in the Upper and Lower Mantle," BULL. SEISMOL. SOC. AMERICA, 1964, Vol 54, No 6.

104. G. A. McMechan, "Amplitude Constraints and the Inversion of Canadian Shield Early Rise Explosion Data," BULL. SEISMOL. SOC. AMERICA, 1975, Vol 65, No 5.

105. S. Miyamura, "Determination of Body-Wave Magnitudes for Shallow Earthquakes in the New Zealand and Macquarie Loop Region Using PKP Data," PHYS. EARTH AND PLANET. INTERIORS, 1974, Vol 8, No 2.

106. O. W. Nuttli, "The Amplitudes of Teleseismic P-Waves," BULL. SEISMOL. SOC. AMERICA, 1972, Vol 68, No 1.

107. M. Niazi, L. D. Anderson, "Upper Mantle Structure of Western North America from Apparent Velocities of P-Waves," J. GEOPHYS. RES., 1965, Vol 70, No 18.

108. R. Robinson, H. M. Iyer, "Temporal and Spatial Variations of Travel-Time Residuals in Central California for Novaya Zemlya Events," BULL. SEISMOL. SOC. AMERICA, 1976, Vol 66, No 5.

109. R. Sato, A. F. Espinoza, "Quality Factor Inversion Determination from the Analysis of Body Wave Data," Pt. 1, PURE AND APPL. GEOPHYS., 1967, Vol 67, pp 1-26.

110. M. K. Sengupta, B. R. Julian, "Amplitude-Distance Calibration Curve from Deep-Focus Earthquakes," BULL. SEISMOL. SOC. AMERICA, 1976, Vol 66, No 5.

111. D. W. Simpson, R. F. Meroni, D. W. King, "An Array Study of P-Wave Velocities in the Upper Mantle Transition Zone Beneath Northeastern Australia," BULL. SEISMOL. SOC. AMERICA, 1974, Vol 64, No 6.

112. R. L. Street, "Scaling Northeastern United States-Southeastern Canadian Earthquakes by Their Lg Waves," BULL. SEISMOL. SOC. AMERICA, 1976, Vol 66, No 5.

113. T. L. Teng, "Attenuation of Body Waves and The Q Structure of the Mantle," J. GEOPHYS. RES., 1978, Vol 73, No 6.

114. W. Thatcher, T. S. Hanks, "Source Parameters of Southern California Earthquakes," J. GEOPHYS. RES., 1973, Vol 78, No 35.

115. M. Tsujiura, "Regional Variation of P-Wave Spectrum (1)," BULL. EARTHQUAKE RES. INST. TOKYO UNIV., 1969, Vol 47, No 4.

116. B. E. Tucker, I. N. Brune, "Seismograms, S-Wave Spectra and Source Parameters for Aftershocks of the San Fernando Earthquake" in: "San Fernando, California Earthquake of February 9, 1971," Vol III, Washington, 1973.

117. K. F. Veith, G. E. Clawson, "Magnitude from Short-Period P-Wave Data," BULL. SEISMOL. SOC. AMERICA, 1972, Vol 62, No 2.

118. J. P. Wesley, "Diffusion of Seismic Energy in the Near Range," J. GEOPHYS. RES., 1965, Vol 70, No 20.

119. R. A. Wiggins, D. V. Helmberger, "Upper Mantle Structure of the Western United States," J. GEOPHYS. RES., 1973, Vol 78, No 11.

120. A. D. Zoltan, R. P. Masse, J. P. Gurski, "Regional Attenuation of Short-Period P- and S-Waves in the United States," Geophys. res., 1975, Vol 40, No 1.

6610
CSO: 8144/0481

- END -